SHOCK WAVES IN MIXTURES

OF

LIQUIDS AND AIR BUBBLES

L. NOORDZIJ

SHOCK WAVES IN MIXTURES

OF

LIQUIDS AND AIR BUBBLES

SHOCK WAVES IN MIXTURES

OF

LIQUIDS AND AIR BUBBLES

DOOR

LEENDERT NOORDZIJ

GEBOREN OP 1 DECEMBER 1942 TE ROTTERDAM

DIT PROEFSCHRIFT IS GOEDGEKEURD DOOR DE PROMOTOR

PROF. DR. IR. L. VAN WIJNGAARDEN

AAN JETTY

CONTENTS

GENERAL INTRODUCTION.

In this thesis one-dimensional propagation of waves with finite amplitude is studied. Especially shock waves, in mixtures of randomly distributed gas bubbles in a liquid. We have limited ourselves to mixtures with air bubbles, almost all of the same size, with a radius of order of $10^{-3}m$ and a gas volume fraction of a few percent. This type of flow is characterised by Kosterin (1949) as froth flow or strongly dispersed flow. Therefore the experiments are carried out in the range given in the right-hand side of the diagram in Figure 1.
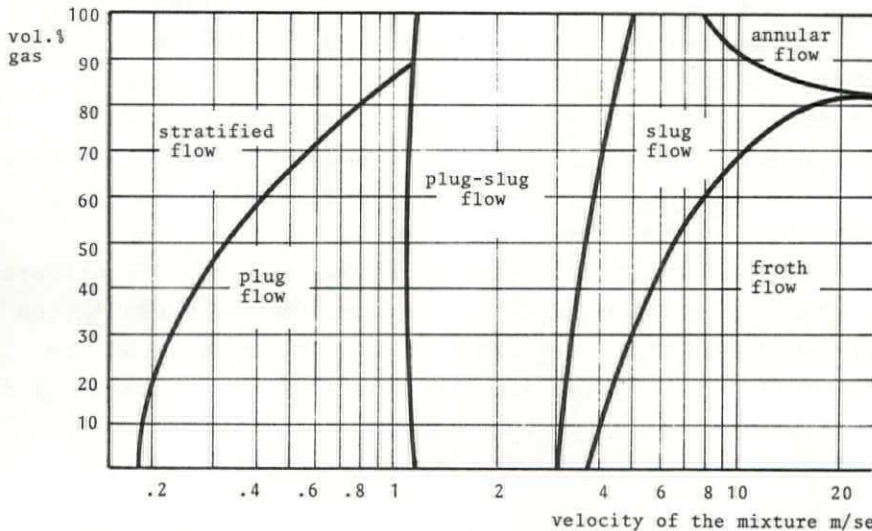
FIGURE 1.Distribution of the gas-liquid flow regions with different topologies for a 1"horizontal pipe, from Kosterin (1949).

To allow a tractable theoretical analysis we restrict ourselves to circumstances where bubbles do not break up under the influence of a pressure gradient. Also no mass-transfer occurs between the two phases in time intervals in which pertinent quantities such as pressure, density, etc. change. Further the bubbles are assumed to remain spherical. From an experimental point of view we restrict ourselves to weak and moderate shocks with pressure ratio's across the shock to about 6.

Even with these restrictions the flow of a heterogeneous

mixture of liquid and bubbles remains complicated. Therefore we employ a model which makes it possible to predict theoretically those quantities which can be measured.

We consider, as described in Van Wijngaarden (1968) and Batchelor (1969), wave propagation through a mixture of bubbles and liquid from the point of view of continuum theory and not as a multiple scattering problem (Foldy,1945). In the continuum theory we start with averaging and introduce average pressure, velocity and density. The averages are over a volume element containing many bubbles, but of linear dimensions small compared with the characteristic length of motion. Thus changes in pertinent quantities occur in distances large with respect to the inter-bubble distance and bubble radius. We therefore describe wave propagation in a fictitious, single phase compressible medium.

The mixture is a compressible medium with compressibility due to the gas phase and density due to the liquid. In most cases a rather low sound speed, as defined later on, can therefore be expected. Furthermore the mixture is considered, in equilibrium state, as a uniform medium. This assumption does not hold completely since in our experiments we are faced with a space-wise density distribution following from gravity. It will appear that this non-uniformity does not invalidate the analysis.

In the analysis of wave propagation through the mixture several types of steady shocks are studied. Some of them have been observed earlier by different investigators. For these shocks, normal shock relations are formulated similar to those in gasdynamics, socalled Rankine - Hugoniot relations. It can be expected that the description of wave propagation in a mixture is, to a large extent, similar to wave propagation in single phase compressible fluids. However, the leading mechanism in formation of a shock wave, non-linear steepening, originates in the case of a mixture for the greater part in the compression phenomenon, whereas in gases this steepening follows from convection.

The other effects which distinguish shocks in mixtures from
shocks in ordinary gases, are effects due to the relative
motion of the bubbles with respect to the surrounding liquid.
This relative motion consists of two types of motion: radial
motion of the liquid near an expanding or compressed bubble
and relative translational motion of the bubble with respect
to the liquid. Both types of flow cause dissipation.
Furthermore there is dispersion of waves caused by the
inertia of the radial flow associated with an oscillating
bubble.

In ordinary gases steepening of a compression wave by con-
vection can be balanced by viscous diffusion, leading to
a steady shock. The thickness of a shock in gases is there-
fore of the order of the mean molecular path (Lighthill,
1956).

For a mixture it is shown to be evident that the bubble
size determines the shock thickness. In mixtures several
types of shocks can be expected. One is based on the balance
of non-linear compression and dissipation due to radial
motion of a bubble. A second is based on the equilibrium
of non-linear compression, dispersion and the associated
dissipation. A third is based on the balance of non-linear
compression and dissipation due to relative translational
motion.

The first one was not encountered in our experiments. For
weak shocks, when the pressure ratio is below a certain
critical value, the third type of shock can appear. As
for the second type of shock it was noticed that the dis-
sipation associated with radial motion dominates the dis-
sipation associated with relative translational motion.
This is in the case of not too weak shocks in mixtures
with a volumetric gas content of a few precent. This leads
to shocks where the overall thickness is determined by the
dispersion effect. These shocks are governed by equations
of the same type as those for long gravity waves on water
of finite depth. Therefore the pressure profile in a steady
shock should look like the surface elevation in an undular

bore. This type of shock, a socalled S_A shock, was found in the experiments and shown in Figure 2.
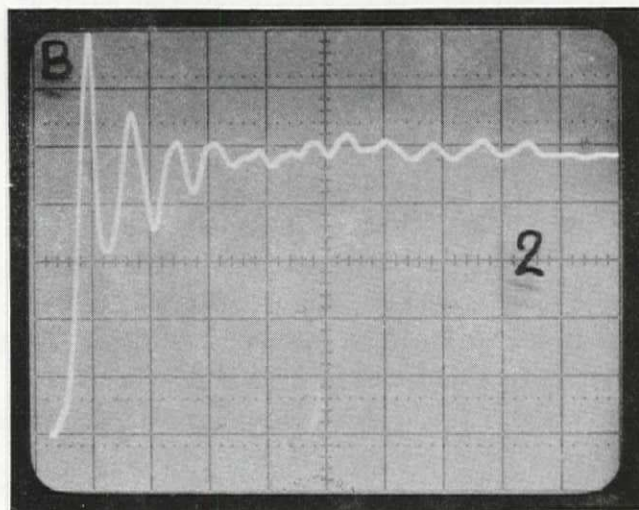
FIGURE 2. A pressure profile typical for a S_A shock, a steep rise in pressure at the front side and waves at the back side.

We observed a gradual change of the shock structure during its passage through a tube of some length. These changes are attributed to the mechanism of relative translational motion between the bubbles and liquid. Therefore we developed a theory, taking in account this relative motion. It will be shown that its effect on the shock structure is similar to the effects of thermal relaxation on gasdynamic waves. The pertinent relaxation time in the present case is the time it takes a bubble to adjust to the liquid velocity through viscous forces. From the theory it follows that this relaxation affects the speed of the wave as well as its structure. In the experiments no verification of this influence on wave speed could be made, it being too small to be measured in dilute mixtures. Comparison of the experimental results concerning the wave structure, with theory, supports our conclusion that the observed changes are due to relative motion indeed. In Figure 3 a pressure profile affected by relaxation is presented.
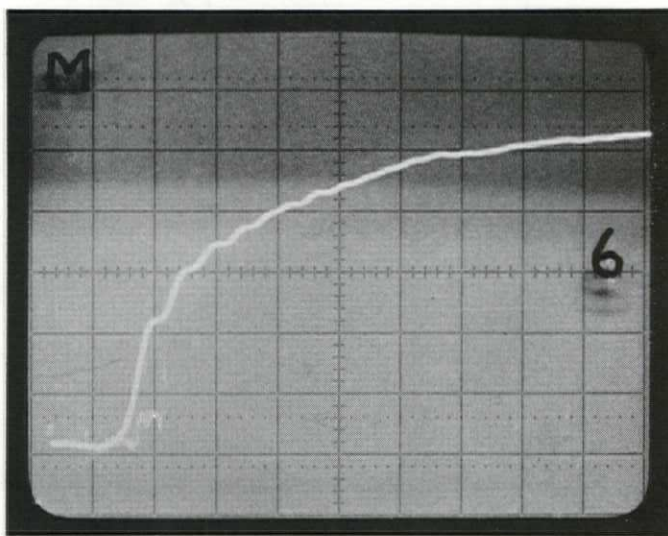
FIGURE 3. A S_B shock.

There is still a steep pressure rise at the front part, but
the pressure does not no longer rise to equilibrium pressure
at the back side. This takes place in a region, which is
much thicker than the front shock, and in which the pressure
slowly oscillating reaches its final value. This type of
shock will be called a S_B shock.
For weak shocks and where dissipation due to radial motion
is smaller than dissipation due to relative translational
motion the shock thickness can be much larger than of a S_A
shock. It is even possible, as already mentioned that a
steady shock appears, of which the structure follows from
a balance of non-linear steepening and resisted relative
translational motion. This we call a S_C shock. The front
shock as well as the oscillations have disappeared. The
pressure profile is almost completely smooth and covers a
region which is at least an order of magnitude larger than
the thickness of a S_A shock. A typical pressure recording
is shown in Figure 4.
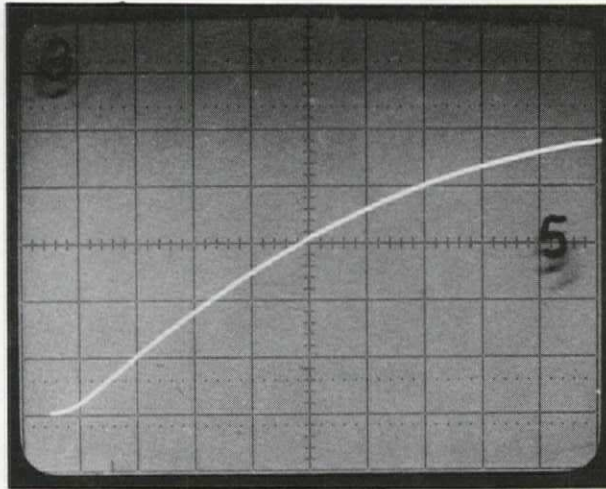
FIGURE 4. A S_c shock.

Having discussed the topics of this thesis it is of inte-
rest to survey previous work on shock waves in liquid-
bubble mixtures.
One of the earliest theoretical and experimental investi-
gations on shock waves in two-phase flow were done by
Ackeret (1930) who studied cavitating water flow in Laval
nozzles. Ackeret formulated Hugoniot relations for the
mixture similar to the relations for shocks in gases. From
these normal shock relations he derived expressions between
the pertinent quantities far in front and far behind the
shock. The structure of the shock and especially the shock
thickness, was estimated from dynamic bubble behaviour.
An extension of the experimental work of Ackeret was re-
ported by Campbell & Pitcher (1958). They illustrated their
theoretical discussion on the Hugoniot relations with ex-
periments on a short gas-liquid shocktube. The bubble beha-
viour of the gas phase was left out of account in their
analysis and accordingly the structure of the shock was not
discussed. They found that the temperature rise accross the
shock was very small for a very large range of conditions.

This leads to simple relations for the shock wave propagation speed. Campbell & Pitcher showed from entropy considerations, that a rarefaction wave cannot propagate without change of form and they argued that a compression wave can be expected to steepen into a shock wave. Their measured shock velocities come close to the predicted values. The bubbles in these experiments have a radius of about $10^{-4}m$, an order of magnitude smaller than the bubbles in our experiments. As will be discussed later on the magnitude of the bubble size is important from a thermal point of view. Bubbles of the size of $10^{-4}m$ are assumed to be in thermal equilibrium with the liquid, whereas larger bubbles can be regarded as thermally insulated. More theoretical work on shock waves in bubbly fluid was reported by Parkin, e.a. (1961). They formulated Hugoniot relations for normal shock waves in cases where the bubbles can be considered as thermally insulated. Also other aspects of air-water mixtures were discussed. They payed attention to dissolving of air bubbles, effects of surface tension and heat conduction between the bubbles and the liquid. Parkin e.a. also pointed to the importance of the inertia effects following from radial motion on the structure of the shock. Their qualitatively predicted shock structure is not supported by our theory, because their discussion on the S_B shock was based on thermal relaxation. They did not present experiments. Eddington (1970) also performed experiments on normal shocks and concluded that there is a good correspondence between the experiments and the results following from Hugoniot relations. The shock structure, as found in his experiments may be quite different from the shock in bubble-liquid mixtures, because the topology of the air-water mixture varied during these experiments. More detailed investigations on the structure of shock waves were reported by Crespo (1969) and Van Wijngaarden (1970). Crespo discussed propagation of a plane shock wave through a mixture with equal temperatures on both sides of the shock. He found a structure which is similar to the profile of Figure 2. However the

waves behind the shock were stronger attenuated than one
might conclude from the attenuation in our experiments.
This was due to the fact that Crespo assumed that the heat
flow, through which attenuation is largely determined, is
dominated by the heat resistance at the liquid side of the
bubble. Noordzij (1971) showed with experimental results
that heat flow from bubble to liquid is dominated by heat
resistance at the gas side and the contribution to attenua-
tion was found large enough to account for the experimen-
tally observed attenuation. Van Wijngaarden (1970) indepen-
dently formulated the equation describing the structure of
the shock. He dropped relative translational motion and
found an estimate for the shock thickness and the wave length
of the waves behind the shock. Experiments on S_A type of
shocks are reported in Noordzij (1971) and Van Wijngaarden
(1972b). Theory and experiments on the S_A-S_C shocks and espe-
cially theory concerning relaxation is reported by Noordzij
and Van Wijngaarden (1973).

The theory for the S_A-S_C shocks is presented together with
a large number of experimental results. For this we first
discuss, in chapter 1, the dynamic behaviour of an indivi-
dual bubble immersed in a liquid. In chapter 2 general
properties and the equations of motion for a liquid-bubble
mixture are discussed. In chapters 3-5 different types of
shock profiles will be analysed.

The influence of relative motion on the development of the
shock is discussed in chapter 6 in terms of relaxation,
introduced in the complete set of equations.

Gravity plays a role in our experiments according to the
experimental set up, resulting in a small relative velocity
of the bubbles. But this velocity can be neglected with re-
spect to the shock induced velocity. Due to gravity there
is a pressure and a density distribution in the equilibrium
state. Actually when we are discussing shocks, we consider
shocks propagating through a non-uniform medium. It will
appear, as discussed in chapter 7, that effects following
from this non-uniformity are sufficiently accounted for,

if we introduce local quantities for describing the structure of the shock. As a matter of fact this non-uniform medium enables us to study propagation of waves through mixtures where density is a slowly changing function of the space-wise coordinate. Using the socalled Whitham rule as described in Whitham (1958), we are able to present the change in propagation velocity as a function of the equilibrium quantities.

In chapter 8 the experimental set up is described and the experiments are compared with theory.

For the sake of simplicity we assumed isothermal behaviour of the gas phase. Where necessary corresponding relations following from adiabatic behaviour were summarized.

CHAPTER 1.

THE MOTION OF A SINGLE BUBBLE IMMERSED IN AN INFINITE
INCOMPRESSIBLE LIQUID.

§1. *INTRODUCTION.*

For describing wave propagation in a liquid-bubble mixture
it is necessary to know the equations governing the motion
of an individual bubble relative to the liquid.
Two types of bubble motion are of importance for our model
of the mixture flow. The first one is radial motion of the
bubble surface. Due to liquid inertia and gas compressibi-
lity an individual bubble is capable to execute radially
symmetrical oscillations. In a mixture this inertia causes
a dispersion effect on waves. The other motion is the rela-
tive translational motion of a bubble. Viscous friction
associated with relative motion causes a relaxation effect
on a wave. We assume in our theoretical model that this
relative motion does not disturb the spherical symmetry of
the bubble.

§2. *RADIAL MOTION OF THE BUBBLE SURFACE.*

In this section we describe briefly the motion of liquid
surrounding a contracting or expanding bubble. An equation
will be derived for the bubble radius $R=R(t)$, t denoting
time. This equation describing volume oscillations of a
bubble is well-known in literature, see a.o. Lamb (1932).
The liquid is assumed to be incompressible and the gas in
the bubble homogeneous. From a velocity potential Φ

$$\Phi = - R^2 \frac{dR/dt}{r} \quad , \tag{1.1}$$

by applying Bernoulli's law between a point on the bubble
surface and a point far away in the liquid, we find that
the compression or expansion of the bubble is governed by

$$P_g - P_\infty = \rho_l \left\{ R \frac{d^2R}{dt^2} + \frac{3}{2} (\frac{dR}{dt})^2 \right\} . \qquad (1.2)$$

Surface tension, vapour pressure and effects of the radial viscous stress are left out of account. The various quantities in (1.2) are given in Figure 5; ρ_l is the density of the liquid.
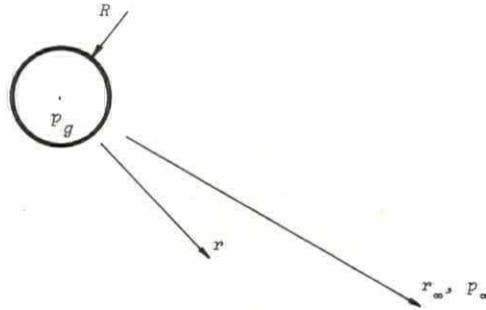
FIGURE 5. An individual bubble in a mixture. At the bubble radius $r = R$ the pressure is p_g. Far away $(r \to r_\infty)$ the pressure is p_∞.

A physical interpretation of (1.2) is that the difference between p_g and p_∞ is brought about by the inertia of the liquid being accelerated with respect to the interface in radial direction. This inertia is the cause of a dispersion effect on pressure waves through bubbly mixtures.
Assuming the gas to be isothermal we find for the angular frequency ω_B of free volume oscillations (with small amplitude) about the equilibrium radius R_o, from (1.2)

$$\omega_B = \frac{1}{R_o} (\frac{3p_\infty}{\rho_l})^{\frac{1}{2}} . \qquad (1.3)$$

For our experimental circumstances with $R_o=10^{-3}m$, $p_o=10^5$ N/m^2 and $\rho_l=10^3 kg/m^3$, ω_B is of order 10^4. It can be expected that for waves at frequencies ω below 10^3 sec.$^{-1}$ a bubbly fluid can be treated as a homogeneous medium in which the bubbly character of the gas phase may be ignored. When the gas phase behaves adiabatically ω_B becomes, as derived by Minnaert (1933),

$$\omega_B' = \frac{1}{R_o}(\frac{3\gamma p_\infty}{\rho_l})^{\frac{1}{2}} , \qquad (1.4)$$

γ is the ratio between the specific heat at constant pressure and the specific heat at constant density. Whether the gas phase behaves either isothermally or adiabatically has been investigated by Plesset (1964) for bubble oscillations at arbitrary frequencies. Plesset discussed results in terms of the characteristic lengths R_o, $D_g/\omega R_o$, the scale associated with the heat penetration depth in the bubble, and the acoustic wave length in the gas phase λ_g. As long as the latter is large with respect to the bubble radius R_o and $D_g/(\omega R_o)$, pressure and temperature within the bubble are uniform and the bubble oscillations are isothermal when $D_g/\omega >> R_o^2$ and adiabatic when $D_g/\omega << R_o^2$. At very high frequencies with $\lambda_g < R_o$ the oscillations are again isothermal; the surrounding liquid is no longer significant for the bubble interior. In general the oscillations of a bubble are therefore isothermal both for low and high frequencies and adiabatic in an intermediate range. A complete description of the heat processes would require an energy equation both for the liquid and the gas phase with proper boundary conditions. However, for our analysis the following approximations are sufficient. In our experiments for the air bubbles, having a radius of order $10^{-3}m$, the typical frequencies are just in the intermediate range. This is shown as follows:

Consider the case for shock waves with velocity of order $10^2 m/sec$ and thickness of order $10^{-2}m$. This leads to frequencies typical for our experiments of order 10^4.

The associated wave length λ_g in air is of order $10^{-2}m$ which is an order of magnitude larger than the bubble size. Hence acoustical variations of temperature and pressure within a bubble may be neglected. The thermal penetration depth in the bubble is of order $(D_g/\omega)^{\frac{1}{2}}$. With a frequency of order $10^4 sec^{-1}$ and a thermal diffusivity $D_g=18\times10^{-6}m^2/sec$ for air, the penetration depth becomes $10^{-4}m$, which is negligible small with respect to the bubble size. Adiabatic behaviour of the air bubble during the passage of the shock is therefore a realistic assumption. (Of course ultimately the bubble adjusts to the temperature of the liquid).

Hitherto we left out of account in equation (1.2) effects of viscosity, surface tension etc.

The full equation incorparating the various effects, reads:

$$p_g + p_v - \frac{2\sigma}{R} = p_\infty + \rho_l \{R \frac{d^2R}{dt^2} + \frac{3}{2}(\frac{dR}{dt})^2 + \delta\omega_B'R \frac{dR}{dt} \} , \qquad (1.5)$$

with σ the coefficient of surface tension, p_v the vapour pressure, δ a damping constant incorporating effects following from normal viscous stress etc. and ω_B' defined by (1.4). In the next section, we discuss the damping coefficient δ. Equation (1.5) applies to bubbles moving with the liquid. Actually the liquid velocity differs from the bubble velocity. The contribution of this to (1.5) is of order $\rho_l(v-u)^2$, with $(v-u)$ the relative velocity of the bubble with respect to the liquid). This quantity is of order $10^3 N/m^2$, and can therefore be neglected.

For our experimental circumstances we can further neglect the influence of vapour pressure with respect to $p_g \sim 10^5 N/m^2$

$$p_v \sim 10^3 \ N/m^2 \ .$$

The influence of surface tension is of no importance:

$$\frac{\sigma}{2R} \sim 10^2 \ N/m^2 \ .$$

The equation to be used, describing damped volume oscillations of a bubble, reduces to

$$p_g - p_\infty = \rho_l \left\{ R \frac{d^2R}{dt^2} + \frac{3}{2}(\frac{dR}{dt})^2 + \delta\omega_B' R \frac{dR}{dt} \right\} . \qquad (1.6)$$

Later on equation (1.6) will be substituted in the equations describing the hydrodynamics of a liquid-bubble mixture. It is reasonable to suppose (Van Wijngaarden, 1964), when the bubbles are sufficiently far apart, that the ambient pressure for one bubble p_∞ is the local pressure in the continuum theory, as will be discussed in the following chapter.

§3. THE ATTENUATION OF THE VOLUME OSCILLATIONS; δ.

There are various mechanisms which cause attenuation of the volume oscillations of a bubble. If the liquid surrounding a bubble were incompressible and the gas phase behaved purely isothermally or adiabatically the most important contribution to attenuation would follow from viscous dissipation associated with the radial motion near an expanding or contracting bubble. In this case the last term in the right-hand side of equation (1.6) is determined by normal viscous stress and equals

$$2\mu_l \frac{\partial^2 \phi}{\partial r^2} ,$$

with μ_l the dynamic viscosity of the liquid.
The equation for the bubble oscillations becomes, using (1.1)

$$p_g - p_\infty = \rho_l \left\{ R \frac{d^2R}{dt^2} + \frac{3}{2}(\frac{dR}{dt})^2 + \frac{4\nu_l}{R} \frac{dR}{dt} \right\} , \qquad (1.7)$$

with ν_l the kinematic viscosity of the liquid.
However the liquid is not purely incompressible and a bubble executing volume oscillations expends a portion

of its energy by radiating spherical sound waves. Also
the gas does not behave purely isothermally or adiabati-
cally. It will appear that the most important damping
mechanism stems from this thermal process in the gas phase.
During expansion and compression heat is conducted from
the liquid to the bubble and visa versa, causing a phase
difference between the pressure in the bubble and the
external pressure. This can be described in terms of a
damping coefficient. Several authors discussed the attenu-
ation associated both with acoustical radiation and ther-
mal conduction. For this the reader is referred to a survey
in Van Wijngaarden (1972a).

In equation *(1.6)* the term including the factor δ repre-
sents the various damping effects in a formal way, since
only for small amplitude oscillations and small values of
δ the various effects can simply be added. However for our
purposes we find a sufficiently satisfactory damping constant
if we assume δ to be the sum of the different effects:

$$\delta = \delta_{vr} + \delta_{ac} + \delta_{th} \, , \qquad\qquad (1.8)$$

with : δ_{vr} the contribution due to normal viscous stress

δ_{ac} the contribution due to acoustic radiation

δ_{th} the contribution due to thermal conduction.

δ_{vr} has been discussed already and becomes

$$\delta_{vr} = \frac{4\mu_l \omega'_B}{3\gamma p_\infty} \, ,$$

or

$$\delta_{vr} = \frac{4\nu_l}{\omega'_B R_o^2} \, . \qquad\qquad (1.9)$$

The contribution δ_{ac} becomes (Devin, 1959)

$$\delta_{ac} = \frac{\omega'_B R_o}{c_l} \qquad\qquad (1.10)$$

with c_l the sound velocity in the liquid. In general δ_{ac}
is a function of the forced frequency (Meyer&Skudrzyk, 1953).

We assume δ_{ac} to be constant and take its value at reso-
nance as a first approximation. δ_{ac} is found from calcula-
tions in which the bubble is treated as a simple sound source
and the bubble radius is considered small with respect to
the wave length of the radiated sound.

An expression for δ_{th} can be approximated from calculations
of Pfriem (1940) and becomes

$$\delta_{th} = \frac{3(\gamma-1)}{2R_o} \left(\frac{2D_g}{\omega'_B}\right)^{\frac{1}{2}} . \tag{1.11}$$

Also we took δ_{th} under resonance conditions. For air bubbles
this expression is

$$\delta_{th} = 1.7 \times 10^{-4} (\omega'_B)^{\frac{1}{2}} . \tag{1.12}$$

These approximations of the thermal contribution are based
on linearizations of the dynamic equation for the bubble
and of its heat equation, using proper boundary conditions.
Due to its great heat capacity the liquid is assumed to be
isothermal in this approximation.

In most of our experiments thermal dissipation dominates
other dissipation mechanisms discussed so far. Other
mechanisms leading to thermal adjustment are: forced and
free convection in the bubble. These effects and also those
following from vaporization and condensation are left out
of account because they are beyond the scope of this thesis.

§4. *THE RELATIVE TRANSLATIONAL MOTION OF A BUBBLE.*

In general there is no evidence that a body immersed in a
liquid will move at the same local liquid velocity under
the influence of a pressure gradient in the liquid. There-
fore the equation of motion describing relative trans-
lational motion is of interest. With an ultimately vanishing
pressure gradient the bubble velocity equals eventually the
liquid velocity, because of viscocity.

Batchelor (1969) has shown the importance of dissipation

associated with relative motion for pressure waves in bubble-
liquid mixtures. Crespo (1969) and Van Wijngaarden (1970)
introduced the equation of motion in the context of basic
equations from which the structure of the shock can be found.
For derivation of this equation it is necessary to know the
different forces on a bubble.

Due to the negligible inertia of the gas, the gas in the
bubble can freely move about so there is hardly no constraint
on the tangential velocity of the liquid at the boundary
of a bubble (Levich, 1962). There are only the constraints
of continuity of tangential stress and the vanishing of
relative normal velocity in this case. The only boundary
layer of importance is a boundary layer for the velocity
gradient, the neglect of which is, in a first approximation,
legitimate (see e.g. Levich, 1962). Therefore the motion
of a bubble can be determined from potential theory.
Knowing the potential of translational motion of a sphere
the dissipation associated with this motion can be calcu-
lated. Since velocity gradients are not of larger order
of magnitude within the boundary layer than outside of it,
the rate of energy dissipation per unit volume is of the
same order throughout the liquid. So the total rate of dis-
sipation is dominated by the contribution of the considerable
larger region of irrotational flow outside the layer in
contrast with a rigid body. From the dissipation through
the whole of the liquid coupled with relative motion we can
find an expression for the frictional force exerted on
the bubble.

By equating the rate of dissipation in the liquid to a
frictional force times the relative velocity, we find for
the frictional force F,

$$F = 12\pi\mu_l R(v-u) \quad, \tag{1.13}$$

where v is the velocity of the bubble and u of the sur-
rounding liquid (Levich, 1949).

Note that this force is just twice the Stokes resistance for a solid sphere at small Reynolds numbers. Here, in contrast with Stokes flow, the Reynolds number must be large enough for inertia forces to dominate over viscous forces.

The validity of *(1.13)* is according to Levich (1962) restricted to Reynolds numbers of about *800*, because at larger numbers the bubbles are significantly deformed. It is of interest for a discussion of the experimental results to give for these oblate bubbles an approximate resistance based on Levich's model.

According to Levich (1962) this drag becomes:

$$F' = 12\pi\mu_l \frac{S}{h}(v-u) \quad , \qquad (1.14)$$

where S is the area and h the thickness of the deformed bubble in the direction of motion. In the following theoretical analysis we assume the bubble to remain spherical. When the liquid contains surface active agents and contains only a few bubbles Levich's model ceases to be valid. The presence of surface active agents leads to an apparent no slip condition at the interface. In suspensions as we will use, Levich's model for a bubble is realistic (Levich 1962, p.448), because for not too low gas concentrations the concentration of agents divided by the total gas-liquid interface is low enough.

The other force on the bubble follows from the ambient pressure gradient $\partial p/\partial x$ and equals $-V \partial p/\partial x$. Associated with this each bubble represents an impulse as defined by Kelvin (Lamb 1932, §119). This is the impulse of the system bubble and liquid. Kelvin introduced this impulse to solve the problem connected with the momentum of the liquid. The momentum of the liquid depends on the shape of the surface at infinity and is therefore indeterminate. The socalled Kelvin impulse for a bubble is, relative to the liquid, of magnitude

$$\frac{1}{2} \rho_l V(v-u) \quad , \qquad (1.15)$$

corresponding with the inertia of the mass of the liquid
occupying a volume half that of the bubble, usually called
the added or virtual mass, times the relative velocity.
Since the bubble is considered as massless, the rate of
change of its Kelvin impulse equals the external forces,
which are the force due to the ambient pressure gradient
and the friction exerted by the liquid.
The equation of motion for the bubble is, taking these
forces together,

$$\frac{1}{2} \rho_l \frac{d}{dt}\{V(v-u)\} + 12\pi\mu_l R(v-u) = -V\frac{\partial p}{\partial x} . \qquad (1.16)$$

Initially the volume of the bubble can be taken as constant
(Woo & Paslay, 1967). In that case and for low viscosity
(1.16) reduces, using the equation of motion for the liquid

$$\rho_l \frac{du}{dt} + \frac{\partial p}{\partial x} = 0 ,$$

to

$$3 \frac{du}{dt} \simeq \frac{dv}{dt} . \qquad (1.17)$$

In a situation where u and v are initially zero, as in our
experimental circumstances when a shock wave propagates in
a mixture at rest, we find

$$v \simeq 3 u .$$

Of course the viscosity is not zero and with a vanishing
pressure gradient the bubble velocity ultimately equals
the liquid velocity. We describe this process in a mix-
ture in more detail in the chapters 5 and 6.
Associated with the relative motion of the bubble there
appears liquid motion which is called drift. Darwin (1953)
showed that in potential flow associated with the motion
of a sphere through a liquid at rest, a mass of liquid is
displaced equal to the hydrodynamic or virtual mass

of the sphere. This displacement, drift, equal to $1/2 \, \rho_l V$ is in the direction of motion. We must account for this effect in the equations of motion and mass conservation in mixtures of liquid and bubbles.

§5. *THE RATE OF DISSIPATION ASSOCIATED WITH BOTH RELATIVE TRANSLATIONAL AND RADIAL MOTION OF THE BUBBLE.*

It is of interest to find the leading mechanism of wave attenuation in mixtures. For this we compare the rate of dissipation associated with relative translational and radial motion.
The rate of dissipation associated with translational motion of a bubble with a socalled free boundary is found to be, (Batchelor, 1967),

$$E_t = 12\pi\mu_l R(v-u)^2 \ . \tag{1.18}$$

The rate of dissipation associated with radial motion is found from the attenuation term in *(1.5)*

$$\rho_l \delta\omega_B' R \, \frac{dR}{dt} \quad .$$

The rate of dissipation becomes, (Batchelor, 1967),

$$E_r = \rho_l \delta\omega_B' R 4\pi R^2 (\frac{dR}{dt})^2 \ . \tag{1.19}$$

This is of course an approximation because δ contains contributions from linearized equations.
The ratio between E_r and E_t is

$$\frac{E_r}{E_t} = \frac{\delta\omega_B' \, R^2}{v_l(v-u)^2} \, (\frac{dR}{dt})^2 \ . \tag{1.20}$$

To find the magnitude of this ratio we introduce a time scale relevant for the change in pertinent quantities. This scale is based on the shock propagation velocity U, which is of order $10^2 m/sec$ and the shock thickness d,

which is of order $10^{-2}m$.

The scale is

$$\omega^{-1} = \frac{d}{U} = O(10^{-4})sec .$$

Accordingly dR/dt is approximated by ωR.

Also we need an estimate for $v-u$. For that we use a relation which will be derived later on in this thesis. $v-u$ becomes approximately for not too weak shocks

$$v-u = U\beta ,$$

with β the gas volume fraction of the mixture. $\beta=O(10^{-2})$.

Using the just derived expressions, the ratio E_r/E_t becomes

$$\frac{\delta\omega_B'R^2}{v_l\beta} \frac{R^2}{\beta d^2} .$$

For the moderate shocks in our experiments, this quantity is of order 10^3. So dissipation is largely governed by radial motion. Only in the case of weak shocks this no longer holds and the ratio becomes of order unity. Then the suggestion of Batchelor (1969), that relative translational motion is important, is supported.

§6. CONCLUSIONS.

In this chapter we discussed the motion of a single bubble immersed in a liquid. As will appear later on the different aspects of this motion, radial as well as translational, will be of importance in analysing waves of small and finite amplitude through mixtures.

We conclude that dissipation associated with radial motion plays an important rôle in attenuation of waves. Furthermore radial motion will be important for dispersion effects on waves in these mixtures.

In this chapter we adopted Levich's model for the frictional force. From experiments discussed in chapter 8 we will verify the reliability of this model.

CHAPTER 2.

GENERAL PROPERTIES AND EQUATIONS OF MOTION FOR A MIXTURE
OF LIQUID AND GAS BUBBLES.

§1. *INTRODUCTION*.

In this chapter we consider wave propagation through mixtures
of bubbles and liquid. For many purposes it is sufficient
to consider the mixture as a homogeneous fluid. Provided
the length scale of motion is sufficiently large compared
with the average distance between the randomly distributed
bubbles. In this the simplest model the pressure in the
bubble equals the pressure in the liquid. For low frequen-
cies this model is supported by experiments (Silberman,1957).
At higher frequencies wave propagation becomes more and
more complicated, because of bubble oscillations. One
approach is to adopt a model where wave propagation is
considered as a multiple scattering problem. However this
approach is beyond the scope of this thesis. For a review
on this subject the reader is referred to Van Wijngaarden
(1972a).
In this thesis we adopt the model in which a continuum
theory can be constructed. In this theory we start by intro-
ducing average quantities. These are average pressure,
velocity and density, where the averaging is over a volume
element of the mixture containing many bubble, but of
linear dimensions small with respect to the characteristic
length of motion.
At higher frequencies the bubble behaviour of the gas phase
becomes important and the equality of the pressure in the
bubble and the pressure in the liquid is lost. We assume
that the relation between the local pressure in the liquid
p and the pressure in the bubble p_g is the same as for an
isolated bubble as given in the foregoing chapter where p_∞
is replaced by p.
This model enables us to write down simple equations for

wave propagations in mixtures of bubbles and liquid.
For convenience some assumptions for these mixtures are
repeated. We assume that the bubbles are all of the same
size and they execute volume oscillations. Further the
bubbles are considered as gas filled cavities, which do
not break up or cluster together. Mass transfer between
the two phases is let out of account, because desolution
times are much larger than a characteristic time related
with wave motion (Parkin e.a., 1961). As already mentioned
in the general introduction gravity plays a rôle in our
experiments. However its influence on wave propagation is
discussed elsewhere in this thesis. Also induced relative
translational motion is left out of account in the analysis
of this chapter.
In the following section we derive the equation of state of
the mixture.

§2. THE EQUATION OF STATE.

Throughout the analysis the liquid is assumed to be incom-
pressible except for the damping effect associated with
sound radiation from a bubble.
A modification of the equations caused by compressibility
can be found in Batchelor (1969). In the following we de-
note quantities belonging to the gas phase with subscript
g; those belonging to the liquid with l. In most of the
practical cases and also in our experiments the gas volume
fraction β is not larger than a few percent. It is defined
as the volume occupied by the gas in a unit volume of the
mixture,

$$\beta = n \; \frac{4}{3} \; \pi R^3 = nV \quad , \qquad (2.1)$$

where n is the number density of the bubbles.
The mass density ρ of the mixture follows from the density
of the liquid, ρ_l, and the density of the gas, ρ_g. For small
values of β we may neglect the contribution of the gas, $\rho_g \beta$,

and we find for ρ

$$\rho = \rho_l (1 - \beta) \quad . \tag{2.2}$$

When the bubbles move with the liquid the mass of the gas in a unit mass of the mixture is constant

$$\frac{d}{dt}\left[\frac{\rho_g \beta}{\rho_l (1-\beta)}\right] = 0,$$

or

$$\frac{\rho_g \beta}{1-\beta} = constant \quad . \tag{2.3}$$

In a homogeneous mixture where $p = p_g$ and for isothermal circumstances (2.3) changes into

$$\frac{p\beta}{1-\beta} = constant \quad , \tag{2.4}$$

and for adiabatic circumstances

$$p\left(\frac{\beta}{1-\beta}\right)^\gamma = constant \quad . \tag{2.5}$$

(2.4) and (2.5) are the equations of state.

§3. *THE SOUND VELOCITY.*

For the isothermal sound velocity $c = (dp/d\rho)^{\frac{1}{2}}$ we find from (2.2) and (2.4)

$$c^2 = \frac{p}{\rho_l \beta (1-\beta)} \quad . \tag{2.6}$$

The adiabatic speed of sound becomes, with (2.2) and (2.5)

$$c^2 = \frac{\gamma p}{\rho_l \beta (1-\beta)} \tag{2.7}$$

We see from (2.6) and (2.7) that for $\beta \to 0$ we have to account for the compressibility of the liquid and for $\beta \to 1$ the con-

tribution of the density of the gas phase to the density
of the mixture.

In most of the practical cases we are dealing with β neither
very close to zero nor to unity. So the relations (2.6) and
(2.7) are used throughout this thesis. In our experiments
c is of order $10^2 m/sec$.

The results for the speed of sound waves of low frequency
were already found by Mallock (1910).

For a survey on sound velocities in a bubbly fluid the reader
is referred to Van Wijngaarden (1972a).

In the case of a homogeneous theory with disappearing bubble
radius or large wave length, Hsieh & Plesset (1961) found
that wave propagation is isothermal. This is also supported
by the experiments of Silberman (1957).

As follows from the investigations in the foregoing chapter
the adiabatic speed of propagation is of importance for
short wave length. In that case we are also dealing with
effects following from dispersion.

§4. *EQUATIONS OF MOTION.*

In this section we pay attention to the hydrodynamics of
the mixture for the homogeneous case.

The homogeneous theory is defined through stating $p=p_g$.
However, in our theory we allow for a difference between
p and p_g which is associated with radial viscous stress
near the bubble.

Using (1.7), the relation between p and p_g becomes

$$p_g - p = \frac{4\mu_l}{R} \frac{dR}{dt} .$$
(2.8)

The equation of mass conservation becomes

$$\partial\rho/\partial t + \partial(\rho u)/\partial x = 0 ,$$
(2.9)

where t is the time-wise variable, x the space-wise variable
and u the mixture velocity.

The equation of motion for the mixture is

$$\rho\, du/dt = -\partial p/\partial x .$$
(2.10)

The equation of continuity for the number density n is

$$\frac{\partial n}{\partial t} + \frac{\partial}{\partial x}(nu) = 0 \quad , \qquad (2.11)$$

or with $V\rho_g = constant$ and (2.1)

$$\frac{\partial}{\partial t}(\beta\rho_g) + \frac{\partial}{\partial x}(\beta\rho_g u) = 0 \quad .$$

With (2.9) and the fact that the mass of the bubble is constant we find from (2.11)

$$\frac{nV\rho_g}{1-\beta} = constant \quad ,$$

or

$$\frac{\beta\rho_g}{1-\beta} = constant \quad ,$$

as already presented in eqation (2.3).
With $V\rho_g = constant$ we obtain

$$\frac{n}{1-\beta} = constant \quad . \qquad (2.12)$$

With (2.1) and (2.12), (2.8) yields

$$P_g - p = \frac{4}{3}\mu_l \, ln\frac{\beta}{1-\beta} \quad . \qquad (2.13)$$

Substitution of ρ from (2.2) into (2.13) gives

$$P_g - p = -\frac{4}{3}\frac{\mu_l}{\rho\beta}\frac{d\rho}{dt} \quad . \qquad (2.14)$$

From the equations (2.9), (2.10) and (2.14) we finally obtain the equation of motion which will be subject of further discussion in the next section

$$\frac{\partial u}{\partial t} + u\frac{\partial u}{\partial x} = -\frac{1}{\rho}\frac{\partial p_g}{\partial x} + \frac{1}{\rho}\frac{\partial}{\partial x}(\frac{4\mu_l}{3\beta}\frac{\partial u}{\partial x}) \quad . \qquad (2.15)$$

The last term in the right-hand side of *(2.15)* describes
the effect of radial viscous stress near the bubbles in a
mixture. This term can be interpreted as the contribution
of the socalled volume viscosity $4\mu_l/3\beta$. The derivation of
volume viscosity for a suspension of bubbles in liquid based
on dissipation in the mixture is already given by Taylor
(1954). The term shows that effects of shear stress in the
liquid can be neglected safely when $\beta = O(10^{-2})$. This being
so in our experiments.

§5. *WAVE PROPAGATION IN A MIXTURE OF GAS BUBBLES AND LIQUID.*

In this section we discuss acoustical wave propagation. The
equations are completely similar to those in gasdynamics.
For this the reader is referred to a survey in Lighthill
(1956). First we drop the term representing dissipation
in *(2.15)*. Using $c^2 = (dp/d\rho)$, we find from a linearization
of *(2.9)* and *(2.15)* the well-known wave equation for waves
of small amplitude

$$\frac{\partial^2 u}{\partial t^2} = c_o^2 \frac{\partial^2 u}{\partial x^2} \quad , \tag{2.16}$$

where subscript o refers to equilibrium circumstances.
c_o^2 is defined through *(2.6)*.
If we consider the infuence of viscosity as represented
in the last term of the right-hand side of *(2.15)*, the
equation describing waves of small amplitude becomes

$$\frac{\partial^2 u}{\partial t^2} - c_o^2 \frac{\partial^2 u}{\partial x^2} = c_o^2 \frac{4\mu_l}{3p_o} \frac{\partial^3 u}{\partial t \partial x^2} \quad . \tag{2.17}$$

The term in the right-hand side represents attenuation of
the sound wave by diffusion. The factor $(4\mu_l/3p_o)c_o^2$ is
usually called the diffusivity and we denote this factor
with Γ. We now briefly illustrate the diffusion. Looking
for solutions proportional to *exp(iωt)* *(2.17)* changes
into:

$$(c_o^2 + \Gamma i \omega) \frac{\partial^2 u}{\partial x^2} + \omega^2 u = 0 . \qquad (2.18)$$

From equation (2.18) we see that a progressive wave is of the form

$$u \propto exp \left[i \omega \left\{ t - \frac{x}{(c_o^2 + \Gamma i \omega)^{\frac{1}{2}}} \right\} \right]. \qquad (2.19)$$

With $c_o^2 \gg \Gamma \omega$, (2.19) becomes

$$u \propto exp \left\{ - \frac{\Gamma \omega^2}{2 c_o^3} x \right\} exp \left\{ i \omega (t - {}^x/{}_{c_o}) \right\} . \qquad (2.20)$$

The first factor shows that an initial sinusoidal wave is unaltered by diffusion. Now we consider a general signal with a given frequency spectrum $u(\omega)$ for $x=0$,

$$u = u_o(t) = \int_{-\infty}^{\infty} e^{i \omega t} u(\omega) d\omega , \qquad (2.21)$$

and for $x \neq 0$ we find with (2.20)

$$u = \int_{-\infty}^{\infty} exp \left\{ - \frac{\Gamma \omega^2}{2 c_o^3} x \right\} exp \left\{ i \omega (t - {}^x/{}_{c_o}) \right\} u(\omega) d\omega . \qquad (2.22)$$

Using the transform of $exp(-\Gamma \omega^2 x / 2 c_o^3)$ we find from inverse transformation of (2.22),

$$u = \frac{c_o}{(2 \pi \Gamma x / c_o)^{\frac{1}{2}}} \int_{-\infty}^{\infty} u_o(s) \, exp \left[- \frac{(t - s - {}^x/{}_{c_o})^2}{2 \Gamma x / c_o^3} \right] ds , \qquad (2.23)$$

u is the time mean of $u_o(s)$ weighted according to a Gaussion distribution centred on $s = t - {}^x/{}_{c_o}$ with standard deviation $(\Gamma x / c_o)^{\frac{1}{2}} / c_o$. This accentuates the reason for calling Γ the diffusivity of sound since the wave spreads out with increasing x. For example an initial step function changes into an error function. Ultimately a wave disappears. We will show further on that this spreading of the wave by diffusion can be altered by non-linearity.

§6. NON-LINEAR WAVE PROPAGATION.

In this section we discuss plane waves of finite amplitude travelling in an undisturbed region of the mixture and use the simple wave analysis of gasdynamics. In particular we are interested in those cases where non-linearity leads to formation of a steady shock wave.

In gasdynamics shock waves are formed as a result of a balance between steepening by convection and the tendency to spread out by diffusion.

In the case of a bubbly liquid the term producing diffusion is already discussed and we therefore pay attention to the process of steepening. For this we use the general approach of Riemann (1859).

The equations *(2.9)* and *(2.10)* can be written in the following form, using *(2.6)*,

and
$$
\left.
\begin{aligned}
\left(\frac{\partial}{\partial t} + (u+c)\frac{\partial}{\partial x}\right)J_+ &= 0 \\[2ex]
\left(\frac{\partial}{\partial t} + (u-c)\frac{\partial}{\partial x}\right)J_- &= 0 \; ,
\end{aligned}
\right\}
\qquad (2.24)
$$

where J_+ and J_- are the Riemann invariants

and
$$
\left.
\begin{aligned}
J_+ &= u + \int(dp/\rho c) \\[1ex]
J_- &= u - \int(dp/\rho c) \; .
\end{aligned}
\right\}
\qquad (2.25)
$$

From *(2.24)* it follows that J_+ and J_- remain constant along each characteristic, respectively

and
$$
\begin{aligned}
C_+ &= dx/dt = u+c \\
C_- &= dx/dt = u-c \; .
\end{aligned}
$$

The socalled characteristic directions are well-known quantities in discussing wave propagation as a result of hyperbolic differential equations. (Courant & Friedrichs, 1948).

If the waves travel from the left to the right into the undisturbed region indicated with subscript *o* we have on

a "left" characteristic C_-, with $u=0$

$$\int (dp/\rho c) = constant,$$

or with (2.6)

$$\int (dp/\rho c) = c_o \beta_o \, ln(\beta_o/\beta) = constant,$$

where we neglect β in comparison with unity and used, from (2.4) and (2.6)

$$c \approx c_o(\beta_o/\beta).$$

From the undisturbed region, where $\beta=\beta_o$, we find therefore

$$u - \int (dp/\rho c) = 0.$$

For a C_- characteristic we finally obtain

$$u = \int (dp/\rho c).$$

Using the results from a C_- characteristic the speed $u+c$ in the positive direction is found to be

$$u+c = \int (dp/\rho c) + c = c_o(1 + \frac{\beta_o - \beta}{\beta} + \beta_o ln\frac{\beta_o}{\beta}). \qquad (2.26)$$

From (2.26) it follows that any acoustic wave form will continually change. This can be seen as follows: the compressed part of the wave, $\beta<\beta_o$, travels faster than the expanding part, $\beta>\beta_o$.

We see from (2.26) that the excess in speed stems from two effects. The first,

$$c_o\frac{\beta_o - \beta}{\beta},$$

follows from the fact that the sound velocity is larger in the compressed part than in the expanding part. The second from a positive value of u in the compressed part and a negative one in the expanding part. From (2.26) we see that the latter effect is relatively unimportant in contrast with a simple wave in ordinary gas.

For a mixture the ratio between the first and the second effect is:

$$\frac{1}{\beta_o} \frac{\beta_o/\beta - 1}{ln(\beta_o/\beta)} \quad .$$

With β_o only a few percent the second effect, usually called the convective part, is unimportant. Then the change in wave form stems from the compression part. This process is called steepening by compression. As already mentioned this is in contrast with a simple wave in an ordinary gas. In that case the speed of the wave is, Lighthill (1956),

$$u+c = c_o(1 + \frac{c-c_o}{c_o} + \frac{2}{\gamma-1} \frac{c-c_o}{c_o}) \, ,$$

and the ratio between the compression part and the convective part becomes $(\gamma-1)/2$. From this we see that the steepening in an ordinary gas is governed by convection.

From gasdynamics it is known that this steepening eventually leads to the formation of a shock wave when the steepening is balanced by diffusion. Analogous with the theory for gases we may attempt to predict the structure of the shock and especially the shock thickness in a mixture of bubbles and liquid.

For weak shocks in gases the profile of the shock is a *tanh*, with argument equal to the running coordinate along the wave times the ratio of the excess in wave velocity and the dissipation coefficient resulting from shear viscosity, volume viscosity and heat conduction (see e.g. Lighthill, 1956). Using this for the mixture, we find that for a mean compression $(\beta_o-\beta_1)/2$, the excess in wave velocity becomes

$$c_o \frac{\beta_o-\beta_1}{2\beta_1} \, ,$$

where β_o is the gas volume fraction for the low pressure side and β_1 for the high pressure side.

Using (2.6) and (2.17) we find for the dissipation coefficient

$$(4\mu_l/3p_o)c_o^2 \simeq (4/3)(\nu_l/\beta_o) \, .$$

In terms of β the profile of the shock becomes

$$\beta = \frac{\beta_o + \beta_1}{2} - \frac{\beta_o - \beta_1}{2} \, tanh\,[-\frac{3}{8} \frac{c_o(\beta_o-\beta_1)\beta_o}{\beta_1 \nu_l}(x-Ut)]\,, \qquad (2.27)$$

where U is the velocity of the shock which is intermediate between $u+c$ before and behind the shock. So we find for U

$$U \simeq c_o(1 + \frac{\beta_o - \beta_1}{2\beta_1})\,.$$

This relation is also found later on where we discuss different types of steady shock waves.

(2.27) can be found by substitution of $(\partial/\partial t)=U(\partial/\partial x)$ in the equations (2.4), (2.9)-(2.11) and (2.14) when seeking a wave of steady form which propagates with velocity U. This solution is given by Van Wijngaarden (1970).

For an estimate of the shock thickness we use for completeness the total damping constant instead of the partial contribution $\delta_{vr}=(4\nu_l/\omega_B^! R_o^2)$. Using (1.8) and (2.6) the equation for the shock profile becomes:

$$\beta = \frac{\beta_o + \beta_1}{2} - \frac{\beta_o - \beta_1}{2} \, tanh\,[\frac{(3\gamma\beta_o)^{\frac{1}{2}}}{2R_o\delta}\frac{\beta_o}{\beta_1}(\frac{\beta_o}{\beta_1} - 1)(x-Ut)]\,. \qquad (2.28)$$

The thickness of the shock is defined as twice the value of $x-Ut$ for which the $tanh$ in (2.28) assumes the value $0,99$. The argument of the $tanh$, is about 3 in this case. So the thickness of the shock wave d becomes:

$$d \simeq 2\,\frac{R_o\delta}{(\beta_o)^{\frac{1}{2}}}\frac{\beta_1}{\beta_o-\beta_1}\,. \qquad (2.29)$$

Under the conditions for our experiments, with weak shocks, defined by $(\beta_o-\beta_1)/\beta_o=0(10^{-1})$, $\beta_o=0(10^{-2})$, $R_o=0(10^{-3}m)$ and $\delta=0(10^{-1})$, d is

$$d \sim 10^{-2}m\,.$$

If we assume that (2.29) also holds for moderate shocks with $(\beta_o-\beta_1)/\beta_o=0(1)$ and other quantities equal we find

for d

$$d \sim 10^{-3} m \quad .$$

In our experiments the measured thicknesses are of order $10^{-1} m$ and $10^{-2} m$ for weak and moderate shocks respectively. This suggests that shock waves in a bubbly fluid with $R_o \sim 10^{-3} m$ and $\beta_o \sim 10^{-2}$, are structured by a different mechanism. For this we introduce in the governing equation the inertia of the liquid near the bubble. This will be discussed in the following section.

§7. *WAVES INCLUDING THE INERTIA OF THE LIQUID NEAR THE BUBBLES.*

Again we start by discussing waves of small amplitude. For this we introduce the difference between p and p_g from *(1.6)* in the basic set of equations.

By linearization of the equations *(1.6)*, *(2.9)-(2.11)* and with $\delta=0$, we obtain

$$\frac{\partial^2 p}{\partial t^2} = c_o^2 \frac{\partial^2 p}{\partial x^2} + \frac{c_o^2}{(\omega_B)^2} \frac{\partial^4 p}{\partial x^2 \partial t^2} \quad , \qquad (2.30)$$

where c_o and ω_B are sound velocity and resonance frequency for isothermal circumstances.

Seeking solutions of *(2.30)* in the form of a progressive wave

$$p \propto exp\{i(kx-\omega t)\} \quad ,$$

we obtain by substituting this in the equation *(2.30)* a relation between ω and the wave number k. The relation is known as the dispersion equation (Van Wijngaarden, 1968),

$$\frac{\omega}{k} = \frac{c_o}{(1+k^2 c_o^2/\omega_B^2)^{\frac{1}{2}}} \quad ,$$

or

$$\frac{\omega}{k} = c_o \{1-(\frac{\omega}{\omega_B})^2\}^{\frac{1}{2}} \quad .$$

$$(2.31)$$

From this we see that the phase velocity ω/k depends on
the wave number and accordingly each wave travels with its
own velocity, which is large for small values of ω and be-
comes zero for $\omega \to \omega_B$. Only for long waves $(k \to 0)$ the wave
propagation is non-dispersive. Otherwise dispersion leads
to a continuous change of waves of general (non-sinusoidal)
form. This type of dispersion is usually called frequency
dispersion and its effect is a spreading of the wave. This
spreading can be altered by non-linear steepening.
For a dispersive system as represented by (2.31) the group
velocity $d\omega/dk$ is smaller than the phase velocity.
When dissipation, characterized by δ, is included in equation
(2.30) the dispersion relation becomes

$$\frac{\omega}{k} = c_o \left\{ 1 - (\frac{\omega}{\omega_B})^{\frac{1}{2}} - i(\gamma)^{\frac{1}{2}} \frac{\omega}{\omega_B} \delta \right\}^{\frac{1}{2}} , \qquad (2.32)$$

This equation is also given in van Wijngaarden (1972a),
who mentioned that (2.32) is identical with a similar rela-
tion following from scattering theory. Silberman (1957)
showed for this relation good agreement with experiments.
We therefore conclude that our approach of the hydrody-
namics of the mixture through a continuum theory is sup-
ported by these results.

§8. SHOCK WAVES IN A DISPERSIVE MEDIUM.

The non-linear or compression effect, discussed in §6, leads
to steepening of a given wave profile. This effect is also
called amplitude dispersion. Frequency dispersion however
leads to spreading of this profile. In the case of waves
with moderate amplitude, Van Wijngaarden (1968) showed that
the two effects can be combined in one hydrodynamic equa-
tion. For this we consider a pressure disturbance of mode-
rate strength propagating through the mixture at rest. In
the undisturbed state all quantities have the subscript o.
Moderate strength means in this case that we use an approxim-
ation one order beyond the linear approximation.

We take the effects following from non-linear steepening, dissipation and dispersion together, and write $p=p_o(1+\epsilon p')$, $\beta=\beta_o(1+\epsilon\beta')$, $p_g=p_o(1+\epsilon p_g')$, $u=\epsilon c_o\beta_o u'$, e.t.c. with ϵ a small quantity. This is introduced in the equations (1.6), (2.1) and $(2.9)-(2.11)$. Terms of order ϵ^2 and lower are retained, terms however of order $\epsilon^2\beta_o$ are discarded. We omit further details, for this the reader is referred to the Appendix 2, and give directly, dropping the primes, for a wave propagating in positive direction:

$$\frac{\partial p}{\partial t} + c_o\frac{\partial p}{\partial x} + \epsilon c_o p\frac{\partial p}{\partial x} + \frac{c_o^3}{2\omega_B^2}\frac{\partial^3 p}{\partial x^3} - \frac{(\gamma)^{\frac{1}{2}}c_o^2\delta}{2\omega_B}\frac{\partial^2 p}{\partial x^2} = 0 \ . \qquad (2.33)$$

In (2.33) c_o^3/ω_B^2 and $c_o^2\delta/\omega_B$ are small quantities. For $\epsilon=0, \delta=0$ and $\omega_B\to\infty$ we have an acoustic wave again. When $\delta=0$ we have an equation of the type of the Korteweg-De Vries equation describing the propagation of long gravity waves on liquid of finite depth. Van Wijngaarden (1968) discussed this equation for a mixture of gas bubbles and liquid, where we have

$$\frac{\partial p}{\partial t} + c_o\frac{\partial p}{\partial x} + \epsilon c_o p\frac{\partial p}{\partial x} + \frac{c_o^3}{2\omega_B^2}\frac{\partial^3 p}{\partial x^3} = 0 \ . \qquad (2.34)$$

The third and the fourth term represent amplitude and frequency dispersion respectively. Solutions in which both tendencies balance each other are well known. One of these solutions is the solitary wave on which we come back in the following chapter. We are interested in shock wave type of solutions of (2.33). Solutions starting at a given pressure level and asymptotically reaching a higher pressure. Without frequency dispersion we have the case as discussed in one of the foregoing sections: Solutions where non-linear steepening is balanced by diffusion. As mentioned this leads to a shock thickness which is an order of magnitude too small in comparison with experimental results for both weak and moderate shocks. On the other hand, neglecting

diffusion, no steady shock wave solutions of *(2.34)* are
known (Van Wijngaarden, 1972a). However, several investi-
gators showed that in the case of water waves unsteady
solutions in the form of a bore, or shock wave as given in
Figure 2, appear in finite time intervals. Here the model
equation without dissipation $(\delta=0)$ is *(2.34)*.
Peregrine (1966) presented numerical solutions, but whether
or not these solutions become steady for t tending to infi-
nity was not shown. Benjamin e.a. (1972) proved that for
any finite time the equation has a solution with the cha-
racter as shown in Figure 2. However the existence of a
steady profile was not proven.
Steady solutions representing shock waves following from
the balance of non-linear steepening and frequency dis-
persion can not be expected therefore from *(2.34)*.
Looking for steady solutions in the form of a shock wave
we return to the equation *(2.33)* with $\delta\neq0$. This equation,
a combination of the Korteweg-De Vries equation and Burger's
equation (Lick, 1970) has solutions of the type of a shock
wave. Several investigators such as Grad & Hu (1967),
Johnson (1970) and Pfrisch & Sudan (1971) discussed an
equation of the type of *(2.33)*.They showed the existence
of steady shock-like solutions of the Korteweg-De Vries
equation with dissipation.

§*9. CONCLUSIONS.*

In this chapter we considered wave propagation through a
mixture of bubbles and liquid. The mixture was considered
as a continuum and we used results following from conti-
nuum mechanics. The various contributions of the liquid
and the gas phase were accounted for. Especially the bubble
behaviour of the gas phase and the associated radial motion
of the liquid near the bubbles are important for investi-
gation of waves of high frequencies. This motion leads to
socalled frequency dispersion. Another important effect
associated with wave propagation in mixtures is, that the

steepening of the wave is governed by compression in stead of convection.

We found in contrast to what happens in gases, that shock waves in liquid-bubble mixtures can be structured by the three mechanisms, steepening by compression, frequency dispersion and dissipation associated with radial motion. In the next chapter we discuss a steady shock wave following from these effects.

CHAPTER 3.

STRUCTURE OF A STEADY SHOCK WAVE WHEN THE SPEED OF THE GAS
PHASE EQUALS THE SPEED OF THE LIQUID.

§1. *INTRODUCTION.*

In this chapter we look at steady shock waves structured
by non-linear steepening, dispersion and dissipation. To
get a first insight in the overall character of the shock
structure, we neglect relative translational motion of the
gas phase with respect to the liquid. For our experimental
circumstances this is unrealistic as will be shown later
on. However, the analysis of this chapter suits to serve
the discussion of some general properties of shock waves
in liquid-bubble mixtures.
Equations already discussed by various investigators such
as Ackeret (1930), Campbell & Pitcher (1958) and Parkin e.a.
(1961), relating quantities far in front and far behind
the shock, are derived. Investigations of Crespo (1969),
Noordzij (1971) and Van Wijngaarden (1972b) on the struc-
ture of the shock are summarized.
To compare this theory with the experiments, parameters
describing the shock structure are derived.

§2. *BASIC EQUATIONS.*

We consider time dependent flow in x direction of a liquid-
bubble mixture. The mixture velocity averaged over a small
volume yet containing many bubbles is u. The mixture den-
sity is ρ. The contribution by the gas phase to ρ can be
safely neglected. ρ is therefore related to the liquid
density ρ_l and the gas volume fraction β by

$$\rho = \rho_l (1-\beta) , \qquad (3.1)$$

with $\beta \ll 1$.
The equation of mass conservation for the mixture is,

$$\frac{\partial \rho}{\partial t} + \frac{\partial}{\partial x}(\rho u) = 0 \; . \tag{3.2}$$

The equation of conservation of the number density n is

$$\frac{\partial n}{\partial t} + \frac{\partial}{\partial x}(nu) = 0 \; . \tag{3.3}$$

The equation of motion for the mixture is

$$\frac{du}{dt} = -\frac{1}{\rho}\frac{\partial p}{\partial x} \; . \tag{3.4}$$

The pressure in the bubble p_g and the local pressure in the liquid p are related through

$$p_g - p = \rho_l \left\{ R \frac{d^2 R}{dt^2} + \frac{3}{2}(\frac{dR}{dt})^2 + \delta \omega_B' R \frac{dR}{dt} \right\} \; . \tag{3.5}$$

Assuming that the bubbles are spherical and have locally all the same radius R, we have

$$\beta = \frac{4}{3} \pi n R^3 \; . \tag{3.6}$$

Using the fact that the mass of the bubble, $\rho_g V$, is an invariant and for isothermal circumstances also $p_g V$, (3.3) can also be written as

$$\frac{\partial}{\partial t}(p_g \beta) + \frac{\partial}{\partial x}(p_g \beta u) = 0 \; . \tag{3.7}$$

From (3.2) and (3.7) we find

$$\frac{d}{dt}\left(\frac{p_g \beta}{1-\beta}\right) = 0 \; . \tag{3.8}$$

In the following section we summarize the steady equations describing relations between quantities far in front and far behind the shock, the socalled Hugoniot relations.

§3. THE HUGONIOT RELATIONS.

We briefly summarize the known results and derive expressions which are used throughout this thesis for describing shocks.

We consider a shock wave moving with constant speed U in negative x direction. The situation is illustrated in Figure 6.
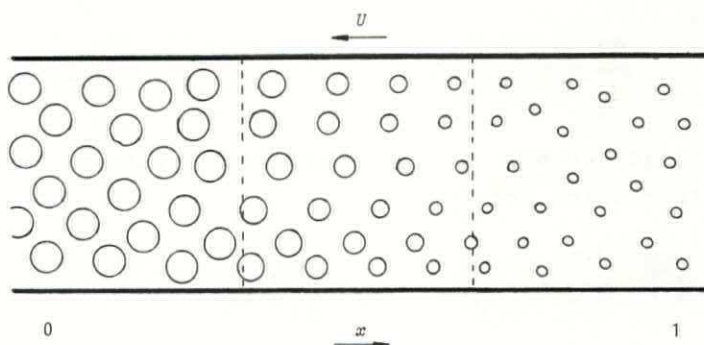
FIGURE 6. Shock wave in a mixture, travelling with speed U from $x=\infty$ (side 1) to $x=-\infty$ (side 0).

The equations $(3.1)-(3.8)$ are written in independent variables x and t. We transform these into x',t, where $x'=x+Ut$. In the new frame the shock wave is steady and so $(\partial/\partial t)_{x'}$ is zero. Carrying out this transformation on (3.2), we obtain, omitting the prime on x',

$$\frac{\partial}{\partial x}\left(\rho_l(1-\beta)(U+u)\right) = 0 . \tag{3.9}$$

Integration gives

$$\rho_l(1-\beta_o) \, U = \rho_l(1-\beta)(U+u_1) , \tag{3.10}$$

where upstream quantities are indicated with o and downstream quantities with 1.

Transformation and integration of the equation of motion, using mass conservation, gives

$$\rho_l(1-\beta_o)U^2 + p_o = \rho_l(1-\beta_1)(U+u_1)^2 + p_1 . \qquad (3.11)$$

In addition we deal with an energy equation for the mixture and accordingly two new variables are introduced: the temperature of the liquid and that of the gas. Relative to the huge heat capacity of the liquid, the temperature rise of the liquid through the shock is small. This was already suggested by Ackeret (1930) and proved by Campbell and Pitcher (1958).
We briefly summarize the results of Campbell & Pitcher. For this we introduce the exact expression for the density of the mixture

$$\rho = \rho_l(1-\beta) + \rho_g\beta ,$$

and from the equation of state for a perfect gas we find, using the expression for ρ

$$\frac{p}{T} \beta \left\{ \frac{1}{\rho-\rho_l(1-\beta)} \right\} = constant , \qquad (3.12)$$

with T the temperature of the gas which was assumed to be equal to the liquid temperature.
We introduce the small quantity ϕ

$$\phi = \frac{\beta\rho_g}{\rho_l(1-\beta)} , \qquad (3.13)$$

where $\beta\rho_g$ in the denominator is neglected with respect to $\rho_l(1-\beta)$. Now we rewrite (3.12). From (2.3) it follows that ϕ is constant. With (3.13), (3.12) yields

$$\frac{p_o}{T_o} \left\{ \frac{1+\phi}{\rho_o} - \frac{1}{\rho_l} \right\} = \frac{p_1}{T_1} \left\{ \frac{1+\phi}{\rho_1} - \frac{1}{\rho_l} \right\} . \qquad (3.14)$$

The energy relation, which equates the work done on a unit mass of the mixture to the increase of its internal and kinetic energies, states that

$$\frac{p_o}{\rho_o} + \left(\frac{h}{1+\phi}\right)T_o + \frac{1}{2}U^2 = \frac{p_1}{\rho_1} + \left(\frac{h}{1+\phi}\right)T_1 + \frac{1}{2}(U+u_1)^2 , \qquad (3.15)$$

with $h=h_l+\phi h_{vg}$. h_l is the specific heat of the liquid and h_{vg} is the specific heat of the gas at constant density. From (3.7)-(3.10) we find for the temperature rise $\Delta T=T_1-T_o$ across the shock, assuming $\Delta T/T_o<<1$

$$\Delta T = \frac{(p_1/p_o)^2-1}{2p_1/p_o} \frac{\beta_o \rho_{go}}{\rho_l} \frac{K_g T_o}{h_l} , \qquad (3.16)$$

where K_g is the gas constant, h is replaced by h_l and ϕ is neglected with respect to unity.

For our experimental circumstances (3.16) yields

$$\Delta T < 10^{-2} \ ^0C .$$

As Campbell & Pitcher indicated, the expressions relating pressure, density and velocity on the two sides of the shock assume a simple form when ΔT is neglected and the sacrifice of accuracy in the process is very small indeed.

From (3.5) it follows that far in front and far behind the shock the pressure in the bubble equals the pressure in the liquid. (3.8) therefore gives a relation between the pressure in the liquid and the gas volume fraction, far in front and far behind the shock

$$\frac{p_o \beta_o}{1-\beta_o} = \frac{p_1 \beta_1}{1-\beta_1} . \qquad (3.17)$$

In the course of the analysis we will use besides β, also the mass concentration. That is the volume of gas in a unit mass of the mixture and is denoted by α/ρ_l. The relation between α and β is

$$\alpha = \frac{\beta}{1-\beta} \quad . \tag{3.18}$$

From $(3.10), (3.11), (3.17)$ and (3.18) the following relations are derived:

for u_1

$$\frac{u_1}{U} = \frac{\alpha_1 - \alpha_o}{1 + \alpha_o} = -\frac{\alpha_o}{1 + \alpha_o} \left\{ 1 - p_o \frac{(1 + \alpha_o)^2}{\rho_l \alpha_o U^2} \right\} \quad , \tag{3.19}$$

for the pressure ratio p_1/p_o

$$\frac{p_1}{p_o} = \frac{\rho_l U^2 \alpha_o}{p_o (1 + \alpha_o)^2} \quad . \tag{3.20}$$

Using

$$c_o^2 = \frac{p_o}{\rho_l \beta_o (1 - \beta_o)} \quad ,$$

or in terms of α:

$$c_o^2 = \frac{p_o}{\rho_l \alpha_o} (1 + \alpha_o)^2 \tag{3.21}$$

we find for the Machnumber M_o, defined as the ratio between the shock speed U and the sound velocity in the undisturbed state c_o, from (3.20) and (3.21)

$$M_o^2 \equiv \frac{U^2}{c_o^2} = \frac{p_1}{p_o} \quad , \tag{3.22}$$

or with (3.17) and (3.18)

$$M_o^2 = \frac{\alpha_o}{\alpha_1} \quad . \tag{3.23}$$

(Note that from (3.22) and (3.23) we get for weak shocks

$$U = c_o \left(1 + \frac{\alpha_o - \alpha_1}{2\alpha_1} \right) \quad ,$$

giving the excess wave velocity as found in chapter 2, §5).
Now we consider the entropy change across the shock. Since
a shock wave is a spontaneous process, any change in entropy
of a unit mass of the mixture on crossing the shock is an
increase. Therefore the temperature rise across the shock
cannot be neglected.

The entropy change follows from integration of

$$dS = \frac{h_l}{T} dT - \left(\frac{\partial}{\partial T}(1/\rho_g)\right)_p dp \quad,$$

where the contribution of the gas phase to h is neglected.
With $p = \rho_g K_g T$, (3.16) and (3.22) the entropy change ΔS
becomes

$$\Delta S = \frac{\beta_o p_o}{\rho_l T_o} \left(\frac{M_o^4 - 1}{2M_o^2} - lnM_o^2\right) . \tag{3.24}$$

This is a positive quantity for $M_o > 1$.

The relations derived so far do not deal with the interior
of the shock. In the next section the equation describing
the interior region of the shock will be derived.

§4. *THE EQUATION DESCRIBING THE STRUCTURE OF THE SHOCK.*

Again we consider a shock wave propagating at constant speed
U in negative x direction. We use the transformation given
in §3 of this chapter.

Carrying out this transformation on (3.2), we find

$$\frac{\partial}{\partial x}\left\{\rho_l(1-\beta)(U+u)\right\} = 0 .$$

Integration gives, upstream condition indicated with o,

$$\rho_l(1-\beta)(U+u) = \rho_l(1-\beta_o) U \quad . \tag{3.25}$$

Integration of the equation of motion gives, with (3.2)

$$\rho_l(1-\beta)(U+u)^2 + p = \rho_l(1-\beta_o) U^2 + p_o . \tag{3.26}$$

Substitution of *(3.25)* into *(3.26)* gives with *(3.18)*, *(3.22)* and c_o from *(3.21)*

$$\frac{p}{p_o} - 1 = M_o^2\left(1 - \frac{\alpha}{\alpha_o}\right) \ . \tag{3.27}$$

For describing the structure of the shock as a function of the running coördinate we eliminate either α or p from *(3.27)*. This can be done by using the relation between p_g and p as given by *(3.5)*. To this end we integrate *(3.8)* and find, with *(3.18)*

$$p_g\alpha = p_o\alpha_o \ . \tag{3.28}$$

We express R in terms of α and use *(3.28)*, this yields

$$\frac{p_g}{p_o} = \frac{R_o^3}{R^3} = \frac{\alpha_o}{\alpha} \ . \tag{3.29}$$

(3.5) becomes with *(3.29)*

$$p_g - p = \frac{\rho_l R_o^2}{3}\left(\frac{\alpha_o}{\alpha}\right)^{\frac{1}{3}}\left[\frac{d^2}{dt^2}\left(\frac{\alpha}{\alpha_o}\right) - \frac{1}{6}\frac{\alpha_o}{\alpha}\left\{\frac{d}{dt}\left(\frac{\alpha}{\alpha_o}\right)\right\}^2 + \right.$$

$$\left. \delta\omega_B' \frac{d}{dt}\left(\frac{\alpha}{\alpha_o}\right)\right] \ . \tag{3.30}$$

From transformation of *(3.30)*, taking $(\partial/\partial t)_x$, zero and omitting the primes, we obtain with $y = (\alpha/\alpha_o)$

$$p_g - p = \frac{\rho_l R_o^2}{3}\left(\frac{1}{y}\right)^{\frac{1}{3}} U^2\left[\{1+2\alpha_o(y-1)\}\frac{d^2y}{dx^2} - \frac{1+2\alpha_o(1-2y)}{6y}\left(\frac{dy}{dx}\right)^2 + \right.$$

$$\left. \frac{\delta\omega_B'}{U}\{1+\alpha_o(y-1)\}\frac{dy}{dx}\right] \ . \tag{3.31}$$

In *(3.31)* we neglect terms with coefficients of $0(\alpha_o^2)$ and higher between the square brackets.
Substitution of p from *(3.31)* in *(3.27)*, elimination of p_g through *(3.28)*, using c_o^2 as given by *(3.21)* and M_o^2 as

given by *(3.22)*, finally yields

$$y^{\frac{2}{3}}\left[(1+2\alpha_o y)\frac{d^2y}{d\eta^2} - \frac{1-4\alpha_o y}{6y}\left(\frac{dy}{d\eta}\right)^2 + \delta^\Delta\left\{1+\alpha_o(y+1)\right\}\frac{dy}{d\eta}\right] +$$

$$(1-y)(y-M_o^{-2}) = 0 \ , \quad (3.32)$$

where $\eta=x(3\alpha)^{\frac{1}{2}}/R_o$ and $\delta^\Delta=\delta\omega_B'R_o/U(3\alpha_o)^{\frac{1}{2}}$.
In deriving *(3.32)* terms with coefficients of $O(\alpha_o^2)$ and
higher between the square brackets were neglected.
Taking into account that for our experimental circumstances
$y = 1$ at maximum, $\alpha_o=O(10^{-2})$ and $\delta^\Delta=O(10^{-1})$, *(3.32)*
reduces to

$$y^{\frac{2}{3}}\left[\frac{d^2y}{d\eta^2} - \frac{1}{6y}\left(\frac{dy}{d\eta}\right)^2 + \delta^\Delta\frac{dy}{d\eta}\right] + (1-y)(y-M_o^{-2}) = 0 \ . \quad (3.33)$$

From *(3.33)* or *(3.32)* the structure of the shock can be
derived in terms of $y=\alpha/\alpha_o$ or, with help of *(3.27)*, in
terms of the pressure ratio p/p_o.

§5. *THE STRUCTURE OF THE SHOCK.*

We investigate the structure of the shock as described by
(3.32) or *(3.33)*. Different features of the structure are
already known. Crespo (1969) presented numerical solutions
of the full set of equations. He found for the shock struc-
ture an exponential steepening at the front part and waves
at the back side, as schemetically shown in Figure 7.
Crespo did not present explicit expressions for the shock
thickness d and the wave length Λ as illustrated in Figure 7.
Van Wijngaarden (1970, 1972b) and Noordzij (1971) discus-
sed a simplified version of *(3.33)*. Shock thickness d and
wave length Λ were estimated. A reasonable agreement with
experimentally obtained results was found. Van Wijngaarden
(1970) considered the following simplified version of *(3.33)*

$$\frac{d^2y}{d\eta^2} + \delta_{vr}^{\Delta} \frac{dy}{d\eta} + (1-y)(y-M_o^{-2}) = 0, \qquad (3.34)$$

where only the viscous contribution to δ^{Δ} was considered. Non-linear derivatives are left out of account because the outskirts of the shock were discussed. This equation describes the balance of dispersion and non-linear steepening by compression. These are respectively the first and the third term of (3.34). Some dissipation is needed for a steady shock.
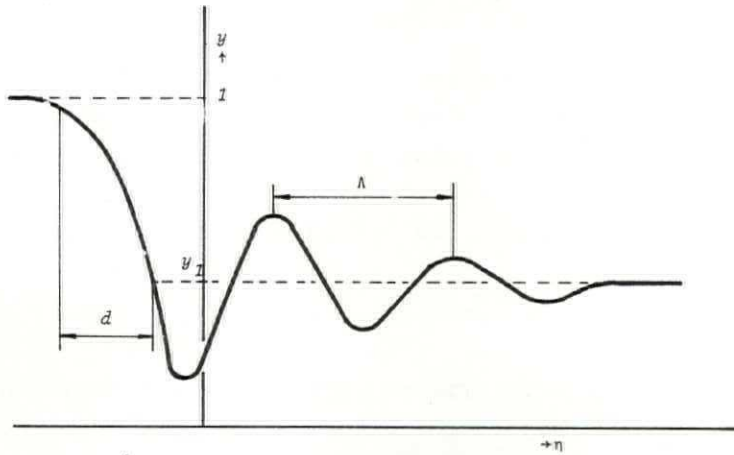
FIGURE 7. In this Figure the profile of the shock is illustrated in terms of y as a function of η.

When dispersion is left out of account in (3.34) a solution in the form of a $tanh$, as discussed in chapter 2, is found. The thickness of the shock is found to be of order

$$\frac{R_o \delta_{vr}^{\Delta}}{(\alpha_o)^{\frac{1}{2}}} \frac{1}{P_{1/p_o}-1} \qquad (3.35)$$

This model for the shock wave, even in the case of δ^{Δ} instead of δ_{vr}^{Δ}, only holds for very small bubbles. This follows from the following reasoning. During the passage of the shock a bubble is compressed to a smaller radius. The time required for this is of order ω_B^{-1}. On the other hand the time of passage of a shock with thickness d is of order d/c_o.

Hence we have $(d/c_o)>\omega_B^{-1}$ or using *(1.3)* and *(3.21)*

$$d > \frac{R_o}{(\delta_o)^{\frac{1}{2}}}$$ *(3.36)*

Only for bubbles much smaller than in our experiments, *(3.35)* exceeds d from *(3.36)*.

If we omit the dissipation term in *(3.34)* we obtain

$$\frac{d^2y}{d\eta^2} + (1-y)(y-M_o^{-2}) = 0 \quad .$$ *(3.37)*

This equation has the form to which the Korteweg - De Vries equation, as discussed in chapter 2, reduces when we look for steady solutions. The solution of *(3.37)* becomes

$$y = 1 - \frac{3}{2}(1-M_o^{-2}) \; sech^2\left(\eta(1-M_o^{-2})^{\frac{1}{2}}/2\right) \; ,$$ *(3.38)*

the well-known solitary wave, which is no shock wave type solution.

Now we consider the outskirts of *(3.34)*, closely following the analysis of Van Wijngaarden (1970).

From linearization of *(3.34)* for y near *1* we obtain

$$1 - y \; \propto \; exp\left[-\delta_{vr}^{\Delta}\eta/2 \; + \; \eta\{\delta_{vr}^{\Delta 2}/4 \; + \; (1-M_o^{-2})\}^{\frac{1}{2}}\right] \; .$$ *(3.39)*

For our experiments, with $\delta_{vr}^{\Delta}=O(10^{-1})$ and $M_o^2-1>10^{-1}$ this means that the front part of the shock is mainly determined by the balance of non-linear steepening and dispersion. Van Wijngaarden approximated the shock thickness, on the basis of *(3.39)*, by

$$\frac{constant}{(1-M_o^{-2})^{\frac{1}{2}}} \; ,$$ *(3.40)*

or in dimensional form

$$\frac{R_o}{(3\alpha_o)^{\frac{1}{2}}} \frac{constant}{(1-M_o^{-2})^{\frac{1}{2}}} \quad .$$ *(3.41)*

Noordzij (1971) presented, using this approximation, an estimate for the *constant*. This was done as follows, see Figure 8:

The solution for y from (3.39) which is only valid near $y=1$, was continued up till $y=y_1$.
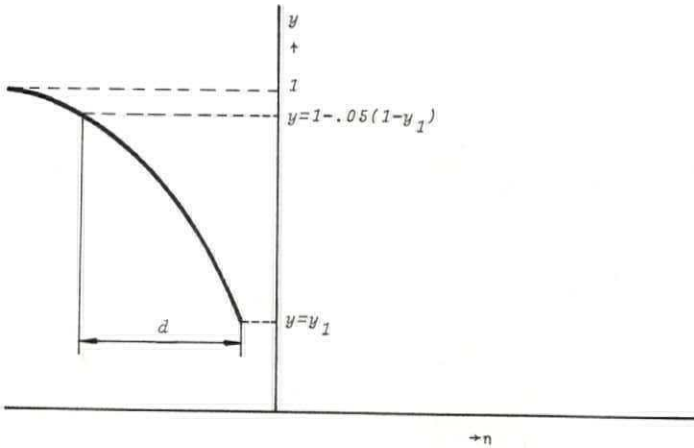
FIGURE 8. The construction of the shock thickness d.

When we define d as the distance between the points where $y=y_1$ and, of course arbitrary, $y=1-.05(1-y_1)$, we obtain

$$d = \frac{R_o}{(3\alpha_o)^{\frac{1}{2}}} \frac{\ln 20}{(1-M_o^{-2})^{\frac{1}{2}}} \ . \qquad (3.42)$$

This estimate was in good agreement with the experiments reported by Noordzij (1971) and Van Wijngaarden (1972b). Another estimate for the shock thickness can be found, Noordzij (1971), from an investigation of an equation of the type of (3.34) by Johnson (1970). Johnson showed that the front part of the shock closely follows the asymptotic solution for $\delta_{vr}^{\Delta} \to 0$. This solution is the solitary wave as given by (3.38). Again defining d as the distance between the points where $y=y_1$ and $y=1-.05(1-y_1)$, we obtain for the shock thickness d :

$$d = \frac{R_o}{(3\alpha_o)^{\frac{1}{2}}} \frac{2.7}{(1-M_o^{-2})^{\frac{1}{2}}} \cdot \qquad (3.43)$$

This is illustrated in Figure 9.
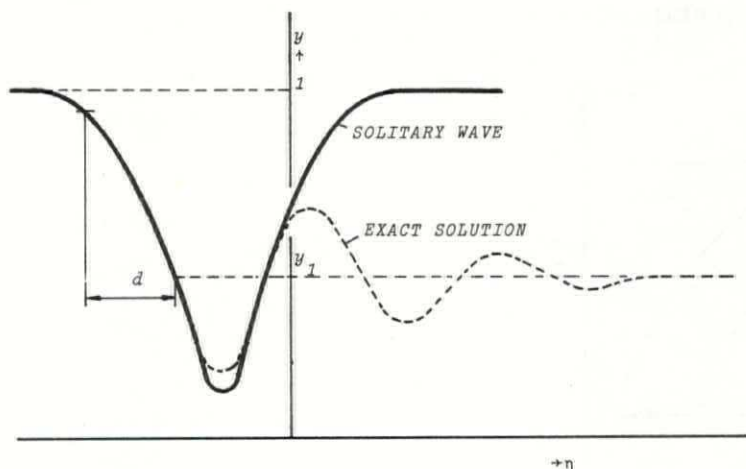
FIGURE 9. Estimate of the shock thickness from the solitary wave.

d from (3.43) is also in good agreement with the experi-
mental results in Noordzij (1971), considering the ob-
tained experimental accuracy of about 10%.
For weak shocks the dissipation term becomes important.
From a perturbation of the solitary wave (Johnson, 1970),
a rather complicated expression arises including δ_o^Δ.
However, linearization near the front part leads to a
simple expression for the modified shock thickness

$$d = \frac{R_o}{(3\alpha_o)^{\frac{1}{2}}} \frac{\ell n 20}{(1-M_o^{-2})^{\frac{1}{2}} - \delta_o^\Delta/2} \cdot \qquad (3.44)$$

In this thesis we therefore base the discussion of the
shock structure on the method of analysing the outskirts.
The choice of the latter approximation method is also based
on the fact that we want to find out the influence of α_o
and non-linear effects on both the shock thickness and at
the back side of the shock later on.

So far we discussed a linearized version of *(3.32)*. Now we pay attention to the equations *(3.32)* and *(3.33)* because we want to investigate the influence of the quantities $(1+2\alpha_o)$ and $y^{2/3}$.

From linearization of *(3.32)* near the front part of the shock, the shock thickness is found to be

$$d = \frac{R_o}{(3\alpha_o)^{1/2}} \frac{(1+\alpha_o)\,ln20}{(1-M_o^{-2})^{1/2} - \delta_o^{\Delta}/2} \quad . \tag{3.45}$$

In our experiments, $\alpha = O(10^{-2})$ and d reduces to *(3.44)*. Therefore we discuss further details of the shock structure from *(3.33)*.

We summarize the results for the back side of the shock. As shown in Figure 7, waves appear at the back side of the shock. They have the equilibrium value $y=y_1=M_o^{-2}$, which follows fróm *(3.33)* with disappearing derivatives for $\eta\to\infty$. To analyse the back side of the shock we linearize *(3.33)* for y near y_1 and obtain for $y-M_o^{-2}$

$$y - M_o^{-2} \propto exp\left[-\eta\delta_1^{\Delta}/2 + \eta\left\{(\delta_1^{\Delta})^2/4 - (1-M_o^{-2})M_o^{4/3}\right\}^{1/2}\right], \tag{3.46}$$

with $\delta_1^{\Delta}=\delta_o^{\Delta}M_o^{-4/3}$.

From this expression some important features are obtained. When $(\delta_1^{\Delta}/2)>>(1-M_o^{-2})^{1/2}$, *(3.46)* reduces to

$$y - M_o^{-2} \propto exp\left[-\eta\frac{(1-M_o^{-2})M_o^{4/3}}{\delta_1^{\Delta}}\right] \quad . \tag{3.47}$$

This also results from the expression for a profile where dissipation balances compression as shown in chapter 2 by equation *(2.28)*. However for most of our experiments

$$(\delta_1^{\Delta})^2/4 << 1-M_o^{-2} \quad ,$$

and the expression under the square root in *(3.46)* is negative. Waves appear at the back side of the shock.

This wavy behaviour was experimentally verified in Noordzij (1971) and Van Wijngaarden (1972b).
The associated wave length Λ becomes

$$\Lambda = \frac{R_o}{(3\alpha_o)^{\frac{1}{2}}} \frac{2\pi M_o^{\frac{1}{3}}}{(M_o^2-1)^{\frac{1}{2}}} \quad . \tag{3.48}$$

From this we find a frequency $\omega = 2\pi U/\Lambda$. Inserting Λ from (3.48) and using (3.21) and the relation $U^2/c_o^2 = p_1/p_o$, we can write ω as

$$\omega = \frac{1}{R_1} \left\{ \frac{3p_1(1-{}^\alpha 1/\alpha_o)}{\rho_l} \right\}^{\frac{1}{2}} \quad .$$

The expression for ω_B at the high pressure side (c.f. 1.3) is

$$\omega_B = \frac{1}{R_1} \left(\frac{3p_1}{\rho_l} \right)^{\frac{1}{2}} \quad .$$

ω becomes with this

$$\omega = \omega_B (1-{}^\alpha 1/\alpha_o)^{\frac{1}{2}} \quad .$$

For weak shocks ω is always rather below ω_B. For strong shocks, ${}^\alpha o/\alpha_1 \to \infty$, ω approaches ω_B and wave propagation is no longer possible as follows from the discussion in §7 of chapter 2.
The damping of the waves is found from the factor

$$exp\left[-\frac{\delta_1^\Delta}{2} \frac{(3\alpha_o)^{\frac{1}{2}}}{R_o} \right] \quad . \tag{3.49}$$

Van Wijngaarden (1970) showed similar equations as (3.48) and (3.49) with δ_{vr}^Δ instead of δ_1^Δ. This leads to a too small amount of attenuation of the waves behind the shock. Crespo (1969), who also found a relation for the wave length, introduced a too large amount of attenuation, because he suggested heat conduction in the liquid near the bubble

to be the leading mechanism.

Noordzij (1971) showed that the contribution of δ^Δ to attenuation was large enough to account for the damping observed in his experiments.

To facilitate the experiments we introduce the number of waves, N, in which the amplitude decreases by a factor e^{-1}, say. From (3.48) and (3.49) we find for this number

$$N = \frac{1}{\pi} \frac{(M_o^2-1)^{\frac{1}{2}}}{M_o^{\frac{1}{3}} \delta_1^\Delta} \quad . \tag{3.50}$$

Before summarizing some conclusions on the shock wave relations we present in the following section relations resulting from adiabatic theory.

§6. THE ADIABATIC RELATIONS FOR THE SHOCK.

As already mentioned the gas phase in our experiments does not behave isothermal. We therefore derive the pertinent expressions for adiabatic circumstances. First we pay attention to the Hugoniot relations.

In §2 of this chapter we found that when the bubbles move with the liquid the mass of the gas in a unit mass of the mixture is constant:

$$\frac{d}{dt}\left\{\frac{\rho_g \beta}{\rho_l(1-\beta)}\right\} = 0 \quad . \tag{3.51}$$

Using the adiabatic relation, $p_g \propto \rho_g^\gamma$, (3.51) yields

$$p_g\left(\frac{\beta}{1-\beta}\right)^\gamma = \text{constant} \quad , \tag{3.52}$$

or $\qquad p_g \alpha^\gamma = \text{constant} \quad . \tag{3.53}$

From (3.53) we find the relation for the isentropic sound speed c_{ad}, with $p_g \rightarrow p$,

$$c_{ad}^2 = dp/d\rho = \gamma p_o(1+\alpha_o)^2/\rho_l \alpha_o \quad , \tag{3.54}$$

and the speed of sound in the adiabatic theory exceeds the isothermal speed of sound by a factor $(\gamma)^{\frac{1}{2}}$.

From (3.53) it follows that the relation between the pressure and α far in front and far behind the shock becomes

$$p_o \alpha_o{}^\gamma = p_1 \alpha_1{}^\gamma \quad . \tag{3.55}$$

For a steady flow field the transition relations concerning mass and momentum are

$$\rho_l (1-\beta_o) \, U = \rho_l (1-\beta_1)(U+u_1) \quad , \tag{3.56}$$

and

$$\rho_l (1-\beta_o) \, U^2 + p_o = \rho_l (1-\beta_1)(U+u_1)^2 + p_1 \quad . \tag{3.57}$$

From (3.55)-(3.57) we find:

for u_1

$$\frac{u_1}{U} = -\frac{\alpha_o}{1+\alpha_o} \left\{ 1 - \left(\frac{p_o}{p_1} \right)^{1/\gamma} (1+\alpha_o) \right\} \quad , \tag{3.58}$$

for the pressure ratio p_1/p_o

$$\frac{p_1/p_o - 1}{1 - \left(p_o/p_1 \right)^\gamma} = \frac{\rho_l U^2 \alpha_o}{p_o (1+\alpha_o)^2} \quad . \tag{3.59}$$

In terms of the Machnumber $M_o = U/c_o$, where c_o is defined by (3.21), (3.59) is rewritten as

$$M_o^2 = \frac{p_1/p_o - 1}{1 - \left(p_o/p_1 \right)^{1/\gamma}} \quad , \tag{3.60}$$

or

$$M_o^2 = \frac{\left(\alpha_o/\alpha_1 \right)^\gamma - 1}{1 - \alpha_1/\alpha_o} \quad . \tag{3.61}$$

Besides the conservation of mass and momentum we have an energy equation. When the gas phase follows the isentropic

law, the temperature rise across the shock can simply be deduced for a given pressure ratio. If we assume no temperature rise for the liquid there will be no increase of entropy across the shock. However a shock is a spontaneous process and we therefore expect ΔS to be larger than zero. The energy equation for the mixture becomes

$$\frac{h_l}{1+\phi} T_{l1} + \frac{\phi h_{vg}}{1+\phi} T_{g1} + \frac{1}{2}(U+u_1)^2 + \frac{p_1}{\rho_1} =$$

$$\frac{h_l}{1+\phi} T_{lo} + \frac{\phi h_{vg}}{1+\phi} T_{go} + \frac{1}{2} U^2 + \frac{p_o}{\rho_o} \quad , \tag{3.62}$$

with $T_{lo}=T_{go}$.

Using the relation $T_{g1}=T_{go}\left(p_1/p_o\right)^{1-1/\gamma}$ we find from (3.14), (3.56) and (3.62) for the temperature increase $\Delta T=T_{l1}-T_{lo}$

$$\Delta T = \frac{p_o \phi}{\rho_{go} 2 h_l} \left\{\frac{p_1}{p_o}+1\right\} \left\{1-\left(\frac{p_o}{p_1}\right)^{1/\gamma}\right\} . \tag{3.63}$$

Using ϕ defined by (3.13), ΔT becomes

$$\Delta T = \frac{\beta_o p_o}{2\rho_l h_l} \left\{\frac{p_1}{p_o}+1\right\} \left\{1-\left(\frac{p_o}{p_1}\right)^{1/\gamma}\right\} . \tag{3.64}$$

This is again a negligible quantity.
The increase in entropy is

$$\Delta S = \frac{h_l}{1+\phi} \ln(\frac{T_{l1}}{T_{lo}}) . \tag{3.65}$$

With $\Delta T/T_{lo}<<1$, (3.65) changes into

$$\Delta S = \frac{\beta_o p_o}{2\rho_l T_{lo}} \left\{\frac{p_1}{p_o}+1\right\} \left\{1-\left(\frac{p_o}{p_1}\right)^{1/\gamma}\right\} , \tag{3.66}$$

where ϕ is neglected with respect to unity.

With the adiabatic relations known, we describe the shock structure.

For a steady shock we find from the momentum equation

$$M_o^2(1-y) = p/p_o - 1 \quad . \tag{3.67}$$

Substitution of p from (3.31), the relation between p and p_g, in (3.67), using (3.53) and the expression for c_o^2 as given by (3.21), equation (3.67) finally yields

$$y^{\frac{2}{3}} \left[(1+2\alpha_o y) \frac{d^2 y}{d\eta^2} - \frac{1-4\alpha_o y}{6y} \left(\frac{dy}{d\eta} \right)^2 + \delta^{\Delta} \left\{ 1+\alpha_o(y+1) \right\} \frac{dy}{d\eta} \right] +$$

$$y(1-y) + M_o^{-2} y(1-y^{-\gamma}) = 0 \quad . \tag{3.68}$$

An estimate for the shock thickness is found from linearization of (3.68) near $y=1$. The differential equation for $1-y=y'(<<1)$ is

$$\frac{d^2 y'}{d\eta^2} + \delta_o^{\Delta} \frac{dy'}{d\eta} - y'(1-\gamma M_o^{-2}) = 0 \quad , \tag{3.69}$$

where α_o is neglected with respect to unity.
The shock thickness is

$$d = \frac{R_o}{(3\alpha_o)^{\frac{1}{2}}} \frac{\ln 20}{(1-\gamma M_o^{-2})^{\frac{1}{2}} - \delta_o^{\Delta}/2} \quad . \tag{3.70}$$

Linearization of (3.68) at the back side of the shock, for y is near y_1, yields, using (3.61),

$$\frac{d^2 y''}{d\eta^2} + \delta_1^{\Delta} \frac{dy''}{d\eta} + \frac{y''}{y_1^{\frac{2}{3}}} (\gamma M_o^{-2} y_1^{-\gamma} - y_1) = 0 \quad , \tag{3.71}$$

with $y-y_1=y''(<<1)$.

From (3.71) a wavy behaviour appears for $y-y_1$ with wave length Λ_{ad}

$$\Lambda_{ad} = \frac{R_o}{(3\alpha_o)^{\frac{1}{2}}} \frac{2\pi y_1^{\frac{1}{3}}}{(\gamma M_o^{-2} y_1^{-\gamma} - y_1)^{\frac{1}{2}}} \; . \tag{3.72}$$

The number of waves, N, in which the amplitude of these waves decreases by a factor e^{-1}, is

$$N = \frac{(\gamma M_o^{-2} y_1^{-\gamma} - y_1)^{\frac{1}{2}}}{\pi \delta_1^\Delta y_1^{\frac{1}{3}}} \; . \tag{3.73}$$

§7. CONCLUSIONS.

As suggested at the end of chapter 2 we found in this chapter a shock wave structured by compression, dispersion and dissipation. The front part of the shock is mainly determined by the balance of compression and dispersion. Only for very weak shocks dissipation becomes important. However for weak shocks another mechanism needs to be included as we will see in the following chapters. At the back side of the shock waves appear, which are damped in 10 wave lengths at most.

We conclude further that for strong shocks, $M_o^2 \to \infty$, the frequency of the waves approaches the resonant frequency of the bubbles ω_B. From the analysis of chapter 2 it follows that these waves are no longer possible. Other effects such as breaking up of the bubbles become important. However this type of shocks are beyond the scope of this thesis.

In this chapter we discussed shock waves in mixtures where the bubbles are assumed to move with the liquid everywhere. In terms of the equation of motion of a bubble (1.17) this means that the viscosity of the liquid is very high. For our experiments this is unrealistic. We therefore discuss in the following chapter the other extreme, where the bubble translation with respect to the liquid is not resisted by a viscous force.

CHAPTER 4.[⊗]

STRUCTURE OF A STEADY SHOCK WAVE IN THE CASE WHERE THE
BUBBLE TRANSLATION WITH RESPECT TO THE LIQUID IS NOT
RESISTED BY VISCOSITY.

§1. *INTRODUCTION*.

We now include the relative translational velocity of the
bubble in the discussion of steady shock waves. The extreme,
where the bubble velocity is not resisted by viscosity,
is considered.
From the equations of motion describing this flow, diffe-
rent important expressions are derived such as sound velo-
city, etc. From the governing equations it will appear that
the shock structure is completely similar to the structure
as found in the foregoing chapter. However, the structure
will be based on an other sound velocity and consequently
on an other Machnumber. When the gas volume fraction is
sufficiently small, $\beta_o = 0(10^{-2})$, there is practically no dif-
ference between the relations derived in this and those of
the foregoing chapter.
We derive Hugoniot relations, shock thickness, etc. At the
end of this chapter the corresponding adiabatic relations
are summarized.

§2. *EQUATIONS OF MOTION INCLUDING RELATIVE TRANSLATIONAL*
VELOCITY OF THE BUBBLE.

In this section some already known relations are repeated
for convenience. We consider time dependent flow in x
direction. The liquid velocity, averaged over a small volume
of the mixture containing many bubbles, is u, the gas velo-
city v and the mixture density is ρ.
The density is found from

$$\rho = \rho_l (1-\beta) . \qquad (4.1)$$

⊗

Parts of the results of this chapter and the following chapters will
be published in Noordzij & Van Wijngaarden (1973).

The concentration by mass, α/ρ_l, is given by

$$\alpha = \frac{\beta}{1-\beta} \; .$$ (4.2)

Now we include relative translational velocity $v-u$ in the governing equations.

As described in chapter 1 we adopt Levich's model for the bubble translation. Darwin (1953) showed that in potential flow of a sphere through a liquid at rest, a mass of liquid is displaced equal to the virtual or hydrodynamic mass, $\rho_l V/2$, of the sphere. V is the volume of the sphere. This is sometimes called drift (Darwin). The liquid displacement is in the direction of the sphere's motion. We will understand by u the liquid velocity which locally exists at large distance from a bubble.

The number of bubbles passing through a surface at right angles with u and moving with u is $n(v-u)$. Therefore the displaced mass is, using Darwin's results, $\rho_l Vn(v-u)/2$, or with (2.1),

$$\rho_l \beta(v-u)/2 \; .$$ (4.3)

Therefore the equation of mass conservation becomes,

$$\frac{\partial \rho}{\partial t} + \frac{\partial}{\partial x}\left\{\rho u + \rho_l \beta(v-u)/2\right\} = 0 \; .$$ (4.4)

The equation of conservation of the number density n is

$$\frac{\partial n}{\partial t} + \frac{\partial}{\partial x}(nv) = 0 \; .$$ (4.5)

Associated with the motion of the bubble in potential flow, each bubble represents an impulse, as defined by Kelvin (Lamb 1932, §119), relative to the liquid of magnitude

$$\rho_l V(v-u)/2 \; .$$

The number of bubbles passing through a unit surface at rest, normal to the flow, is nv. The associated Kelvin impulse is, (Van Wijngaarden, 1970),

$$\rho_l \beta(v-u) \ .$$

The momentum equation for the mixture is, including this Kelvin impulse,

$$\frac{\partial}{\partial t}\left\{\rho u + \rho_l \beta(v-u)/2\right\} + \frac{\partial}{\partial x}\left\{p + \rho u^2 + \rho_l \beta v(v-u)/2\right\} = 0 \ . \qquad (4.6)$$

The equation describing unresisted bubble translation is found from $(1.1\overset{b}{?})$ with $\mu_l = 0$,

$$\frac{1}{2}\rho_l \frac{d}{dt}V(v-u) = -V\frac{\partial p}{\partial x} \ . \qquad (4.7)$$

The equation relating the pressure in the bubble to the pressure in the liquid is

$$p_g - p = \rho_l\left\{R\frac{D^2 R}{Dt^2} + \frac{3}{2}(\frac{DR}{Dt})^2 + \delta\omega_B'R\frac{DR}{Dt}\right\} , \qquad (4.8)$$

with

$$\frac{D}{Dt} = \frac{\partial}{\partial t} + v\frac{\partial}{\partial x} \ .$$

The effect of relative translational motion in (4.8) is neglected. This would give an extra term of order $\rho_l(v-u)^2$ which can be ignored as shown in chapter 1.
In the following section we derive equations relating the quantities far in front and far behind the shock.

§3. THE HUGONIOT RELATIONS.

We consider a shock wave moving with constant speed in negative x direction. The equations $(4.1)-(4.8)$ are transformed from the x,t frame into the x',t frame, with $x'=x+Ut$.

In this new frame the shock is assumed to be steady and therefore $(\partial/\partial t)_x$, is zero. Transformation of (4.4) and (4.6) and integration of the resulting relations gives: for the mass conservation

$$\rho_l(1-\beta_o)U = \rho_l(1-\beta_1)(U+u_1) + \rho_l\beta_1(v_1-u_1)/2 \qquad (4.9)$$

for the momentum equation

$$p_o + \rho_l(1-\beta_o)U^2 = p_1 + \rho_l(1-\beta_1)(U+u_1)^2 +$$

$$\rho_l\beta_1U(v_1-u_1) . \qquad (4.10)$$

The constant of integration follows from the assumption $v=u=0$ ahead of the shock $(x \to -\infty)$. Because we have $u_1/U = 0(\beta_o)$, it follows from (4.6) and (4.7) that $(v_1-u_1)/U = 0(\beta_o)$. We will use approximate forms of the equations, in which terms of order β_o^3 are left out of account. Therefore $U+v_1$ is taken equal to U in the third term of the right-hand side of (4.10).

Transformation and integration of (4.5) gives, using the constancy of mass of a bubble,

$$\beta\rho_g(U+v) = \beta_o\rho_{go}U . \qquad (4.11)$$

Using the isothermal relation $p_g \propto \rho_g$, (4.11) yields

$$\frac{p_g}{p_o} = \frac{\beta_o}{\beta} \frac{U}{U+u}\left(1 - \frac{v-u}{U}\right) + 0(\alpha^2) . \qquad (4.12)$$

Considering the order of approximation in (4.12), $U/(U+u)$ can be replaced through $(1-\beta)/(1-\beta_o)$ as can be seen from (4.9). Then, with (4.2), (4.12) becomes

$$\frac{p_g}{p_o} = \frac{\alpha_o}{\alpha}\left(1 - \frac{v-u}{U}\right) . \qquad (4.13)$$

Using (4.13), the pressure ratio p_1/p_o is,

$$\frac{p_1}{p_o} = \frac{\alpha_o}{\alpha_1}\left\{1 - \frac{v_1 - u_1}{U}\right\} . \tag{4.14}$$

An expression for the relative velocity $v-u$ is found from transformation and integration of (4.7). First we formulate (4.7) in terms of β. With (4.5), (4.7) yields

$$\frac{D}{Dt}\left\{\beta(v-u)\right\} = -\frac{2\beta}{\rho_l}\frac{\partial p}{\partial x} - \beta(v-u)\frac{\partial v}{\partial x} . \tag{4.15}$$

Substitution of $\partial p/\partial x$ from (4.6) into (4.15), transformation and integration finally gives, with help of (4.1) and (4.4),

$$\frac{v_1 - u_1}{U} = \alpha_o \frac{\alpha_o}{\alpha_1}\left\{\left(\frac{\alpha_1}{\alpha_o}\right)^2 - 1\right\} . \tag{4.16}$$

p_1/p_o from (4.14) changes with (4.16) into

$$\frac{p_1}{p_o} = \frac{\alpha_o}{\alpha_1} - \alpha_o\left\{1 - \left(\frac{\alpha_o}{\alpha_1}\right)^2\right\} . \tag{4.17}$$

This relation indicates the difference with the case where the bubbles move with the liquid. In the latter case the pressure ratio is found to be

$$\frac{p_1}{p_o} = \frac{\alpha_o}{\alpha_1} .$$

With $\alpha_o = 0(10^{-2})$, the difference between this and p_1/p_o from (4.17) is small.
Substitution of (4.9) into (4.10) gives

$$\frac{p_1}{p_o} - 1 = \frac{\alpha_o \rho_l U^2}{p_o(1+\alpha_o)^2}\left(1 - \frac{\alpha_1}{\alpha_o}\right) . \tag{4.18}$$

Using the definition of M_o^2 from (3.22) we find from (4.18)

and *(3.20)*

$$\frac{p_1}{p_o} = 1 + M_o^2\left(1 - \frac{\alpha_1}{\alpha_o}\right) \quad,$$

or with *(4.17)*

$$M_o^2 = \frac{p_1}{p_o} + \alpha_o\left(\frac{p_1}{p_o} + 1\right) \quad. \qquad (4.19)$$

So far we did not introduce the sound velocity in the re-
lations between quantities far in front and far behind the
shock. For later purposes we derive the sound velocity for
a mixture in which the bubble is free to move with respect
to the liquid.

§4. *THE SOUND VELOCITY.*

The sound velocity for a mixture in which bubble motion is
not resisted by viscosity, is given by Crespo (1969). This
velocity, c_f, is

$$c_f^2 = \frac{p_o}{\rho_l \alpha_o}(1+4\alpha_o) \quad, \qquad (4.20)$$

or

$$c_f^2 = c_o^2(1+2\alpha_o) \quad. \qquad (4.21)$$

The relation for c_o is found from an equation of state.
(chapter 2). We investigate whether such an equation can
be derived for the unresisted case.
First we derive the relation for c_f in a steady frame of
motion. From $p_g = p$, *(4.13)* and *(4.16)*, omitting subscript *1*,
we obtain for p

$$\frac{p}{p_o} = \frac{\alpha_o}{\alpha}\left[1 - \alpha_o\frac{\alpha_o}{\alpha}\left\{\left(\frac{\alpha}{\alpha_o}\right)^2 - 1\right\}\right] \quad. \qquad (4.22)$$

$(\alpha_o - \alpha)/\alpha$ is assumed to be small with respect to unity in
the case of acoustical wave propagation.
With $c_f^2 \equiv (dp/d\rho)$ and $\alpha \to \alpha_o$, we find from *(4.22)*

$$c_f^2 = c_o^2 (1+2\alpha_o) . \qquad (4.23)$$

The speed of sound c_f in a mixture, in which relative motion is not resisted by viscous forces, is larger by a factor $1+\alpha_o$ or $1+\beta_o$ than in a mixture in which the bubbles move with the liquid. The physical reason is that due to relative motion the gas concentration is locally less than it would have been with bubbles moving with the liquid. This gives the mixture a greater stiffness and accordingly a higher sound velocity.

Secondly, for small disturbances, an equation for c_f can be derived from instationary theory. From (4.5) we find, using $p_g=p$, the homogeneous theory,

$$\frac{d}{dt}(p\beta) + p\beta \frac{\partial u}{\partial x} + \frac{\partial}{\partial x}(p\beta(v-u)) = 0 . \qquad (4.24)$$

Note that

$$\frac{d}{dt} = \frac{\partial}{\partial t} + u \frac{\partial}{\partial x} . \qquad (4.25)$$

(4.4) changes, with help of (4.25), into

$$\frac{d}{dt}(1-\beta) + (1-\beta)\frac{\partial u}{\partial x} + \frac{1}{2} \frac{\partial}{\partial x}(\beta(v-u)) = 0 . \qquad (4.26)$$

From a combination of (4.24) and (4.26) we find

$$\frac{d}{dt}(p\beta) - \frac{p\beta}{1-\beta} \frac{d}{dt}(1-\beta) + \frac{\partial}{\partial x}(p\beta(v-u)) -$$

$$\frac{p\beta}{2(1-\beta)} \frac{\partial}{\partial x}(\beta(v-u)) = 0 . \qquad (4.27)$$

In the following we omit the last term in the left-hand side of (4.27), which is $O(\beta)$ times the third term. From (4.5) and (4.25), (4.7) becomes

$$\frac{1}{2} \rho_l \frac{d}{dt} \left(\beta (v-u) \right) = - \beta \frac{\partial p}{\partial x} . \tag{4.28}$$

(4.6) becomes

$$\rho_l (1-\beta)\frac{du}{dt} + \frac{1}{2} \rho_l \frac{d}{dt} \left(\beta (v-u) \right) = - \frac{\partial p}{\partial x} . \tag{4.29}$$

Combination of (4.28) and (4.29) gives

$$\frac{d}{dt} \left(\beta (v-u) \right) = 2\beta \frac{du}{dt} . \tag{4.30}$$

Using the fact that small quantities are considered, (4.30) can be integrated to

$$\beta (v-u) = 2\beta u ,$$

or

$$p\beta (v-u) = 2p\beta u . \tag{4.31}$$

From substitution of (4.31) into (4.27), we obtain

$$\frac{d}{dt}(p\beta) - \frac{p\beta}{1-\beta} \frac{d}{dt}(1-\beta) + \frac{\partial}{\partial x}(2p\beta u) = 0 . \tag{4.32}$$

When small disturbances are considered, (4.26) reduces to

$$\frac{d\beta}{dt} = (1-\beta)\frac{\partial u}{\partial x} ,$$

or

$$\frac{2p\beta}{1-\beta} \frac{d\beta}{dt} = \frac{\partial}{\partial x}(2p\beta u) . \tag{4.33}$$

Substitution of (4.33) into (4.32) finally yields

$$\frac{d}{dt} \left\{ ln \left(\frac{p\beta}{\rho_l (1-\beta)^3} \right) \right\} = 0 ,$$

or
$$\frac{p\beta}{\rho_l(1-\beta)^3} = constant \ . \tag{4.34}$$

From this we find for the sound velocity c_f,

$$c_f^2 = \frac{p}{\rho_l \beta(1-\beta)}(1+2\beta) \ . \tag{4.35}$$

Using $\alpha=\beta/(1-\beta)$, (4.35) changes into (4.20). A simple relation between p and β, as given by (4.34), could not be found for the general case.

Now we return to the Hugoniot relations as given in §2. Defining $M_f^2 \equiv U^2/c_f^2$, we find for the relation between M_f and M_o, using (4.2) and (4.35),

$$M_f^2 = (1-2\alpha_o)M_o^2 \ . \tag{4.36}$$

With (4.36), (4.19) becomes

$$M_f^2 = \frac{p_1}{p_o}\left\{1-\alpha_o(1-\frac{p_o}{p_1})\right\} \ . \tag{4.37}$$

For a given pressure ratio p_1/p_o and given α_o, (4.19) or (4.37) specifies the speed of propagation of the wave. Note that for values of p_1/p_o near unity, (4.37) reduces to

$$\frac{U^2}{c_f^2} = \frac{p_1}{p_o} \ .$$

Comparison with $(U/c_o)^2 = p_1/p_o$ shows that weak shock waves propagate at a velocity near c_f, when relative motion is not resisted by friction, and at a velocity near c_o when resisted.

§5. *THE EQUATIONS DESCRIBING THE STRUCTURE OF THE SHOCK.*

We consider a shock wave which propagates at constant speed U in negative x direction. Transformation of equation (4.4)

from the x,t into the x',t frame yields, omitting the prime on x',

$$\frac{\partial}{\partial x}\left\{\rho_l(1-\beta)(U+u) + \rho_l\beta(v-u)/2\right\} = 0 \ . \tag{4.38}$$

Integration gives, upstream quantities indicated with subscript o

$$\rho_l(1-\beta)(U+u) + \rho_l\beta(v-u)/2 = \rho_l(1-\beta_o)U \ . \tag{4.39}$$

This equation can be written down directly by formulating the constancy of mass flow in the moving frame of reference. The complication, caused by relative motion, makes a formal derivation useful. The shock induced velocity u is, as follows from (4.39),

$$u = \frac{\beta-\beta_o}{1-\beta} U - \frac{\beta}{2(1-\beta)}(v-u) \ .$$

Here the use of α as defined by (4.2) gives a simpler expression. u becomes

$$u = \beta_o U\left(\frac{\alpha}{\alpha_o} -1\right) - \alpha(v-u)/2 \ . \tag{4.40}$$

The momentum gained by mass flow $\rho_l(1-\beta_o)U$ during the passage of the shock is, at station x, $\rho_l(1-\beta_o)Uu$. The Kelvin impulse of the bubbles, to order β^3, is $\rho_l\beta U(v-u)$. Whence the momentum equation is

$$p_o = p + \rho_l(1-\beta_o)Uu + \rho_l\beta U(v-u)/2 \ . \tag{4.41}$$

This equation results also from a transformation in x',t of equation (4.6) thereby using (4.39). (Writing down the equation of conservation of momentum directly, one might be inclined to put

$$\frac{d}{dx}\left\{ p + \rho_l(1-\beta)(U+u)^2 + \rho_l \beta U(v-u)/2 \right\} = 0 \,,$$

counting $\rho_l(1-\beta)(U+u)^2$ as the momentum of the mean flow and adding the Kelvin impulse. This is erroneous because the mass flow in the moving frame is not $\rho_l(1-\beta)(U+u)$ but larger than this by $\rho_l \beta(v-u)/2$.
The correct form is

$$\frac{d}{dx}\left\{ p + \rho_l(1-\beta)(U+u)^2 + \rho_l \beta U(v-u) \right\} = 0 \,,$$

from which (4.41) follows upon using (4.39)).
Substitution of (4.40) into (4.41) gives, with help of (4.2), (3.20) and (3.22),

$$\frac{p}{p_o} - 1 = M_o^2(1-y) \,, \tag{4.42}$$

where $y=\alpha/\alpha_o$.
In order to find the shock structure we eliminate p or y from (4.42). For this we use (4.13) and the relation between p_g and p from (4.8). First we transform (4.8). From the isothermal relation $p_g V=p_o V_o$ and (4.13) it follows that

$$\frac{R^3}{R_o^3} = \frac{V}{V_o} = y\left(1+ \frac{v-u}{U}\right) \,. \tag{4.43}$$

Using (4.43), the transformation of DR/Dt from (4.8) gives

$$\frac{DR}{Dt} \rightarrow \frac{R(U+v)}{3} \frac{V_o}{V} \frac{d}{dx}\left[\frac{\alpha}{\alpha_o}\left(1- \frac{v-u}{U}\right)\right] + O(\alpha^3) \,. \tag{4.44}$$

For estimating the order of approximation the derivative d/dx is replaced by $(\alpha_o/R_o^2)^{\frac{1}{2}}$, which is connected with the length scale on which pertinent quantities change, as found in the foregoing chapter. Substitution of p from (4.8) in (4.22), using (4.13) and the relation for M_o^2, equation (4.42)

finally yields, omitting non-linear derivatives such as $(dy/d\eta)^2$,

$$y^{\frac{2}{3}}\left[(1+4\alpha_o y)\frac{d^2 y}{d\eta^2} + \delta^\Delta \frac{dy}{d\eta}\right] + (1-y)(y-M_o^{-2}) +$$

$$M_o^{-2}\frac{v-u}{U} = 0 , \qquad (4.45)$$

with $\eta=x(3\alpha_o)^{\frac{1}{2}}/R_o$.

In (4.45) we presented an approximative term including $y(v-u)/U$. Actually the term would appear to be more complicated. However, we discuss the shock structure with help of an analysis of the outskirts. Therefore the approximation does not sacrify the accuracy.

From (4.16) it follows that

$$y(v-u)/U = \alpha_o(y^2-1) . \qquad (4.46)$$

For M_o^{-2} we obtain, using (4.17) and (4.19)

$$M_o^{-2} = y_1 - \alpha_o(1+y_1), \qquad (4.47)$$

where $y_1 = \alpha_1/\alpha_o$.

With (4.46) and (4.47), (4.45) yields

$$y^{\frac{2}{3}}\left[(1+4\alpha_o y)\frac{d^2 y}{d\eta^2} + \delta^\Delta \frac{dy}{d\eta}\right] = \frac{(1-y)(y_1-y)(y+\alpha_o)}{y} . \qquad (4.48)$$

This second order differential equation describes the shock structure in the case where bubble translation is not resisted by viscous forces. This equation differs only slightly from (3.33) because the factor $(y+\alpha_o)/y$ does not make much difference in the region of interest, $y_1 \geq y \geq 1$. The features of the solution of (4.45) are the same as those of (3.33): a sharp decrease of y from 1 to y_1, followed by damped oscillations around $y=y_1$.

Again from linearization near the outskirts of the shock, the structure will be determined. For the front part we

linearize *(4.48)* near $y=1$ and look for solutions which disappear for $\eta \to -\infty$. With $y=1-y'$ and $y'<<1$, *(4.48)* changes into

$$(1+4\alpha_o)\frac{d^2y'}{d\eta^2} + \delta_o^\Delta\frac{dy'}{d\eta} - y'(1-y_1)(1+\alpha_o) = 0 \;, \qquad (4.49)$$

or with *(4.36)* and *(4.46)*

$$(1+4\alpha_o)\frac{d^2y'}{d\eta^2} + \delta_o^\Delta\frac{dy'}{d\eta} - y'(1-M_f^{-2}) = 0 \;. \qquad (4.50)$$

From this we obtain for y

$$1-y \propto exp\left[\left\{-\frac{\delta_o^\Delta}{2} + \frac{(1-M_f^{-2})^{\frac{1}{2}}}{1+2\alpha_o}\right\}\eta\right]. \qquad (4.51)$$

Accordingly in the expression for the shock thickness as given by *(3.42)*, M_f will enter in the place of M_o. However, the difference between these expressions for the shock thickness (the one with M_o^{-2} and the one with M_f^{-2}) is within the error of the experimentally obtained values. The shock thickness becomes

$$d_A = \frac{R_o}{(3\alpha_o)^{\frac{1}{2}}}\frac{(1+2\alpha_o)ln20}{(1-M_f^{-2})^{\frac{1}{2}}-\delta_o^\Delta/2} \approx \frac{R_o}{(3\alpha_o)^{\frac{1}{2}}}\frac{ln20}{(1-M_o^{-2})^{\frac{1}{2}}-\delta_o^\Delta/2} \;, \qquad (4.52)$$

with $M_o^2 = p_1/p_o$.
The front part of the shock follows from a balance of dispersion and compression.
For the back side of the shock we linearize *(4.48)* with respect to the small quantity $y-y_1$ and find for y

$$y-y_1 \propto exp\left(-\frac{\delta_1^\Delta\eta}{2}\right) exp\left[\pm i\eta\left\{\frac{(1-y_1)(y_1+\alpha_o)}{y_1^3(1+4\alpha_o y_1)}\right\}^{\frac{1}{2}}\right]. \qquad (4.53)$$

The wave length Λ_A is found to be

$$\Lambda_A = \frac{2\pi R_o}{(3\alpha_o)^{\frac{1}{2}}} \frac{(1+2\alpha_o y_1)y_1^{\frac{1}{3}}}{[1-M_f^{-2}+\alpha_o(1-y_1)^2/y_1]^{\frac{1}{2}}} . \tag{4.54}$$

Within the experimental error, Λ_A is

$$\Lambda_A = \frac{R_o}{(3\alpha_o)^{\frac{1}{2}}} \frac{2\pi M_o^{\frac{1}{3}}}{(M_o^2-1)^{\frac{1}{2}}} . \tag{4.55}$$

This is equal to the wave length derived in the foregoing chapter.

The number of waves, N, in which the amplitude decreases by a factor e^{-1} is, using (4.53) and (4.54),

$$N = \frac{(M_o^2-1)^{\frac{1}{2}}}{\pi \delta_1^{\Delta} M_o^{\frac{1}{3}}} . \tag{4.56}$$

In all our experiments, this quantity is smaller than 10. With shock thickness, wave length and attenuation of the waves known, we are able to describe the shocks. These shocks are called S_A shocks. A pressure recording of the shock profile is shown in Figure 10.
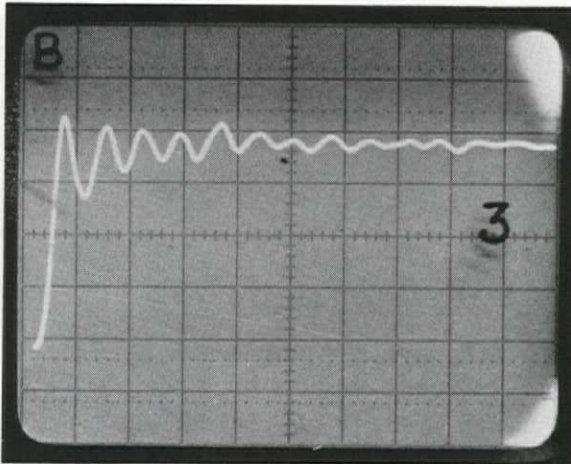
FIGURE 10. A pressure recording typical for flow with unresisted bubble velocity. A S_A shock.

§6. *THE ADIABATIC RELATIONS FOR THE SHOCK.*

From *(4.11)* and the relation $p_g \propto \rho_g^\gamma$ we find for the relation between the pressure in the bubble and the pressure far in front of the shock

$$\frac{p_g}{p_o} = \left(\frac{\alpha_o}{\alpha}\right)^\gamma \left(1-\gamma \frac{v-u}{U}\right) . \tag{4.57}$$

The relation for *(v-u)/U* is

$$y(v-u)/U = \alpha_o(y^2-1) . \tag{4.58}$$

For the homogeneous theory with $p \to p_g$, we find from *(4.57)* and *(4.58)* for the sound velocity c_{fad}

$$c_{fad}^2 = \frac{\gamma p_o}{\rho_l \alpha_o}(1+4\alpha_o) , \tag{4.59}$$

or $\qquad c_{fad}^2 = \gamma c_f^2 = \gamma(1+2\alpha_o)c_o^2 . \tag{4.60}$

For a steady flow field the relations concerning mass and momentum are

$$\rho_l(1-\beta_o)U = \rho_l(1-\beta_1)(U+u_1) + \rho_l\beta_1(v_1-u_1)/2 , \tag{4.61}$$

and

$$p_o + \rho_l(1-\beta_o)U^2 = p_1 + \rho_l(1-\beta_1)(U+u_1)^2 +$$

$$\rho_l\beta_1 U(v_1-u_1) . \tag{4.62}$$

The pressure ratio across the shock, p_1/p_o, becomes

$$\frac{p_1}{p_o} = \left(\frac{\alpha_o}{\alpha_1}\right)^\gamma \left(1-\gamma \frac{v_1-u_1}{U}\right) . \tag{4.63}$$

Using *(4.58)*, p_1/p_o is

$$\frac{p_1}{p_o} = \left(\frac{\alpha_o}{\alpha_1}\right)^\gamma \left\{1-\gamma\alpha_o\left(\frac{\alpha_1}{\alpha_o} - \frac{\alpha_o}{\alpha_1}\right)\right\} . \tag{4.64}$$

From (4.61) and (4.62) we find for the pressure ratio

$$\frac{p_1}{p_o} - 1 = \frac{\rho_l\alpha_o U^2}{p_o(1+\alpha_o)}\left(1- \frac{\alpha_1}{\alpha_o}\right) . \tag{4.65}$$

With help of (4.64) the ratio α_o/α_1 becomes

$$\frac{\alpha_o}{\alpha_1} = \left(\frac{p_1}{p_o}\right)^{1/\gamma} + \alpha_o\left\{1-\left(\frac{p_1}{p_o}\right)^{2/\gamma}\right\} . \tag{4.66}$$

Substitution of α_o/α_1 into (4.65) gives, using $M_o \equiv U/c_o$,

$$M_o^2 = \frac{p_1/p_o-1}{1-\left(p_o/p_1\right)^{1/\gamma}}\left[1+\alpha_o\left\{1+\left(\frac{p_o}{p_1}\right)^{1/\gamma}\right\}\right]. \tag{4.67}$$

For convenience we summarize some other relations between M_o^2, $y_1 = \alpha_1/\alpha_o$ and p_1/p_o :

$$\frac{p_1}{p_o} = y_1^{-\gamma}\left\{1+\gamma\frac{\alpha_o}{y_1}(1-y_1^2)\right\} , \tag{4.68}$$

$$M_o^2 = \frac{y_1^{-\gamma}-1}{1-y_1} + \gamma\alpha_o(1+y_1)/y_1^{(\gamma+1)} . \tag{4.69}$$

With help of the foregoing relations the structure of the shock can be described.

For a steady shock wave we have, from the momentum equation

$$\frac{p}{p_o} -1 = M_o^2(1-y) . \tag{4.70}$$

Substitution of p, from (4.8), the relation describing the volume oscillations of the bubble, into (4.68), using (4.57) and (4.58) finally yields

$$y^{\frac{2}{3}} \left[(1+4\alpha_o y)\frac{d^2 y}{d\eta^2} + \delta^\Delta \frac{dy}{d\eta} \right] + y(1-y) + y(1-y^{-\gamma})M_o^{-2} +$$

$$\gamma\alpha_o y^{-\gamma}(y^2-1)M_o^{-2} = 0 \quad . \qquad (4.71)$$

From linearization near the front part we find for the shock thickness, using $M_{fad}^{-2}=(1+2\alpha_o)\gamma M_o^{-2}$,

$$d_A = \frac{R_o}{(3\alpha_o)^{\frac{1}{2}}} \frac{(1+2\alpha_o)\ln 20}{(1-M_{fad}^{-2})^{\frac{1}{2}} - \delta_o^\Delta/2} \quad . \qquad (4.72)$$

Within the experimental error d_A becomes

$$d_A = \frac{R_o}{(3\alpha_o)^{\frac{1}{2}}} \frac{\ln 20}{(1-\gamma M_o^{-2})^{\frac{1}{2}} - \delta_o^\Delta/2} \quad . \qquad (4.73)$$

In (4.73) M_o^2 is defined through (3.60).
Within the experimental error the relations for Λ and N are identical to (3.72) and (3.73) respectively.

§7. CONCLUSIONS.

In this chapter we discussed shock waves, socalled S_A shocks, in mixtures where bubble translational velocity is not resisted by viscous forces. A shock profile is found, practically identical to that found in chapter 3: a steep front followed by damped waves at the back side. We did not compute the temperature rise and entropy change across the shock. The relations (3.16) and (3.24) are hardly affected by relative velocity.

In this and the foregoing chapter we analysed shock structures for two extreme circumstances. The first extreme is that the bubbles move with the liquid. This means that the viscosity is assumed to be very large. The other extreme is based on a negligibly small viscosity. Bubble velocity differs from the liquid velocity.

In the following chapter we discuss the more realistic case where initially generated relative translation is ultimately resisted by viscous forces.

CHAPTER 5.

STRUCTURE OF A STEADY SHOCK WAVE WHEN THE SPEED OF THE GAS
PHASE ULTIMATELY EQUALS THE SPEED OF THE LIQUID.

§1. *INTRODUCTION.*

In this chapter we discuss steady shock waves with ultimately
zero relative translational velocity of the bubble. So the
relations between quantities far in front and far behind the
shock, the Hugoniot relations, are equal to those discussed
in chapter 3. However, the shock structure will be signi-
ficantly modified by viscous effects associated with relative
motion. A typical profile is shown in Figure 11.
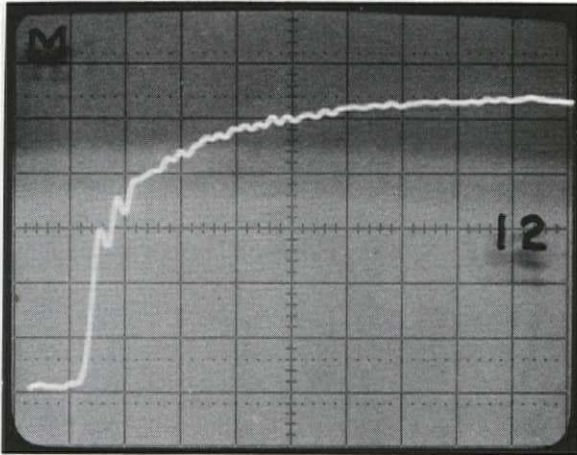
FIGURE 11. A pressure recording typical for flow with resisted
bubble velocity. A S_B shock.

The shock structure, as shown in Figure 11, depends on both
the gas volume fraction and the pressure ratio. Below a
critical value of the pressure ratio, the steep front of the
S_B shock disappears. The pressure profile is almost entirely
smooth. This we call a S_C shock.
In this chapter we summarize the Hugoniot relations. From
the equations of motion, including viscous forces, the rela-
tions which determine the shock structure are derived. At

the end of this chapter the corresponding adiabatic relations are summarized.

§2. *EQUATIONS OF MOTION.*

Most of the equations were already derived in the foregoing chapters. For convenience we briefly summarize the known relations. Furthermore we include viscosity in the equation of motion of a bubble.

We consider time dependent flow. The liquid velocity is u and the gas velocity is v. Both quantities averaged over a small volume of the mixture containing many bubbles. The density of the mixture is defined by

$$\rho = \rho_l (1-\beta), \qquad (5.1)$$

and the mass concentration, α/ρ_l, by

$$\alpha = \frac{\beta}{1-\beta} . \qquad (5.2)$$

The relation between β and the bubble radius R is

$$\beta = \frac{4}{3} \pi n R^3 . \qquad (5.3)$$

In the mixture the equation of mass conservation is, including drift effects (chapter 4),

$$\frac{\partial \rho}{\partial t} + \frac{\partial}{\partial x} \{\rho u + \rho_l \beta (v-u)/2\} = 0 . \qquad (5.4)$$

The equation of conservation of the number density n is

$$\frac{\partial n}{\partial t} + \frac{\partial}{\partial x}(nv) = 0. \qquad (5.5)$$

The momentum equation is, including Kelvin impulse (chapter 4),

$$\frac{\partial}{\partial t}\{\rho u + \rho_l \beta(v-u)/2\} + \frac{\partial}{\partial x}\{p + \rho u^2 + \rho_l \beta v(v-u)/2\} = 0 . \tag{5.6}$$

Now the equation describing the translational velocity of the bubble includes the friction force and is (c.f. 1.16)

$$\frac{1}{2}\rho_l \frac{d}{dt}\{V(v-u)\} + 12\pi\mu_l R(v-u) = -V\frac{\partial p}{\partial x} . \tag{5.7}$$

Furthermore we have the equation for bubble pressure p_g and liquid pressure p

$$p_g - p = \rho_l\left\{ R\frac{D^2R}{Dt^2} + \frac{3}{2}(\frac{DR}{Dt})^2 + \delta\omega_B'R\frac{DR}{Dt} \right\} , \tag{5.8}$$

with

$$\frac{D}{Dt} = \frac{\partial}{\partial t} + v\frac{\partial}{\partial x} . \tag{5.9}$$

§3. THE HUGONIOT RELATIONS.

The relations between quantities far in front and those far behind the shock become rather simple. Far in front and far behind the shock the velocity of the gas phase equals the liquid velocity. Therefore the Hugoniot relations are equal to those derived in chapter 3. We summarize these for convenience. The expression for the liquid velocity u_l behind the shock is, using (3.21),

$$\frac{u_1}{U} = -\frac{\alpha_o}{1+\alpha_o}\left(1 - \frac{c_o^2}{U^2}\right) . \tag{5.10}$$

For the Machnumber M_o we have

$$M_o \equiv \frac{U}{c_o} = \left(\frac{p_1}{p_o}\right)^{\frac{1}{2}} , \tag{5.11}$$

or

$$M_o^2 = \alpha_o/\alpha_1 , \tag{5.12}$$

and accordingly

$$\frac{p_1}{p_o} = \frac{\alpha_o}{\alpha_1} \ . \tag{5.13}$$

We also use the equation

$$\frac{p_1}{p_o} = \frac{\alpha_o \rho_l U^2}{p_o (1+\alpha_o)^2} \ . \tag{5.14}$$

§4. THE EQUATIONS DESCRIBING THE SHOCK STRUCTURE.

We consider a shock wave moving with constant speed U in negative x direction. The equations (5.1)-(5.8) are transformed from the x, t-frame into the x', t-frame with $x'=x+Ut$. In this new frame the shock is steady and so $(\partial/\partial t)_x$, is zero. Carrying out this transformation on (5.4), we obtain, omitting the prime on x',

$$\frac{\partial}{\partial x} \left\{ \rho_l (1-\beta)(U+u) + \rho_l \beta(v-u)/2 \right\} = 0 \ . \tag{5.15}$$

Integration gives

$$\rho_l (1-\beta)(U+u) + \rho_l \beta(v-u)/2 = \rho_l (1-\beta_o) U \ , \tag{5.16}$$

where upstream quantities are indicated with subscript o. The shock induced velocity u follows from (5.2) and (5.16),

$$u = \beta_o U \left(\frac{\alpha}{\alpha_o} - 1 \right) - \alpha(v-u)/2 \ . \tag{5.17}$$

From transformation and integration of (5.6) we find for the momentum equation in the moving frame of reference

$$p_o + \rho_l (1-\beta_o) U^2 = p + \rho_l (1-\beta)(U+u)^2 + \rho_l \beta U(v-u) \ . \tag{5.18}$$

Substitution of (5.17) into (5.18), use of the equations (5.12)-(5.14), gives for the momentum equation

$$\frac{p}{p_o} - 1 = M_o^2(1-y) + O(\alpha^2) , \qquad (5.19)$$

with $y = \alpha/\alpha_o$.

From (5.19) we want to find the equation describing the shock structure in terms of either p or y. We follow the method given in §5 of chapter 4. Transformation of (5.8) by use of (4.44), substitution of p from this new equation into (5.19), use of the isothermal relation $p_g V = p_o V_o$, finally gives for (5.19), with help of (4.43),

$$y^{\frac{2}{3}}\left[(1+4\alpha_o y)\frac{d^2 y}{d\eta^2} + \delta^{\Delta}\frac{dy}{d\eta}\right] + (1-y)(y-M_o^{-2}) +$$

$$\frac{v-u}{U} M_o^{-2} = 0 , \quad (5.20)$$

with $\eta = x(3\alpha_o)^{\frac{1}{2}}/R_o$.

Non-linear derivatives are neglected because the outskirts will be discussed.

For determining the shock structure we need an expression for $(v-u)/U$. Therefore we consider the equation of motion of a single bubble (5.7). With the help of (5.3), (5.5) and (5.9), (5.7) is changed into

$$\frac{D}{Dt}\{\beta(v-u)\} + 24\pi\mu_l nR(v-u) = -\frac{2\beta}{\rho_l}\frac{\partial p}{\partial x} - \beta(v-u)\frac{\partial v}{\partial x} . \quad (5.21)$$

Substitution of $\partial p/\partial x$ from (5.6) into (5.21) and transformation of (5.21) finally yields, with help of (5.17),

$$\frac{d}{d\eta}\left(y\frac{v-u}{U}\right) + \frac{\sigma}{y^{\frac{2}{3}}}y\frac{v-u}{U} - 2\alpha_o y\frac{dy}{d\eta} + O(\alpha^2) = 0 , \qquad (5.22)$$

with

$$\sigma = \frac{18\nu_l}{UR_o}\frac{1}{(3\alpha_o)^{\frac{1}{2}}} . \qquad (5.23)$$

In some cases $y^{\frac{2}{3}}$, in the term containing σ, can be taken

equal to unity. Upon integration of *(5.22)* we obtain omitting terms of order α^2

$$y \frac{v-u}{U} = \alpha_o \int_{-\infty}^{\eta} \frac{dy^2}{d\eta'} exp\left[-\sigma(\eta-\eta')\right] d\eta' . \qquad (5.24)$$

In determining the constant of integration it is assumed that ahead of the shock $(\eta \to -\infty)$ $v=u=0$. Actually there is a small relative velocity caused by buoyancy. Thanks to the addition of glycerine to the liquid this velocity is only a few *cm/sec*. The shock induced velocity is of order αU and therefore much larger in most of the experiments. The basic set of equations is given by the system of equations *(5.20)* and *(5.22)* as well by the system *(5.20)* and *(5.24)*. With the help of both systems we discuss the outskirts of the shock. For $\sigma \to 0$, shocks as discussed in chapter 4 are derived and so are shocks, as discussed in chapter 3, for $\sigma \to \infty$. Before starting the discussion of the shock structure we make some remarks regarding to the equation describing relative motion; *(5.22)*. For most of our experiments σ is of order 10^{-2} and at maximum of order 10^{-1} in some of the experiments. On the scale of $\eta=O(1)$, that is on the scale of the shock thickness d_A as defined by *(4.52)*, the term representing the viscous force in *(5.22)* is unimportant, because $(v-u)/U=O(\alpha)$. However on the scale $\sigma\eta=O(1)$, viscous effects associated with relative motion plays a dominant rôle. These features will largely determine the shock structure.

For sake of completeness we combine equations *(5.20)* and *(5.24)* to an integro-differential equation

$$y^{\frac{2}{3}}\left[(1+4\alpha_o)\frac{d^2y}{d\eta^2} + \delta^\Delta\frac{dy}{d\eta}\right] + (1-y)(y-M_o^{-2}) +$$

$$\alpha_o \frac{M_o^{-2}}{y} \int_{-\infty}^{\eta} \frac{dy^2}{d\eta'} exp\left[-\sigma(\eta-\eta')\right] d\eta' = 0 . \qquad (5.25)$$

In the next section, where we analyse the shock structure, we will use the system of equations (5.20) and (5.22) as well equation (5.25)

§5. THE SHOCK STRUCTURE.

We substitute $y(v-u)/U$ from (5.20) into (5.22) and find a third order differential equation. Following the procedure of the foregoing chapters, this equation will be linearized in order to analyse the shock structure from the outskirts of the shock.

To investigate the front part of the shock we linearize the differential equation in this region, where $y'(=1-y)$ is the small quantity. The resulting equation is

$$\frac{d^3y'}{d\eta^3} + \left(\frac{\delta^\Delta}{1+4\alpha_o} + \sigma\right)\frac{d^2y'}{d\eta^2} - \frac{1-M_o^{-2}-2\alpha_o M_o^{-2}}{1+4\alpha_o}\frac{dy'}{d\eta} -$$

$$\frac{\sigma}{1+4\alpha_o}(1-M_o^{-2})y' = 0 \ . \quad (5.26)$$

For the front part we seek solutions which disappear when $\eta \to -\infty$. To find the solutions we have to solve the third order differential equation (5.26). To this end a general method is summarized in Appendix 1. In this section the results are presented.

In general there are three solutions of (5.26). However, not all are useful. This depends on the condition that the solution needs to vanish when $\eta \to -\infty$. As follows from the analysis in Appendix 1, there are two important cases which lead to different solutions. So we will properly distinguish these two cases. Their appearance depends on the pressure ratio across the shock. The first is represented through

$$M_o^2 = \frac{p_1}{p_o} < 1+2\alpha_o \ .$$

From Appendix 1 it follows, under this condition, that the solution for y is

$$1-y \propto exp\left[\frac{\sigma\eta(M_o^2-1)}{1+2\alpha_o-M_o^2}\right] . \qquad (5.27)$$

This solution, which describes the front part, disappears when $\eta\to-\infty$. From (5.27) a shock thickness d' can be defined

$$d' \sim \frac{R_o}{(3\alpha_o)^{\frac{1}{2}}} \frac{1+2\alpha_o-M_o^2}{\sigma(M_o^2-1)} \, ln20 . \qquad (5.28)$$

This is at least an order of magnitude larger than the shock thickness derived in the foregoing chapters. In this case the front part follows from a balance of non-linear compression with dissipation associated with relative motion. (5.27) represents the front part of a smooth profile, the S_C shock. The second case is represented by the condition

$$M_o^2 > 1+2\alpha_o .$$

Under this condition the solution for y is

$$1-y \propto exp\left[-\frac{\eta\delta_o^{\Delta}}{2} + \frac{\eta(1-M_o^{-2}-2\alpha_o M_o^{-2})^{\frac{1}{2}}}{1+2\alpha_o}\right]. \qquad (5.29)$$

The shock thickness d_A becomes

$$d_A = \frac{R_o}{(3\alpha_o)^{\frac{1}{2}}} \frac{(1+2\alpha_o)ln20}{(1-M_o^{-2}-2\alpha_o M_o^{-2})^{\frac{1}{2}}-\delta_o^{\Delta}/2} . \qquad (5.30)$$

With the help of the definition of M_f^2, (4.37), d_A can also be presented in terms of M_f

$$d_A = \frac{R_o}{(3\alpha_o)^{\frac{1}{2}}} \frac{(1+2\alpha_o)ln20}{(1-M_f^{-2})^{\frac{1}{2}}-\delta_o^{\Delta}/2} . \qquad (5.31)$$

For most of our experiments this is the same as the shock thickness derived in chapter 4. We already mentioned, on the scale of d_A, that in the front of the shock viscous effects are unimportant.

Now we pay attention to the back side of the shock. We linearize the third order differential equation in this region, where $y''(=y-y_1)$ is the small quantity. The resulting differential equation for y'' is

$$\frac{d^3y''}{d\eta^3} + (\delta_1^\Delta + \sigma M_o^{2/3})\frac{d^2y''}{d\eta^2} + \frac{M_o^2-1+2\alpha_o}{1+4\alpha_o M_o^{-2}} M_o^{-\frac{2}{3}}\frac{dy''}{d\eta} +$$

$$\frac{\sigma(M_o^2-1)}{1+4\alpha_o M_o^{-2}} y'' = 0 . \qquad (5.32)$$

For the backside we seek solutions disappearing when $\eta \to \infty$. To this end we use the analysis of Appendix 1. The solution for y consists of two parts. The first part is proportional to

$$exp\left[-\frac{\eta\sigma M_o^{\frac{2}{3}}(M_o^2-1)}{M_o^2-1+2\alpha_o}\right] . \qquad (5.33a)$$

This term originates in the viscous effects associated with relative translational motion. The pressure changes on the scale $\sigma\eta$.

The second part is proportional to

$$exp\left[-\frac{\eta}{2}\left\{\delta_1^\Delta + \frac{\sigma 2\alpha_o M_o^{\frac{2}{3}}}{M_o^2-1+2\alpha_o}\right\}\right] exp\left[\pm i\eta\left\{\frac{(M_o^2-1+2\alpha_o)M_o^{\frac{4}{3}}}{M_o^2+4\alpha_o}\right\}^{\frac{1}{2}}\right] . (5.33b)$$

This represents damped pressure oscillations. This wavy behaviour was already found in the foregoing chapter, but with a slightly different attenuation factor. In this term the expression containing the factor σ becomes important when $M_o^2-1=O(\alpha_o)$ and accordingly $M_o^{\frac{2}{3}}$ can be taken unity. We see that the solution for y, or for the pressure ratio, at the back side of the shock consists of a profile slowly changing to equilibrium, (5.33a), with damped oscillations superimposed, (5.33b).

Thus we found two types of shock structure, the appearance of which depends on a critical value of the pressure ratio. One type is described by the system of equations (5.27),

(5.33a) and (5.33b). This we call a S_C shock. This shock
will receive more attention in the following section. The
other type is represented through the system of equations
(5.31), (5.33a) and (5.33b). We call this a S_B shock, with
which the present section is concerned. A pressure recor-
ding for a S_B shock is shown in Figure 12.
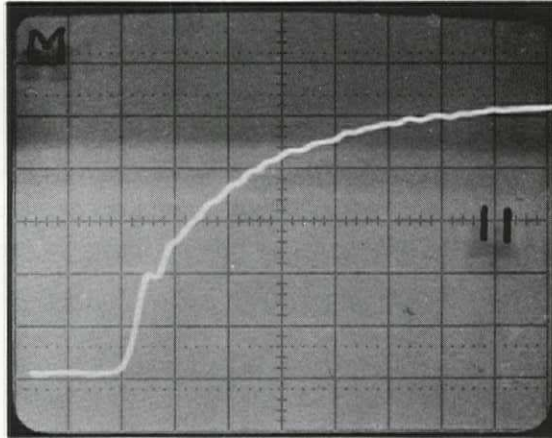
FIGURE 12. A pressure recording typical for a S_B shock.

In this Figure we see a profile that considerably differs
from that of a S_A shock (c.f. Figure 10). In the S_B shock
there is still a steep rise at the front, but the pressure
does no longer rise to its equilibrium value at the back
side. This takes place in a region which is much larger than
that of the front shock. In this region at the back side
the pressure reaches its final value slowly oscillating.
The wave length Λ follows from (5.33b) and yields, with
$\alpha_o=O(10^{-2})$, $\delta^\Delta=O(10^{-1})$ and $\sigma=O(10^{-2})$ in most of our expe-
riments,

$$\Lambda = \frac{2\pi R_o}{(3\alpha_o)^{\frac{1}{2}}} \left| \frac{M_o^{\frac{2}{3}}}{M_o^2-1+2\alpha_o} \right|^{\frac{1}{2}} . \qquad (5.34)$$

There is no essential difference with the wave length
represented by (4.55).

The number of waves, N, in which the amplitude decreases by a factor e^{-1}, is found from $(5.33b)$ and (5.34) and is

$$N = \frac{1}{\pi} \left\{ \frac{M_o^2 - 1 + 2\alpha_o}{M_o^{\frac{2}{3}}} \right\}^{\frac{1}{2}} \frac{M_o^2 - 1 + 2\alpha_o}{(M_o^2 - 1 + 2\alpha_o) \delta_1^{\Delta} + 2\sigma} \quad . \qquad (5.35)$$

Besides by the shock thickness d_A and wave length Λ, a S_B shock is also characterised by two other quantities. The first is the length of the region where the pressure slowly reaches its equilibrium value as shown in Figure 12. The second is the pressure p^* located at the point of intersection of the steep front part and the smooth back side of the shock. The different quantities for a S_B shock are once more illustrated in Figure 13.
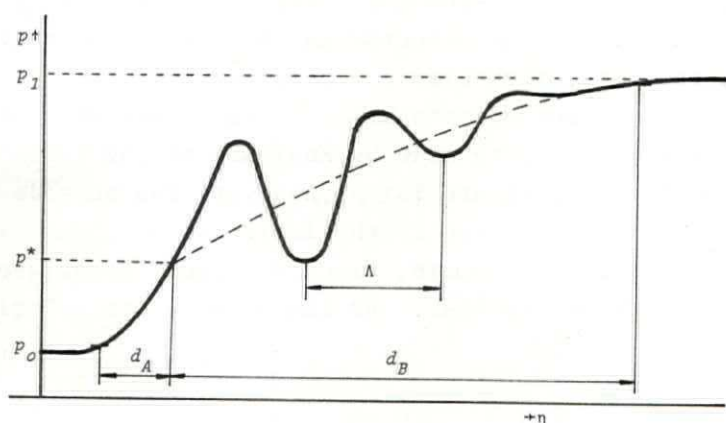
FIGURE 13. In this Figure the pressure profile of the shock wave is shown. Important quantities such as d_A, Λ, p^* and d_B are marked.

The region of length d_B is determined by viscous effects, as can be seen from $(5.33a)$. By stretching the η scale through the factor σ, to

$$\xi = \sigma\eta , \qquad (5.36)$$

(5.22) becomes

$$\frac{d}{d\xi}\left(y \; \frac{v-u}{U}\right) + y^{\frac{2}{3}}y \; \frac{v-u}{U} - 2\alpha_o y \; \frac{dy}{d\xi} = 0 \; . \qquad (5.37)$$

For the investigations of the back side of the shock, $y^{-\frac{2}{3}}$ in (5.37) can be taken equal to unity. Then we obtain from (5.24) and (5.36)

$$y \; \frac{v-u}{U} = \alpha_o \int_{-\infty}^{\xi} \frac{dy^2}{d\xi'} \; exp \left[-(\xi-\xi')\right] d\xi' \; . \qquad (5.38)$$

To find p^* and d_B the following approach is chosen: On ξ scale the front shock can be considered as a discontinuity. In front of this discontinuity the pressure is p_o and behind it p^*. At the back side, a region where steepening is balanced by dispersion goes over into a region where it is balanced by viscous effects. In the transition region therefore, the three mechanisms, non-linear compression, dispersion and viscous effects are of equal importance. A detailed study can only be made by analysis of the full equation (5.20). An estimate for p^*, however, can be made in various ways. One of them is the following: In the front shock, on η scale, viscous effects associated with relative motion are small and the propagation velocity must obey (4.19)

$$\frac{U^2}{c_o^2} = \frac{p^*}{p_o}\left\{1+\alpha_o\left(1+\frac{p_o}{p^*}\right)\right\} \; .$$

However, U^2/c_o^2 follows from conservation of mass and of momentum in the whole wave and is, (eq.5.11),

$$\frac{U^2}{c_o^2} = \frac{p_1}{p_o} \; ,$$

whence

$$\frac{p_1}{p_o} = \frac{p^*}{p_o}\left\{1+\alpha_o\left(1+\frac{p_o}{p^*}\right)\right\} \; . \qquad (5.39)$$

The pressure recordings from the experiments give $p-p_o$ relative to the pressure jump p_1-p_o. For this we introduce F_{is} which is defined through

$$F_{is} = \frac{p^*/p_o - 1}{p_1/p_o - 1} .$$

From this and (5.39) we have at $p=p^*$

$$F_{is} = 1 - \alpha_o \frac{p_1/p_o + 1}{p_1/p_o - 1} . \qquad (5.40)$$

It is easily verified that p^* becomes equal to zero, to order α_o^2, when

$$p_1/p_o = 1+2\alpha_o .$$

Which is the threshold for the existence of a smooth profile, the S_C shock. For strong shocks p^* is practically equal to p_1.

The value of y associated with p^*, y^* is, using (5.11), (5.19) and (5.40),

$$y^* = y_1 + \alpha_o(1+y_1) . \qquad (5.41)$$

From this value of y^* or with p^* and the relation for the smooth profile at the back side of the shock, (5.33a), the length of the smooth region, d_B, can be estimated. d_B follows from the distance in which y changes from y^* to $y_1 + .05(y^*-y_1)$, say. From (5.33a) and (5.41) we obtain

$$\frac{d_B}{U\tau} = \left(1 + \frac{2\alpha_o}{M_o^2-1}\right) \frac{\ell n 20}{M_o^{\frac{2}{3}}} , \qquad (5.42)$$

with

$$\tau = \frac{R_o^2}{18\nu_\ell} . \qquad (5.43)$$

Experimentally, it is beyond the accuracy of the measured profile, for us to locate the distance where $y-y_1$ is a small fraction, 5%, say, of y^*-y_1. It is only possible to indicate

$y-y_1$ as a small fraction of p_1-p_0.

With the help of $(5.33a)$, (5.40) and (5.41) we find for d_B

$$\frac{d_B}{U\tau} = \left(1+ \frac{2\alpha_o}{M_o^2-1}\right)M_o^{-\frac{2}{3}}ln\{20(1-F_{is})\} \ . \tag{5.44}$$

The equation for the thickness of the front shock, d_A, also needs some modification. Actually d_A follows from the distance in which y changes from 1 to y^* instead of to y_1. The latter value gives (5.29). For d_A we have the same comment on the accuracy of the approximation as we had for d_B. From (5.28) and (5.40) we find for d_A, the distance in which y changes from $1-.05(1-y_1)$ to y^*,

$$d_A = \frac{R_o}{(3\alpha_o)^{\frac{1}{2}}} \frac{(1+2\alpha_o)ln(20F_{is})}{(1-M_f^{-2})^{\frac{1}{2}}-\delta_o^{\Delta}/2} \ . \tag{5.45}$$

So far we discussed the structure of a S_B shock, which will appear for $p_1/p_0>1+2\alpha_o$. Before starting the discussion of steady shocks with $p_1/p_0<1+2\alpha_o$, we first analyse a S_B shock in a slightly different way. This may serve the insight of the S_B shock.

In the region $y^*<y\leq1$ relative motion is not resisted by viscous friction and we may take here $\sigma=0$ in the system of equations (5.20) and (5.22) and equation (5.25). From these equations we find, using (5.41),

$$\frac{(1-y)(y^*-y)(y+\alpha_o)}{y} = y^{\frac{2}{3}}\left[(1+4\alpha_o y)\frac{d^2y}{d\eta^2} + \delta^{\Delta}\frac{dy}{d\eta}\right] \ . \tag{5.46}$$

This equation is similar to equation (4.48) with y^* instead of y_1, valid for a S_A shock, as could be expected. This shock is discussed in chapter 4 and (5.46) needs no further discussion here. The equilibrium points are at $y=1$ and at $y=y^*$. Linearization at the front, near $y=1$, gives

$$1-y \propto exp\left[- \frac{\eta\delta_o^{\Delta}}{2} + \frac{\eta\{1-y_1(1+2\alpha_o)\}^{\frac{1}{2}}}{1+2\alpha_o}\right] \ . \tag{5.47}$$

Since here $y_1 = p_0/p_1 = M_0^{-2}$ and $c^2 = c_f^2(1-2\alpha_0)$, this may be written as (4.51), which emphasizes that both the front part of a S_A shock and that of a S_B shock are of the same type. At the beginning of this section we already discussed the front part of a S_B shock as represented by equation (5.28). This equation shows the influence of viscous friction by the factor σ. The neglect of σ is justified for most of our experiments and accordingly this results in equation (5.47).

The back side, excluding the oscillations, is governed by the balance between non-linear steepening and the effects following from viscous friction connected with relative translational motion. For this purpose the η scale of the equation (5.25) is stretched by the factor σ. We obtain

$$(1-y)(M_0^{-2}-y) - \alpha_0 \frac{M_0^{-2}}{y} \int_{-\infty}^{\xi} \frac{dy^2}{d\xi'} exp\left[-(\xi-\xi')\right] d\xi' =$$

$$y^{\frac{2}{3}}\left[\sigma^2(1+4\alpha_0)\frac{d^2y}{d\xi^2} + \sigma\delta^{\Delta}\frac{dy}{d\xi}\right], \qquad (5.48)$$

with $\xi=\sigma\eta$.

The pertinent equation for the back side is (5.48) with $\sigma\to0$. On ξ scale the front shock is a discontinuity and taking $\xi=0$ at this discontinuity, we write

$$y = 1 + \left\{(y_1-1)+f(\xi)\right\}H(\xi) , \qquad (5.49)$$

where H is Heaviside's unit step function.

With a view on (5.41) $f(\xi)$ is of order α_0. When we neglect, in inserting (5.49) into (5.48), terms of order α_0^2 the integral reduces to

$$\int_{-\infty}^{0} (y_1^2-1)\delta(\xi')exp\left[-(\xi-\xi')\right] d\xi' ,$$

where $\delta(\xi)$ is the Dirac delta function.
The integral equals

$$(y_1^2 - 1)exp-\xi \; .$$

From (5.48) we obtain for f

$$f = \alpha_o (1+y_1) exp-\xi \; .$$

Together with (5.49) this gives for $\xi \geqslant 0$

$$y = y_1 + \alpha_o (1+y_1) exp-\xi \; . \qquad (5.50)$$

This relation for $y-y_1$ is similar to $(5.3\overset{\alpha}{\underset{\vee}{3}})$. The latter represents the smooth profile at the back side of the shock when

$$\frac{M_o^{2/3}(M_o^2 - 1)}{M_o^2 - 1 + 2\alpha_o}$$

is taken unity.

At $\xi=0$, the location of the discontinuity, (5.50) gives

$$y^* = y_1 + \alpha_o (1+y_1)$$

which supports the independently obtained estimate (5.41) for y^*. With help of (5.11) and (5.19), we deduce from (5.50) that the pressure profile at the back side is

$$\frac{p/p_o - 1}{p_1/p_o - 1} = 1 - \alpha_o \frac{p_1/p_o + 1}{p_1/p_o - 1} exp-\xi \; . \qquad (5.51)$$

At $\xi=0$ F_{is} as given by (5.40) is recovered.

§6. *THE STRUCTURE OF A SMOOTH SHOCK; A S_c SHOCK.*

In this section we investigate shocks without the steep front part. This occurs when the pressure ratio is below a certain critical value. A pressure recording of a S_c shock is shown in Figure 14.
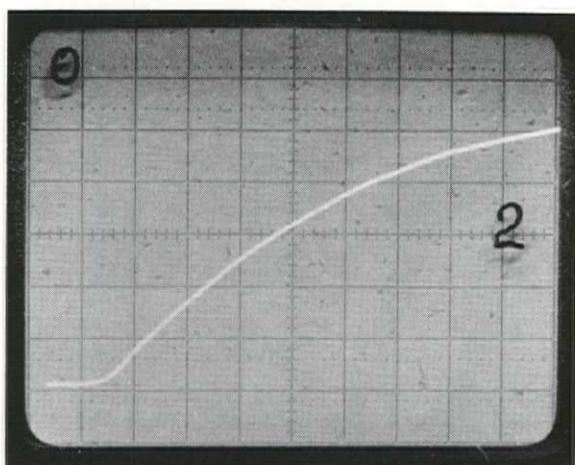
FIGURE 14. A pressure recording typical for a S_C shock.

In the foregoing section we described already the front part and the backside of this profile. For a S_C shock the viscous forces are important throughout the profile. The scale on which quantities change is the ξ scale instead of the η scale. The pertinent equation describing S_C shocks is equation (5.48). For $\sigma \to 0$ the right-hand side vanishes and the equation describes a transition in which non-linear steepening is resisted by effects connected with relative motion. In §5 we found that this is only possible for

$$M_o^2 = P_1/p_o < 1+2\alpha_o .$$

Since y lies between unity and M_o^{-2}, $1-y$ and $M_o^{-2}-y$ are of order α_o in these waves. Then, to order α_o^3, (5.48) can be simplified to

$$(1-y)(M_o^{-2}-y) - 2\alpha_o \int_{-\infty}^{\xi} \frac{dy}{d\xi'} \, exp\left[-(\xi-\xi')\right] d\xi' = 0 . \qquad (5.52)$$

When we introduce the quantities ψ and λ by

$$y = \{(1+M_o{}^2) + \psi(1-M_o{}^2)\}/2 , \qquad (5.53)$$

$$\lambda = \frac{2\alpha_o}{M_o^2-1} , \qquad (5.54)$$

and require that $\psi=0$, half way between $y=1$ and $y=M_o^{-2}$, is at $\xi=0$, we obtain

$$(1-\psi)^{1-\lambda} (1+\psi)^{1+\lambda} = exp-\xi . \qquad (5.55)$$

For $1-\lambda<0$, which amounts to $p_1/p_o<1+2\alpha_o$, as follows from (5.54), this represents a wave profile in which ψ decreases smoothly from 1 to -1, y accordingly from 1 to M_o^{-2}. The dimensionless pressure p/p_o is related with ψ, from (5.19) and (5.53), by

$$p/p_o = \{(1+M_o^2) + \psi(1-M_o^2)\}/2 , \qquad (5.56)$$

or, with $M_o^2 = p_1/p_o$, by

$$\frac{p/p_o-1}{p_1/p_o-1} = (1-\psi)/2 . \qquad (5.57)$$

From (5.55) and (5.56) it follows that the dimensionless pressure rises from 1 to $(M_o^2+1)/2$ over a distance which is, in terms of ξ, a few times, 3 say, $\lambda-1$. Using (5.54) and remembering that $2\alpha_o$ can be written as $(c.f.4.21)$ $(c_f/c_o)^2-1$ we derive

$$3(\lambda-1)= 3 \frac{c_f^2-U^2}{U^2-c_o^2} .$$

The rise of $(M_o^2+1)/2$ to M_o^2 takes place over a distance $3(\lambda+1)$ or

$$3 \frac{c_f^2+U^2-2c_o^2}{U^2-c_o^2} .$$

This shows that the front part of the shock is much thinner than the back side. The overall shock thickness is found from the distance in which ψ changes from $+1$ to -1. Using the expressions for ψ, λ and ξ, we find from (5.55) for the thickness d_C

$$\frac{d_C}{U\tau} = \frac{4\alpha_o}{M_o^2-1} \, ln20 \, .$$

(5.58)

For convenience we give the profile for a S_C shock once more in terms of y,

$$y(1-y)^{1-\lambda} \, (y-M_o^{-2})^{1+\lambda} = exp-\xi \, .$$

(5.59)

§7. THE ADIABATIC THEORY.

The Hugoniot relations are already given in chapter 3. For the pressure ratio we have

$$p_1/p_o = \left(\alpha_o/\alpha_1\right)^\gamma \, .$$

(5.60)

The Machnumber is related with p_1/p_o by

$$M_o^2 = \frac{p_1/p_o-1}{1-\left(p_o/p_1\right)^{1/\gamma}} \, .$$

(5.61)

The sound velocity, c_{ad}, is

$$c_{ad}^2 = \gamma p_o (1+\alpha_o)^2/(\rho_1\alpha_o) \, .$$

(5.62)

Furthermore we summarize the quantities such as shock thickness, wave length and the length of the smooth profile. The relation between the pressure in the bubble and the pressure far in front of the shock is, (c.f.4.57),

$$\frac{p_g}{p_o} = \left(\frac{\alpha_o}{\alpha}\right)^\gamma \left(1 - \gamma \, \frac{v-u}{U}\right) \, .$$

(5.63)

For a steady shock wave the momentum equation is

$$^p/p_o - 1 = M_o^2(1-y) . \qquad (5.64)$$

Transformation of (5.8) by use of (4.44), substitution of p from the resulting equation into (5.64) and use of (5.63), gives

$$y^{\frac{2}{3}}\left[(1+4\alpha_o y)\frac{d^2y}{d\eta^2} + \delta^\Delta \frac{dy}{d\eta}\right] + y(1-y) + M_o^{-2}y(1-y^{-\gamma}) +$$

$$y\frac{v-u}{U}\gamma M_o^{-2}y^{-\gamma} = 0 . \qquad (5.65)$$

With the equation for $y(v-u)/U$, (5.22), we find for the equation describing the front part of the shock

$$\frac{d^3y'}{d\eta^3} + (\delta_o^\Delta + \sigma)\frac{d^2y'}{d\eta^2} - \frac{1-\gamma M_o^{-2} - 2\alpha_o \gamma M_o^{-2}}{1+4\alpha_o}\frac{dy'}{d\eta} -$$

$$\frac{\sigma(1-\gamma M_o^{-2})}{1+4\alpha_o}y' = 0 , \qquad (5.66)$$

with $y'=1-y$.
$(1+2\alpha_o)\gamma M_o^{-2}$ can be taken equal to M_{fad}^{-2}.
Using the results of Appendix 1, we obtain from (5.66), when $^p1/p_o$ is smaller than the critical value

$$1 + \frac{4\gamma\alpha_o}{1+\gamma} , \qquad (5.67)$$

for y

$$1-y \propto exp\left[\frac{\sigma\eta(M_o^2-\gamma)}{2\alpha_o\gamma+\gamma-M_o^2}\right] . \qquad (5.68)$$

This represents the front part of a S_C shock.
For

$$^p1/p_o > 1 + {}^{4\gamma\alpha}o/(\gamma+1) , \qquad (5.69)$$

or

$$M_o^2 > \gamma(1+2\alpha_o) ,$$

the solution for y becomes

$$1-y \propto exp\left[-\eta\delta_o^\Delta/2 + \frac{\eta(1-M_{fad}^2)^{\frac{1}{2}}}{1+2\alpha_o}\right] . \qquad (5.70)$$

With help of (5.22) and (5.65) we find for y^*

$$y^* = y_1 + \alpha_o\gamma \frac{1-y_1^2}{\gamma-M_o^2 y_1^{\gamma+1}} . \qquad (5.71)$$

To express this in terms of the pressure ratio p^*/p_o, we introduce F_{ad} which is defined through

$$F_{ad} = \frac{p^*/p_o-1}{p_1/p_o-1} .$$

From this and (5.71) we have at $p=p^*$

$$F_{ad} = 1 - \gamma\alpha_o \frac{p_1/p_o\{1+(p_o/p_1)^{1/\gamma}\}}{\gamma p_1/p_o-(p_o/p_1)^{1/\gamma}M_o^2} . \qquad (5.72)$$

The thickness of the front shock d_A, based on y^* and using the comment on the experimental accuracy, is estimated from the distance in which y changes from $1-.05(1-y_1)$ to y^*. From (5.70) we obtain

$$d_A = \frac{R_o}{(3\alpha_o)^{\frac{1}{2}}} \frac{(1+2\alpha_o)ln(20F_{ad})}{(1-M_{fad}^{-2})^{\frac{1}{2}}-\delta_o^\Delta/2} . \qquad (5.73)$$

The profile at the back side is found from a linearization of the equations (5.22) and (5.65). The resulting differential equation for $y''(=y-y_1)$ is

$$\frac{d^3y''}{d\eta^3} + \left\{\delta_1^\Delta+\frac{\sigma}{y_1^{2/3}}\right\}\frac{d^2y''}{d\eta^2} + \frac{G_1}{y_1^{\frac{2}{3}}(1+4\alpha_o y_1)}\frac{dy''}{d\eta} + \frac{\sigma G_2 y''}{y_1^{\frac{4}{3}}(1+4\alpha_o y_1)}=0, \quad (5.74)$$

with

$$G_1 = G_2 + 2\alpha_o \gamma M_o^{-2} y_1^{1-\gamma} , \qquad (5.75)$$

and

$$G_2 = \frac{\gamma M_o^{-2}}{y_1^\gamma} - y_1 . \qquad (5.76)$$

From (5.74) it follows that the function describing the smooth profile in this region is proportional to

$$exp\left[-\frac{\sigma \eta G_2}{G_1 y_1^{\frac{2}{3}}}\right] . \qquad (5.77)$$

The thickness of this region, d_B, is found to be

$$\frac{d_B}{U\tau} = y_1^{\frac{2}{3}} \frac{G_1}{G_2} \ln\left\{20(1-F_{ad})\right\}. \qquad (5.78)$$

The expression for the wave length is

$$\Lambda = \frac{2\pi R_o}{(3\alpha_o)^{\frac{1}{2}}} \frac{y_1^{\frac{1}{3}}(1+2\alpha_o y_1)}{G_1^{\frac{1}{2}}} . \qquad (5.79)$$

The attenuation of the waves is found from the factor

$$exp\left[-\eta(\delta_1^{\Lambda}+G_3)/2\right] , \qquad (5.80)$$

with

$$G_3 = \frac{2\alpha_o \gamma \sigma}{M_o^2 G_1 y_1^{\gamma-\frac{1}{3}}} . \qquad (5.81)$$

The number of waves in which the amplitude decreases by a factor e^{-1}, is

$$N \simeq \frac{G_1^{\frac{1}{2}}}{y_1^{\frac{1}{3}}\pi(\delta_1^{\Lambda}+G_3)} . \qquad (5.82)$$

Now we return to the smooth profile or S_C shock. The resulting equation is found from (5.65) and is

$$y(1-y) + M_o^{-2}y(1-y^{-\gamma}) + y \frac{v-u}{U} \gamma M_o^{-2} y^{-\gamma} = 0 \ . \qquad (5.83)$$

From this equation and (5.22) we find for y

$$y(1-y)^{1-\ell} (y-y_1)^{1+\ell} = exp-\xi \ , \qquad (5.84)$$

with $\qquad \ell = \dfrac{2\alpha_o \gamma}{M_o^2 - \gamma} \ .$

For $\ell < 1$, which amounts to the critical value for the pres-
sure ratio, (5.84) represents the profile of a S_C shock
for adiabatic circumstances.
The expression for the thickness of the S_C shock is found
to be

$$\frac{d_C}{U\tau} = 2\ell \ln 20 \ . \qquad (5.85)$$

§8. CONCLUSIONS.

In this chapter we investigated shock waves, where, in
contrast to chapter 4, relative velocity of the bubbles
is resisted by viscous friction. These are S_B and S_C shocks.
We found that the profiles are considerably modified by
these viscous effects. The modification was found in two
ways:
The first is that the pressure oscillations at the back
side of the shock no longer take place around the equili-
brium value p_1. The oscillations start already near p^*,
which is between p_1 and p_o. This modification is very small
for large pressure ratio's as follows from (5.40). For weak
shocks however p^* clearly differs from p_1 as will be shown
in the experiments. The front part of this S_B shock is
similar to that of a S_A shock.
The second is that when the pressure ratio is smaller than
a certain critical value the profile is entirely smooth.

The steep front part as well as the oscillations no longer
appear. This we called a S_C shock.

CHAPTER 6.

RELAXATION EFFECTS ON SHOCK WAVES IN LIQUID-BUBBLE MIXTURES.

§1. *INTRODUCTION.*

In the foregoing chapters several shocks, such as S_A, S_B and S_C shocks were investigated. In experiments by Noordzij (1971) and Van Wijngaarden (1972b) S_A shocks were observed. These experiments were carried out in a shock tube of one meter length. After a longer distance viscous forces connected with relative translational motion become effective. Then the profiles of S_B and S_C shocks as discussed in chapter 5 can be observed. The shock tube, in which these shocks are observed, is schematically drawn in Figure 15.
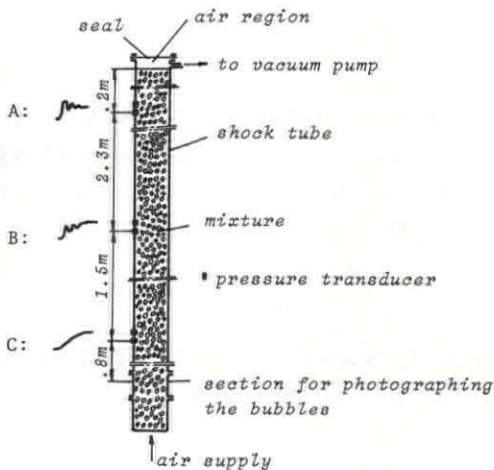
FIGURE 15. Experimental setup for measurements on shock waves. (A description will be given in chapter 8).

During its passage along the tube the profile of a pressure wave was recorded at three stations marked A, B and C in Figure 15. A is about *.2m* from the top of the tube, B at *2.5m* and C is at *4m*. At A a S_A shock appears, at B a S_B shock and finally at C a S_C shock. To illustrate the changing form, the pressure recordings are shown in

Figure 16.

A   B   C
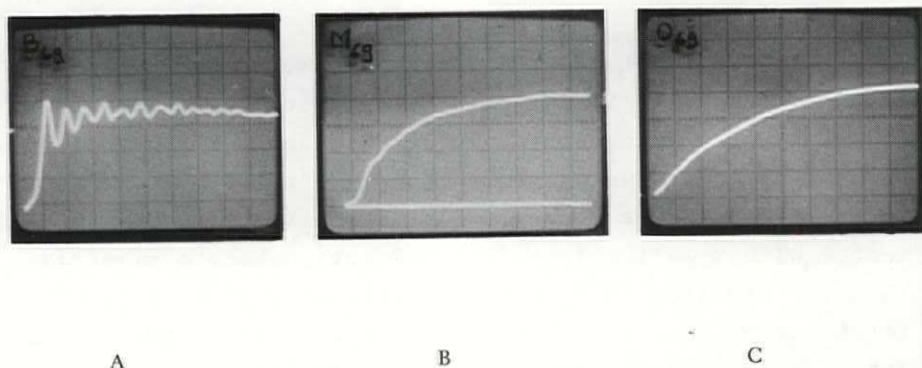
FIGURE 16. Several shock profiles recorded at the stations A, B and
C along the tube as indicated in Figure 15.

This change in profile cannot be explained with the sta-
tionary theory in the foregoing chapters. To gain insight
in the change in profile of the wave we consider the com-
plete set of unsteady equations in this chapter.

§2. *EQUATIONS OF MOTION.*

We consider time dependent flow. The liquid velocity is u
and the gas velocity is v, both quantities averaged over
a small volume.
The mixture density ρ is defined through

$$\rho = \rho_l (1-\beta) . \qquad (6.1)$$

The mass concentration, α/ρ_l, is defined through

$$\alpha = \frac{\beta}{1-\beta} . \qquad (6.2)$$

In the following we will take advantage of the fact that
in our experiments β and α are small, of order 10^{-2}.

Further we have

$$\beta = 4\pi n R^3/3 . \tag{6.3}$$

The equation of mass conservation is

$$\frac{\partial \rho}{\partial t} + \frac{\partial}{\partial x}\{\rho u + \rho_l \beta (v-u)/2\} = 0 . \tag{6.4}$$

The momentum equation is

$$\frac{\partial}{\partial t}\{\rho u + \rho_l \beta (v-u)/2\} + \frac{\partial}{\partial x}\{p + \rho u^2 + \rho_l \beta v (v-u)/2\} = 0 . \tag{6.5}$$

The equation of motion for a bubble is

$$\frac{1}{2}\rho_l \frac{d}{dt}\{V(v-u)\} + 12\pi\mu_l R(v-u) = -V\frac{\partial p}{\partial x} . \tag{6.6}$$

To express this in terms of β, we note that

$$\frac{Dn}{Dt} = -n\frac{\partial v}{\partial x} , \tag{6.7}$$

where

$$\frac{D}{Dt} = \frac{\partial}{\partial t} + v\frac{\partial}{\partial x} .$$

We combine this with (6.6) to

$$\rho_l \frac{D}{Dt}\{\beta(v-u)/2\} + 12\pi\mu_l nR(v-u) = -\beta\frac{\partial p}{\partial x} -$$

$$\frac{\rho_l}{2}\beta(v-u)\frac{\partial v}{\partial x} . \tag{6.8}$$

From (6.4) it follows that u is of order β. (6.5) and (6.6) show also that $v-u$ and $\partial p/\partial x$ are of order β. The leading terms in (6.8) are of order β^2 and the last term on the right-hand side is of order β^3. Since β is small we discard

this term, which reduces *(6.8)* to

$$\frac{\partial}{\partial t}\{\beta(v-u)\} + \frac{18\nu_l}{R_o^2} \beta(v-u) = -\frac{2\beta}{\rho_l} \frac{\partial p}{\partial x} , \qquad (6.9)$$

where we reduced the material derivative to the local deri-
vative $\partial/\partial t$, since $u(\partial u/\partial x)$ and $v(\partial u/\partial x)$ are of order β^2.
To the order of approximation in β, considered here, it is
permitted to take R in the coefficient of the viscous term
in *(6.8)* constant. We choose for this the value R_o in the
undisturbed state.
Since, with a view on *(6.5)*, $-\partial p/\partial x$ in the right-hand side
of *(6.9)* may be replaced by $\rho_l(\partial u/\partial t)$ in the present approxim-
ation, an alternative form of *(6.9)* is

$$\frac{\partial}{\partial t}\{\beta(v-u)\} + \frac{18\nu_l}{R_o^2} \beta(v-u) = 2\beta \frac{\partial u}{\partial t} . \qquad (6.10)$$

This equation describes a relaxation process with charac-
teristic time τ, given by

$$\tau = \frac{R_o^2}{18\nu_l} . \qquad (6.11)$$

For times $t \ll \tau$ relative motion is not resisted by friction.
Friction becomes effective at large times and, provided
$\partial u/\partial t$ tends to zero at large time, relative motion ceases
eventually. Similar "rate" processes occur in gasdynamic
shocks. Their socalled relaxation effects on shocks are
well understood in gasdynamics (Lighthill 1956, Whitham
1959, Ockendon&Spence 1969). Once the analogy is recognized,
the application of this theory to shocks in bubbly suspen-
sions can be made.
For most of our experiments, with bubbles of radius $10^{-3}m$
and $\nu_l=10^{-5}m^2/sec$, τ is about $10^{-2}sec$.
For isothermal circumstances we have, with $\rho_g V$ as an
invariant of the motion,

$$\frac{\partial}{\partial t}(p_g \beta) + \frac{\partial}{\partial x}(p_g \beta v) = 0 \; . \tag{6.12}$$

A difference between p and p_g is brought about by both the inertia of the liquid and various damping mechanisms. In an expression for $p-p_g$ all these effects are represented by strongly non-linear terms. However, both the coefficients involved and the bubble radii are small. So, as shown in the foregoing chapters (c.f.3.34), the leading contributions in the difference between p and p_g are represented by the right-hand side of

$$\frac{p_g-p}{\rho_l R_o^2} = \frac{\partial^2}{\partial t^2}\left(\frac{R}{R_o}\right) + \delta\omega_B' \frac{\partial}{\partial t}\left(\frac{R}{R_o}\right) \; . \tag{6.13}$$

Terms neglected in the right-hand side of (6.13) are of $O(\alpha)$ and of higher order.

In the dispersion equation (6.13) we also neglect the small effect of relative motion. When $v-u=0$, the mass of the gas in a unit mass of the mixture is constant. Since $p_g \propto \rho_g$ this means that $p_g \alpha$ is constant and equal to $p_o \alpha_o$. Together with $p_g R^3 = p_o R_o^3$ and the expression for the speed of sound

$$c_o^2 = \frac{p_o(1+2\alpha_o)}{\rho_l \alpha_o} \; , \tag{6.14}$$

we write for (6.13)

$$\frac{p_g-p}{p_o} = \frac{R_o^2}{3\alpha_o^2 c_o^2}\left\{\frac{\partial^2 \alpha}{\partial t^2} + \delta\omega_B' \frac{\partial \alpha}{\partial t}\right\} \; . \tag{6.15}$$

For convenience we summarize the equations here obtained, thereby slightly rearranging the terms in (6.4) and (6.5), and neglecting in (6.5) terms of order β^3

$$\rho = \rho_l(1-\beta) \; , \tag{6.16}$$

$$\alpha = \frac{\beta}{1-\beta} \simeq \beta(1+\beta) \; , \tag{6.17}$$

$$\frac{\partial \rho}{\partial t} + u \frac{\partial \rho}{\partial x} + \rho \frac{\partial u}{\partial x} = - \frac{\partial}{\partial x}\left\{\rho_l \beta(v-u)/2\right\} , \qquad (6.18)$$

$$\rho \frac{\partial u}{\partial t} + \rho u \frac{\partial u}{\partial x} + \frac{\partial p}{\partial x} = - \frac{\partial}{\partial t}\left\{\rho_l \beta(v-u)/2\right\}, \qquad (6.19)$$

$$\frac{\partial}{\partial t}(p_g \beta) + v \frac{\partial}{\partial x}(p_g \beta) + p_g \beta \frac{\partial v}{\partial x} = 0 . \qquad (6.20)$$

$$\left(\frac{\partial}{\partial t} + \tau^{-1}\right)\beta(v-u) = - \frac{2\beta}{\rho_l} \frac{\partial p}{\partial x} , \qquad (6.21)$$

$$\frac{p_g - p}{p_o} = \frac{R_o^2}{3\alpha_o^2 c_o^2}\left\{\frac{\partial^2 \alpha}{\partial t^2} + \delta\omega_B' \frac{\partial \alpha}{\partial t}\right\} , \qquad (6.22)$$

$$c_o^2 = \frac{p_o}{\rho_l \alpha_o}(1+2\alpha_o) . \qquad (6.23)$$

§3. THE EFFECTS OF RELATIVE TRANSLATIONAL MOTION ON WAVE PROPAGATION.

The new aspect, we wish to investigate, is the relative motion. To obtain some insight, we first disregard all other effects and consider small amplitude waves with

$$p_g = p .$$

Linearization of (6.18)-(6.21) leads to:

$$\frac{\partial}{\partial t}(1-\beta) + (1-\beta_o)\frac{\partial u}{\partial x} = - \frac{\beta_o}{2} \frac{\partial}{\partial x}(v-u) , \qquad (6.24)$$

$$\frac{\partial u}{\partial t} + \beta_o c_o^2 \frac{\partial \tilde{p}}{\partial x} = - \frac{\beta_o}{2} \frac{\partial}{\partial t}(v-u) , \qquad (6.25)$$

$$\frac{\partial \beta}{\partial t} + \beta_o\left\{\frac{\partial \tilde{p}}{\partial t} + \frac{\partial}{\partial x}(v-u) + \frac{\partial u}{\partial x}\right\} = 0 , \qquad (6.26)$$

$$\frac{\partial}{\partial t}(v-u) + \tau^{-1}(v-u) = - \frac{2p_o}{\rho_l} \frac{\partial \tilde{p}}{\partial x} \, , \qquad (6.27)$$

where

$$\tilde{p} = \frac{p-p_o}{p_o} \, .$$

Addition of (6.24) and (6.26) gives

$$\frac{\partial u}{\partial x} + \beta_o \frac{\partial \tilde{p}}{\partial t} = - \frac{3\beta_o}{2} \frac{\partial}{\partial x}(v-u) \, .$$

Elimination of u between this equation and (6.25) gives with use of (6.27)

$$\frac{\partial}{\partial x}(v-u) = - \tau \left(c_f^2 \frac{\partial^2 \tilde{p}}{\partial x^2} - \frac{\partial^2 \tilde{p}}{\partial t^2} \right) \, , \qquad (6.28)$$

where

$$c_f^2 = c_o^2 (1+2\beta_o) \, . \qquad (6.29)$$

c_f is discussed in chapter 4.
Substitution of (6.28) into (6.27) yields finally

$$\frac{\partial}{\partial t} \left(c_f^2 \frac{\partial^2 \tilde{p}}{\partial x^2} - \frac{\partial^2 \tilde{p}}{\partial t^2} \right) + \tau^{-1} \left(c_o^2 \frac{\partial^2 \tilde{p}}{\partial x^2} - \frac{\partial^2 \tilde{p}}{\partial t^2} \right) = 0 \, . \qquad (6.30)$$

For times $t \ll \tau$ the solutions of (6.30) are waves propagating with speed c_f as defined by (6.29). Eventually the waves given by (6.30) travel with velocity c_o. We find for a wave travelling to the right, c.f. Appendix 2,

$$\frac{\partial}{\partial t} \left(c_f \frac{\partial \tilde{p}}{\partial x} + \frac{\partial \tilde{p}}{\partial t} \right) + \tau^{-1} \left(c_o \frac{\partial \tilde{p}}{\partial x} + \frac{\partial \tilde{p}}{\partial t} \right) = 0 \, . \qquad (6.31)$$

This equation, resembling relaxation, is extensively studied by Whitham (1959).
In the following sections we discuss general aspects of this equation. Much is based on investigations by Lighthill (1956) and Whitham (1959). They discussed relaxation in

gasdynamics and magneto-hydrodynamics respectively.

§4. *A GENERAL DISCUSSION ON RELAXATION.*

Our main attention will be given to linear wave propaga-
tion because non-linear wave propagation can be inferred
from the corresponding linear equations. The equation of
interest is *(6.31)*.
First we present some general properties of the solutions
of *(6.31)*. A more detailed analysis is given in the fol-
lowing section.
If $\tau^{-1}<0$, $\tilde{p}$ increases indefinitely. If $\tau^{-1}>0$, the solution
remains finite when c_o lies between c_f and 0.
For $\tau/t>>1$, *(6.31)* can be reduced to

$$\frac{\partial}{\partial t}\left(\frac{\partial}{\partial t} + c_f\frac{\partial}{\partial x}\right)\tilde{p} = 0 \;, \qquad (6.32)$$

and for $\tau/t<<1$ to

$$\left(\frac{\partial}{\partial t} + c_o\frac{\partial}{\partial x}\right)\tilde{p} = 0 \;. \qquad (6.33)$$

How the solutions of these approximate equations are matched
to the boundary conditions is extensively discussed in a
survey by Whitham (1959).
The question to be answered is, how do the lower order terms
modify the solution of *(6.32)* and how do the higher order
terms modify *(6.33)*.
For $\tau^{-1}>0$ and $c_f>c_o>0$, the effects of the lower order terms
on the waves given by *(6.32)* produce an exponential decay
of amplitude. Therefore the main part of the wave moves
ultimately according to *(6.33)*. The higher order terms pro-
duce a diffusion of this wave. So, for long enough time,
the signal diffuses ultimately. For a non-linear problem
where c_o itselfs depends on $\tilde{p}$, this diffusion can be balan-
ced by non-linear effects leading to a steady shock pro-
file.

§5. EXACT SOLUTIONS OF THE LINEARIZED EQUATIONS.

In this section we present a more detailed discussion on the effects mentioned in the foregoing section.
The conditions for solutions which remain finite, are derived from periodic solutions of the linearized equation (6.31). The solutions periodic in x are

$$\tilde{p} \propto exp(ikx-\theta t) \ .$$

Substitution of this into (6.31) gives

$$(ikc_f-\theta)\theta - \tau^{-1}(ikc_o-\theta) = 0 \ . \tag{6.34}$$

For $kc_f\tau \gg 1$, relatively short waves, we find for θ

$$\theta_1 = ikc_f + \tau^{-1} \frac{c_f-c_o}{c_o} \ , \tag{6.35}$$

and

$$\theta_2 = \tau^{-1} \frac{c_o}{c_f} \ . \tag{6.36}$$

These solutions increase indefinitely unless $\tau^{-1}>0$ and $c_f>c_o>0$. Further we see that the short waves correspond to the higher order wave speed c_f and they are exponentially damped.
For $kc_f\tau \ll 1$, relatively long waves, we find

$$\theta_3 = ikc_o + k^2\tau(c_f-c_o)c_o \ , \tag{6.37}$$

and

$$\theta_4 = \tau^{-1} + ik(c_f-c_o) \ . \tag{6.38}$$

The solution given by (6.37) corresponds to the lower order waves with speed c_o; the k^2-factor in the real part indicates diffusion (c.f. §5, chapter 2). The solution given by (6.38) rapidly damps out through the factor $exp(-t/\tau)$. Solutions periodic in t give similar results (Whitham, 1959) which will not be discussed here.

Now we investigate the more general signalling problem, for the linear case, starting from zero initial disturbance with data prescribed on $x=0$. Then all possible types of waves occur and the development in dependence on x and t is discussed.

The boundary conditions are

$$\tilde{p} = \frac{\partial \tilde{p}}{\partial t} = 0 \, , \quad t=0, \ x>0$$

$$\tilde{p} = \tilde{p}_o(t) \, , \qquad x=0, \ t>0 \qquad\qquad (6.39)$$

We use Laplace transformation defined by

$$\bar{p}(s,x) = \int_0^\infty e^{-st} \tilde{p} \, dt. \qquad\qquad (6.40)$$

Inserting this in (6.31), we obtain

$$\bar{p} = \bar{p}_o exp\left[- \frac{s(s+\tau^{-1})}{c_f s + c_o \tau^{-1}} \, x \right] , \qquad\qquad (6.41)$$

with

$$\bar{p}_o = \int_0^\infty e^{-st} \tilde{p}_o \, dt \ .$$

The solution for $\tilde{p}$ is found to be

$$\tilde{p} = \frac{1}{2\pi i} \int_L \bar{p}_o exp\left[st - \frac{s(s+\tau^{-1})}{c_f s + c_o \tau^{-1}} \, x \right] ds \, , \qquad (6.42)$$

where L is the path, $Re \ p = constant$, to the right of all singularities.

With help of tables of Laplace transforms (Erdelyi, 1954) we obtain from (6.42)

$$\tilde{p} = exp\left[- \frac{\tau^{-1}}{c_f}\left(1- \frac{c_o}{c_f}\right)x \right]\left[\int_0^\infty \left(\frac{\partial \tilde{p}_o}{\partial \xi} + \frac{c_o}{c_f} \tau^{-1}\tilde{p}_o\right) H(t-\xi- \frac{x}{c_f}) \times \right.$$

$$exp\left[- \frac{\tau^{-1}}{c_f}(t-\xi- \frac{x}{c_f})\right] I_o\left[2\tau^{-1}\left\{(t-\xi- \frac{x}{c_f})\frac{c_o}{c_f^2}\left(1- \frac{c_o}{c_f}\right)x \right\}^{\frac{1}{2}}\right] d\xi \, ,$$

where I_o is the modified Bessel function of the second kind.

However, relevant properties of the solution can be shown in a more direct and clear way by using approximative methods. For this we return to (6.41).

Near the wave front $x=c_f t$, we use for (6.41) an expansion for large values of s. This changes (6.41) into

$$\bar{p}(s) = exp\left[-\frac{\tau^{-1}}{c_f}\frac{c_f-c_o}{c_f}x\right]\bar{p}_o \, exp\left[-\frac{sx}{c_f}\right] . \qquad (6.43)$$

The solution for $\tilde{p}$ is

$$\tilde{p} = exp\left[-\frac{\tau^{-1}}{c_f}\frac{c_f-c_o}{c_f}x\right]\tilde{p}_o(t-\frac{x}{c_f}) . \qquad (6.44)$$

This just represents the higher order wave which is exponentially damped near the wave front. Thus the main part of the disturbance is away from the wave front. Therefore we use an approximation for large values of t. An asymptotic expansion for large t is found by using the method of the steepest descents (Morse & Feshbach, 1953). We write the exponent in (6.42) as

$$t\left\{s-\frac{s(s+\tau^{-1})}{c_f s+c_o \tau^{-1}}\frac{x}{t}\right\} . \qquad (6.45)$$

The main contribution to the integral in (6.42) stems from the region where

$$\frac{df}{ds} = 0, \qquad (6.46)$$

with

$$f = s - \frac{s(s+\tau^{-1})}{c_f s+c_o \tau^{-1}}\frac{x}{t} \equiv s - \frac{x}{t}f_1 . \qquad (6.47)$$

The saddle point, at $s=s_1$, is determined by (6.46), which becomes, with help of (6.47),

$$1 - \frac{2s_1 + \tau^{-1}}{c_f s_1 + c_o \tau^{-1}} \frac{x}{t} + \frac{s_1(s_1 + \tau^{-1})c_f}{(c_f s_1 + c_o \tau^{-1})^2} \frac{x}{t} = 0 . \qquad (6.48)$$

The zeros of (6.48) are

$$s_1' = -\tau^{-1} \frac{c_o}{c_f} \left\{ 1 - \left(1 - \frac{c_f}{c_o} \frac{c_o^{-x/t}}{c_f^{-x/t}} \right)^{\frac{1}{2}} \right\}$$

and

$$s_1'' = -\tau^{-1} \frac{c_o}{c_f} \left\{ 1 + \left(1 - \frac{c_f}{c_o} \frac{c_o^{-x/t}}{c_f^{-x/t}} \right)^{\frac{1}{2}} \right\}$$

$$(6.49)$$

This represents two saddle points.

The path L in (6.42) is completed to a closed contour with a path through the saddle points. We assume that $\bar{p}_o$ possesses no singularities within the contour.

From the method of the steepest descents it can be found that the main contribution to the integral becomes

$$\bar{p}_o(s_1) \frac{exp\left[t(s_1 - f_1(s_1)^x/t) \right]}{(2\pi t |d^2 f/ds^2|_{s=s_1})^{\frac{1}{2}}} , \qquad (6.50)$$

where

$$\left(\frac{d^2 f}{ds^2} \right)_{s=s_1} = 2 \frac{x}{t} \frac{\tau^{-2} c_o (c_f - c_o)}{c_f s_1 + c_o \tau^{-1}} .$$

From comparison with (6.49) it follows that the exponential in (6.50) takes its maximum from the saddle point at $s=s_1'$, as represented by the first line in (6.49). Evaluation of this expression yields that this maximum occurs when $s_1'=0$ and we see from (6.48) or (6.49) that

$$\frac{x}{t} = c_o . \qquad (6.51)$$

Therefore the maximum in the disturbance moves with the speed of the lower order waves, c_o.

Using $s_1=0$, (6.50),which represents the maximum, becomes

$$\frac{\bar{p}_o(0)}{(4\pi x(c_f - c_o)/(c_o^2 \tau^{-1}))^{\frac{1}{2}}} , \qquad (6.52)$$

or

$$\frac{c_o}{\{4\pi(c_f-c_o)x\tau\}^{\frac{1}{2}}} \int_0^\infty \tilde{\tilde{p}}_o(t)dt \, , \qquad (6.53)$$

where we assume the integral to be finite.

We see that the maximum value decreases with $x^{-\frac{1}{2}}$, which is typical for diffusion. Thus the diffusive effect of the higher order derivatives is demonstrated.

In the following section we will discuss the foregoing effects once more from a direct approximation of (6.31).

§6. *APPROXIMATE SOLUTIONS OF THE LINEARIZED EQUATION.*

For $t/\tau \ll 1$ we use the approximation

$$\frac{\partial}{\partial t} \simeq -c_f \frac{\partial}{\partial x} \, ,$$

c.f. Appendix 2.

With this, (6.31) can be approximated by

$$\left(\frac{\partial}{\partial t} + c_f \frac{\partial}{\partial x}\right)\frac{\partial \tilde{p}}{\partial x} + \tau^{-1} \frac{c_f-c_o}{c_f} \frac{\partial \tilde{p}}{\partial x} = 0 \, . \qquad (6.54)$$

The solution of which is

$$\tilde{p} = g_1(t - \frac{x}{c_f}) \, exp\left[-\frac{\tau^{-1}}{c_f} \frac{c_f-c_o}{c_f} x\right]. \qquad (6.55)$$

This result is similar to (6.44).

For the lower order waves corresponding to c_o, (6.31) may be approximated by using

$$\frac{\partial}{\partial t} \simeq -c_o \frac{\partial}{\partial x} \, ,$$

for the higher order derivatives.

This gives

$$\frac{c_f - c_o}{\tau^{-1}} c_o \frac{\partial^2 \tilde{p}}{\partial x^2} = \frac{\partial \tilde{p}}{\partial t} + c_o \frac{\partial \tilde{p}}{\partial x} \;. \qquad (6.56)$$

The left-hand side represents diffusion of the waves propagating with speed c_o. This can be examined by Laplace transformation of (6.56). Using the definition (6.40) and the boundary conditions (6.39) for (6.56), we obtain for $\bar{p}$

$$\bar{p} = \bar{p}_o exp \left[\frac{x \tau^{-1}}{2(c_f - c_o)} \left(1 - \left\{ 1 + \frac{4 s (c_f - c_o)}{c_o \tau^{-1}} \right\}^{\frac{1}{2}} \right) \right] \;.$$

Expanding the square root for small s, $\bar{p}$ becomes

$$\bar{p} = \bar{p}_o exp \left[- \frac{s x}{c_o} \right] exp \left[s^2 \frac{c_f - c_o}{c_o^2 \tau^{-1}} x \right] \;. \qquad (6.57)$$

With help of tables of Laplace transforms (Campbell & Forster, 1948) $\tilde{p}$ becomes

$$\tilde{p} = \frac{c_o}{\left\{ 4 \pi \tau (c_f - c_o) x \right\}^{\frac{1}{2}}} \int_0^t \tilde{p}_o(\xi) exp \left[- \frac{(t - \xi - x/c_o)^2}{4(c_f - c_o) \tau x / c_o^2} \right] d\xi \;. \qquad (6.58)$$

This represents a time mean value of $\tilde{p}_o$ weighted according to a Gaussian distribution centred on $\xi = t - x/c_o$, with standard deviation

$$\left| \frac{2 \tau (c_f - c_o) x}{c_o^2} \right|^{\frac{1}{2}} \;. \qquad (6.59)$$

Here the diffusion effect is once more indicated. Since the effect of diffusion is to smear out a wave according to a spatial standard deviation as given by (6.59). As extreme case, a "step-function" wave would with this theory become an error integral wave form as the wave progresses. When $\left\{ 4(c_f - c_o) \tau x / c_o^2 \right\}^{\frac{1}{2}}$ is much smaller than a typical time scale in $\tilde{p}_o(t)$, (6.58) is approximated by

$$\tilde{p} \simeq \tilde{p}_o(t - x/c_o) \;.$$

This is only possible for finite t and x. On the other hand, when $\{4(c_f-c_o)\tau x/c_o^2\}^{\frac{1}{2}}$ is much larger than that time scale, (6.58) is approximated by (6.53).

§7. NON-LINEAR WAVE PROPAGATION; SHOCK WAVES.

The non-linear equation, now including the effects of dispersion and dissipation, is, c.f. Appendix 2,

$$\frac{\partial}{\partial t}\{S_A(c_f)\} + \tau^{-1}S_A(c_o) = 0 , \qquad (6.60)$$

where

$$S_A(c) \equiv c\,\frac{\partial \tilde{p}}{\partial x} + \frac{\partial \tilde{p}}{\partial t} + c\tilde{p}\,\frac{\partial \tilde{p}}{\partial x} + \frac{c^3}{2\omega_B^2}\frac{\partial^3 \tilde{p}}{\partial x^3} - \frac{(\gamma)^{\frac{1}{2}}\delta c^2}{2\omega_B}\frac{\partial^2 \tilde{p}}{\partial x^2} . \qquad (6.61)$$

The non-linear contribution is represented by $c\tilde{p}(\partial\tilde{p}/\partial x)$. First some general remarks about (6.60) are made. For times $t \ll \tau$ the second term in (6.60) can be left out of account and the wave is governed by

$$S_A(c_f) = 0 . \qquad (6.62)$$

This equation is the same as (2.33) with c_f instead of c_o. As mentioned in chapter 2, this equation has a stationary solution in which the pressure profile has the form as shown in Figure 16-A. The results for these steady solutions are summarized in chapter 3 for $\tau \to 0$ and in chapter 4 for $\tau \to \infty$. To this class of solutions belongs the profile observed in section A of the shock tube. This shock, a S_A shock, is determined by the highest order derivatives. The non-linear term must be balanced with the dispersion term, which gives for the shock thickness d_A

$$d_A \sim \frac{R_o}{(\beta_o)^{\frac{1}{2}}}\frac{1}{(p_1/p_o-1)^{\frac{1}{2}}} . \qquad (6.63)$$

d_A amounts to a few centimeters for not too weak shocks.

Since τ is of order $10^{-2} sec$ in most of our experiments and c_f of order $10^2 m/sec$, the relaxation process becomes effective after the wave has travelled the distance of the order of one meter. Numerical computations on equation (6.62) showed that the solution does not change appreciably after travelling a couple of centimeters. Therefore we may assume that the wave form as observed at station A, represents the steady solution of (6.62).

For times $t > \tau$, after the wave has propagated over a distance $c_f \tau$, the relaxation mechanism becomes important. Its effect on a wave is, as we have seen, diffusive. In an acoustic wave this diffusion is not resisted and the wave diffuses out ultimately. In a non-linear wave however, this diffusion is resisted by non-linear steepening. Thus a steady profile is possible in which the mechanisms are balanced. This only occurs when the shock strength is less than a certain critical value. To find these shocks we return to equation (6.60) and present a more detailed discussion on this equation.

The lowest order approximation of (6.60) is given by $\tau \to 0$, or more precisely when $t/\tau >> 1$. This approximation is

$$c_o \frac{\partial \tilde{p}}{\partial x} + \frac{\partial \tilde{p}}{\partial t} + c_o \tilde{p} \frac{\partial \tilde{p}}{\partial x} = 0 \ . \tag{6.64}$$

When the continuous solutions of this equation break down, the solutions contain discontinuities in pressure and velocity. This is what we usually call a shock. To find the structure of the shock, or the continuous solution, higher order terms need to be introduced in (6.64). This leads to

$$\frac{\partial}{\partial t}\left\{ c_f \frac{\partial \tilde{p}}{\partial x} + \frac{\partial \tilde{p}}{\partial t} + c_f \tilde{p} \frac{\partial \tilde{p}}{\partial x} \right\} +$$

$$\tau^{-1}\left\{ c_o \frac{\partial \tilde{p}}{\partial x} + \frac{\partial \tilde{p}}{\partial t} + c_o \tilde{p} \frac{\partial \tilde{p}}{\partial x} \right\} = 0 \ . \tag{6.65}$$

The highest order derivatives represent the diffusion effect on the lower order ones. Stationary solutions from (6.65) were discussed in chapter 5; we call the resulting profile a S_C shock. The appearance of such a shock can be expected when the disturbance velocity U satisfies the condition

$$c_o < U < c_f , \qquad (6.66)$$

because for a smooth profile, the wavelets at the front travel at maximum at the speed c_f, related to c_o by

$$c_f = c_o (1+\beta_o) . \qquad (6.67)$$

Furthermore the wave travels at the speed which is, for our waves (c.f. chapter 5), related to c_o by

$$\frac{U}{c_o} = (\frac{\tilde{p}_1}{p_o})^{\frac{1}{2}} .$$

Since the wave is steady, the speed of the front equals U, whence

$$\frac{p_1}{p_o} < 1+2\beta_o . \qquad (6.68)$$

This critical value for the pressure ratio was also given in chapter 5, where steady shock profiles are investigated. To the class of profiles, which appear under the condition as given in (6.68), belongs the one observed at station C of the shock tube. It is shown in Figure 16. The threshold for adiabatic circumstances is

$$\frac{p_1}{p_o} < 1 + \frac{4\gamma}{\gamma+1} \beta_o .$$

The thickness d_C of a S_C shock can be estimated with help of the non-linear term $c_o \tilde{p}(\partial\tilde{p}/\partial x)$ and the diffusion term $\tau c_o (c_f - c_o)(\partial^2\tilde{p}/\partial x^2)$ from (6.56), which must be of equal magnitude in these waves. It follows that

$$d_C \sim \frac{\tau c_o \left({}^c f^2 / c_o^2 - 1 \right)}{p_{1/p_o} - 1} , \qquad (6.69)$$

which, with a view on (6.67) and (6.68), is of order of a
meter. d_C as given by (6.69) is of the same order as d_C
given by (5.58).

When the speed of a S_C shock, U, exceeds the wave front
speed, c_f, of the higher order terms in (6.65), a new dis-
continuity appears, since the only disturbance which can
move with a velocity larger than c_f is an other shock wave.
To find the structure of this shock, higher order terms
need to be introduced in (6.65). The equation describing
these shocks is represented by (6.60). So when p_{1/p_o} ex-
ceeds $1+2\beta_o$ no entirely smooth profile or S_C shock is
possible and the diffusion resisted wave is preceeded by
a thin shock of the S_A type. The strength of this front
shock, p^*/p_o, is given in chapter 5. This is the type of
wave shown in Figure 16, a socalled S_B shock, where the
thin region of order of magnitude given by (6.63) is fol-
lowed by a much thicker region with thickness as given in
(6.69).

When $t \ll \tau$, the structure of the shock is, as we have shown,
described by the highest order derivatives in (6.60). This
solution, a S_A shock, occurs only in a finite time interval.
Ultimately the shock is described by the second term in
(6.60) and smeared out by diffusion following from the
highest order derivatives.

In this section we discussed the types of shocks and the
influence of relaxation qualitatively. Quantitave results
incorporating effects from relaxation can be found from the
steady solutions. For this the reader is referred to the
chapters 4 and 5.

§8. DISCUSSION ON RELAXATION.

The theory predicts effects of relaxation on the speed of
propagation of the wave and the form of the pressure profile.

In our opinion the change in pressure profile as demonstra-
ted in Figure 16 and amply discussed in chapter 8 is caused
by relaxation. It might be asked whether this relaxation
must be necessarily due to the dynamics of the relative
motion, and not due to a gradual transition from adiabatic
to isothermal behaviour. There is a strong argument against
this. Without a complete theory at hand, it is clear that
the two velocities of sound occuring in a thermal relaxation
theory are the isothermal sound speed c_o and the adiabatic
sound speed $(\gamma)^{\frac{1}{2}}c_o$. The argument is:
When a steady state of the shock has been reached, involving
no further steepening, the weak sound wavelets in the front
of the shock travel at the same speed as the main part of
the shock. The wavelets at the front travel at maximum at
the speed $(\gamma)^{\frac{1}{2}}c_o$. So the condition is

$$U < (\gamma)^{\frac{1}{2}}c_o \quad .$$

For the whole wave we have

$$\frac{P_1}{P_o} = \frac{U^2}{c_o^2} \quad .$$

So the condition becomes

$$\frac{P_1}{P_o} < \gamma = 1.4 \quad . \tag{6.70}$$

This was noticed also by Crespo (1969).
Our measurements clearly show as will be demonstrated later
on, that smooth profiles do appear only at a much smaller
pressure ratio, corresponding with:

$$\frac{P_1}{P_o} < 1 + \frac{4\gamma\alpha_o}{1+\gamma} \quad ,$$

following from relaxation of relative motion as given in
chapter 5. Another, though weaker, argument is that the
time necessary for thermal adjustment of the bubble, about
$0.3R_o^2/D_g$, D_g being thermal diffusivity in air, is conside-

rably larger than the relaxation time associated with resisted relative motion. The latter is estimated, as we have shown, as $R_o^2/18\nu$, which is with $\nu=10^{-5}m^2/sec$ and $D_g=18\times10^{-6}m^2/sec$ one third of the thermal relaxation time. In the following we present, as an illustration, thermal relaxation in the same way as we did for relative motion. For this we have to introduce the energy equation for a bubble and the gas in the bubble can no longer be treated as homogeneous (Chapman & Plesset, 1971). When we consider wave propagation the connected set of equations, including the energy equation can not be rearranged easily into a relaxation equation. To discuss this relaxation we therefore use a rather rough approximation based on a mean heat transfer coefficient. This coefficient depends on the gas properties and we consider the gas in the bubble to be homogeneous. From a heat balance for the bubble and the penetration thickness we find for the transfer coefficient κ

$$\kappa = 3 \; \frac{D_g}{R_o^2} \; \frac{\pi R^3 \rho_g h_{vg}}{3\pi R^2} \, , \qquad (6.71)$$

where h_{vg} is the specific heat at constant density. The factor 3 before D_g/R_o^2 is of course arbitary. This approximate heat transfer coefficient is used in the energy equation for a bubble to estimate the heat flow.
We first disregard effects following from dispersion, attenuation and relative motion of the bubble. We use the system of equations as given at the end of section 2, completed with the energy equation for the bubble

$$4\pi R^2 \kappa (T_o - T_g) = \frac{4\pi R^3 \rho_g}{3(\gamma-1)} \left\{ \frac{1}{\rho_g} \frac{dp_g}{dt} - \frac{\gamma p_g}{\rho_g^2} \frac{d\rho_g}{dt} \right\}. \qquad (6.72)$$

T_o is the temperature of the liquid, which is assumed to behave isothermal, as long as no entropy changes are considered. Using $p=p_g$ and $v=u$, then linearization of (6.18), $(6.17)-(6.19)$ and (6.20) leads to, omitting details,

$$\frac{\partial}{\partial t}\left\{\gamma c_o^2 \frac{\partial^2 \tilde{p}}{\partial x^2} - \frac{\partial^2 \tilde{p}}{\partial t^2}\right\} + \frac{3D_g}{R_o^2}\left\{c_o^2 \frac{\partial^2 \tilde{p}}{\partial x^2} - \frac{\partial^2 \tilde{p}}{\partial t^2}\right\} = 0. \qquad (6.73)$$

The linearization scheme for finding (6.73) is completely similar to that used for deriving (6.31).

For times $t \ll R_o^2/3D_g$ the solutions of (6.73) are waves propagating with speed $(\gamma)^{\frac{1}{2}}c_o$, the speed for insulated bubbles. Ultimately the waves given by (6.73) travel with c_o, the speed for which the bubbles are in thermal equilibrium with the liquid. As already mentioned the time necessary for thermal adjustment exceeds the time connected with relative motion by a factor 3.

Merely for curiosity we give the equation where both relaxation mechanisms are combined in one equation:

$$\frac{\partial^2}{\partial t^2}\left\{\gamma c_f^2 \frac{\partial^2 \tilde{p}}{\partial x^2} - \frac{\partial^2 \tilde{p}}{\partial t^2}\right\} + \tau^{-1} \frac{\partial}{\partial t}\left\{\gamma c_o^2 \frac{\partial^2 \tilde{p}}{\partial x^2} - \frac{\partial^2 \tilde{p}}{\partial t^2}\right\} +$$

$$\tau_{th}^{-1} \frac{\partial}{\partial t}\left\{c_f^2 \frac{\partial^2 \tilde{p}}{\partial x^2} - \frac{\partial^2 \tilde{p}}{\partial t^2}\right\} + \tau_{th}^{-1}\tau^{-1}\left\{c_o^2 \frac{\partial^2 \tilde{p}}{\partial x^2} - \frac{\partial^2 \tilde{p}}{\partial t^2}\right\} = 0 \quad , \qquad (6.74)$$

with

$$\tau = \frac{R_o^2}{18\nu} \text{ and } \tau_{th} = \frac{R_o^2}{3D_g} \quad .$$

(6.74) will not further be discussed.

The argument for the appearance of a thermal relaxation shock profile can also be illustrated from the stationary solution. Using continuity and momentum equations for the mixture and continuity for the gas phase, completed with the energy equation, we find in a frame moving with the shock velocity U for $y = \alpha/\alpha_o$

$$\frac{\gamma(M_o^{-2}+1) - y(1+\gamma)}{(1-y)(y-M_o^{-2})} \frac{dy}{dx} = -\frac{3D_g}{UR_o^2} \quad . \qquad (6.75)$$

The solution for y becomes

$$(1-y)^T (y-M_o^{-2})^\Xi = exp\left[- \frac{3D_g}{UR_o^2} x\right] , \qquad (6.76)$$

where

$$T = \frac{M_o^2-\gamma}{M_o^2+1} ,$$

and

$$\Xi = \frac{\gamma M_o^2-1}{1-M_o^{-2}} .$$

For $M_o^2 < \gamma$, or $U < (\gamma)^{\frac{1}{2}} c_o$, this represents a wave profile in which y decreases smoothly from 1 to M_o^{-2}.
When $M_o^2 > \gamma$ a discontinuity appears and higher order derivatives need to be involved. The equation describing a steady shock wave becomes, including effects of dispersion and dissipation, omitting non-linear derivatives:

$$\frac{d^3y}{d\eta^3} + \delta^0 \frac{d^2y}{d\eta^2} + \left\{ \gamma \frac{1-y}{y} + \frac{M_o^{-2}}{y} - 1 \right\} \frac{dy}{d\eta} +$$

$$\sigma_{th} \left\{ 1-y+M_o^{-2}- \frac{M_o^{-2}}{y} + \frac{d^2y}{d\eta^2} + \delta^0 \frac{dy}{d\eta} \right\} = 0 , \qquad (6.77)$$

where

$$\sigma_{th} = \frac{3D_g}{UR_o^2} \frac{R_o}{(3\alpha_o)^{\frac{1}{2}}} .$$

$\delta^0 = \delta_{vr}^\Delta + \delta_{ac}^\Delta$. The solution for the front part of the shock becomes for $M_o^2 > \gamma$

$$1-y \propto exp\left[\eta(1-M_{ad}^{-2})^{\frac{1}{2}}\right] ,$$

with $M_{ad}^2 = M_o^2/\gamma$. In the front part the gas phase behaves adiabatically.
For $M_o^2 < \gamma$ the smooth profile represented by (6.76) is recovered and approximated through

$$1-y \propto exp\left[\sigma_{th}\eta \frac{M_o^2-1}{\gamma-M_o^2}\right] .$$

The back side of the shock is governed by the balance of non-linear steepening and thermal relaxation. By stretching η with σ_{th} the smooth profile at the back side can be found. On this new scale the front shock can be treated as a discontinuity. In front of the discontinuity (c.f. Figure 17) the pressure is p_o, at the back side p_{ad}^*, say.
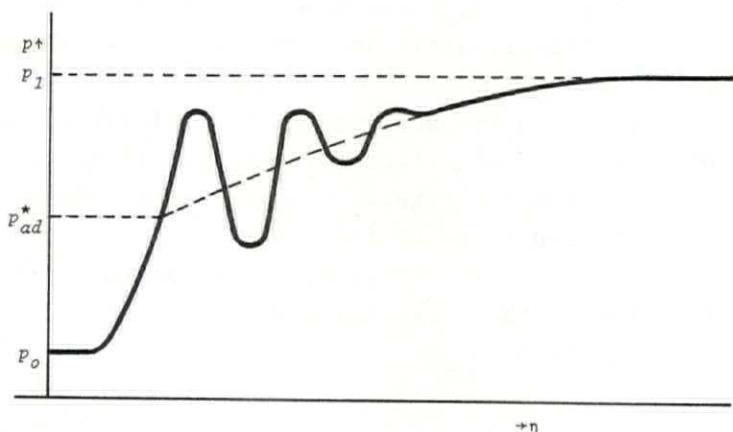
FIGURE 17. A shock profile typical for thermal relaxation.

An estimate for the value of p_{ad}^* can be found from the same argument as that for the estimate of p^* in §5 of chapter 5. In the front shock, on η scale, thermal effects are unimportant and the bubbles behave insulated. From the adiabatic theory it follows that the propagation velocity must obey equation (3.60), so

$$\frac{U^2}{c_o^2} = \frac{p_{ad}^*/p_o - 1}{1 - (p_o/p_{ad}^*)^{1/\gamma}} . \qquad (6.78)$$

However for the whole wave U^2/c_o^2 must obey the isothermal relation (3.22)

$$U^2/c_o^2 = p_1/p_o .$$

From this relation and (6.78), p_{ad} is found to be

$$\frac{p_1}{p_o} = \frac{p^*_{ad}/p_o - 1}{1 - (p_o/p^*_{ad})^{1/\gamma}} \quad , \tag{6.79}$$

and we see that p^*_{ad}/p_o only depends on p_1/p_o. For relaxation connected with relative motion, p^*/p_o depends on the gas fraction β_o and on p_1/p_o, which would appear to be the correct relation. This is again an argument against thermal relaxation.

Of course a weakness in the analysis on thermal relaxation is the rather rough approximation for the heat exchange between the bubble and the liquid. However, a more complete analysis is beyond the scope of this thesis.

For completeness we present the system of equations with thermal relaxation, without relative motion:

The continuity equation

$$\frac{\partial \rho}{\partial t} + \frac{\partial}{\partial x}(\rho u) = 0 \; .$$

The momentum equation

$$\rho \frac{\partial u}{\partial t} + \rho u \frac{\partial u}{\partial x} = - \frac{\partial p}{\partial x} \; .$$

Conservation of the number density

$$\frac{\partial n}{\partial t} + \frac{\partial}{\partial x}(nu) = 0 \; .$$

The equations for the gas in the bubble, allowing radial motion in the bubble, in terms of a radial coordinate r, with $r=R$ at the bubble surface, are:

Continuity

$$\frac{\partial \rho_g}{\partial t} + \frac{1}{r^2} \frac{\partial}{\partial r}(\rho_g r^2 v_r) = 0 \; .$$

Momentum

$$\frac{\partial v_r}{\partial t} + v_r \frac{\partial v_r}{\partial r} = - \frac{1}{\rho_g} \frac{\partial p_g}{\partial r} \ .$$

Energy

$$\frac{k_g}{r^2} \frac{\partial}{\partial r} \{ r^2 \frac{\partial T_g}{\partial r} \} = \rho_g h_{vg} \{ \frac{\partial T_g}{\partial t} + \frac{v_r}{r^2} \frac{\partial}{\partial r} (r^2 T_g) \} + \frac{p}{r^2} \frac{\partial}{\partial r} (r^2 v_r) \ ,$$

with k_g as the coefficient of thermal conductivity of the gas. The gas is assumed to be perfect

$$p_g = \rho_g T_g K_c / m \ ,$$

where K_c is the universal gas constant and m its molecular weight.

The boundary conditions are

for $r=0$: $v_r=0$ and T_g remains finite,

for $r=R$: $p(x,t)=p_g(R,x,t)$,

where we assumed dispersion effects to be small, otherwise

for $r=R$:

$$p_g(R,x,t)-p(x,t) = \rho_l \{ R \frac{d^2R}{dt^2} + \delta' \omega_B' \frac{dR}{dt} \} \ .$$

δ' is compounded of effects following from viscous dissipation and acoustic radiation associated with radial motion. The condition for the temperature can be simplified by the assumption that the liquid remains at the equilibrium temperature. This approximation is justified by the fact that the liquid has a much higher conductivity and a much lower diffusivity than the gas. The condition for the temperature becomes therefore

$$T_g(R,x,t) = T_o = constant.$$

Furthermore we have

$$\int_0^R 4\pi r^2 \rho_g \, dr = constant \, ,$$

and

$$n = \frac{3\beta}{4\pi R^3} \, .$$

§9. CONCLUSIONS.

Finally we conclude that a theory is developed which takes into account the relative motion between bubbles and liquid. The theory predicts effects both on wave speed and wave profile. The effect on wave speed is small, $(c_f - c_o)/c_o = O(\beta_o)$. This effect could hardly be measured as will be shown in chapter 8, where the experiments are discussed. The effects on the profile could be measured as shown at the beginning of this chapter in Figure 16. It will be demonstrated later on, from comparison of the experiments with theory, that there is a fair support for stating that the observed changes in wave profile are caused by the relaxation mechanism connected with relative translational motion.

CHAPTER 7.

ONE DIMENSIONAL WAVE PROPAGATION THROUGH A NON-UNIFORM
MEDIUM.

§1. *INTRODUCTION.*

This chapter deals with wave propagation through a non-
uniform mixture of bubbles and liquid. In the foregoing
chapters we treated this mixture as a uniform medium.
However, in our experiments we are faced with non-uni-
formity due to gravity.

In this chapter we want to investigate the influence of
gravity on the relations describing several types of shocks.
To get some insight we first discuss the propagation of
small amplitude waves. From this analysis we investigate
how an initial disturbance is distorted through the non-
uniformity.

Propagation of finite amplitude waves can be inferred from
the linear theory. It will be shown that no significant
modification of the shock structure needs to be carried
through. The propagation velocity of these waves depends
on the space-wise coordinate. To find how Machnumber and
pressure ratio change along this coordinate we use the
analysis of Whitham (1958).

§2. *LINEAR THEORY; WAVES OF SMALL AMPLITUDE.*

We omit dispersion, dissipation and relaxation effects.
We describe wave propagation in terms of the small pressure
disturbance $\tilde{p}$. This disturbance propagates into an undis-
turbed region with a hydrostatic pressure distribution.
The disturbance is defined as the difference between the
actual local pressure and the undisturbed one

$$\tilde{p} = p - p_o, \text{ where } \tilde{p}/p_o \ll 1 .$$

We assume the gas phase to behave isothermally. For con-

venience we recapitulate the continuity equation:

$$\frac{\partial \rho}{\partial t} + \frac{\partial}{\partial x}(\rho u) = 0 \,, \tag{7.1}$$

the momentum equation:

$$\rho \frac{\partial u}{\partial t} + \rho u \frac{\partial u}{\partial x} = - \frac{\partial p}{\partial x} - \rho_l g \,, \tag{7.2}$$

where g is the acceleration of gravity.
Continuity of the gas phase gives

$$\frac{\partial}{\partial t}(p\beta) + \frac{\partial}{\partial x}(p\beta u) = 0 \,. \tag{7.3}$$

When $\beta_o \ll 1$, convective terms such as $\rho u(\partial u/\partial x)$ in (7.2) can be neglected (c.f. chapter 2).
From (7.2) and (7.3) we find

$$\frac{d}{dt}\left(\frac{p\beta}{1-\beta}\right) = 0, \text{ or } \frac{p\beta}{1-\beta} = \text{constant} \,, \tag{7.4}$$

The sound velocity $c \equiv (dp/d\rho)^{\frac{1}{2}}$ is found from (7.4)

$$c^2 = \frac{p}{\rho_l \beta(1-\beta)} \,. \tag{7.5}$$

From (7.4) and (7.5) it follows that

$$(c\beta)^2 = \frac{p\beta}{\rho_l(1-\beta)} = \text{constant} \,, \tag{7.6}$$

throughout the region of interest.
Combining (7.1), (7.2) and (7.5) we obtain

$$\frac{1}{c^2}\frac{\partial^2 p}{\partial t^2} + \frac{\partial p}{\partial t}\frac{\partial}{\partial t}\left(\frac{1}{c^2}\right) = \frac{\partial^2 p}{\partial x^2} \,. \tag{7.7}$$

Introducing the small disturbance $\tilde{p}$ in (7.7), using $dp_o/dx = -\rho_l g$, the hydrostatic pressure distribution, linearization of (7.7) with respect to $\tilde{p}$ finally yields

$$\frac{\partial^2 \tilde{p}}{\partial t^2} = c_o^2(x) \frac{\partial^2 \tilde{p}}{\partial x^2} , \qquad (7.8)$$

where

$$c_o^2 = \frac{p_o}{\rho_l \beta_o (1-\beta_o)} .$$

From (7.8) we see that the signal which propagates is the difference between the actual and the undisturbed pressure. For not too large wave length a socalled short wave approximation for $\tilde{p}$ can be found, when the disturbance is periodic in t.

The equation for $\tilde{p}$ becomes with

$$\tilde{p} = exp(i\omega t) \psi ,$$

$$\frac{d^2 \psi}{dx^2} + \frac{\omega^2}{c_o^2(x)} \psi = 0 . \qquad (7.9)$$

Using the W.K.B.J. approximation (Morse & Fesbach, 1953) with the condition that

$$\frac{1}{c_o} \frac{dc_o}{dx} << \frac{\omega}{c_o} ,$$

we find for $\tilde{p}$

$$\tilde{p} \propto exp(i\omega t) \left\{ \frac{c_o(x)}{\omega} \right\}^{\frac{1}{2}} exp\left[\pm i \int \frac{c_o}{\omega} dx \right] . \qquad (7.10)$$

To a sufficient level of accuracy (7.6) can also be written as

$$c \propto p .$$

With this we see that the amplitude of $\tilde{p}$ changes with p_o
as

$$p_o^{\frac{1}{2}} \, ,$$

and the wave number as p_o.
For a characteristic length of about *2m* these variations
are negligible.

§3. NON-LINEAR WAVE PROPAGATION.

Using $\tilde{p}=p-p_o$ and $c^2 \approx c_o^2(1+2\tilde{p}/p_o)$, *(7.7)* becomes

$$\frac{\partial^2 \tilde{p}}{\partial t^2} - \frac{2}{p_o} \frac{\partial}{\partial t}\left(\tilde{p} \frac{\partial \tilde{p}}{\partial t}\right) = c_o^2 \frac{\partial^2 \tilde{p}}{\partial x^2} \, . \qquad (7.12)$$

The second term in the left-hand side is the leading non-
linear term of the steepening of the wave by compression
(c.f. chapter 2). *(7.12)* once more shows that the signal
which propagates is the difference between the actual and
the undisturbed pressure. However we want to find out in
what way a disturbance, propagating in one direction, is
distorted by gravity.
For this we write

$$p = p_o(1+\epsilon p'), \text{ with } \epsilon p_o p' = \tilde{p} \, ,$$
$$\beta = \beta_o(1+\epsilon \beta'), \text{ with } \epsilon \beta_o \beta' = \tilde{\beta} \, ,$$
$$u = \epsilon c_o \beta_o u' \, , \qquad\qquad (7.13)$$
$$x = x'c_o \tau \, ,$$
$$t = t'\tau \, .$$

p_o and β_o are given functions of x connected with the undis-
turbed hydrostatic pressure distribution.
From *(7.13)* it follows that

$$\frac{\partial}{\partial x} = \frac{1}{c_o \tau}\left\{1- \frac{x}{c_o} \frac{\partial c_o}{\partial x}\right\} \frac{\partial}{\partial x'} \, .$$

With help of (7.6), this can be written as

$$\frac{\partial}{\partial x} = \frac{1}{c_o \tau}\left\{1+ \frac{\rho_l g(1-2\beta_o)x}{P_o}\right\} \frac{\partial}{\partial x'} .$$ (7.14a)

Further we define

$$\left\{1+ \frac{\rho_l g(1-2\beta_o)x}{P_o}\right\} \frac{\partial}{\partial x'} \equiv \frac{\partial}{\partial\theta} .$$ (7.14b)

(7.13), (7.14a) and (7.14b) are introduced in the equations (7.1)-(7.3). Terms of order ε^2 and lower are retained, terms of order $\beta_o \varepsilon^2$ are discarded. The transformed set of equations becomes,

$$\frac{\partial u'}{\partial\theta} - \frac{\partial\beta'}{\partial t'} = \frac{\partial u'\beta_o}{\partial\theta} ,$$ (7.15)

$$\frac{\partial u'}{\partial t'} + \frac{\partial p'}{\partial\theta} = \frac{\rho_l g c_o \tau}{P_o} p' ,$$ (7.16)

$$\frac{\partial p'}{\partial t'} + \frac{\partial\beta'}{\partial t'} = - \beta_o \frac{\partial u'}{\partial\theta} + \varepsilon \frac{\partial p'\beta'}{\partial t'} .$$ (7.17)

From (7.17) we see that $p'+\beta'=0(\varepsilon,\beta_o)$ and with this we find from (7.15) and (7.17)

$$\frac{\partial u'}{\partial\theta} + \frac{\partial p'}{\partial t'} = \frac{\partial u'\beta_o}{\partial\theta} - \beta_o \frac{\partial u'}{\partial\theta} + \varepsilon \frac{\partial p'^2}{\partial t'} .$$ (7.18)

The right-hand side of (7.16) is assumed to be small, of $0(\varepsilon,\beta_o)$. From Appendix 2 it follows that

$$\frac{\partial u'}{\partial\theta} + \frac{\partial u'}{\partial t'} - \frac{\partial p'}{\partial\theta} - \frac{\partial p'}{\partial t'} = 0(\beta_o^2, \varepsilon^2, \varepsilon\beta_o) .$$ (7.19)

Substituting (7.19) into (7.16) and (7.18) we obtain

$$\frac{\partial p'}{\partial t'} + \frac{\partial p'}{\partial \theta} = \frac{\rho_l g c_o \tau}{2 p_o} p' - \varepsilon p' \frac{\partial p'}{\partial \theta} . \qquad (7.20)$$

(7.20) becomes in the laboratorium frame

$$\frac{\partial \tilde{p}}{\partial t} + c_o \frac{\partial \tilde{p}}{\partial x} + c_o \frac{\tilde{p}}{p_o} \frac{\partial \tilde{p}}{\partial x} + \frac{\rho_l g c_o}{2 p_o} \tilde{p} = 0 . \qquad (7.21)$$

The influence of gravity on the signal is given by a c_o dependent on x and the last term in the left-hand side of (7.21). The ratio of this term and the non-linear term is

$$\frac{\rho_l g}{2 (\partial p / \partial x)} , \qquad (7.22)$$

the ratio between the acceleration due to gravity and the local acceleration. When we use as a characteristic length the thickness of a S_C shock, (7.22) becomes

$$\frac{\rho_l g d_C}{2 (p_1 - p_o)} . \qquad (7.23)$$

With $d_C \sim U \tau$, the magnitude of (7.23), for our experimental circumstances, is one third at maximum. Thus (7.21) reduces to

$$\frac{\partial \tilde{p}}{\partial t} + c_o \frac{\partial \tilde{p}}{\partial x} + c_o \frac{\tilde{p}}{p_o} \frac{\partial \tilde{p}}{\partial x} = 0 . \qquad (7.24)$$

As mentioned before, this equation shows that the signal which propagates is the difference between the actual and undisturbed pressure. Addition of a diffusion term in the right-hand side of (7.24) would permit a steady solution, a S_C shock, if c_o and p_o were constants, as in the equations of chapter 6 (c.f. equation 6.64). Our analysis of shock waves sofar was based on the existence of steady profiles propagating with velocity U not dependent on x. In our experiments we measured $\tilde{p}$ as a function of time. With the

transformation $t=x/U$, where U is the propagation velocity averaged over a couple of centimeters, we were able to interprete the time depen.'ent profile in terms of shock thickness and wave length. However, as can be seen from (7.21), the propagation velocity depends on x and in fact steady solutions can no longer be found. So the question is raised: when using the transformation $t=x/U$ for inter-pretation of the experiments, how large is the introduced in accuracy? For this we return to equation (7.20). When we neglect the first term in the right-hand side, we have

$$\frac{\partial p'}{\partial t'} + \frac{\partial p'}{\partial \theta} + \epsilon p' \frac{\partial p'}{\partial \theta} = 0 \ . \qquad (7.25)$$

Adding a diffusion term of the type $\delta(\partial^2 p'/\partial \theta^2)$ to (7.25) gives

$$\frac{\partial p'}{\partial t'} + \frac{\partial p'}{\partial \theta} + \epsilon p' \frac{\partial p'}{\partial \theta} = \delta \frac{\partial^2 p'}{\partial \theta^2} \ . \qquad (7.26)$$

Steady shock-type solutions of (7.26) can be found in a frame (X, t'), where

$$X = \theta - (1+\chi)t' \ .$$

χ is a constant which follows from the conditions ahead and behind the shock.
With this a profile measured in terms of t' can be trans-formed in the θ-plane by

$$dt' = \frac{d\theta}{1+\chi} , \qquad (7.27)$$

θ is a known function of x (c.f. 7.14a and 7.14b). So, with $t'=t/\tau$, a time-wise measured profile can be transformed in a space-wise dependent profile.
Using $d\theta=dx/c_o\tau$, we obtain from (7.27)

$$t = \int \frac{dx}{(1+x)c_o} \ . \tag{7.28}$$

From $c_o \propto p_o$, the dependence of c_o on x is given by

$$c_o = c_{oo} \left\{ 1 - \frac{\rho_l g x}{p_{oo}} \right\} \ , \quad x \leqslant o , \tag{7.29}$$

where quantities with subscript oo are defined at $x=0$, located at the back side of the shock.
Substitution of (7.29) into (7.28) gives

$$t = \frac{x}{(1+x)c_o} \left[-\frac{p_{oo}}{\rho_l g x} \ ln \left\{ 1 - \frac{\rho_l g x}{p_{oo}} \right\} \right] \ . \tag{7.30}$$

Thus the accuracy of the transformation $t=x/U$, with $U=$ constant, can be approximated by the magnitude of the quantity between the square brackets in (7.30). For values of x of the order of the thickness of a S_C shock this quantity can be approximated by

$$\left(1 - \frac{\rho_l g x}{2 p_{oo}} \right) \ . \tag{7.31}$$

(7.31) represents the correction factor of the transformation $t=x/U$. This correction would lead to a slightly stretching of a x-dependent profile for a constant value of U. Neglecting this stretching or taking (7.31) equal to unity we introduce an error which is not larger than the accuracy obtained in the experiments. From this we conclude that no correction for gravity on the structure of the shock needs to be carried through. For comparison with the experiments it is sufficient to use local values for p_o and β_o.
Due to the length of the shock tube we were able to measure U as a function of x. From the Whitham rule we will derive equations describing the dependence of the propagation velocity on x.

§4. *THE WHITHAM RULE.*

In this section we investigate the dependence of the shock
wave velocity U on the coordinate along the shock tube.
Shock wave propagation through a non-uniform medium is
recently studied by Strachan e.a. (1970) and Nunzatio &
Walsh (1972), who extent the theory of Whitham. However,
with a view to the accuracy of our experiments we base our
analysis on the rather simple relations following from the
Whitham rule. This rule gives U as a function of x. In the
present theory we are not dealing with the structure of
the shock. Effects of relative translational motion on the
propagation velocity are small. Thus relative translational
motion is left out of account in the pertinent equations.
For convenience we recapitulate these equations, which
will be written in the characteristic form.
The equations are

$$\frac{\partial \rho}{\partial t} + \frac{\partial}{\partial x}(\rho u) = 0 , \qquad (7.32)$$

$$\rho \frac{\partial u}{\partial t} + \rho u \frac{\partial u}{\partial x} = -\frac{\partial p}{\partial x} - \rho g , \qquad (7.33)$$

$$\frac{\partial p}{\partial t} + u \frac{\partial p}{\partial x} - c^2 \frac{\partial \rho}{\partial t} - c^2 u \frac{\partial \rho}{\partial x} = 0 , \qquad (7.34)$$

(7.33) and *(7.34)* are taken together to

$$\frac{\partial p}{\partial t} + \frac{\partial p}{\partial x}(u \pm c) \pm \rho c \left\{ \frac{\partial u}{\partial t} + (u \pm c) \frac{\partial u}{\partial x} \right\} \pm \rho c g = 0 , \qquad (7.35)$$

or

$$\left\{ \frac{\partial p/\partial t}{u \pm c} + \frac{\partial p}{\partial x} \right\} \pm \rho c \left\{ \frac{\partial u/\partial t}{u \pm c} + \frac{\partial u}{\partial x} \right\} \pm \frac{\rho c g}{u \pm c} = 0 . \qquad (7.36)$$

And in characteristic form

$$dp + \rho c\, du + \frac{\rho c g}{u+c}\, dx = 0 \quad \text{on} \quad \frac{dx}{dt} = u+c , \qquad (7.37a)$$

$$dp - \rho c du - \frac{\rho c g}{u-c} dx = 0 \quad \text{on} \quad \frac{dx}{dt} = u-c . \qquad (7.37b)$$

The Whitham rule states that when the relevant equations are written first in the characteristic form, the differential relations, which must be satisfied along a characteristic, can be applied to the flow quantities just behind the shock wave. Together with the shock relations this rule determines the motion of the shock wave. The shock is treated as a discontinuity in this theory. For S_A and S_B shocks this is a reasonable approximation because pertinent quantities changes on a scale, d_A, which is much smaller than the scale where undisturbed quantities change due to gravity. So the Hugoniot relations, relating quantities far in front and far behind the shock, still apply. For a S_C shock, being much thicker, we assume the Hugoniot relations to hold, of course within the order of approximation determined by a constant value of U.

The differential equation of interest is, $(7.37b)$,

$$dp_1 - \rho_1 c_1 du_1 = \frac{\rho_1 c_1 g}{u_1 - c_1} dx , \qquad (7.38)$$

where subscript 1 indicates quantities just behind the shock. With the Whitham rule we apply the differential relation (7.38) along a characteristic just behind the shock wave. Together with the Hugoniot relations we are able to describe U or related quantities in terms of the equilibrium quantities p_o and β_o. First we present the analysis for isothermal circumstances and summarize afterwards the relations for the adiabatic theory. We use the relations as derived in chapter 3.

For u_1, as given in (3.19)

$$u_1 = - \beta_o U(1-M_o^{-2}) . \qquad (7.39)$$

For p_1, as given in (3.22)

$$P_1 = P_o M_o^2 = \frac{P_o \beta_o}{1-\beta_o} \frac{M_o^2}{\beta_o} (1-\beta_o) \,, \qquad (7.40)$$

where $P_o \beta_o / (1-\beta_o)$ can be treated as a constant. For small enough values of β_o, $P_o \beta_o$ is approximately a constant. Using (2.6), (3.23) and (7.40) we find for $\rho_1 c_1$

$$\rho_1 c_1 = \rho_l (1-\beta_1) \left(\frac{dp}{d\rho}\right)^{\frac{1}{2}} = \rho_l (1-\beta_1) \left\{\frac{P_1}{\rho_l \beta_1 (1-\beta_1)}\right\}^{\frac{1}{2}} =$$

$$\rho_l \left\{\frac{P_o \beta_o}{\rho_l (1-\beta_o)}\right\}^{\frac{1}{2}} M_o^2 \frac{1-\beta_o}{\beta_o} \,. \qquad (7.41)$$

With the help of (3.21) and (3.22), U becomes

$$U = M_o c_o = M_o \left\{\frac{P_o}{\rho_l \beta_o (1-\beta_o)}\right\}^{\frac{1}{2}} = \frac{M_o}{\beta_o} \left\{\frac{P_o \beta_o}{\rho_l (1-\beta_o)}\right\}^{\frac{1}{2}} \,. \qquad (7.42)$$

Substitution of (7.39)-(7.42) in (7.38) gives, using $\alpha_o = \beta_o / (1-\beta_o)$,

$$P_o \alpha_o \, d\left(\frac{M_o^2}{\alpha_o}\right) + P_o \alpha_o \, \frac{M_o^2}{\alpha_o} \, d\left(M_o - \frac{1}{M_o}\right) = -$$

$$\frac{M_o \rho_l g dx}{M_o + \alpha_o (M_o^2 + M_o - 1)/M_o^2} \,, \qquad (7.43)$$

where $P_o \alpha_o$ is a constant and α_o is a known function of x. With $\alpha_o \ll 1$ and $dp_o / dx = -\rho_l g$, (7.43) reduces to

$$\frac{M_o + 1}{M_o - 1} \frac{dM_o}{dx} - \frac{\alpha_o}{P_o \alpha_o} \rho_l g = 0 \,. \qquad (7.44)$$

We obtain for the relation between M_o and p_o:

$$(M_o - 1)^2 \, exp[M_o] \propto \frac{1}{P_o} \,, \qquad (7.45)$$

and for $M_o^2-1<<0(10^{-1})$.

$$M_o^2-1 \propto \left(\frac{1}{p_o}\right)^{\frac{1}{2}} . \tag{7.46}$$

(7.46) is similar to Chisnell's result for a weak shock moving in a duct with changing area (Chisnell, 1955). Using M_{oo} defined at $x=o$, (7.45) and (7.46) become

$$\left\{\frac{M_o-1}{M_{oo}-1}\right\}^2 exp(M_o-M_{oo}) = \left\{1 - \frac{\rho_l g x}{p_{oo}}\right\}^{-1} \tag{7.47}$$

and

$$\frac{M_o^2-1}{M_{oo}^2-1} = \left\{1- \frac{\rho_l g x}{p_{oo}}\right\}^{-\frac{1}{2}} . \tag{7.48}$$

To find relations for adiabatic circumstances we use equations, which can be found at the end of chapter 3:

$$\left.\begin{array}{l} p_1 = \alpha_1^{-\gamma} p_o \alpha_o^{\gamma} \\[2mm] \rho_1 c_1 = \rho_l \alpha_1^{-(\gamma+1)/2} \left\{\frac{\gamma p_o \alpha_o^{\gamma}}{\rho_l}\right\}^{\frac{1}{2}} \\[2mm] U_1 = -\left\{\alpha_o-\alpha_1(1+\alpha_o)\right\} \left|\frac{(\alpha_o/\alpha_1)^{\gamma}-1}{1-\alpha_o/\alpha_1}\right|^{\frac{1}{2}} \alpha_o^{-(\gamma+1)/2} \left\{\frac{\gamma p_o \alpha_o^{\gamma}}{\rho_l}\right\}^{\frac{1}{2}} . \end{array}\right\} \tag{7.49}$$

Substitution of (7.49) into (7.38) gives, using $p_o \alpha_o^{\gamma} =$ constant, a first-order equation for $\alpha_o/\alpha_1(x)$. The solution of which will require a numerical integration. However in the case of weak shocks, $\alpha_o/\alpha_1-1=0(10^{-1})$, we finally obtain

$$\alpha_o/\alpha_1 - 1 \propto \beta_o^{\gamma/2} . \tag{7.50}$$

With

$$M_o^2 = \frac{(\alpha_o/\alpha_1)^{\gamma}-1}{1- \alpha_o/\alpha_1} ,$$

(7.50) can also be written as

$$\frac{M_o^2}{\gamma} - 1 \propto \left(\frac{1}{p_o}\right)^{\frac{1}{2}} . \tag{7.51}$$

Using M_{oo} defined at $x=o$, (7.51) becomes

$$\frac{M_o^2-\gamma}{M_{oo}^2-\gamma} = \left\{1 - \frac{\rho_l g x}{p_{oo}}\right\}^{-\frac{1}{2}} . \tag{7.52}$$

§5. *CONCLUSIONS.*

In this chapter we investigated wave propagation in a non-uniform mixture of liquid and bubbles. We found that the quantity which propagates is the difference between the actual and equilibrium pressure. Effects of gravity on the shock structure are sufficiently incorporated by using local quantities determined by the equilibrium pressure distribution. By using a steady frame of reference we introduced an error, the neglect of which is justified with a view at the experimental accuracy.

From the Whitham rule we found the dependence of the shock propagation velocity on the coordinate along the shock tube.

CHAPTER 8.

EXPERIMENTS; COMPARISON WITH THEORY.

§1. *INTRODUCTION.*

In this chapter we present experimental results and compare
these with theoretical predictions. First a description of
the experimental set up is given. Then the shock propagation
velocity is investigated. The various shock structures such
as S_A, S_B and S_C shocks are compared with theory. Finally
the relations following from the Whitham rule are discussed.

§2. *EXPERIMENTAL SET UP.*

The experiments were carried out in a vertically mounted
cilindrical shock tube with an inner diameter of $5.5 \times 10^{-2} m$
and an outer diameter of $6.5 \times 10^{-2} m$. Two types of these shock
tubes are used. One has a length of about $4.5m$ and consists
of a stainless steel part in which the pressure transducers
are mounted. The upper part of the tube consists of perspex
for determining the gas fraction. The lower part also con-
sists of perspex for photographing the bubbles. The choice
of the stainless steel part was done for minor purposes
such as a reliably mounting of the pressure transducers. The
other shock tube has a length of about $2.5m$ and consists com-
pletely of perspex. Both shock tubes are shown in Figure 18A
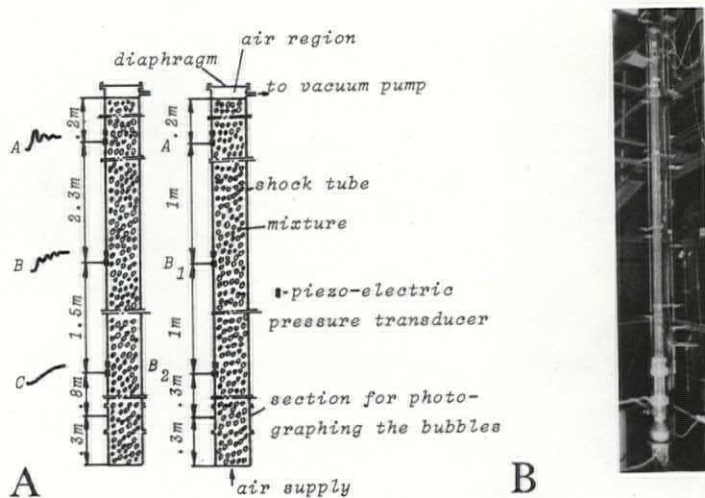
FIGURE 18. A-Experimental set up. B-Photograph of the short shock tube.

where the important dimensions are given. The distance
from the top of the mixture to the first pressure trans-
ducer is only approximative, it serves to indicate where
the different stations are located. The exact values will
be given later on. In Figure 18B a photograph of the short
shock tube is shown.

The experiments were done as follows. The tube is almost
completely filled with an aqueous solution of glycerine
leaving a small air occupied region at the top. An aqueous
solution was used to keep effects from buoyancy as small
as possible. The bulk of the experiments was carried out
with an aqueous solution of *50%* glycerine with a kinematic
viscosity of $.7 \times 10^{-5} m^2/sec$ and a density of *1126 kg/m³*. In
such a solution the velocity of a free rising bubble with
a radius of $10^{-3} m$ is about $10^{-1} m/sec$ (See also Haberman &
Morton 1953). Subsequently the tube is sealed at the top
with a diaphragm as shown in Figure 19A.
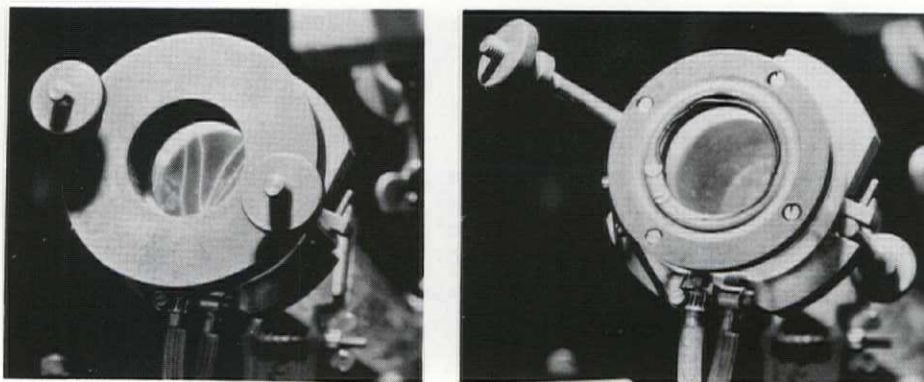
A   B

FIGURE 19. A- The top of the tube sealed with a diaphragm. B- Equip-
ment for puncturing the diaphragm by a hot wire.

A plastic diaphragm with a thickness of about $2.5 \times 10^{-6} m$
is used. The pressure below the diaphragm is, by evacu-
ating the air occupied region, decreased below atmosphe-
ric pressure. Bubbles are supplied through a system of
many capillary tubes at the bottom of the shock tube as

shown in Figure 20.
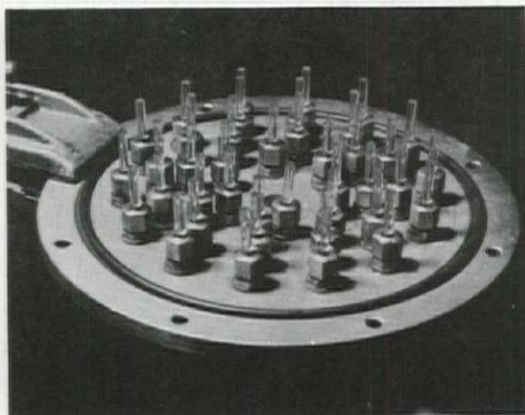
<div style="text-align:center">A   B</div>

FIGURE 20. A- The bottom of the shock tube. The cone enables the moun-
ting of the bottom plate with a number of capillary tubes. B- Detail
of the bottom plate. The capillary tubes have an inner diameter of
$10^{-4}m$, an outer diameter of $5 \times 10^{-3}m$ and a length of $2.5 \times 10^{-2}m$.

The device by which the bubbles are supplied guarantees
that in one experiment the bubbles have locally almost all
the same size. When the mixture is stationary the mean volu-
metric gas content is determined by measuring the increase
in length of the liquid column as a result of the air supply.
From this mean gas content, $\bar{\beta}_o$, the local value of β_o can
be determined from the equilibrium hydrostatic pressure
distribution[⊗]. Also a photograph of the mixture is taken
at a station marked in Figure 18. From this photograph the
bubble size is determined[⊗].

[⊗]
The gas phase is assumed to behave isothermal. With $\beta_o \ll 1$ we have $p_o \beta_o$
is constant. The equilibrium pressure p_o, as a function of x, is:
$p_o = p_{oo} - \rho_l g x$, where $x \leqslant 0$ and p_{oo} is at $x=0$, the top of the mixture. Then
the mean gas content $\bar{\beta}_o$ becomes

$$\bar{\beta}_o = \frac{p_o \beta_o}{\rho_l g L} \, \ln\left\{ 1 + \frac{\rho_l g L}{p_{oo}} \right\} ,$$

where L is the length of the mixture column.
The local value of R_o follows from the isothermal relation

$$R_o = R_{photo} \left\{ \frac{p_{photo}}{p} \right\}^{1/3}.$$

In Figure 21 such a photograph is shown.
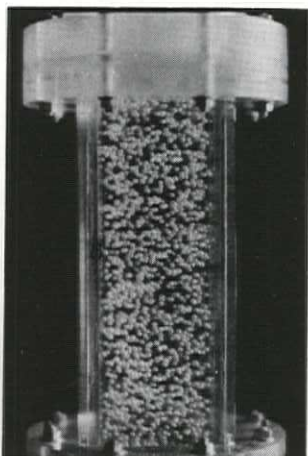
FIGURE 21. Photograph of a liquid-bubble mixture before the passage of a shock wave. $R_{photo}=1.06\times10^{-3}m$, $\bar{\beta}_o=3.2\%$.

After determination of the gas content and the bubble size, a shock wave is produced by puncturing the diaphragm covering the top of the tube there by admitting air of atmospheric pressure. The device for puncturing the diaphragm is shown in Figure 19B. The profile of the shock wave was at its passage along the tube recorded at several stations as indicated in Figure 18. The pressure was recorded by means of piezo-electric pressure transducers. Two of them, mounted in the shock tube wall, are shown in Figure 22.
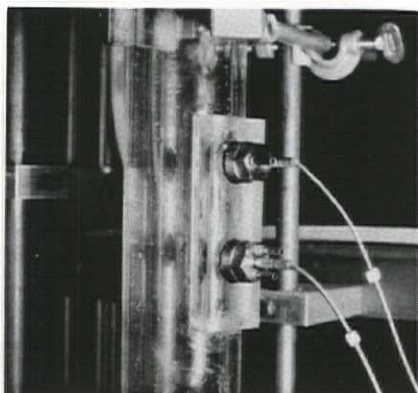
FIGURE 22. Piezo-electric pressure transducers, $5\times10^{-2}m$ apart, mounted in the wall of the shock tube.

The sensitivity of a pressure transducer is about 150×10^{-12} Coulomb/atm with a resolution of 2×10^{-4} atm and an acceleration sensitivity of 2×10^{-3} atm/g. The natural frequency of the transducers is about 5×10^{4} sec^{-1}. The signal from the transducers was amplified in an adapted charge amplifier and afterwards visualized on a storage oscilloscope. Typical pressure recordings were shown in foregoing chapters. To find out which part of the signal was due to the acceleration of the tube wall, we measured the tube wall acceleration by means of an accelerometer with a sensitivity of 20×10^{-12} Coulomb/g. A typical acceleration recording is shown in Figure 23.
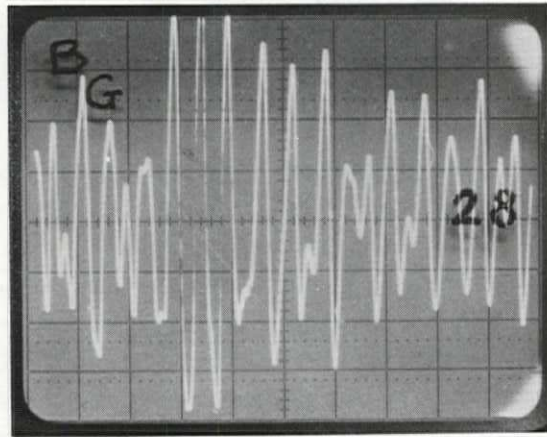
FIGURE 23. An acceleration recording of the tube wall. The peak-peak value represents 80×10^{-12} Coulomb.

From the recorded peak-peak value and the known acceleration sensivity of the pressure transducers it follows that for pressure ratio's smaller than 5, effects from acceleration can be neglected.

To investigate the influence of relaxation associated with resisted translational motion the viscosity of the liquid is changed by using different aqueous solutions. Besides the mentioned solution we used tap water with $\nu_l = 10^{-6}$ m^2/sec and $\rho_l = 1000 kg/m^3$, a solution of 70% glycerine with $\nu_l = 3 \times 10^{-5}$ m^2/sec and $\rho_l = 1170 kg/m^3$ and a solution of 85% glycerine with $\nu_l = 1.1 \times 10^{-4}$ m^2/sec and $\rho_l = 1215 kg/m^3$.

During the experiments it was noticed using the 70% and

85% solutions, that in the tube with a length of 4.5m the free rising bubbles clustered together after a distance of about 3m. This is the reason for using also a short shock tube with a length of about 2.5m. The socalled high viscosity experiments were carried out in the shorter tube.

§3. *PROPAGATION VELOCITY; U.*

This velocity is detected at the various stations along the tube. U is determined from the time interval between the passage of the first and the second transducer as shown in Figure 22. These transducers are $5 \times 10^{-2} m$ apart. In some experiments the distance between these transducers was .25m. As follows from the analysis in chapter 7 variation of U within this distance can be neglected.

From the theory it was found that relaxation predicts effects on the speed of the shock wave and on its structure. The effects on the structure will be discussed in following sections. In this section we pay attention to relaxation effects on the propagation velocity. Because of this it is of interest with which relation for U^2/c_o^2 the experiments agree.

The theoretical expressions for U^2/c_o^2 are, c.f. chapters 4 and 5,

isothermal

> *not resisted*

$$\frac{U^2}{c_o^2} = \frac{p_1}{p_o}\left\{1 + \alpha_o\left(1 + \frac{p_o}{p_1}\right)\right\} ,$$

$$(8.1)$$

> *resisted*

$$\frac{U^2}{c_o^2} = \frac{p_1}{p_o} ,$$

$$(8.2)$$

adiabatic

> *not resisted*

$$\frac{U^2}{c_o^2} = \frac{p_1/p_o - 1}{1 - (p_o/p_1)^{1/\gamma}} \left\{ 1 + \alpha_o (1 + (p_o/p_1)^{1/\gamma}) \right\} , \qquad (8.3)$$

resisted

$$\frac{U^2}{c_o^2} = \frac{p_1/p_o - 1}{1 - (p_o/p_1)^{1/\gamma}} . \qquad (8.4)$$

The value for c_o is given by

$$c_o^2 = \frac{p_o (1 + \alpha_o)^2}{\rho_l \alpha_o} . \qquad (8.5)$$

The different theoretical and experimental values for U^2/c_o^2 are collected in Figure 24, for the isothermal and adiabatic theory respectively.
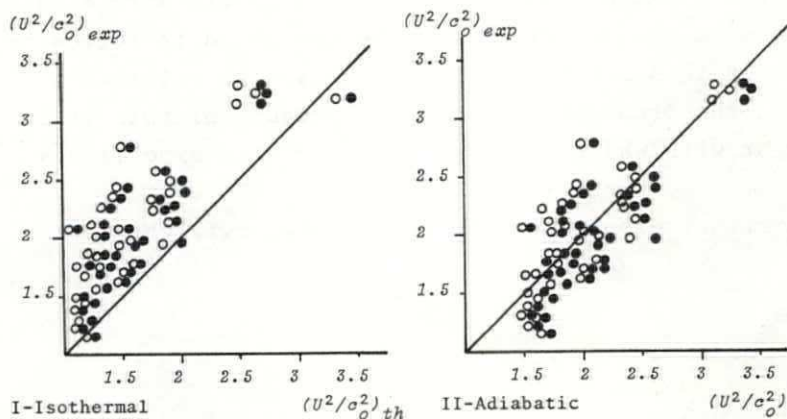
FIGURE 24. In this Figure the different theoretical and experimental values for U^2/c_o^2 are collected for region A. When either the isothermal (resisted, not resisted) or adiabatic (resisted, not resisted) theory fits reasonably in with the experiments, the marks representing that theory would be close to the solid line.
● *exp - not resisted, o exp - resisted.*

The experimental values were obtained in region A of the shock tube (Figure 18) where, for not too large values of the viscosity, x is sufficiently small with respect to $c_f \tau$. This is the distance, as indicated in chapter 6, in which

relaxation becomes effective. In Table A-5, Appendix 3, the values for P_1/p_o, p_o, α_o and U are given. The distance from the top of the mixture to the station where these quantities and the pressure profile were obtained is indicated by x. For each experiment the measured value of U^2, divided by c_o^2, is found as $(U^2/c_o^2)_{exp}$ along the vertical axis. The two different values for the quantity U^2/c_o^2, as given by (8.1) and (8.2) or by (8.3) and (8.4) are registered along the horizontal axis in Figure 24-I and Figure 24-II respectively. When either the isothermal(resisted, not resisted) or adiabatic(resisted, not resisted) theory would fit in with the experiments the marks representing the pertinent theory would be close to the solid line. The conclusion we draw from Figure 24 is that the adiabatic marks are definitely more close to the solid line than the isothermal ones. The difference between the values for U^2/c_o^2 of waves resisted by friction and waves not resisted by friction is, as follows from inspection of Figure 24, of the order of magnitude of the scatter. Thus in this respect the experiments provide no verification.

§4. *THE STRUCTURE OF* S_A *SHOCKS*.

In Figure 25 a typical pressure recording for region A is shown.
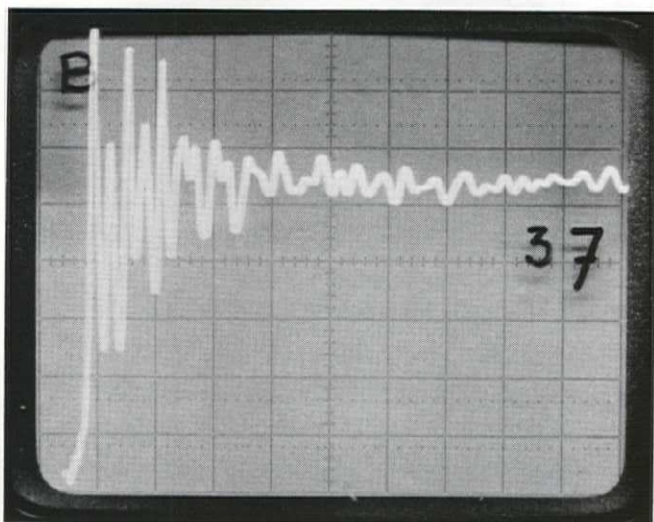
FIGURE 25. A pressure recording typical for region A. $P_1/p_o=1.79$, $\beta_o=3.21\%$, $R_o=1.33\times10^{-3}m$, $U=66m/sec$, $d_A=3.3\times10^{-2}m$ and $\Lambda=3.3\times10^{-2}m$.

This record, and other records to be shown as well, represent the pressure as a function of time at a given station. Comparison with theory, where the pressure is given in terms of a space-wise variable, is possible by the transformation $t=x/U$. U is for each record the propagation velocity. From records as shown in Figure 25 shock thickness d_A, wave length Λ, attenuation of the waves and the shock strength p_1/p_o are determined. Here the expressions for these quantities are summarized. With a view to the discussion of the foregoing section, the expressions for resisted bubble velocity are presented.

The expression for the shock thickness is

$$d_A = \frac{R_o}{(3\alpha_o)^{\frac{1}{2}}} \frac{\ln 20}{(1-\gamma M_o^{-2})^{\frac{1}{2}} - \delta_o^{\Delta}/2} \, , \qquad (8.6)$$

where

$$M_o^2 = \frac{p_1/p_o - 1}{1 - (p_1/p_o)^{1/\gamma}} \, . \qquad (8.7)$$

For the wave length Λ we have

$$\Lambda = \frac{R_o}{(3\alpha_o)^{\frac{1}{2}}} \frac{2\pi y_1^{2/3}}{(\gamma M_o^{-2} y_1^{-\gamma} - y_1)^{\frac{1}{2}}} \, , \qquad (8.8)$$

where

$$y_1 = \left(\frac{p_o}{p_1}\right)^{1/\gamma} \, .$$

The number of waves, N, after which the amplitude of the waves decreases by a factor e^{-1} is

$$N = \frac{(\gamma M_o^{-2} y_1^{-\gamma} - y_1)^{\frac{1}{2}}}{\pi y_1^{2/3} \delta_1^{\Delta}} \, . \qquad (8.9)$$

The shock strength p_1/p_o follows from the sum of the pressure jump across the shock and p_o, divided by p_o.
The choise of expressions following from the adiabatic theory is based on the fact that for region A the propagation velocity is close to the one following from adiabatic theory. Further we define

$$W_1 \equiv \frac{d_A(3\alpha_o)^{\frac{1}{2}}}{R_o}\left\{(1-\gamma M_o^{-2})^{\frac{1}{2}}-\delta_o^\Delta/2\right\} , \qquad (8.10)$$

and

$$W_2 \equiv \frac{\Lambda(3\alpha_o)^{\frac{1}{2}}}{R_o}\frac{(\gamma M_o^{-2}y_1^{-\gamma}-y_1)^{\frac{1}{2}}}{y_1^{2/3}} . \qquad (8.11)$$

It follows from (8.6) and (8.8) that W_1 and W_2 must be constants. In Appendix 3, Table A-5, the experimental values for β_o, p_o, R_o, d_A, Λ, p_1/p_o, W_1 and W_2 are given. The values of W_1 and W_2 averaged over all experiments are 3.8 and 5.8 respectively. The standard deviation in both quatities is about 1. The magnitude of this deviation is for the greater part restricted to the error in the determination of R_o. This error is about 20%. In the Figures A3-1 and A3-2, Appendix 3, the distribution functions for W_1 and W_2 are given respectively. The mean values are indicated. The theoretical value for W_1 is $ln20$ (c.f. eq. 8.6). This value follows from the definition of d_A. d_A is defined as the distance between the points where the pressure starts to rise, $p=p_o+.05(p_1-p_o)$, and the equilibrium pressure $p=p_1$ at the back side of the shock. In the experiments the point where the pressure starts to rise was taken more close to p_o. So the mean value of W_1 exceeds $ln20$. The experimental values of N agree reasonably well with the theoretical predicted values.
To test the influence of some parameters in (8.6) we selected some experiments for which R_o is constant.

In Figure 26 $d_A(3\alpha_o)^{\frac{1}{2}}$ is drawn as a function of

$$\frac{W_1}{(1-\gamma M_o^{-2})^{\frac{1}{2}}-\delta_o^{\Delta}/2} \quad,$$

for constant values of R_o.
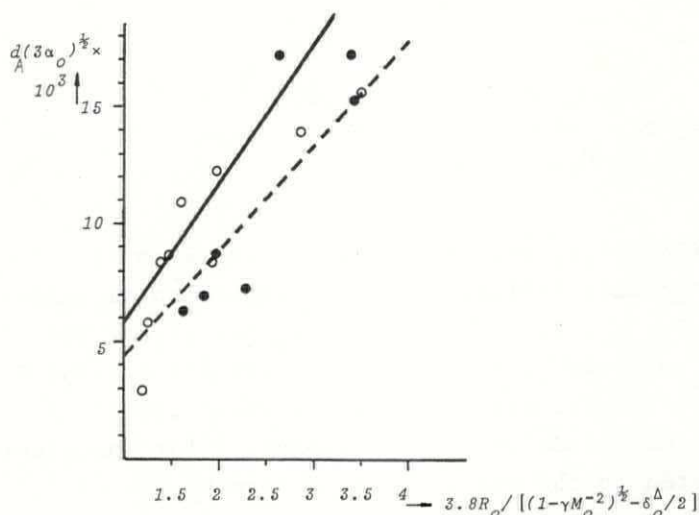
FIGURE 26. $d(3\alpha_o)^{\frac{1}{2}}$ is given as a function of $3.8/\left|(1-\gamma M_o^{-2})^{\frac{1}{2}}-\delta_o^{\Delta}/2\right|$ with R_o as parameter.

----- theory; ● exp: $R_o = 1.16 \times 10^{-3} m.$
——— theory; o exp: $R_o = 1.53 \times 10^{-3} m.$

For W_1 we took the experimentally obtained value of W_1, which is about 3.8. In this Figure the experimentally obtained values for $d_A(3\alpha_o)^{\frac{1}{2}}$ are plotted against $3.8R_o/[(1-\gamma M_o^{-2})^{\frac{1}{2}}-\delta_o^{\Delta}/2]$. Considering the inaccuracy in R_o it follows from Figure 26 that the experimental points fit reasonably in with the theoretical curve. The constant values for R_o are taken from Table A-5 allowing for a spreading of 5%.

In Figure 27 the lines for d/R_o as a function of $1/(3\alpha_o)^{\frac{1}{2}}$ are drawn.
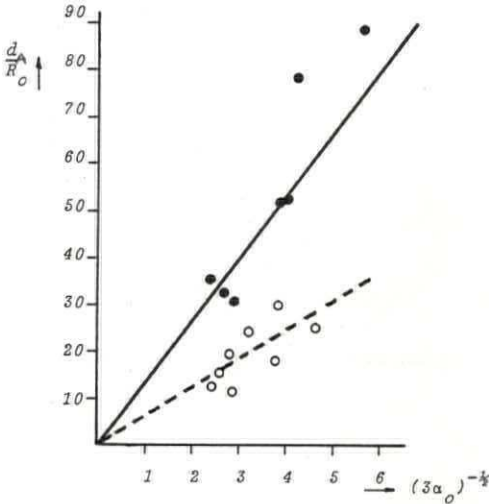
FIGURE 27. d/R_o is given as a function of $(3\alpha_o)^{-\frac{1}{2}}$ with p_1/p_o as a parameter.
----- theory; o exp: $p_1/p_o=1.9$.
——— theory; ● exp: $p_1/p_o=1.12$.

This is done for different constant values of

$$3.8/[(1-\gamma M_o^{-2})^{\frac{1}{2}}-\delta_o^{\Delta}/2] .$$

In most of the experiments we have $\delta_o^{\Delta}/2<<(1-\gamma M_o^{-2})^{\frac{1}{2}}$, so the curves are drawn for constant values of M_o^2, or with (8.7), for constant values of p_1/p_o. The experimentally obtained values are also given.
Considering the inaccuracy in the experimental results it follows from Figure 27 that the experimental points follow the theoretical curve quite satisfactory. In conclusion we may say that equation (8.6) is by the experiments confirmed within the experimental accuracy.
Now the experimental results for the back side of the shock, especially the wavy behaviour of the pressure, are investigated. To test the influence of different quantities on the wave length Λ, as given in (8.8), some experiments for which

R_o is a constant are selected. In Figure 28 we draw $\Lambda(3\alpha_o)^{\frac{1}{2}}$ as a function of $W_2 y_1^{2/3} / (\gamma M_o^{-2} y_1^{-\gamma} - y_1)^{\frac{1}{2}}$.
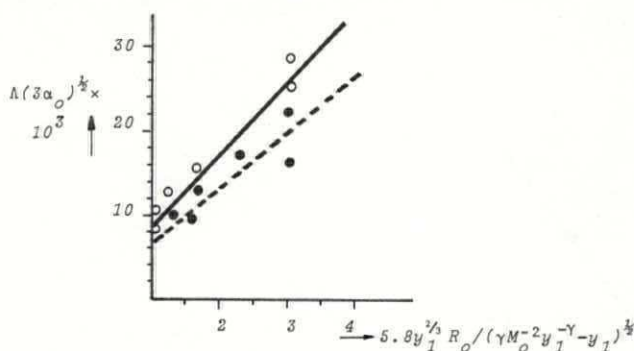
FIGURE 28. $\Lambda(3\alpha_o)^{\frac{1}{2}}$ is given as a function of $5.8 y_1^{2/3} / (\gamma M_o^{-2} y_1^{-\gamma} - y_1)^{\frac{1}{2}}$ with R_o as parameter.
----- theory; ● exp: $R_o = 1.16 \times 10^{-3}$ m.
——— theory; ○ exp: $R_o = 1.5 \times 10^{-3}$ m.

For W_2 the mean experimental value of W_2, which equals 5.8, is used instead of the theoretical value 2π. However, the difference is small.

Also the experimental values for $\Lambda(3\alpha_o)^{\frac{1}{2}}$ are given. It follows from Figure 28 that these values reasonably fit in with the theoretical curve. In Figure 29 the lines for Λ/R_o as a function of $(3\alpha_o)^{-\frac{1}{2}}$ are drawn.
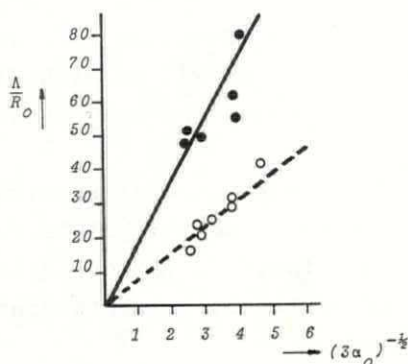
FIGURE 29. Λ/R_o is given as a function of $(3\alpha_o)^{-\frac{1}{2}}$ with p_1/p_o as parameter.
----- theory; ○ exp: $p_1/p_o = 1.84$
——— theory; ● exp: $p_1/p_o = 1.13$.

This is done for different constant values of the pressure ratio. From Figure 29 we see a reasonable correspondence between theory and experiment. We may say that equation (8.8) is by the experiments confirmed within the experimental accuracy.

Finally we conclude that the theoretical predicted dependence of the shock thickness and the wave length on R_o, p_{1/p_o} and α_o is recovered in the experiments.

§5. *THE STRUCTURE OF A S_B SHOCK.*

In Figure 30 a typical pressure recording for region B is shown.
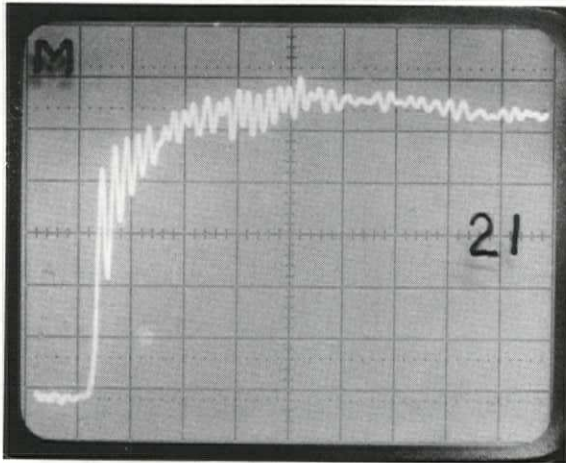
FIGURE 30. A pressure recording typical for region B.
$p_{1/p_o}=1.81$, $\beta_o=1.17\%$, $R_o=1.07\times10^{-3}m$, $U=108m/sec$, $d_A=4.3\times10^{-2}m$, $\Lambda=4.3\times10^{-2}m$, $d_B=.54m$ and $F_{exp}=.61$.

First we are interested in which relation for U^2/c_o^2 agrees with the experiments. Resisted relations are considered

$$U^2/c_o^2 = p_{1/p_o} ,$$

and

$$\frac{U^2}{c_o^2} = \frac{p_{1/p_o}-1}{1-(p_o/p_1)^{1/\gamma}} . \qquad (8.12)$$

This is done because, as shown in Figure 24, the difference between the resisted and not resisted results is of the order of the scatter. On the other hand, following from the

discussion in chapter 6, about region B, when $x/c_f\tau$ exceeds unity, the theory in which non-linear steepening is resisted by relaxation can be expected to hold. For these reasons in Figure 31 the isothermal and adiabatic resisted values for U^2/c_o^2 according to *(8.12)* are registered.
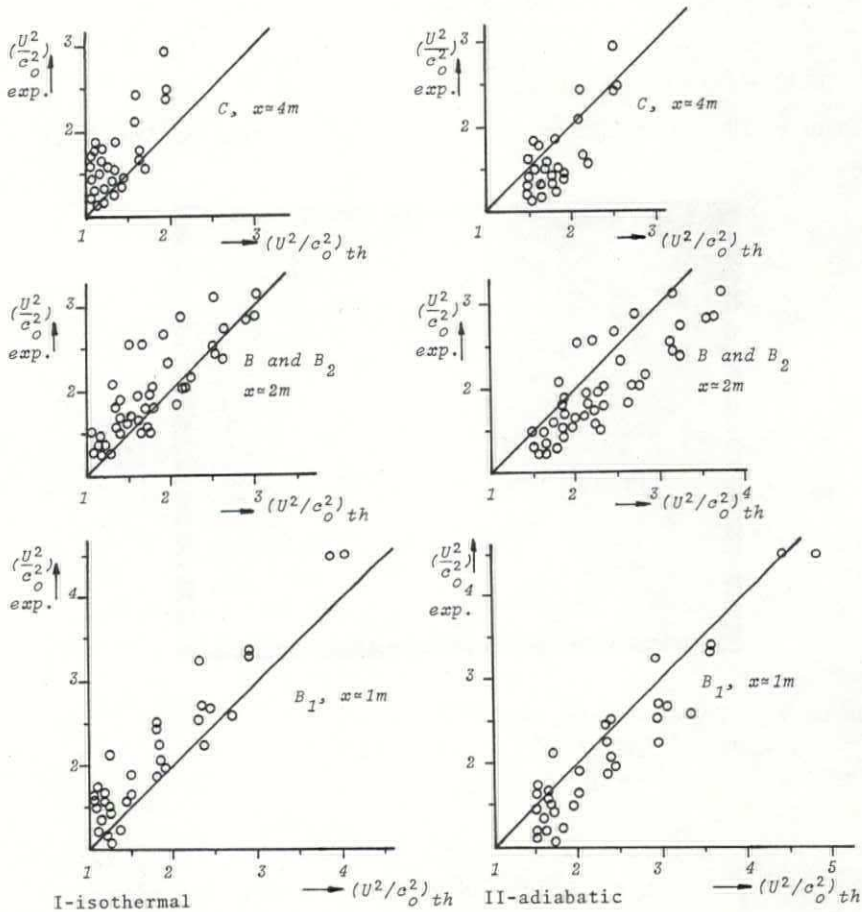
FIGURE 31. In this Figure the different theoretical and experimental values for U^2/c_o^2 as determined at different stations along the shock tube (Figure 18) are collected for S_B shocks. When either the isothermal or adiabatic theory fits in with the experiments, the pertinent marks would be close to the solid line.

o - *experiments*.

The experimental values are determined at the stations B
and C for the long shock tube and at B_1 and B_2 for the
short tube. We presented the results for the different
stations seperately in Figure 31 to find out whether or
not thermal relaxation might become effective. This is
expected to occur after the shock wave has travelled a
distance about 3 times larger than that for translational
relaxation (chapter 6). When either the isothermal or adia-
batic theory would fit in with the experiments, the marks
representing the pertinent theory would fit in with the
experiments. However, from Figure 31 no clear conclusion
can be drawn which of both theories applies for the pro-
pagation velocity. From comparison with Figure 24 we
conclude that thermal relaxation is noticeable.
With a view to the disccussion in §8 of chapter 6 one
might ask whether the relaxation profile as shown in Figure
30 chiefly follows from thermal or translational relax-
ation. An important quantity for relaxation is p^*, the
point of intersection between the steep front part and the
smooth back side of a S_B shock. p^* is found from the follo-
wing relations, with $F \equiv (p^*/p_o - 1)/(p_1/p_o - 1)$,
translational relaxation:
isothermal

$$F_{is} = 1 - \alpha_o \frac{p_1/p_o + 1}{p_1/p_o - 1} , \qquad (8.13)$$

adiabatic

$$F_{ad} = 1 - \gamma \alpha_o \frac{p_1/p_o (1 + (p_o/p_1)^{1/\gamma})}{\gamma p_1/p_o - (p_o/p_1)^{1/\gamma} M_o^2} , \qquad (8.14)$$

and
thermal relaxation

$$\frac{p^*_{ad}/p_o - 1}{1 - (p_o/p^*_{ad})^{1/\gamma}} = \frac{p_1}{p_o} , \qquad (8.15)$$

where the subscript *ad* for p^* indicates the thermal relax-
ation profile.

In Figure 32 the theoretical values from *(8.13)* and *(8.14)* are compared with the corresponding experimental data. The experimental values are collected at B and C for the long tube and at B_1 and B_2 for the short shock tube. The meaning of the solid line is the same as in Figure 31.
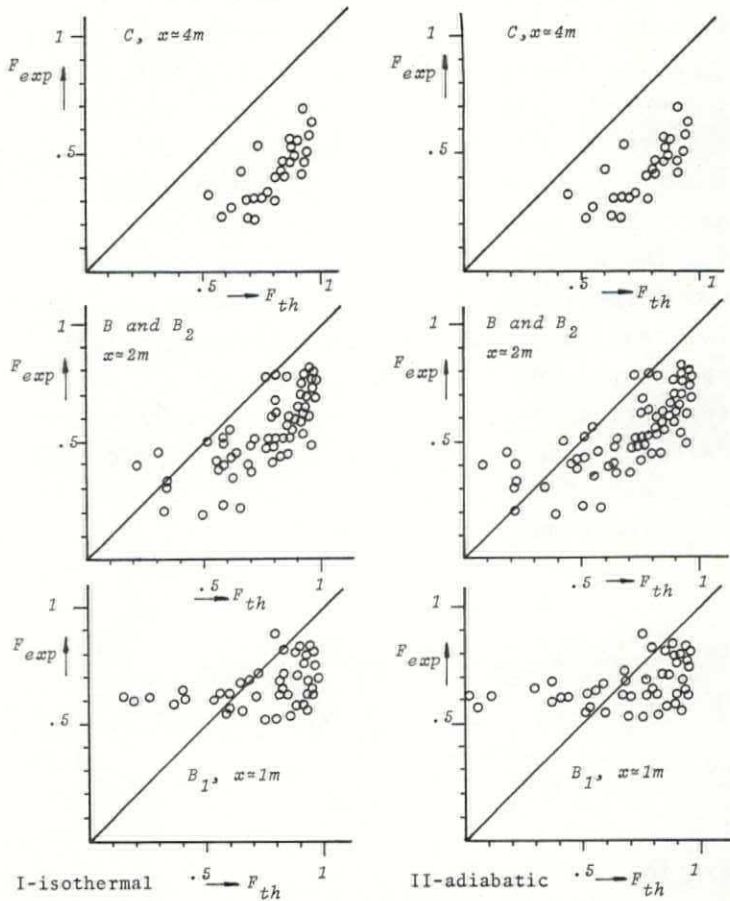
FIGURE 32. In this Figure the different theoretical and experimental values for $F=(p^*/p_o-)/(p_1/p_o-1)$ as determined at different stations along the shock tube are given. When either the isothermal or adiabatic theory fits in with the experiments, the pertinent marks would be close to the solid line.

o - *experiments*.

The experimental values for F, F_{exp}, given in Table A-6, Appendix 3, are registered along the vertical axis. The two different values for the quantity F, as given in *(8.13)* and *(8.14)*, at given p_1/p_o and α_o (Table A-6), are registered along the horizontal axis in Figure 32 I and II respectively.

From comparison of the upper graphs in Figure 32 with the others it follows that deep down the tube, at station C, the marks clearly deviate from the solid line. This indicates that thermal relaxation becomes noticeably as will be explained later on in this section. However, we conclude from Figure 32 that the bulk of the experimental marks are close to the solid line, which indicates translational relaxation. As a support for this conclusion another presentation of F will be given. In Figure 33 F, as given in *(8.14)*, is drawn as a function of p_1/p_o at constant β_o.
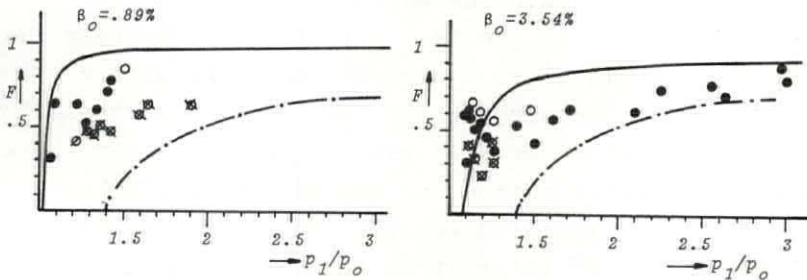
FIGURE 33. $F=(p^*/p_o-1)/(p_1/p_o-1)$ from *(8.14)* (——) is given as a function of p_1/p_o with β_o as parameter. Also the curve for $(p^*_{ad}/p_o-1)/(p_1/p_o-1)$ from *(8.15)* (—·—) is given. *exp:* o-$x \approx 1m$, •-$x \approx 2m$ and ▨-$x \approx 4m$.

For investigation of thermal relaxation we also draw in this Figure $(p^*_{ad}/p_o-1)/(p_1/p_o-1)$ from *(8.15)* as a function of p_1/p_o. This represents the thermal relaxation curve. As discussed in chapter 6, when $x/c_f\tau>1$ translational relaxation can be expected. For the bulk of the experiments with $c_f\tau \approx 1$, this type of relaxation occurs for $x>1$. Only for tap water we have $x>10$. Thermal relaxation can be

expected when $x/c_{ad}\tau_{th}>1$. From the calculations in chapter 6 it follows that this occurs for $x>3m$. So it is reasonable to suppose that deep down the tube the structure of the shock is affected by thermal relaxation. This might explain that in the Figures 32 and 33 the marks for region C, $x\approx4m$, are lower distributed with respect to the curves following from translational relaxation theory. A further support for this relaxation is found from the fact that for $p_1/p_o<1.4$, the threshold for thermal relaxation, F_{exp} clearly differs from zero as follows from Figure 33. As can be seen in this Figure both relaxation curves approach each other with increasing p_1/p_o and accordingly the experimental results are less conclusive. Considering the deviation of the experiments from theory one should keep in mind that F is based on a rough estimate, obtained by matching a dispersion dominated shock with a relaxation dominated one. In the transition region between these, p^* is located and the matching which ignores this transition region, necessarily provides only an approximate value for p^*. With a view to this, the experimental results may be considered as a support for the theory. p^* indicates the transition between the dispersion dominated front shock with unresisted bubble motion and the back side of the shock determined by resisted relative translational motion. So another quantity of interest is the length d_B of this part of the shock. This part of the wave is called the relaxation dominated part of the wave. The experimental values of d_B provide verification of the adopted resistance model for a bubble. We will pay attention to this part of S_B shocks when S_C shocks will be investigated in the following section. Further quantities which determine S_B shocks are the thickness d_A and the wave length Λ. Though the difference between the results for the isothermal and for the adiabatic theory is small we present results following from the adiabatic theory since we assume no thermal relaxation. The expression for the shock thickness d_A is, c.f. chapter 5,

$$d_A = \frac{R_o}{(3\alpha_o)^{\frac{1}{2}}} \frac{ln(20F_{ad})}{(1-\gamma M_o^{-2}(1+2\alpha_o))^{\frac{1}{2}}-\delta_o^{\Delta}/2} \, , \qquad (8.16)$$

where F_{ad} is defined by (8.14).
For the wave length Λ we have

$$\Lambda = \frac{R_o}{(3\alpha_o)^{\frac{1}{2}}} \frac{2\pi y_1^{2/3}}{(\gamma M_o^{-2} y_1^{-\gamma}-y_1+2\alpha_o \gamma y_1^{1-\gamma} M_o^{-2})^{\frac{1}{2}}}. \qquad (8.17)$$

Further we define

$$W_3 \equiv \frac{d_A(3\alpha_o)^{\frac{1}{2}}}{R_o} \left\{(1-\gamma M_o^{-2}(1+2\alpha_o))^{\frac{1}{2}}-\delta_o^{\Delta}/2\right\} \, , \qquad (8.18)$$

and

$$W_4 \equiv \frac{\Lambda(3\alpha_o)^{\frac{1}{2}}}{R_o} \frac{(\gamma M_o^{-2} y_1^{-\gamma}-y_1+2\alpha_o \gamma y_1^{1-\gamma} M_o^{-2})^{\frac{1}{2}}}{y_1^{2/3}} . \qquad (8.19)$$

It follows from (8.16) that W_3 is not a constant. We find
for W_3

$$W_3 = ln\ (20F_{ad}) . \qquad (8.20)$$

W_4, as follows from (8.19), must be a constant and equal
to 2π. In Table A-6, Appendix 3, the experimental results
for β_o, R_o, p_1/p_o, d_A, Λ, W_3 and W_4 are given. Also the
theoretical value for W_3 and points along the tube where
the results were obtained are given. In the Figures A3-3
and A3-4, Appendix 3, the distribution functions for W_3
and W_4 are given respectively. The values of W_3 are col-
lected for $ln(20F_{ad})$ between 2.5 and 3. The mean values
of W_3 and W_4 are also indicated. From these it follows
that with increasing x, $W_3/ln(20F_{ad})$ is an increasing
quantity. For large $x(\sim 4m)$ the deviation is large. This
once more supports the conclusion that for large x thermal
relaxation becomes important. Especially when $p_1/p_o<1.4$
we should have, when thermal relaxation was completely ef-
fective, a smooth profile with a considerably larger thick-
ness. This qualitatively explains the larger values of W_3
for large x. About the deviation of W_4 with respect to 2π,

for $x \sim 4m$, no conclusion can be drawn, since we have only a few experiments. As for S_A shocks we give a graphical presentation for d_A and Λ. For this presentation we took those experiments, considering the deviation of W_3 from the theoretical value, for which $x < 4m$. For d_A we selected some experiments for which p_1/p_o is constant and $\ln(20F_{ad})$ is between 2.5 and 3. In Figure 34 d_A/R_o is drawn as a function of $(3\alpha_o)^{-\frac{1}{2}}$. This is done for different values of $W_3/\left[(1-\gamma M_o^{-2}(1+2\alpha_o))^{\frac{1}{2}}-\delta_o^{\Lambda}/2\right]$. To draw these curves a mean value for W_3, from Figure A3-3, Appendix 3, is taken as obtained from the stations located at $x \sim 1m$ and $x \sim 2m$. We used $W_3 \sim 4.5$.
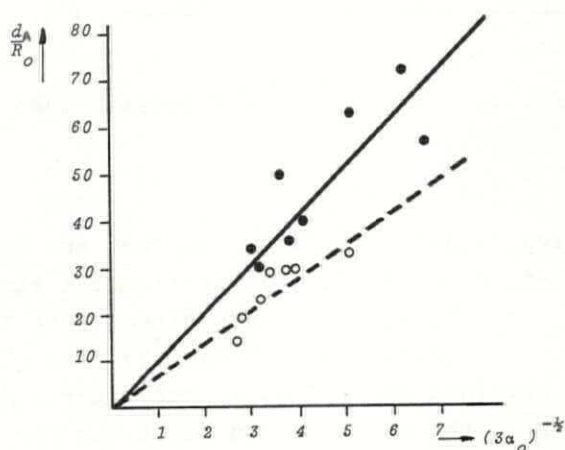
FIGURE 34. d/R_o is given as a function of $(3\alpha_o)^{-\frac{1}{2}}$ with p_1/p_o as parameter.
----- theory; o exp: $p_1/p_o=2.35$.
——— theory; • exp: $p_1/p_o=1.42$.

In most of the experiments $\delta_o^{\Lambda}/2 << (1-\gamma M_o^{-2}(1+2\alpha_o))^{\frac{1}{2}}$. So the curves are drawn for constant values of $M_o^{-2}(1+2\alpha_o)$, or, for not too small values of p_1/p_o for a constant value of p_1/p_o. It follows from Figure 34 that the experiments reasonably fit in with the theory.

For investigation of the experimental results for the wave

length Λ some experiments for a constant value of p_1/p_o are selected. In Figure 35 curves are drawn for Λ/R_o as a function of $(3\alpha_o)^{-\frac{1}{2}}$ according to (8.17) with p_1/p_o as parameter.
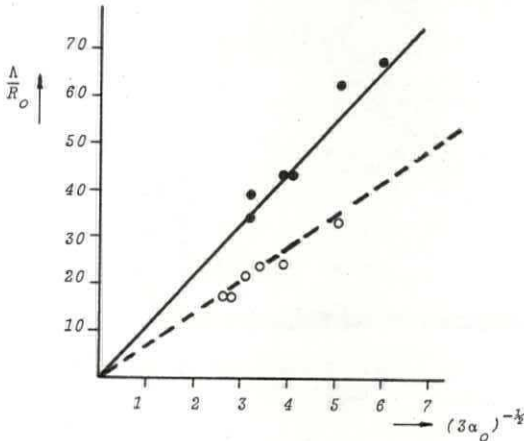
FIGURE 35. Λ/R_o is given as a function of $(3\alpha_o)^{-\frac{1}{2}}$ with p_1/p_o as parameter.
----- theory; o exp: $p_1/p_o=2.35$.
——— theory; ● exp: $p_1/p_o=1.42$.

For W_4 the mean value as obtained from the values at $x\sim 1m$ and $x\sim 2m$ (Figure A3-4, Appendix 3) is used. From Figure 35 we see a good correspondence between theory and experiment. Curves for d_A and Λ with a constant value of R_o are not presented since the variation in R_o is considerably less than the variation in p_1/p_o. Further the selected experiments for graphical presentation are those for which W_3 and W_4 are within 20% of the mean value of both quantities. Finally we conclude that the experiments for d_A and Λ of the S_B shocks, given by (8.16) and (8.17) respectively, confirm the theory quite satisfactory.

§6. *THE STRUCTURE OF S_C SHOCKS AND THE LENGTH d_B OF S_B SHOCKS.*

In Figure 36 a typical pressure recording of a S_C shock is shown.
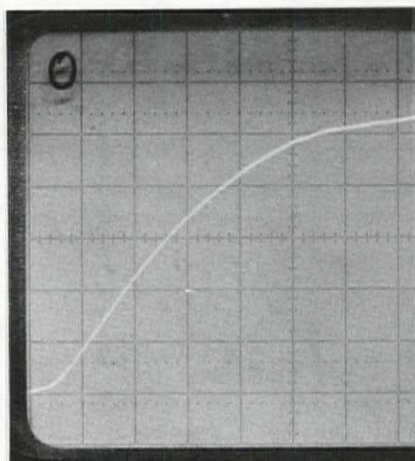
FIGURE 36. A pressure recording typical for a S_C shock.
$p_1/p_o=1.07$, $\beta_o=4.17\%$, $R_o=1.15\times10^{-3}m$, $U=65m/sec$, $d_C=2.1m$ and $1+ 4\alpha_o\gamma/(\gamma+1) =1.1$.

The equation describing the structure of the shock is, adiabatic theory,

$$y(1-y)^{1-\ell}(y-y_1)^{1+\ell} = exp - \frac{x}{U\tau} , \qquad (8.21)$$

where

$$\ell = \frac{2\alpha_o\gamma}{M_o^2-\gamma} .$$

The thickness d_C of the S_C shock is given by

$$\frac{d_C}{U\tau} = 2\ell ln20 . \qquad (8.22)$$

Further we define

$$W_5 \equiv \frac{d_C}{U\tau\ell} \qquad (8.23)$$

A S_C shock occurs when the pressure ratio is below a certain critical value

$$p_1/p_o < 1+ \,^{4\alpha_o\gamma}/_{(\gamma+1)} .$$

In Table A-7, Appendix 3, the experimental results for S_C shocks are collected. There we also summarized the values for $1+2\beta_o$, the corresponding isothermal threshold. If we compare the isothermal as well as the adiabatic threshold with the pressure ratio in Table A-7, it is found that the appearance of S_C shocks answers to the adiabatic relation. For some experiments the propagation velocity U is not given, because the steepness of the profile was too small to permit the measurement of U. One should notice that $d_C/U\tau$ does not depend on U; d_C/U is directly measured, since the experiments give the pressure as function of the time-wise variable x/U. From (8.22) and (8.23) it follws that W_5 is a constant. The values of W_5 are also given in Table A-7. In Figure A3-5, Appendix 3, we give the distribution function for W_5. In this Figure we presented results for two viscosities: $v_l=.7\times10^{-5}m^2/sec$ and $v_l=1.1\times10^{-4}m^2/sec$. The results indicate a strong dependence of W_5 on the viscosity. Since we have only a few experiments for S_C shocks we will take a close look to effects of viscosity on the length of the relaxation profile when we investigate the back side of S_B shocks. First we want to inspect for S_C shocks whether the measured profile is shaped in the way as predicted by the relaxation theory. For this we draw in Figure 37 $(d_C/U\tau)\times$ $(M_o^2/\gamma -1)$ as a function of α_o. We selected those
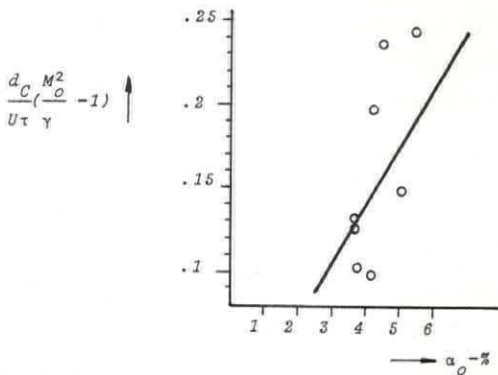
FIGURE 37. $(d_C/U\tau)(M_o^2/\gamma -1)$ as a function of α_o with $W_5=.88$.
o - experiments.

experiments with $v_l=.7\times10^{-5}m^2/sec.$ (There are only two experimental values for $v_l=1.1\times10^{-4}m^2/sec$). W_5 is taken equal to $.88$, the experimentally obtained mean value (see Figure A3-5), which is about one third of the theoretical value $ln20$. From Figure 37 we conclude that the dependence of $d_C(M_o^2-\gamma)/U\tau$ on α_o is in the way as predicted by the theory. In Figure 38 a pressure recording for a S_C shock (thick line) is presented, the theoretical relation (thin line) according to (8.21) is also given.
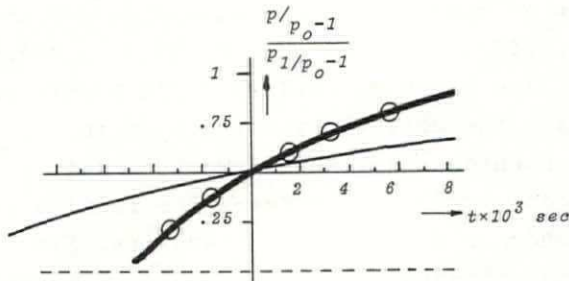
FIGURE 38. $(p/p_o-1)/(p_1/p_o-1)$ as a function of t (thick line). $p_1/p_o=1.08$, $\beta_o=3.7\%$, $R_o=1.17\times10^{-3}m$, $d_C=2.04m$ and $1+4\gamma\alpha_o/(\gamma+1)=1.085$. The thin line is the theoretical curve with $\tau=10^{-2}sec$, according to the adiabatic theory (8.21). Using the transformation $t=x/U$, $(p/p_o-1)\times (p_1/p_o-1)^{-1}$ can be found as a function of the time wise variable and be compared with the experiments. o-Theoretical values for the pressure if τ is one third of the calculated one.

This theoretical relation is found from (8.21) using the transformation $t=x/U$. We see that the theoretical change in pressure takes place in a considerably longer distance than the experimental change in pressure. However, from changing the time wise variable in the theoretical obtained pressure profile, this curve appears to fit in with the experimental curve, though with a relaxation time τ about one third of the theoretical value $R_o^2/18v_l$. Thus the measured profile is shaped in a way predicted by relaxation theory. Apparently the actual value of τ is less than follows from the adopted theoretical model. Explanation of this discrepancy is postponed to the discussion on the length

d_B of S_B shocks.

In Figure 39 another record of a smooth profile is shown.
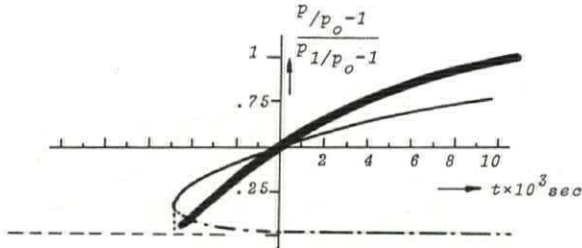
FIGURE 39. A pressure recording (thick line) as in Figure 38. The theoretical curve, thin line, turns back and therefore indicates the occurence of a thin front shock. This could not be observed in the experiments. $p_1/p_o=1.13$ and $1+4\gamma\alpha_o/(\gamma+1)=1.1$.

According to the theory a thin front shock should appear since the pressure ratio exceeds $1+4\gamma\alpha_o/(\gamma+1)$. However, here it is hard to decide from the Figure whether a front shock is present or not.

Now we will pay attention to our model for the resistance of a translating bubble. As indicated the length d_C is a measure for this. We found a discrepancy between theory and experiment. The length d_B of the back side of a S_B shock is also a measure for the bubble resistance. Since we have much more experiments for S_B shocks than for S_C shocks we will discuss relaxation from the experiments for S_B shocks. The theoretical expression for d_B is, c.f. chapter 5,

$$\frac{d_B}{U\tau} = y_1^{2/3}\frac{\gamma M_o^{-2}y_1^{-\gamma}-y_1+2\alpha_o\gamma y_1^{1-\gamma}M_o^{-2}}{\gamma M_o^{-2}y_1^{-\gamma}-y_1}\, \ln\left[20(1-F_{ad})\right]\ . \qquad (8.24)$$

For not too weak shocks (8.24) can be written as

$$\frac{d_B}{U\tau}\frac{y_1^{2/3}}{\ln\left[20(1-F_{ad})\right]} = 1\ . \qquad (8.25)$$

For comparison with W_5 we multiply both sides of *(8.25)* with *ln20* and we define W_6 as

$$W_6 \equiv \frac{d_B}{U\tau} \; \frac{y_1 \, ln20}{ln \; 20(1-F_{exp})} \; . \qquad (8.26)$$

In *(8.26)* F_{exp} in stead of F_{ad} is taken. This is done since we are faced with the inaccuracy in the estimate of p^* represented by F_{ad}. In table A-8, Appendix 3, the experimental results for the back side of S_B shocks are given. In Figure A3-6 of this Appendix the different distribution functions for W_6 are given for different values of the viscosity of the liquid. Also the mean values are indicated. No distinction is made for the stations where the results are obtained. From Figure A3-6 it follows that for $v_l = .7 \times 10^{-5} m^2/sec$ the mean value of W_6 is close to the corresponding value of W_5 *(=.88)* for S_C shocks. Further it can be seen that W_6 changes considerably when we change viscosity. This differs from what the theory predicts in this respect. From the theory we found that W_6 is a constant and approximately equal to *ln(20)*. Only for a viscosity of $3 \times 10^{-5} m^2/sec$ W_6 is in the neighbourhood of this constant. What could be the cause of the discrepancy between theory and experiment?

Our theoretical model for the bubble resistance from which we found the relaxation time τ is based on Levich's resistance for a bubble. This leads to a relaxation time $\tau = R_o^2/18v_l$. Only for viscosities of about $3 \times 10^{-5} m^2/sec$ and $R_o \sim 10^{-3} m$ we get near this relaxation time. Levich's resistance for a bubble applies when inertia forces exceed the viscous forces, so for Reynolds numbers sufficiently larger than unity. According to Levich (1962) the validity of his model is restricted to Reynolds numbers up to *800*, because at larger numbers the bubbles are significantly deformed. From our experiments we may conclude that Levich's model applies for a small range of Reynolds numbers. In the following we will base the discussion for the bubble resistance on the Reynolds number. Of course the Reynolds number is no where a constant in the relaxation profile

because, except for a small resulting velocity following
from buoyancy, relative velocity ultimately vanishes. How-
ever, in the front part of the relaxation profile where
the pressure changes significantly, we assume in a certain
range of Reynolds numbers a typical resistance model to
hold. To explain the experimental results qualitatively,
we first investigate the range of Reynolds numbers asso-
ciated with the different viscosities. To find an estimate
for the magnitude of the Reynolds numbers we assume unre-
sisted bubble motion in the front part of the relaxation
profile. The relative velocity, $v-u$, is in this case ap-
proximated by, c.f. chapter 4,

$$v-u = 2U\beta_o(1-p_o/p_1) . \qquad (8.27)$$

With β_o a few percent, U about $100m/sec$ and p_1/p_o of the
order of unity in most of our experiments we find for the
various Reynolds numbers

$$
\begin{aligned}
\nu_l &= 10^{-6}m^2/sec : & Re &\sim 4000, \\
\nu_l &= .7\times10^{-5}m^2/sec : & Re &\sim 600, \\
\nu_l &= 3\times10^{-5}m^2/sec : & Re &\sim 200, \\
\nu_l &= 1.1\times10^{-4}m^2/sec : & Re &\sim 50.
\end{aligned}
\qquad (8.28)
$$

From (8.28) we see that for tap water, $\nu_l=10^{-6}m^2/sec$, the
Reynolds number largely exceeds the upper value of 800 as
indicated by Levich. The bubbles are strongly deformed and
behave as small discs. From Haberman & Morton (1953) we
can approximate the bubble resistance with a constant value
for the drag coefficient C_D of about 1.5. The drag coeffi-
cient based on Levich's model, $C_D=48/Re$, amounts to 10^{-2}
in this case. Even for a free rising bubble in water $C_D=48/Re$
is unrealistic. From Appendix 4 it follows that for $C_D=1.5$
the length of the smooth region is about $1m$. This is in
good correspondence with the experimental results for d_B
with $\nu_l=10^{-6}m^2/sec$ as follows from Table A-8. For this model
of the resistance the free boundary of the bubble surface is
of no importance. $C_D\sim1.5$ is also found for a solid disc.
Though we cannot indicate a relaxation time for this resis-

tance model, it explains the length of d_B quite satisfactory.
For $\nu_l = .7 \times 10^{-5} m^2/sec$ we found for S_C shocks a relaxation
time which is about one third of the theoretical one. From
Figure A3-6 and Table A-8 a relaxation time of this magnitude
for S_B shocks can be found. (8.28) gives a Reynolds number
of about 600. If we suppose that Levich's model still holds,
a reasonable explanation for this lower relaxation time is
found in the bubble deformation. In our opion an important
effect in this connection is that during the acceleration,
relative to the liquid, the bubbles do not remain spherical
as assumed in the calculations. The bubbles adopt an oblate
shape, which increases the resistance in comparison with a
sphere as follows from equation (1.14) in chapter 1. We mea-
sured the velocity of bubbles of 1mm effective radius rising
in the mixture under the influence of gravity. We found a
resistance force which was about 1.5 times Levich's friction
force. Since during acceleration by the passing pressure
wave the bubbles are considerably more deformed than when
rising in a hydrostatic pressure field the actual value of
τ could be easily 2 or 3 times smaller than the calculated
one based on a spherical shape. A larger drag coefficient
and accordingly a smaller value of d_B can be found if we
assume solidification of the bubble surface by surface ac-
tive agents. However for gas fractions as in our experiments
a significant influence of surface active agents is not rea-
listic (Levich 1962, p.448).
For $\nu_l = 3 \times 10^{-5} m^2/sec$, which corresponds with Reynolds numbers
of about 200 we see from Figure A3-6 a good correspondence
with the theoretical value for $W_6 (= ln20)$. This indicates
that for these Reynolds numbers Levich's model and the
connected relaxation time correspond with the experimen-
tal results.
For $\nu_l = 1.1 \times 10^{-4} m^2/sec$, which corresponds with Reynolds num-
bers of about 50 we found, as can be seen from Figure A3-6,
a value for W_6 which is about 3 times the theoretical value
$R_o^2 / 18\nu_l$. What could be the cause of this larger relaxation
time or a lower resistance? For Reynolds numbers smaller

than unity this factor 3 could be explained by using Hadamard-Rybczynski (1911) formula for a fluid sphere. This formula gives a drag coefficient equal to 16/Re or exactly 1/3 of Levich's drag coefficient. However the Reynolds number still exceeds unity even for this large viscosity. A possible explanation for this lower resistance can be found from an improved estimate of the drag of a bubble with a free surface. This is given in Moore (1963). Moore calculated also the dissipation of energy in the boundary larger at the bubble surface and found for the drag coefficient

$$c_D = \frac{48}{Re} \left\{ 1 - \frac{2.2}{Re^{\frac{1}{2}}} \right\} .$$ (8.29)

For 10<Re<100, the fraction between brackets varies from .3 to .8. With this lower drag coefficient it can be expected that the length of the smooth back side will be larger than d_B from (8.25). In Figure 40 we illustrate the different relations for c_D as a function of the Reynolds number.
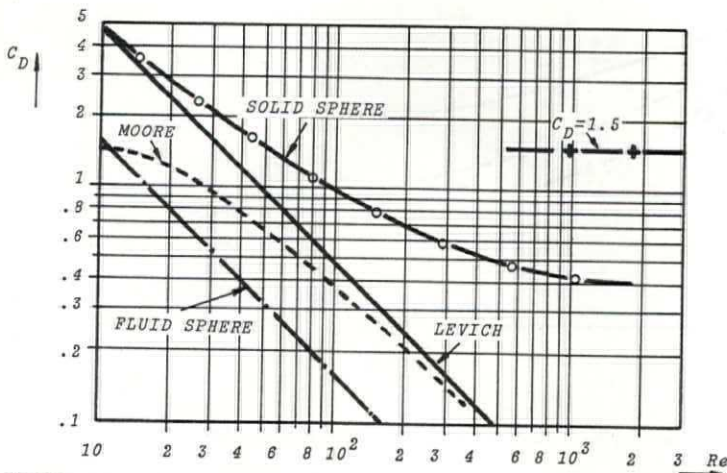
FIGURE 40. c_D for various models of a bubble as a function of the Reynolds number.

For low Reynolds number, or high viscosity, the length of the profile is explained by the C_D as given in *(8.29)*. With increasing Reynolds numbers the bubble resistance come close to Levich's model. For large Reynolds numbers the bubble deformation becomes important and C_D changes to a constant value of *1.5*.

§7. *THE WHITHAM RULE.*

We found in chapter 7 that the Machnumber changes along the shock tube as given by

$$\left\{\frac{M_o-1}{M_{oo}-1}\right\}^2 \ exp\left[(M_o-M_{oo})\right] = \frac{1}{1-\rho_l gx/p_{oo}} \ , \tag{8.30}$$

for isothermal circumstances.
For adiabatic circumstances we have, for $M_o^2/\gamma-1=0(10^{-1})$,

$$\left\{\frac{M_o^2-\gamma}{M_{oo}^2-\gamma}\right\}^2 = \frac{1}{1-\rho_l gx/p_{oo}} \ . \tag{8.31}$$
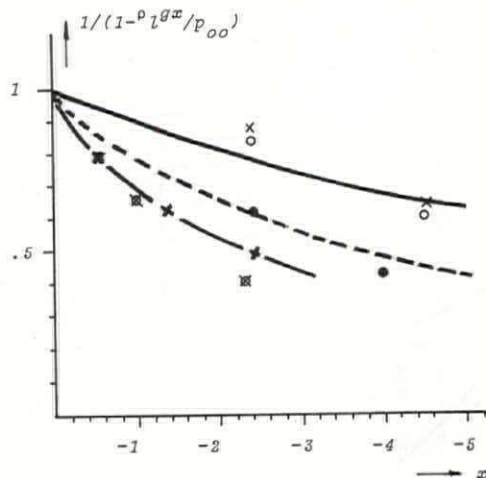
FIGURE 41. In this Figure we draw $(1-\rho_l gx/p_{oo})^{-1}$ as a function of x for different values of p_{oo}.
────── *theory* ; o *exp - isothermal* $p_{oo}=.934\times10^5 N/m^2$.
            × *exp - adiabatic*.
----- *theory* ; ● *exp - isothermal* $p_{oo}=.399\times10^5 N/m^2$.
—+— *theory* ; ✖ *exp - isothermal* $p_{oo}=.246\times10^5 N/m^2$.

In Figure 41 we draw $(1-\rho_l gx/p_{00})^{-1}$ as a function of x for different values of p_{00}. Also the experimental values for the left-hand side of (8.30) and (8.31) are given. Since we only measured at three stations along the shock tube, where one of them is at $x \sim o$, this Figure is less conclusive. However it follows from this Figure that the few marks reasonably fit in with the theoretical curve.

§8. CONCLUSIONS;

We found in the experiments shocks, structured as predicted by the theory. A reasonably good agreement with theory was found for the dispersion dominated shock, S_A shocks, and the dispersion dominated part of S_B shocks. Especially with respect to the thickness of the steep front shock and the waves at the back side of the shocks.

Furthermore the relaxation theory for explaining the gradual change in wave profile from S_A into S_B or S_C shocks, when a shock passes a bubbly mixture is supported by the experiments. The theory predicts effects both on wave speed and wave profile. The effect on wave speed is so small that it was not possible to measure this. The effect on the profile could be measured. Comparison with theory shows, however for a small range of viscosities that the observed changes in profile are caused by the relaxation mechanism associated with, initially generated and finally resisted relative motion between bubbles and liquid. We found S_C shocks shaped in a way predicted by relaxation theory, for $v_l=.7 \times 10^{-5} m^2/sec$, however with a smaller relaxation time. The length of the smooth part of S_B shocks fits in with the theory in a small range of viscosities near $v_l=3 \times 10^{-5} m^2/sec$. Without a complete theory at hand we indicated, qualitatively, that for much smaller and larger values of the viscosity the experimental profiles can be expected. A detailed discussion on i.e. the influence of bubble deformation on the shock structure is beyond the scope of this thesis.

Finally we conclude that the shock propagation velocity can be predicted as a function of the coordinate along the shock

tube by using the Whitham rule. These results support the application of local equilibrium quantities and the Hugoniot relations for shock wave propagation through a bubbly mixture with a given density and pressure distribution.

APPENDIX 1.

In chapter 5 we found a third order differential equation for the front part and the back side of the shock. In this Appendix we determine the solutions.

For the front part we have the following differential equation

$$\frac{d^3y'}{d\eta^3} + a_1 \frac{d^2y'}{d\eta^2} + a_2 \frac{dy'}{d\eta} + a_3 y' = 0, \qquad (A1.1)$$

where

$$a_1 = \frac{\delta_o^\Delta}{1+4\alpha_o} + \sigma ,$$

$$a_2 = - \frac{1-M_o^{-2}-2\alpha_o M_o^{-2}}{1+4\alpha_o} , \qquad (A1.2)$$

$$a_3 = - \frac{\sigma(1-M_o^{-2})}{1+4\alpha_o} .$$

$$\delta_o^\Delta = \frac{R_o}{(3\alpha_o)^{\frac{1}{2}}} \frac{(\delta\omega_B')_o}{U} ,$$

and

$$\sigma = \frac{18\nu_l}{UR_o} \frac{1}{(3\alpha_o)^{\frac{1}{2}}} . \qquad (A1.3)$$

We seek solutions in the form of $y'=e^{\Psi\eta}$. This gives, with (A1.1),

$$\Psi^3 + a_1\Psi^2 + a_2\Psi + a_3\Psi = 0 . \qquad (A1.4)$$

Now the zeros of this cubic equation are determined. For this the magnitude of the coefficients a_1, a_2 and a_3 is of interest for simplification of the rather complicated roots of (A1.4). For the magnitude of a_1, a_2 and a_3 we consider different cases such as high viscosity, $\nu=0(10^{-4})$, normal viscosity, $\nu=0(10^{-5})$, weak shocks, $M_o^2-1=0(10^{-1})$, and moderate shocks, $M_o^2-1=0(1)$. The different orders of magnitude

for a_1, a_2 and a_3 are given in Table A-1.

TABLE A-1

	$\nu=O(10^{-5})$		$\nu=O(10^{-4})$	
	$M_o^2-1=O(10^{-1})$	$M_o^2-1=O(1)$	$M_o^2-1=O(10^{-1})$	$M_o^2-1=O(1)$
a_1	>0 $O(10^{-1})$	>0 $O(10^{-1})$	>0 $O(10^{-1})$	>0 $O(10^{-1})$
a_2	$M_o^2<1+2a_o$: >0 $O(10^{-1})$ | $O(10^{-1})$; <0	<0 $O(1)$	$M_o^2<1+2a_o$: >0 $O(10^{-1})$ | $O(10^{-1})$; <0	<0 $O(1)$
a_3	<0 $O(10^{-3})$	>0 $O(10^{-2})$	>0 $O(10^{-2})$	>0 $O(10^{-1})$

We define the quantities s, q and a by

$$s = a_2 - a_1^2/3,$$

$$q = 2a_1^3/27 - a_1 a_2/3 + a_3, \qquad (A1.5)$$

$$a = s^3/27 + q^2/4.$$

In Table A-2 the orders of magnitude of s, q and a are given.

TABLE A-2

	$\nu=O(10^{-5})$			$\nu=O(10^{-4})$		
	$M_o^2-1=O(10^{-1})$		$M_o^2-1=O(1)$	$M_o^2-1=O(10^{-1})$		$M_o^2-1=O(1)$
	$M_o^2<1+2a_o$			$M_o^2<1+2a_o$		
s	>0 $O(a_2)$	<0 $O(a_2)$	<0 $O(a_2)$	>0 $O(a_2)$	<0 $O(a_2)$	<0 $O(a_2)$
q	<0 $O(-\frac{a_1 a_2}{3})$	>0 $O(-\frac{a_1 a_2}{3})$	>0 $O(-\frac{a_1 a_2}{3})$	>0 $O(-\frac{a_1 a_2}{3}+a_3)$	>0 $O(-\frac{a_1 a_2}{3}+a_3)$	>0 $O(-\frac{a_1 a_2}{3}+a_3)$
a	>0 $O(\frac{s^3}{27})$	<0 $O(\frac{s^3}{27})$	<0 $O(\frac{s^3}{27})$	>0 $O(\frac{s^3}{27})$	<0 $O(\frac{s^3}{27})$	<0 $O(\frac{s^3}{27})$

We further define

$$E_1 = \left\{-q/2 + a^{\frac{1}{2}}\right\}^{1/3},$$

$$E_2 = -\left\{q/2 + a^{\frac{1}{2}}\right\}^{1/3}. \qquad (A1.6)$$

The roots are found by standard methods (Abramowitz & Stegun, 1965). The method is known as the method of Cardanus. The sign of a, Table A-2, is of importance for determination of the roots. If $a>0$, we have one real root and a pair of complex conjucate roots. If $a<0$, all roots are real. The case $a=0$, all roots real and at least two of them are equal, is of no practical importance. It indicates the transition of a S_B shock into a S_C shock.

First we discuss $a>0$ and accordingly $M_o^2<1+2\alpha_o$.
The roots of $(A1.4)$ are

$$\Psi_1 = E_1 + E_2 - a_1/3 \, ,$$

and $\left.\begin{array}{l}\end{array}\right\}$ $(A1.7)$

$$\Psi_{2,3} = -(E_1+E_2)/2 - a_1/3 \pm i\sqrt{3}(E_1-E_2)/2 \, .$$

The solution for y' is

$$y' = D_1 e^{\Psi_1 \eta} + D_2 e^{\Psi_2 \eta} + D_3 e^{\Psi_3 \eta} \, . \qquad (A1.8)$$

Considering the magnitude of the different quantities as given in the Tables A-1 and A-2 we find for the real part of the complex roots in $(A1.7)$, with E_1+E_2 approximated by $-q/a_2$,

$$- a_1/2 + a_3/(2a_2) \, . \qquad (A1.9)$$

For $M_o^2<1+2\alpha_o$ the quantity represented by $(A1.9)$ is negative. Thus D_2 and D_3 as given in $(A1.8)$ are equal to zero. Ψ_1 becomes

$$- a_3/a_2 \, ,$$

and this quantity exceeds zero for $M_o^2<1+2\alpha_o$. The solution for y' is

$$y' \propto exp\left[\frac{\sigma\eta(M_o^2-1)}{1+2\alpha_o-M_o^2}\right] . \qquad (A1.10)$$

Secondly we have $a<0$ and accordingly $M_o^2>1+2\alpha_o$.

The solutions are

$$\Psi_1 = 2\left(-\frac{s}{3}\right)^{\frac{1}{2}}\cos\left(\frac{\Omega}{3}\right) - a_1/3 \; ,$$

$$\Psi_2 = 2\left(-\frac{s}{3}\right)^{\frac{1}{2}}\cos\left(\frac{\Omega}{3}+\frac{2\pi}{3}\right) - a_1/3 \; , \qquad (A1.11)$$

$$\Psi_3 = 2\left(-\frac{s}{3}\right)^{\frac{1}{2}}\cos\left(\frac{\Omega}{3}+\frac{4\pi}{3}\right) - a_1/3 \; ,$$

where

$$\cos\Omega = -\frac{q/2}{(-s^3/27)^{\frac{1}{2}}} \; . \qquad (A1.12)$$

From the Tables A-1 and A-2 it follows that

$$\cos\Omega = - O(10^{-1}) \; .$$

With this the roots Ψ_1, Ψ_2 and Ψ_3 as given in $(A1.11)$ can be approximated.
The solution for y' is

$$y' = L_1 e^{\Psi_1 n} + L_2 e^{\Psi_2 n} + L_3 e^{\Psi_3 n} \; . \qquad (A1.13)$$

Ψ_1 becomes

$$\Psi_1 = (-a_2)^{\frac{1}{2}} + \frac{a_1 a_2 - 3a_3}{6|a_2|} - a_1/3 \; , \qquad (A1.14)$$

which is a positive quantity.
For Ψ_2 we have

$$\Psi_2 = -(-a_2)^{\frac{1}{2}} - a_1/3 \; ,$$

which is a negative quantity.
Ψ_3 becomes

$$\Psi_3 = \frac{a_3}{|a_2|} < 0 \; .$$

Thus L_2 and L_3 as given in $(A1.13)$ are equal to zero and y' becomes

$$y' \propto exp\left[-\frac{\eta \delta_o^\Delta}{2} + \frac{\eta(1-M_o^{-2}-2\alpha_o M_o^{-2})^{\frac{1}{2}}}{1+2\alpha_o}\right] .$$

The differential equation for the back side of the shock is

$$\frac{d^3 y''}{d\eta^3} + b_1 \frac{d^2 y''}{d\eta^2} + b_2 \frac{dy''}{d\eta} + b_3 y'' = 0 , \qquad (A1.15)$$

where

$$b_1 = \frac{\delta_1^\Delta}{1+4\alpha_o M_o^{-2}} + \sigma M_o^{\frac{2}{3}} ,$$

$$b_2 = \frac{M_o^{\frac{4}{3}}(1-M_o^{-2}+2\alpha_o M_o^{-2})}{1+4\alpha_o M_o^{-2}} , \qquad (A1.16)$$

$$b_3 = \frac{\sigma(M_o^2-1)}{1+4\alpha_o M_o^{-2}} .$$

$$\delta_1^\Delta = \frac{R_o}{(3\alpha_o)^{\frac{1}{2}}} \frac{(\delta\omega_B')_1}{U} . \qquad (A1.17)$$

We seek solutions for y'', as given in $(A1.15)$, in the form of

$$y'' = e^{\Psi \eta} .$$

We obtain for Ψ

$$\Psi^3 + b_1 \Psi^2 + b_2 \Psi + b_3 = 0 . \qquad (A1.18)$$

The different orders of magnitude of b_1, b_2 and b_3 are given in Table A-3.

TABLE A-3

	$v=0(10^{-5})$		$v=0(10^{-4})$	
	$M_o^2-1=0(10^{-1})$	$M_o^2-1=0(1)$	$M_o^2-1=0(10^{-1})$	$M_o^2-1=0(1)$
b_1	>0 $0(10^{-1})$	>0 $0(10^{-1})$	>0 $0(10^{-1})$	>0 $0(10^{-1})$
b_2	>0 $0(10^{-1})$	>0 $0(1)$	>0 $0(10^{-1})$	>0 $0(1)$
b_3	>0 $0(10^{-3})$	>0 $0(10^{-2})$	>0 $0(10^{-2})$	>0 $0(10^{-2})$

In Table A-4 the orders of magnitude of s, q and a are given.

TABLE A-4

| | $v=0(10^{-5})$ | | $v=0(10^{-4})$ | |
	$M_o^2-1=0(10^{-1})$	$M_o^2-1=0(1)$	$M_o^2-1=0(10^{-1})$	$M_o^2-1=0(1)$
s	>0 $0(b_2)$	>0 $0(b_2)$	>0 $0(b_2)$	>0 $0(b_2)$
q	<0 $0(-\dfrac{b_1 b_2}{3})$	<0 $0(-\dfrac{b_1 b_2}{3})$	>0 $0(-\dfrac{b_1 b_2}{3}+a_3)$	>0 $0(-\dfrac{b_1 b_2}{3}+a_3)$
a	>0 $0(\dfrac{s^3}{27})$	>0 $0(\dfrac{s^3}{27})$	>0 $0(\dfrac{s^3}{27})$	>0 $0(\dfrac{s^3}{27})$

This Table shows that a exceeds zero and we expect a wavy behaviour of y''.

Ψ_1 becomes

$$\Psi_1 = - \frac{b_3}{b_2} .$$

With the help of $(A1.16)$ this finally yields

$$\Psi_1 = - \sigma \frac{M_o^{\frac{2}{3}}(M_o^2-1)}{M_o^2-1+2\alpha_o} . \qquad (A1.19)$$

This root represents the smooth part of y''.
E_1-E_2 is approximated by

$$E_1-E_2 = \frac{2(\dfrac{b_2}{a_2})^{\frac{1}{2}}}{\sqrt{3}} .$$

With this we find for the roots Ψ_2 and Ψ_3, as given in $(A1.7)$,

$$\Psi_{2,3} = - (b_1 - b_3/b_2)/2 \pm i(b_2)^{\frac{1}{2}}. \qquad (A1.20)$$

Using $(A1.16)$ we find for $\Psi_{2,3}$ as given in $(A1.20)$

$$\Psi_{2,3} = - \frac{1}{2}\left[\frac{\delta_1^\Delta}{1+4\alpha_o M_o^{-2}} + \frac{\sigma 2\alpha_o M_o^{-\frac{2}{3}}}{M_o^2-1+2\alpha_o}\right] \pm i\left[\frac{M_o^2-1+2\alpha_o}{M_o^{\frac{2}{3}}(1+4\alpha_o M_o^{-2})}\right]^{\frac{1}{2}} . \qquad (A1.21)$$

This represents the attenuated wavy behaviour of y''.

APPENDIX 2.

Here we present the linearization scheme to find the equation which describes wave propagation in one direction. We summarize the pertinent equations

$$\rho = \rho_l (1-\beta) \,, \tag{A2.1}$$

$$\frac{\partial \rho}{\partial t} + u \frac{\partial \rho}{\partial x} + \rho \frac{\partial u}{\partial x} = - \frac{\partial}{\partial x} \left\{ \rho_l \beta (v-u)/2 \right\} \,, \tag{A2.2}$$

$$\rho \frac{\partial u}{\partial t} + \rho u \frac{\partial u}{\partial x} + \frac{\partial p}{\partial x} = - \frac{\partial}{\partial t} \left\{ \rho_l \beta (v-u)/2 \right\} \,, \tag{A2.3}$$

$$\frac{\partial}{\partial t}(p_g \beta) + v \frac{\partial}{\partial x}(p_g \beta) + p_g \beta \frac{\partial v}{\partial x} = 0 \,, \tag{A2.4}$$

$$\left(\frac{\partial}{\partial t} + \tau^{-1} \right) \left\{ \beta (v-u) \right\} = - \frac{2\beta}{\rho_l} \frac{\partial p}{\partial x} \,, \tag{A2.5}$$

$$p_g - p = \frac{R_o^2 p_o}{3\beta_o^2 c_o^2} \left[\frac{\partial^2 \beta}{\partial t^2} + \delta' \omega_B \frac{\partial \beta}{\partial t} \right], \tag{A2.6}$$

where

$$\delta' = (\gamma)^{\frac{1}{2}} \delta \,.$$

$$c_o^2 = \frac{p_o}{\rho_l \beta_o (1-\beta_o)} \,. \tag{A2.7}$$

We introduce

$$u = \epsilon \beta_o c_o u' \,,$$
$$v = \epsilon \beta_o c_o v' \,,$$
$$p = p_o (1+\epsilon p') \,,$$
$$p_g = p_o (1+\epsilon p_g') \,,$$
$$\beta = \beta_o (1+\epsilon \beta') \,,$$
$$t = \tau t' \,,$$
$$x = c_o \tau x' \,. \tag{A2.8}$$

ε is chosen so that the maximum of the functions u', etc, for some given initial value, is of order unity.

(A2.8) is introduced in the equations (A2.1)-(A2.6). Terms of order ε^2, $\varepsilon\beta_o$ and lower are retained, terms of order $\varepsilon^2\beta_o$ and higher are discarded. The terms in (A2.6) representing dispersion and attenuation are assumed to be small, at least of $O(\varepsilon)$.

(A2.2) becomes

$$\frac{\partial u'}{\partial x'} - \frac{\partial \beta'}{\partial t'} = \beta_o\left\{\frac{\partial u'}{\partial x'} - \frac{1}{2}\frac{\partial}{\partial x'}(v'-u')\right\} . \qquad (A2.9)$$

(A2.3) becomes

$$\frac{\partial u'}{\partial t'} + \frac{\partial p'}{\partial x'} = \beta_o\left\{\frac{\partial p'}{\partial x'} + \frac{\partial u'}{\partial t'} - \frac{1}{2}\frac{\partial}{\partial t'}(v'-u')\right\} . \qquad (A2.10)$$

(A2.4) becomes

$$\frac{\partial p'_g}{\partial t'} + \frac{\partial \beta'}{\partial t'} = -\beta_o\left\{\frac{\partial u'}{\partial x'} + \frac{\partial}{\partial x'}(v'-u')\right\} - \varepsilon\frac{\partial}{\partial t'}(p'_g\beta') . (A2.11)$$

(A2.6) becomes

$$p'_g - p' = -\frac{1}{\omega_B^2\tau^2}\left[\frac{\partial^2\beta'}{\partial t'^2} + \tau\delta'\omega_B\frac{\partial\beta'}{\partial t'}\right] . \qquad (A2.12)$$

(A2.5) becomes

$$\left\{\frac{\partial}{\partial t'} + 1\right\}(v'-u') + 2\frac{\partial p'}{\partial x'} = 2\beta_o\frac{\partial p'}{\partial x'} - 2\beta'\varepsilon\frac{\partial p'}{\partial x'} -$$

$$\varepsilon\left(\frac{\partial}{\partial t'}+1\right)\left\{\beta'(v'-u')\right\} . \qquad (A2.13)$$

Terms in the left-hand side of the equations (A2.9)-(A2.13) are supposed to be of order one when also p_o, β_o, c_o and τ are properly chosen.

To find a wave propagating in one direction we use a method

given in Broer (1964).

When moving in a $(x'+t',t')$ frame, it follows from $(A2.9)$-$(A2.13)$ that

$$
\left.
\begin{aligned}
u' + \beta' &= O(\beta_o) , \\
p' - u' &= O(\beta_o) , \\
p' - p'_g &= O(\varepsilon) , \\
p'_g + \beta' &= O(\beta_o, \varepsilon) .
\end{aligned}
\right\} \tag{A2.14}
$$

With the help of $(A2.14)$ we find from $(A2.11)$ and $(A2.12)$, omitting the primes

$$
\frac{\partial p}{\partial t} + \frac{\partial \beta}{\partial t} = - \beta_o \left\{ \frac{\partial p}{\partial x} + \frac{\partial}{\partial x}(v-u) \right\} + \varepsilon \frac{\partial p^2}{\partial t} +
$$

$$
\frac{1}{\omega_B^2 \tau^2} \left\{ \frac{\partial^3 p}{\partial t^3} + \tau \delta' \omega_B \frac{\partial^2 p}{\partial t^2} \right\} . \tag{A2.15}
$$

$(A2.9)$ and $(A2.15)$ give

$$
\frac{\partial p}{\partial t} + \frac{\partial u}{\partial x} = - \frac{3\beta_o}{2} \frac{\partial}{\partial x}(v-u) + \varepsilon \frac{\partial p^2}{\partial t} +
$$

$$
\frac{1}{\omega_B^2 \tau^2} \left\{ \frac{\partial^3 p}{\partial t^3} + \tau \delta' \omega_B \frac{\partial^2 p}{\partial t^2} \right\} . \tag{A2.16}
$$

From $(A2.14)$ and $(A2.16)$ it follows that

$$
p - u = O(\varepsilon, \beta_o),
$$

and

$$
\frac{\partial}{\partial t} + \frac{\partial}{\partial x} = O(\varepsilon, \beta_o) .
$$

This gives

$$
\frac{\partial u}{\partial x} + \frac{\partial u}{\partial t} - \frac{\partial p}{\partial x} - \frac{\partial p}{\partial t} = O(\varepsilon^2, \varepsilon\beta_o, \beta_o^2) . \tag{A2.17}
$$

Thus the pertinent equations can be reduced with help of $(A2.17)$. This approach is not uniform valid because we only

know that

$$\frac{\partial p}{\partial t} - \frac{\partial u}{\partial t} = O(\varepsilon, \beta_o).$$

Therefore $p-u = O(\varepsilon t)$. So the reduced equations cannot be used for long time intervals.

Substituting *(A2.17)* into *(A2.10)* and *(A2.16)* we obtain

$$2\left\{\frac{\partial p}{\partial t} + \frac{\partial p}{\partial x}\right\} = \beta_o\left\{\frac{\partial p}{\partial x} + \frac{\partial p}{\partial t} - \frac{1}{2}\frac{\partial}{\partial t}(v-u) - \frac{3}{2}\frac{\partial}{\partial x}(v-u)\right\} +$$

$$\varepsilon\frac{\partial p^2}{\partial t} + \frac{1}{\omega_B^2\tau^2}\left\{\frac{\partial^3 p}{\partial t^3} + \tau\delta'\omega_B\frac{\partial^2 p}{\partial t^2}\right\} + O(\varepsilon\beta_o, \beta_o^2) . \qquad (A2.18)$$

With $(\partial/\partial t)+(\partial/\partial x)=O(\varepsilon,\beta_o)$, *(A2.18)* reduces to

$$\frac{\partial p}{\partial t} + \frac{\partial p}{\partial x} = \varepsilon p\frac{\partial p}{\partial t} - \frac{\beta_o}{2}\frac{\partial}{\partial x}(v-u) +$$

$$\frac{1}{2\omega_B^2\tau^2}\left\{\frac{\partial^3 p}{\partial t^3} + \tau\delta'\omega_B\frac{\partial^2 p}{\partial t^2}\right\} . \qquad (A2.19)$$

We rewrite *(A2.13)* to

$$\left(\frac{\partial}{\partial t} + 1\right)\left\{\frac{\beta_o}{2}\frac{\partial}{\partial x}(v-u)\right\} = -\beta_o\frac{\partial^2 p}{\partial x^2} + O(\varepsilon\beta_o, \beta_o^2) . \qquad (A2.20)$$

(A2.19) and *(A2.20)* give

$$\left(\frac{\partial}{\partial t} + 1\right)\left[\frac{\partial p}{\partial t} + \frac{\partial p}{\partial x} + \varepsilon p\frac{\partial p}{\partial x} + \frac{1}{2\omega_B^2\tau^2}\left\{\frac{\partial^3 p}{\partial x^3} - \tau\delta'\omega_B\frac{\partial^2 p}{\partial x^2}\right\}\right] =$$

$$\beta_o\frac{\partial^2 p}{\partial x\partial t} . \qquad (A2.21)$$

The equation for p, the actual pressure, in the laboratorium frame becomes

ERRATA

Contents-Chapter 6-§2	read: motion
page 26-formula (2.15)	read: p_g
page 60-9th line from top	read: (1.16)
page 90-6th line from top	read: (5.33a)
page 148-Figure 26	read: $d_A(3a_o)^{\frac{1}{2}}$
page 149-1st line	read: d_A/R_o
-Figure 27	read: d_A/R_o
page 158-Figure 34	read: d_A/R_o
page 176-Table A-4	read: b_1, b_2 and b_3 in stead of a_1, a_2 and a_3
-10th line from top	read: b_2 in stead of a_2
page 181-1st line	read: $c_f(\dfrac{p-p_o}{p_o})\dfrac{\partial p}{\partial x}$
-2nd line	read: $c_o(\dfrac{p-p_o}{p_o})\dfrac{\partial p}{\partial x}$

$$\frac{\partial}{\partial t}\left[c_f \frac{\partial p}{\partial x} + \frac{\partial p}{\partial t} + c_f \frac{p-1}{p_o} \frac{\partial p}{\partial x} + \frac{c_f^3}{2\omega_B^2} \frac{\partial^3 p}{\partial x^3} - \frac{\delta' c_f^2}{2\omega_B} \frac{\partial^2 p}{\partial x^2}\right] +$$

$$\tau^{-1}\left[c_o \frac{\partial p}{\partial x} + \frac{\partial p}{\partial t} + c_o \frac{p-1}{p_o} \frac{\partial p}{\partial x} + \frac{c_o^3}{2\omega_B^2} \frac{\partial^3 p}{\partial x^3} - \frac{\delta' c_o^2}{2\omega_B} \frac{\partial^2 p}{\partial x^2}\right] = 0 \quad,$$

where

$$\frac{c_f - c_o}{c_o} = \beta_o \quad.$$

APPENDIX 3.

§1. *EXPERIMENTAL RESULTS FOR S_A SHOCKS.*

TABLE A-5

Experimental results for region A

x	$\dfrac{x}{c_f \tau}$	$P_o \times 10^{-5}$	β_o	$R_o \times 10^3$	$\dfrac{P_1}{P_o}$	U	$d_A \times 10^2$	$\Lambda \times 10^2$	N_{th}	N_{exp}	W_1	W_2	exp. number
m		N/m^2	%	m		m/sec	m	m					
.26	.3	.967	1.82	1.14	1.08	100	11	14	2	4	3.78	7.57	5-3
.2	.04	.928	3.28	1.32	1.09	61	4.9	6.7	2	5	2.71	4.32	4-31
.26	.42	.967	3.98	1.26	1.10	61	7.3	9.1	2	4	4.92	7.52	5-2
.26	.47	.967	6.2	1.31	1.10	47	6.6	7.5	2	7	4.81	7.05	5-1
.07	.12	.919	5.47	1.33	1.11	53	4.7	6.3	2	4	3.59	5.84	4-43
.16	.18	.918	1.05	1.13	1.13	100	10	18	2	5	4.63	9.3	4-1
.19	.18	.921	2.19	1.41	1.13	73	7.2	8.7	2	4	3.73	5.09	4-2
.19	.22	.921	3.9	1.50	1.13	57	4.5	7.4	2	5	2.9	5.55	4-3
.27	.05	.924	5.03	1.47	1.13	57	9.1	7.4	3	4	6.77	6.5	5-22
.27	.45	.934	1.46	1.29	1.13	53	4.2	6.3	2	4	3.33	5.87	5-5
.27	.38	.934	2.12	1.17	1.13	76	6.1	6.4	2	3	3.78	4.54	5-6
.27	.05	.924	1.88	1.18	1.14	78	9.4	9.4	2	4	5.61	6.28	5-23
.20	.04	.861	3.30	1.38	1.17	63	6.3	8.9	3	4	4.67	7.43	4-29
.06	.12	.85	6.18	1.32	1.18	47	3.3	3.7	3	4	3.39	4.66	4-46
.18	.27	.852	4.29	1.35	1.18	52	3.1	3.6	3	5	2.73	3.68	4-7
.21	.18	.855	1.8	1.47	1.19	75	6	6.7	3	5	3.31	4.17	4-5
.2	.28	.854	3.6	1.37	1.19	53	3.7	5.8	3	5	3.05	5.49	4-4
.27	.39	.866	1.4	1.08	1.2	94	4.7	6.6	3	5	3.22	5.07	5-8
.26	.09	.855	5.2	1.30	1.22	63	8.8	10	3	5	9.52	12.7	5-24
.26	.46	.865	4.15	1.26	1.22	56	4.5	4.5	3	4	4.56	5.26	5-8
.26	.53	.865	7.11	1.30	1.22	42	2.5	-	-	-	3.05	-	5-9
.26	.05	.855	1.78	1.18	1.23	75	7.5	7.5	3	7	5.55	6.24	5-25
.2	.04	.793	3.45	1.39	1.24	67	5	5.3	3	5	4.45	5.41	4-33
.08	.1	.785	3.84	1.41	1.26	63	4.4	5.1	3	4	4.22	5.55	4-48
.14	.23	.78	4.36	1.35	1.28	51	2.6	2.6	3	5	2.77	3.21	4-7
.19	.25	.785	3.7	1.37	1.29	60	2.7	4.8	3	5	2.74	5.61	4-8
.21	.25	.788	2.6	1.41	1.30	75	3.4	4.5	3	5	2.82	4.28	4-9
.27	.47	.798	4.43	1.29	1.31	54	3.3	3.8	3	5	3.9	5.3	9-11
.27	.35	.798	1.15	1.09	1.31	96	3.8	5.8	2	6	2.85	4.87	5-12
.26	.04	.787	5.32	1.58	1.33	54	8.1	8.1	4	5	8.82	10.3	5-26
.26	.04	.788	1.87	1.38	1.33	86	10.3	11.2	4	5	7.9	9.8	5-27
.09	.1	.718	1.3	1.28	1.38	106	4.3	6.4	3	3	3.07	5.28	4-50
.09	.13	.718	3.7	1.43	1.38	61	3.7	4.3	3	3	2.33	5.35	4-51

TABLE A-5

(continuation)

x	$\frac{x}{c_f^\tau}$	$p_o \times 10^{-5}$	β_o	$R_o \times 10^3$	$\frac{p_1}{p_o}$	U	$d_A \times 10^2$	$\Lambda \times 10^2$	N_{th}	N_{exp}	W_1	W_2	exp. number
m		N/m²	%	m		m/sec	m	m					
.26	.42	.732	1.69	1.13	1.46	96	3.8	5.8	3	5	3.89	6.8	5-15
.21	.04	.658	3.74	1.44	1.47	67	3.7	4.7	4	4	4.32	6.44	4-35
.07	.09	.65	3.15	1.44	1.5	73	3.6	4.3	4	6	4.02	5.68	4-54
.19	.25	.649	4.3	1.54	1.5	52	2.3	2.6	4	4	2.83	3.72	4-10
.09	.09	.65	1.23	1.34	1.51	88	3.1	2.6	4	5	2.33	2.33	4-53
.21	.26	.652	2.69	1.45	1.52	67	3	-	-	-	3.1	-	4-11
.21	.26	.652	1.12	1.17	1.55	94	3.8	5.2	4	5	3.2	5.18	4-12
.27	.49	.664	1.49	1.05	1.61	85	3.4	5.1	4	5	3.8	6.7	5-18
.19	.05	.665	2.95	1.25	1.62	68	3.4	4.1	4	4	4.5	6.5	5-35
.2	.04	.667	1.96	1.17	1.62	77	3.8	4.6	4	5	4.5	6.4	5-36
.19	.04	.598	3.21	1.33	1.79	66	3.3	3.3	4	4	4.7	5.7	5-37
.2	.04	.599	1.53	1.16	1.79	96	2.9	4.8	4	4	3.3	6.6	5-38
.21	.31	.602	2.31	1.3	1.8	78	3.9	3.8	4	6	3.9	5.6	5-40
.19	.25	.6	5.01	1.65	1.81	51	2.5	2.5	4	4	3.6	4.5	5-39
.13	.25	.508	5.58	1.46	1.85	41	1.8	2	4	5	3.2	4.4	4-15
.21	.35	.516	2.32	1.26	1.9	66	2.3	3.6	4	5	3.1	6	4-13
.18	.32	.513	4	1.47	1.91	54	1.6	3.6	4	4	2.4	5.6	4-14
.21	.04	.522	4.24	1.56	1.91	56	3.1	3.6	5	4	4.4	6.5	4-37
.28	.31	.399	5.83	1.88	2.49	45	2.7	2.3	5	4	4.7	4.8	4-64
.18	.34	.377	5.34	1.54	2.51	47	2.1	2.1	5	5	3.9	5.3	4-18
.2	.05	.386	4.44	1.5	2.55	59	2.4	2.9	5	3	4.2	7	4-39
.16	.32	.376	3.79	1.41	2.62	54	1.9	3.5	5	5	3.4	7.8	4-16
.2	.42	.313	2.34	1.33	3.1	74	1.7	2.6	5	4	2.6	5.7	4-21
.19	.36	.311	4.09	1.55	3.16	55	1.6	1.6	5	4	2.9	4.1	4-20
.14	.27	.306	6	1.66	3.2	48	1.4	1.4	5	4	2.9	4.1	4-19
.22	.43	.331	3.05	1.39	3.34	56	2.2	2.2	5	3	3.9	5.6	5-43
.22	.47	.246	3.27	1.47	4.04	63	1.3	1.4	5	4	2.2	3.7	4-22
.17	.42	.24	5.3	1.54	4.24	48	.7	-	-	-	1.5	-	4-23
.12	.22	.236	7.05	1.92	4.31	39	.8	-	-	-	1.6	-	4-24
.21	.64	.178	4.44	1.44	6.16	57	1.1	-	-	-	2.5	-	4-27
.16	.37	.172	6.32	1.79	6.33	46	.7	-	-	-	1.5	-	4-26
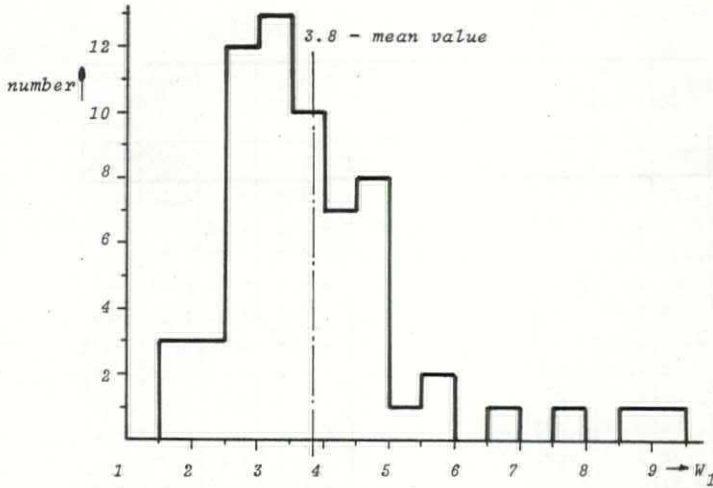
FIGURE A3-1. Distribution function for W_1. The mean value is 3.8 and the standard deviation is about 1.
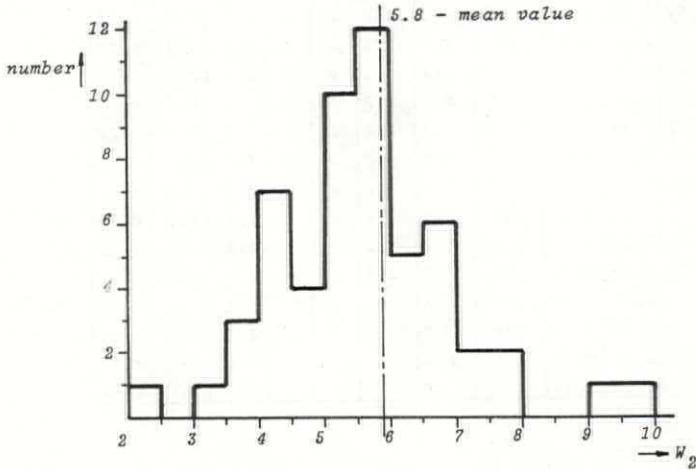
FIGURE A3-2. Distribution function of W_2. The mean value is 5.8 and the standard deviation is about 1.

§2. EXPERIMENTAL RESULTS FOR S_B SHOCKS.

TABLE A-6

Experimental results for S_B shocks

x	$\dfrac{x}{c_f \tau}$	$P_o \times 10^{-5}$	β_o	$R_o \times 10^3$	$\dfrac{p_1}{p_o}$	U	$d_A \times 10^2$	$\Lambda \times 10^2$	W_3	W_4	$\ln(20 \times F_{ad})$	F_{exp}	$\nu_L \times 10^6$	exp. number
m		N/m^2	$\%$	m		m/sec	m	m					$\dfrac{m^2}{sec}$	
2.5	3.1	1.23	1.39	1.08	1.07	111	16.7	11.1	4.5	6.4	2.34	.52	7	4-70
4.1	5.1	1.36	.97	.94	1.08	143	17.1	-	5.8	-	2.66	.31	7	4-41
2.2	32	1.18	3.4	1.38	1.09	63	7.5	-	3.5	-	.55	.4	110	5-31
2.2	2	1.14	1.77	1.32	1.89	93	13.9	11.1	4.2	5.3	2.38	.55	7	4-2
2.2	2.4	1.14	3.14	1.40	1.09	71	10	8.6	1.9	5	1.31	.45	7	4-3
2.3	3.4	1.19	3.24	1.18	1.09	71	11.3	-	1.01	-	.38	.34	7	5-2
2.2	3.4	1.14	.85	1.05	1.10	125	12.5	12.5	4.1	5.2	2.75	.63	7	4-1
4.5	.7	1.34	3.46	1.30	1.10	75	19	-	3.7	-	1.12	.4	1	5-22
4.5	.7	1.34	1.3	1.04	1.10	121	21	17	8.2	9.2	2.62	.53	1	5-23
1.2	22	1.06	3.79	1.43	1.11	52	11.3	9.3	1.5	6.2	.90	.62	110	5-31
1.2	1.1	1.03	1.96	1.36	1.12	76	10.6	9.1	3.8	4.9	2.46	.67	7	4-2
1.2	1.3	1.03	3.48	1.45	1.12	66	9.9	6.6	3	4.5	1.78	.64	7	4-3
2.3	3.5	1.16	3.6	1.20	1.12	63	8.8	-	2.7	-	1.54	.3	7	5-5
2.3	3	1.15	1.72	1.09	1.12	90	9.9	9	4.4	5.8	2.56	.4	7	5-6
2.2	33	1.10	1.4	1.22	1.13	91	7.3	6.4	3	3.5	2.68	.78	110	4-32
4.1	5.6	1.29	1.47	1.01	1.14	119	14.3	-	7.6	-	2.7	.33	7	4-44
4.1	5.9	1.29	2.43	1.10	1.14	94	15.1	-	7.8	-	2.41	.27	7	4-45
2.5	4.4	1.12	4.69	1.21	1.15	55	8.2	-	3	-	1.47	.33	7	4-46
2.5	3.9	1.12	2.79	1.15	1.15	73	10.9	7.2	5.8	6.2	2.37	.43	7	4-45
2.5	3.7	1.12	4.68	1.21	1.15	55	9.3	-	3.4	-	1.47	.33	7	4-46
2.2	2.9	1.08	2.9	1.27	1.15	69	5.2	6.8	2.5	5.4	2.33	.5	7	4-5
2.2	3.2	1.0/	3.4	1.25	1.15	63	5.1	-	2.4	-	2.15	.5	7	4-4
4.5	1	1.27	3.47	1.14	1.16	75	15	-	8.5	-	2.19	.32	1	5-24
2.2	1.8	1.J8	1.43	1.36	1.16	94	6.6	9.4	3.1	5.1	2.7	.79	7	4-6
2.6	3.7	1.13	1.69	1.06	1.16	86	11.2	8.6	2.81	6.2	2.67	.47	7	4-44
2.2	39	1.11	3.18	1.35	1.16	61	9.1	-	3.31	-	2.27	.42	110	6-32
1.2	19	.984	1.59	1.26	1.17	82	10.7	9.8	4.2	6.3	2.73	.98	110	4-32
2.3	3	1.09	1.12	1.0	1.18	111	11.1	8.8	6.2	6.1	2.82	.45	7	5-7
1.2	1.6	.97	3.23	1.31	1.18	57	5.7	4.5	3.1	3.9	2.36	.62	7	4-5
1.2	1.8	.96	3.79	1.29	1.18	56	6.7	5.6	3.6	5.3	2.20	.6	7	4-4
4.5	.7	1.27	1.2	1.03	1.18	128	17	13	9.2	8.7	2.8	.46	1	5-25
1.2	22	.99	3.56	1.4	1.19	52	8.8	7.2	3.8	6.3	2.32	.54	110	5-32
2.3	4.4	1.09	5.7	1.21	1.19	50	6	-	2.6	-	1.47	.2	7	5-9
2.3	3.7	1.09	3.3	1.16	1.19	66	8	-	5.3	-	2.41	.35	7	5-8

TABLE A-6 *(continuation 1)*

x	$\dfrac{x}{c_f \tau}$	$p_o \times 10^{-5}$	β_o	$R_o \times 10^3$	$\dfrac{p_1}{p_o}$	U	$d_A \times 10^2$	$\Lambda \times 10^2$	W_3	W_4	$ln(20 \times F_{ad})$	F_{exp}	$\nu_l \times 10^6$	exp. number
m		N/m^2	%	m		m/sec	m	m					$\dfrac{m^2}{sec}$	
4.1	5.3	1.22	3.6	1.29	1.2	75	11.9	-	7.2	-	2.34	.23	7	4-47
4.1	5	1.22	2.46	1.22	1.2	86	13.8	-	8.6	-	2.61	.68	7	4-48
2.2	32	1.04	1.75	1.32	1.2	86	8.6	8.6	4.3	5.9	2.74	.68	110	4-34
1.2	1	.97	1.59	1.41	1.21	81	8.1	6.5	4	4	2.78	.64	7	4-6
4.1	4.9	1.22	.69	.91	1.21	167	16.7	13.3	9.2	8.7	2.91	.46	7	4-49
2.2	40	1.04	2.82	1.31	1.22	62	6.8	-	3.7	-	2.59	.51	110	5-33
2.5	3.4	1.05	4.18	1.36	1.22	57	8.5	-	5.3	-	2.29	.38	7	4-47
2.5	3.3	1.06	2.85	1.28	1.22	66	8.6	-	5.5	-	2.57	.48	7	4-48
2.1	3.3	1	3.4	1.24	1.22	62	4.3	6.2	3	6.4	2.46	.45	7	4-7
2.2	3	1.01	2.9	1.26	1.23	69	4.8	-	3.3	-	2.58	.52	7	4-8
2.2	2.4	1.01	2.04	1.3	1.23	77	5.4	-	3.3	-	2.72	.62	7	4-9
2.5	3.3	1.06	.81	.95	1.23	119	11.9	8.3	6.9	5.7	2.9	.64	7	4-49
4.5	7	1.27	2.79	1.11	1.23	74	11.8	-	9.2	-	2.61	.22	7	5-11
4.5	5.2	1.27	.73	.93	1.23	134	13.4	10.8	7.6	7.2	2.91	.41	7	5-12
4.5	.7	1.2	3.48	1.37	1.24	75	11	11	7.6	10.3	2.51	.42	1	5-26
1.2	18	.92	1.98	1.37	1.26	91	11.8	10.9	6.3	8.6	2.77	.82	110	4-34
1.1	1.8	.89	3.8	1.29	1.26	57	4.5	4.5	3.4	5.2	2.48	.55	7	4-7
4.5	.6	1.2	1.23	1.2	1.26	122	12	12	7.3	8.7	2.86	.52	1	5-27
1.2	1.7	.9	3.24	1.31	1.27	60	5.4	4.2	4.1	4.5	2.6	.61	7	4-8
2.3	3.7	1.02	3.47	1.1	1.27	63	8.1	-	6.8	-	2.57	.37	7	5-11
4.1	6.3	1.15	3.52	1.19	1.27	69	5.6	-	4.7	-	2.56	.3	7	4-52
4.1	5	1.16	2.29	1.22	1.28	85	6.8	6.8	5.2	6.9	2.75	.38	7	4-51
2.3	4.1	1.02	6.12	1.28	1.28	47	5.7	-	4.3	-	2.08	.19	7	5-20
2.3	2.8	1.02	.9	1	1.28	115	9.2	8	5.9	6.1	2.9	.53	7	5-12
1.2	1.4	.9	2.29	1.35	1.29	70	5.6	4.9	3.9	4.5	2.75	.67	7	4-9
1.2	23	.92	3.18	1.36	1.29	51	7.7	8.2	5	8.6	2.64	.52	110	5-33
4.1	3.7	1.16	.81	1.09	1.29	139	8.3	11.4	4.7	7.5	2.92	.46	7	4-50
2.5	4.1	.99	4.12	1.25	1.31	58	6.9	-	6.2	-	2.54	.4	7	4-52
2.2	44	.98	2.95	1.28	1.31	60	5.4	7.1	3.8	7.9	2.69	.51	110	5-34
2.6	3.3	.99	2.68	1.29	1.32	74	7.4	5.1	2.1	5.9	2.73	.48	7	4-51
4.5	6	1.02	1.03	.96	1.33	128	12.8	7.7	9.8	7.1	2.9	.45	7	5-15
4.5	6.8	1.02	2.58	1.12	1.34	77	7.7	5.4	7.3	6.7	2.73	.3	7	5-14
2.2	31	.9	2.04	1.32	1.34	88	7.9	8.8	5.6	8.3	2.81	.78	110	4-36
4.1	3.5	1.09	.74	1.13	1.37	128	6.4	10.3	3.8	7.2	2.94	.5	7	4-53

TABLE A-6 (continuation 2)

x	$\dfrac{x}{c_f\tau}$	$P_o \times 10^{-5}$	β_o	$R_o \times 10^3$	$\dfrac{p_1}{p_o}$	U	$d_A \times 10^2$	$\Lambda \times 10^2$	W_3	W_4	$ln(20 \times F_{ad})$	F_{exp}	$\nu_L \times 10^6$	exp. number
m		N/m^2	$\%$	m		m/sec	m	m					$\dfrac{m^2}{sec}$	
4.1	4.7	1.09	1.88	1.21	1.37	89	7.1	8	5.9	8.3	2.84	.46	7	4-54
4.1	4.3	1.09	2.57	1.37	1.37	85	6.8	-	5.6	-	2.78	.42	7	4-55
2.3	4.4	.95	6.4	1.28	1.37	46	5.5	-	5.6	-	2.32	.23	7	5-13
2.3	3.3	.953	1.3	1.03	1.37	109	6.6	6.6	5.4	6.6	2.89	.58	7	5-15
2.3	3.1	.952	3.3	1.21	1.38	65	6.5	-	7.6	-	2.72	.41	7	5-14
2.2	2.8	.87	3.2	1.39	1.39	59	4.1	4.7	3.7	5.6	2.73	.52	7	4-10
1.2	25	.86	3.36	1.34	1.4	52	8.2	5.2	6.8	6.5	2.72	.52	110	5-34
2.2	2.5	.87	2.01	1.31	1.41	76	5.3	5.7	4.3	5.8	2.84	.6	7	4-11
2.6	2.3	.92	.87	1.19	1.41	116	9.3	9.3	5.8	7	2.93	.7	7	4-53
2.5	3.1	.92	2.2	1.28	1.41	85	8.5	6.8	7.4	7.5	2.83	.57	7	4-54
2.5	2.8	.92	3.04	1.45	1.42	69	8.2	-	7.2	-	2.76	.52	7	4-55
2.2	2.6	.87	.83	1.06	1.42	119	9.5	8.3	6.8	7	2.94	.76	7	4-12
4.5	9	1.13	5.28	1.15	1.43	52	6.3	-	7.9	-	2.56	.23	7	5-16
4.5	7	1.13	2.6	1.12	1.43	76	7.6	6.8	8.1	9.5	2.8	.4	7	5-17
4.5	6.8	1.13	.87	.88	1.43	126	6.3	7.6	5.5	7.9	2.9	.47	7	5-18
1.2	21	.783	2.36	1.39	1.48	66	4.9	5.9	3.9	6.7	2.84	.8	110	4-36
1.2	1.6	.76	3.68	1.46	1.48	54	4.9	3.3	4.8	4.3	2.74	.62	7	4-10
2.3	4.8	.88	6.8	1.25	1.5	44	4.4	-	5.6	-	2.47	.22	7	5-16
2.3	3.8	.89	3.34	1.21	1.51	63	4.4	4.4	5.1	6.8	2.77	.44	7	5-17
2.3	3.7	.89	1.12	.95	1.51	109	5.4	5.4	5.2	6.4	2.93	.61	7	5-18
1.2	1.5	.76	.96	1.11	1.51	116	7	5.8	5.4	5.4	2.94	.83	7	4-12
1.2	1.4	.76	2.3	1.37	1.53	70	4.9	4.9	4.6	5.8	2.86	.7	7	4-11
2.2	46	.766	1.99	1.22	1.54	91	7.3	8.2	5.3	10.1	2.88	.74	110	4-38
4.1	4.9	.954	.88	1.03	1.6	143	7.1	7.1	6.1	7.4	2.95	.57	7	4-61
4.1	4.7	.953	2.76	1.38	1.61	88	5.3	6.1	5.5	8.4	2.84	.56	7	4-59
2.2	2.7	.82	3.66	1.49	1.62	59	4.7	4.4	5.1	6.5	2.79	.56	7	5-39
2.2	3	.82	1.69	1.17	1.62	93	5.6	5.6	5.6	7.1	2.91	.65	7	5-40
4.5	5.9	.999	.88	.96	1.65	134	4.7	5.3	4.5	6.1	2.95	.63	7	5-21
4.5	6.2	.997	2.47	1.22	1.67	78	4.7	3.9	5.5	6	2.87	.48	7	5-20
2.6	3.2	.79	2.31	1.33	1.69	89	8	5.4	8.5	7.3	2.83	.6	7	4-60
2.6	3.2	.786	1.07	1.1	1.69	100	6	5	5.5	5.7	2.94	.48	7	4-61
2.5	3.1	.79	3.35	1.47	1.72	62	6.2	3.7	6.9	5.6	2.83	.62	7	4-59
4.5	8.3	.997	4.65	1.21	1.72	56	3.9	3.4	5.9	7.1	2.75	.4	7	5-19
2.2	3.4	.74	1.6	1.12	1.74	81	3.2	5.6	3.6	7.9	2.92	.72	7	4-13

TABLE A-6 *(continuation 3)*

x	$\dfrac{x}{c_{f^{\tau}}}$	$p_o \times 10^{-5}$	β_o	$R_o \times 10^3$	$\dfrac{p_1}{p_o}$	U	$d_A \times 10^2$	$\Lambda \times 10^2$	W_3	W_4	$ln(20 \times F_{ad}$	F_{exp}	$\nu_l \times 10^6$	exp. number
m		N/m^2	%	m		m/sec	m	m					$\dfrac{m^2}{sec}$	
2.1	3.7	.73	3.89	1.3	1.74	56	2.8	3.4	3.8	6.3	2.81	.6	7	4-15
2.2	3.2	.73	2.8	1.31	1.77	60	3.3	3.6	4	5.8	2.87	.65	7	4-14
2.3	3.4	.749	3.18	1.34	1.77	64	2.6	2.6	3.2	4.3	2.84	.55	7	5-20
2.3	3.3	.75	1.17	1.07	1.81	108	4.3	4.3	4.5	5.7	2.95	.61	7	5-21
1.2	27	.647	2.36	1.3	1.81	75	6	6	6.3	9.1	2.89	.75	110	4-38
2.3	4.5	.75	6.2	1.33	1.81	46	2.7	2.7	4.3	6.4	2.7	.48	7	5-19
1.2	2	.63	1.91	1.18	1.83	86	4.3	4.3	5.1	6.6	2.91	.79	7	4-13
1.2	1.8	.62	3.3	1.38	1.83	57	2.8	2.3	3.6	3.9	2.85	.71	7	4-14
1.2	2.2	.58	1.92	1.15	1.85	78	4.7	4.7	5.7	7.4	2.91	.62	7	5-40
1.2	1.9	.58	4.14	1.46	1.87	52	4.1	3.9	5.4	7.1	2.8	.53	7	5-39
1.1	2.1	.62	4.58	1.37	1.91	50	3	–	4.4	–	2.8	.62	7	4-15
2.2	52	.63	1.91	1.2	1.93	86	4.3	6	4.7	9.5	2.92	.79	110	4-40
4.1	4.7	.818	2.19	1.36	1.96	100	5	5	5.7	7.5	2.9	.69	7	4-63
4.1	4.4	.814	2.86	1.48	1.97	79	4	4.4	4.6	6.9	2.88	.43	7	4-64
2.2	3.3	.69	1.87	1.19	1.99	88	3.5	3.5	4.3	5.7	2.92	.68	7	5-42
2.2	3	.69	3.91	1.48	2	62	3.1	3.1	4.1	5.8	2.84	.6	7	5-41
2.6	3.6	.65	1.4	1.17	2.08	88	3.5	3.5	4	5.2	2.95	.73	7	4-62
2.5	2.9	.65	3.6	1.6	2.11	58	2.9	2.9	3.6	5	2.9	.6	7	4-64
2.2	3	.6	1.04	1.13	2.13	122	4.9	5.5	5	7.4	2.96	.8	7	4-17
2.5	3.1	.65	2.75	1.45	2.17	66	2.6	2.6	3.2	4.5	2.9	.63	7	4-63
2.2	3.8	.6	2.39	1.21	2.2	69	3.4	4.1	4.8	8	2.92	.76	7	4-16
2.2	3.8	.6	3.37	1.32	2.25	60	3	3	4.5	6.4	2.88	.73	7	4-18
1.2	30	.511	2.36	1.29	2.33	77	3.8	4.6	4.8	8.7	2.92	.84	110	4-40
1.2	2.2	.49	4.13	1.41	2.33	53	2.6	2.4	4.1	5.4	2.86	.83	7	4-18
1.2	2.2	.49	2.93	1.29	2.34	62	3.7	3.1	5.5	6.5	2.9	.79	7	4-16
1.2	2.6	.44	2.19	1.17	2.38	70	3.5	2.8	5.5	5.7	2.93	.64	7	5-42
1.2	1.8	.49	1.28	1.21	2.38	88	3.9	3.9	4.4	6	2.96	.8	7	4-17
1.2	2.3	.443	4.56	1.45	2.46	49	2	2.5	3.2	5.9	2.85	.57	7	5-41
2.2	3.8	.53	1.43	1.11	2.51	93	2.8	2.8	3.6	5	2.95	.74	7	4-21
2.2	3	.53	2.39	1.29	2.54	79	4	3.6	5.6	7.2	2.93	.82	7	4-20
2.1	3.6	.53	3.49	1.39	2.56	58	2.3	2.9	3.6	6.6	2.89	.76	7	4-19
2.2	3.8	.55	1.83	1.17	2.62	86	2.6	2.6	3.6	5.1	2.94	.77	7	5-44
2.2	3.4	.55	3.76	1.47	2.63	57	2	2.3	3	5.2	2.89	.7	7	5-43

TABLE A-6 (continuation 4)

x	$\frac{x}{c_f \tau}$	$P_o \times 10^{-5}$	β_o	$R_o \times 10^3$	$\frac{P_1}{P_o}$	U	$d_A \times 10^2$	$\Lambda \times 10^2$	W_3	W_4	$\ln(20 \times F_{ad})$	F_{exp}	$\nu_l \times 10^6$	exp. number
m		N/m^2	%	m		m/sec	m	m					$\frac{m^2}{sec}$	
1.1	2.1	.42	4.41	1.5	2.72	48	2.4	2.4	3.8	5.9	2.87	.83	7	4-19
1.2	2.1	.42	1.8	1.2	2.9	85	3	3.3	4.2	6.9	2.92	.74	7	4-21
1.2	2.1	.42	3.02	1.4	2.91	65	3.2	2.6	4.9	5.9	2.87	.78	7	4-20
2.2	4.5	.46	2.77	1.24	3.04	70	2.8	2.1	4.7	5.3	2.93	.79	7	4-23
2.2	4	.39	2.77	1.36	3.47	67	2	2.7	3.3	7	2.95	.81	7	4-26
1.2	2.4	.36	2.26	1.3	3.6	66	2	1.6	3	3.9	2.95	.8	7	4-22
1.2	3.3	.31	2.26	1.14	3.67	75	1.9	2.6	3.3	7.2	2.95	.62	7	5-44
1.2	2.8	.31	4.63	1.43	3.71	53	2.4	2.4	4.5	7.6	2.89	.57	7	5-43
1.2	2.6	.35	3.64	1.36	4.05	63	1.9	1.9	3.5	5.9	2.92	.55	7	4-23
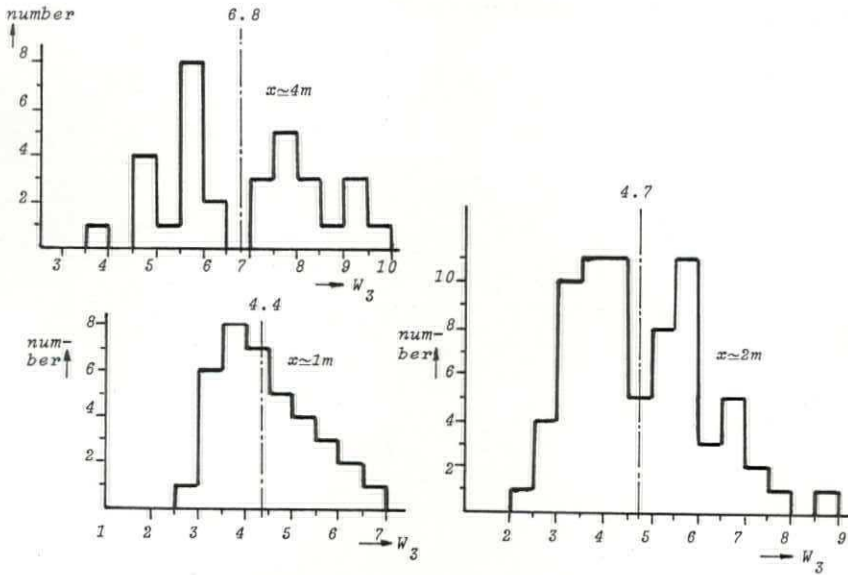
FIGURE A3-3. Distribution function for W_3. The mean values are indicated.
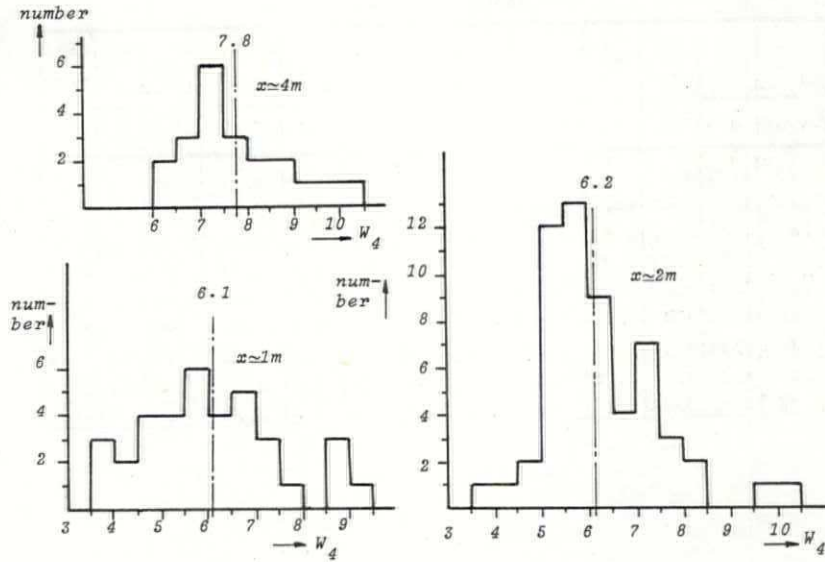
FIGURE A3-4. Distribution function for W_4. The mean values are indicated.

§3. EXPERIMENTAL RESULTS FOR S_C SHOCKS.

TABLE A-7

Experimental results for S_C shocks

x	$\dfrac{x}{c_f\tau}$	$P_o \times 10^{-5}$	β_o	$R_o \times 10^3$	$\dfrac{P_1}{P_o}$	$1+2\beta_o$	$\dfrac{1+\frac{4\gamma\beta_o}{1+\gamma}}{}$	U	d_C	$\dfrac{d_C}{U}\times 10^3$	W_5	$\nu_l \times 10^6$	$\tau \times 10^2$	exp. number
m		N/m²	%	m				m/sec	m	sec		$\dfrac{m^2}{sec}$	sec	
4.1	6	1.39	3.77	1.19	1.06	1.08	1.09	-	-	23	.69	7	1.1	4-68
4.1	5.6	1.39	2.58	1.13	1.06	1.05	1.06	-	-	18	.93	7	1	4-69
2.2	37	1.21	3.02	1.33	1.07	1.06	1.07	66	.68	9	4.5	110	.1	5-30
2.5	3.9	1.23	4.29	1.24	1.07	1.09	1.1	59	1	15	.5	7	1.2	4-68
2.5	3.6	1.23	2.94	1.18	1.07	1.06	1.07	70	.98	12	.54	7	1.1	4-69
4.5	7.4	1.44	4.17	1.15	1.07	1.08	1.1	65	2.1	33	1.22	7	1	5-1
4.1	6.1	1.36	3.67	1.17	1.08	1.07	1.09	-	-	20	.93	7	1.1	4-43
4.1	6.2	1.36	3.7	1.17	1.08	1.07	1.09	-	-	20	.88	7	1	4-43
1.2	21	1.09	3.35	1.37	1.08	1.07	1.08	53	.8	13	6.88	110	.1	5-30
2.3	3.9	1.19	5.05	1.22	1.09	1.1	1.12	55	.91	24	.76	7	1.2	5-1
2.5	4	1.19	4.19	1.22	1.09	1.08	1.1	58	.99	15	.61	7	1.2	4-43
2.5	4	1.19	4.22	1.22	1.09	1.08	1.1	59	1	15	.61	7	1.2	4-43
4.5	7.7	1.4	4.48	1.15	1.1	1.09	1.1	65	1.95	30	1.38	7	1	5-4
2.3	4.1	1.16	5.45	1.22	1.11	1.11	1.13	51	1.53	30	1.17	7	1.2	5-4
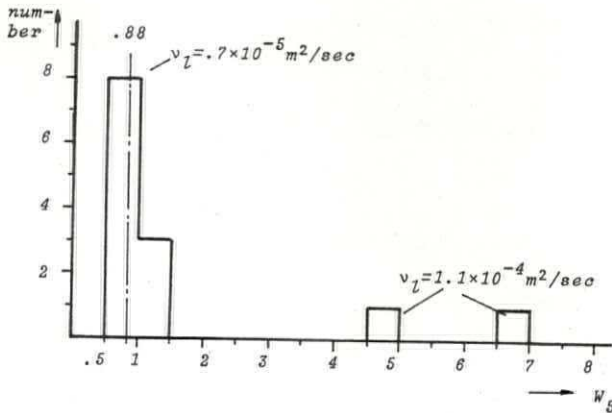
FIGURE A3-5. Distribution function of W_5 for $\nu_l = .7\times 10^{-5} m^2/sec$ and $\nu_l = 1.1\times 10^{-4} m^2/sec$. The mean value for W_5, $W_5 = .88$, is indicated for $\nu_l = .7\times 10^{-5} m^2/sec$.

§4. EXPERIMENTAL RESULTS FOR THE SMOOTH BACK SIDE OF S_B SHOCKS.

TABLE A-8

Experimental results

x	$\dfrac{x}{c_f \tau}$	$p_o \times 10^{-5}$	β_o	$R_o \times 10^3$	$\dfrac{p_1}{p_o}$	U	d_B	$\dfrac{d_B}{U} \times 10^3$	W_δ	$\nu_l \times 10^3$	$\tau \times 10^2$	F_{exp}	exp. number
m		N/m^2	%	m		m/sec	m	sec		$\dfrac{m^2}{sec}$	sec		
1.2	4.5	1.11	1.4	1.33	1.05	114	1.02	9	2.81	30	.33	.68	6-1
2.5	3.1	1.23	1.39	1.08	1.07	111	1	9	.93	7	.91	.52	4-70
4.1	5.1	1.36	.97	.94	1.08	143	1.43	10	1.3	7	.71	.31	4-41
2.2	32	1.18	3.4	1.38	1.09	63	.73	12	7.2	110	.11	.4	5-31
1.2	5.5	1.08	3.53	1.5	1.09	63	.63	10	1.89	30	.42	.59	6-2
1.2	5.4	1.08	2.64	1.41	1.09	76	.68	9	2.2	30	.37	.6	6-3
1.2	4	1.08	1.41	1.41	1.09	98	.78	8	2.66	30	.37	.68	6-4
2.3	3.4	1.19	3.24	1.18	1.09	71	.78	11	.64	7	1.1	.34	5-2
4.5	.7	1.34	3.46	1.3	1.1	75	2.26	30	.23	1	9.4	.4	5-22
4.5	.7	1.34	1.3	1.04	1.1	121	1.2	10	.17	1	6	.53	5-23
2.2	.4	1.12	2.9	1.23	1.1	81	.48	6	.07	1	8.5	.7	4-29
1.2	22	1.06	3.79	1.43	1.11	52	.62	12	9	110	.11	.62	5-31
1.2	5.8	1.04	3.63	1.48	1.12	62	.61	10	2.17	30	.41	.58	6-5
1.2	5.8	1.04	2.58	1.36	1.12	79	.64	8	2.44	30	.34	.63	6-6
1.2	4.6	1.04	1.58	1.37	1.12	104	.63	6	2.37	30	.35	.71	6-7
2.3	.4	1.12	4.15	1.38	1.12	63	1.88	30	.24	1	9.9	.63	5-22
2.3	.4	1.12	1.55	1.11	1.12	106	1.22	12	.23	1	6.8	.68	5-23
2.3	3.5	1.16	3.6	1.2	1.12	63	.88	14	.84	7	1.1	.3	5-5
2.3	3	1.15	1.72	1.09	1.12	90	.9	10	1.1	7	.95	.4	5-6
2.2	33	1.1	1.4	1.22	1.13	91	.46	5	10.4	110	.08	.78	4-32
4.1	5.6	1.29	1.47	1.01	1.14	119	1.55	13	1.59	7	.81	.33	4-44
4.1	5.9	1.29	2.43	1.1	1.14	94	1.13	12	1.05	7	.96	.27	4-45
2.5	4.4	1.12	4.69	1.21	1.15	55	.77	14	.86	7	1.2	.33	4-46
2.5	3.9	1.12	2.79	1.15	1.15	73	.73	10	.86	7	1.1	.43	4-45
2.5	3.7	1.12	4.68	1.21	1.15	55	.77	14	.86	7	1.2	.33	4-46
2.2	2.9	1.08	2.9	1.27	1.15	69	.48	7	.52	7	1.3	.5	4-5
2.2	3.2	1.07	3.4	1.25	1.15	63	.44	8	.51	7	1.2	.5	4-4
2.2	.4	1.06	2.7	1.29	1.15	83	.5	12	.14	1	9.2	.58	4-31
4.5	1	1.27	3.47	1.14	1.16	75	1.13	15	.17	1	7.2	.32	5-24
2.2	1.8	1.08	1.43	1.36	1.16	94	.85	9	1.15	7	1.5	.79	4-6
2.6	3.7	1.13	1.69	1.06	1.16	86	.78	9	1.09	7	.88	.47	4-44
2.2	39	1.11	3.18	1.35	1.16	61	.61	10	8.4	110	.1	.42	5-32

TABLE A-8 (continuation 1)

x	$\dfrac{x}{c_f^\tau}$	$p_o \times 10^{-5}$	β_o	$R_o \times 10^3$	$\dfrac{p_1}{p_o}$	U	d_B	$\dfrac{d_B}{U} \times 10^3$	W_6	$\nu_l \times 10^6$	$\tau \times 10^2$	F_{exp}	exp. number
m		N/m^2	%	m		m/sec	m	sec		$\dfrac{m^2}{sec}$	sec		
2.3	3	1.09	1.12	1	1.18	111	1.22	11	1.63	7	.79	.45	5-7
1.2	1.6	.97	3.23	1.31	1.18	57	.4	7	.56	7	1.4	.62	4-5
4.5	.7	1.27	1.2	1.03	1.18	128	1.4	11	.21	1	5.9	.46	5-25
2.3	.5	1.05	4.2	1.21	1.19	62	.9	15	.17	1	8.1	.48	5-24
1.2	22	.99	3.56	1.4	1.19	52	.62	12	11	110	.11	.54	5-32
2.3	4.4	1.09	5.7	1.21	1.19	50	1.15	23	1.34	7	1.2	.2	5-9
2.3	3.7	1.09	3.3	1.16	1.19	66	1.19	18	1.52	7	1.1	.35	5-8
4.1	5.3	1.22	3.6	1.29	1.2	75	1.34	18	1.09	7	1.3	.23	4-47
4.1	5	1.22	2.46	1.22	1.2	86	1.12	13	1.05	7	1.2	.31	4-48
2.2	32	1.04	1.75	1.32	1.2	86	.52	6	9	110	.1	.68	4-34
1.2	5.7	.98	3.6	1.52	1.2	61	.61	10	2.45	30	.43	.56	6-8
1.2	4.3	.98	2.71	1.45	1.2	73	.65	8	2.46	30	.38	.61	6-9
2.3	.4	1.05	1.45	1.1	1.2	102	.92	9	.18	1	6.7	.65	5-25
1.2	4.3	.98	1.55	1.44	1.21	93	.65	7	2.8	30	.38	.7	6-10
1.2	1	.97	1.59	1.41	1.21	81	.65	8	.72	7	1.6	.64	4-6
4.1	4.9	1.22	.69	.91	1.21	167	1.33	8	1.57	7	.65	.46	4-49
2.2	40	1.04	2.82	1.31	1.22	62	.49	8	9.4	110	.1	.51	5-23
2.5	3.4	1.05	4.18	1.36	1.22	57	.51	9	.55	7	1.5	.36	4-47
2.5	3.3	1.06	2.85	1.28	1.22	66	.59	9	.69	7	1.3	.48	4-48
2.1	3.3	1	3.4	1.24	1.22	62	.43	7	.58	7	1.2	.45	4-7
2.2	.4	.99	2.8	1.29	1.23	83	.42	10	.11	1	9	.64	4-33
2.2	3	1.01	2.9	1.26	1.23	69	.48	7	.65	7	1.3	.52	4-8
2.2	2.4	1.01	2.04	1.3	1.23	77	.54	7	.69	7	1.3	.62	4-9
2.5	3.3	1.06	.81	.95	1.23	119	.95	8	1.7	7	.72	.64	4-49
4.5	7	1.27	2.79	1.11	1.23	74	1.47	20	1.91	7	1	.22	5-11
4.5	.7	1.2	3.48	1.37	1.24	75	1.2	16	.16	1	10.5	.42	5-26
1.2	18	.92	1.98	1.37	1.26	91	.55	6	12.5	110	.1	.82	4-34
1.1	1.8	.89	3.8	1.29	1.26	57	.4	7	.59	7	1.3	.55	4-7
4.5	.6	1.2	1.23	1.2	1.26	122	1.1	10	.16	1	8	.52	5-27
1.2	1.7	.9	3.24	1.31	1.27	60	.36	6	.56	7	1.4	.61	4-8
2.3	3.7	1.0	3.47	1.1	1.27	63	.94	15	1.31	7	1.1	.37	5-11
4.1	6.3	1.1	3.52	1.19	1.27	69	.83	12	1.03	7	1.1	.3	4-52
4.1	5	1.1	2.29	1.22	1.28	85	.68	8	.75	7	1.2	.38	4-51

TABLE A-8 (continuation 2)

x	$\frac{x}{c_f^\tau}$	$p_o \times 10^{-5}$	β_o	$R_o \times 10^3$	$\frac{p_1}{p_o}$	U	d_B	$\frac{d_B}{U} \times 10^3$	W_6	$\nu_l \times 10^6$	$\tau \times 10^2$	F_{exp}	exp. number
m		N/m^2	%	m		m/sec	m	sec		$\frac{m^2}{sec}$	sec		
2.3	4.1	1.02	6.12	1.28	1.28	47	1.04	22	1.33	7	1.3	.19	5-20
2.3	2.8	1.02	.9	1	1.28	115	.92	8	1.37	7	.8	.53	5-12
2.3	.4	.98	4.26	1.47	1.29	60	.9	15	.13	1	12	.46	5-26
1.2	1.4	.9	2.29	1.35	1.29	70	.42	6	.62	7	1.4	.67	4-9
1.2	23	.92	3.18	1.36	1.29	51	.51	10	11.4	110	.1	.52	5-33
4.1	3.7	1.16	.81	1.09	1.29	139	.97	7	.97	7	.95	.46	4-50
2.3	.3	.98	1.5	1.28	1.3	102	1.5	10	.17	1	9.1	.67	5-27
2.5	4.1	.99	4.12	1.25	1.31	58	.4	7	.58	7	1.2	.4	4-52
2.2	44	.98	2.95	1.28	1.31	60	.42	7	9.42	110	.09	.51	5-34
2.6	3.3	.99	2.68	1.29	1.32	74	.37	5	.44	7	1.3	.48	4-51
4.5	6	1.02	1.03	.96	1.33	128	1.28	10	1.83	7	.73	.45	5-15
4.5	6.8	1.02	2.58	1.12	1.34	77	1.23	16	1.75	7	1	.3	5-14
2.2	31	.9	2.04	1.32	1.34	88	.44	5	10.4	110	.1	.78	4-36
4.1	3.5	1.09	.74	1.13	1.37	128	.64	5	.72	7	1	.5	4-53
4.1	4.7	1.09	1.88	1.21	1.37	89	.71	8	.89	7	1.2	.46	4-54
4.1	4.3	1.09	2.57	1.37	1.37	85	.68	8	.65	7	1.5	.42	4-55
2.3	4.4	.95	6.4	1.28	1.37	46	.6	13	.89	7	1.3	.23	5-13
2.3	3.3	.953	1.3	1.03	1.37	109	.76	7	1.24	7	.85	.58	5-15
2.3	3.1	.952	3.3	1.21	1.38	65	.52	8	.8	7	1.2	.41	5-14
2.2	2.8	.87	3.2	1.39	1.39	59	.4	7	.57	7	1.5	.52	4-10
1.2	25	.86	3.36	1.34	1.4	52	.41	8	10.3	110	.1	.52	5-34
2.2	2.5	.87	2.01	1.31	1.41	76	.38	5	.55	7	1.4	.6	4-11
2.6	2.3	.92	.87	1.19	1.41	116	.47	4	.67	7	1.1	.7	4-53
2.5	3.1	.92	2.2	1.28	1.42	85	.51	6	.67	7	1.3	.57	4-54
2.3	2.8	.92	3.04	1.45	1.42	69	.34	5	.4	7	1.7	.52	4-55
2.2	2.6	.87	.83	1.06	1.42	119	.36	3	.73	7	.9	.76	4-12
4.5	9	1.13	5.28	1.15	1.43	52	1.26	24	2.23	7	1.1	.23	5-16
4.5	7	1.13	2.6	1.12	1.43	76	.91	12	1.48	7	1	.4	5-17
4.5	6.8	1.13	.87	.88	1.43	126	1.26	10	2.34	7	.61	.47	5-18
2.2	.4	.85	2.9	1.32	1.44	71	.43	6	.1	1	9.7	.7	4-35
1.2	21	.783	2.36	1.39	1.48	66	.26	4	8.6	110	.11	.8	4-36
1.2	1.6	.76	3.68	1.46	1.48	54	.36	7	.59	7	1.7	.62	4-10
2.3	4.8	.88	6.8	1.25	1.5	44	.61	14	1.1	7	1.2	.22	5-16

TABLE A-8 *(continuation 3)*

x	$\dfrac{x}{c_f\tau}$	$p_o \times 10^{-5}$	β_o	$R_o \times 10^3$	$\dfrac{p_1}{p_o}$	U	d_B	$\dfrac{d_B}{U} \times 10^3$	W_ε	$\nu_l \times 10^6$	$\tau \times 10^2$	F_{exp}	exp. number
m		N/m^2	$\%$	m		m/sec	m	sec		$\dfrac{m^2}{sec}$	sec		
2.3	3.8	.89	3.34	1.22	1.51	63	.63	10	1.1	7	1.2	.44	5-17
2.3	3.7	.89	1.12	.95	1.51	109	1.09	10	2.3	7	.72	.61	5-18
1.2	1.5	.76	.96	1.11	1.51	116	.51	4	1.3	7	.97	.83	4-12
1.2	1.4	.76	2.3	1.37	1.53	70	.32	5	.55	7	1.5	.7	4-11
2.2	.4	.86	1.5	1.08	1.53	102	.41	4	.11	1	6.4	.64	5-36
2.2	46	.766	1.99	1.22	1.54	91	.27	3	7.4	110	.08	.74	4-38
2.2	.5	.86	2.3	1.15	1.55	86	.43	5	.11	1	7.3	.62	5-35
4.1	4.9	.954	.88	1.03	1.6	143	.57	4	.79	7	.84	.57	4-61
4.1	4.7	.953	2.76	1.38	1.61	88	.53	6	.62	7	1.5	.56	4-59
2.2	2.7	.82	3.66	1.49	1.62	59	.35	6	.51	7	1.8	.56	5-39
2.2	3	.82	1.69	1.17	1.62	93	.37	4	.66	7	1.1	.65	5-40
2.2	.4	.79	1.2	1.06	1.62	106	.32	4	.1	1	6.2	.73	5-38
4.5	5.9	.999	.88	.97	1.65	134	.67	5	1.22	7	.75	.63	5-21
4.5	6.2	.997	2.47	1.22	1.67	78	.39	5	.62	7	1.2	.48	5-20
2.2	.5	.97	2.4	1.21	1.67	71	.29	4	.08	1	8.1	.54	5-37
2.6	3.2	.79	2.31	1.33	1.68	89	.36	5	.5	7	1.4	.6	4-60
2.6	3.2	.786	1.07	1.1	1.69	100	.4	4	.63	7	.96	.48	4-61
2.5	3.1	.79	3.35	1.47	1.72	62	.31	5	.5	7	1.7	.62	4-59
4.5	8.3	.997	4.63	1.21	1.72	56	.67	12	1.37	7	1.2	.4	5-19
2.2	3.4	.74	1.6	1.12	1.74	81	.24	3	.63	7	1	.72	4-13
2.1	3.7	.73	3.89	1.3	1.74	56	.17	3	.37	7	1.3	.6	4-15
2.2	3.2	.73	2.8	1.31	1.77	60	.18	3	.42	7	1.4	.65	4-14
2.3	3.4	.749	3.28	1.34	1.77	64	.32	5	.56	7	1.4	.55	5-20
2.3	3.3	.75	1.17	1.07	1.81	108	.54	5	1.05	7	.91	.61	5-21
1.2	27	.647	2.36	1.3	1.81	75	.3	4	9.7	110	.09	.75	4-38
2.3	4.5	.75	6.2	1.33	1.81	46	.36	8	.8	7	1.4	.48	5-19
1.2	2	.63	1.91	1.18	1.83	86	.22	3	.58	7	1.1	.79	4-13
1.2	1.8	.62	3.3	1.38	1.83	57	.17	3	.41	7	1.5	.71	4-14
1.2	2.2	.58	1.92	1.15	1.85	78	.31	4	.71	7	1	.62	5-40
1.2	1.9	.58	4.14	1.46	1.87	52	.31	6	.56	7	1.7	.53	5-39
1.1	2.1	.62	4.58	1.37	1.91	50	.15	3	.35	7	1.5	.62	4-15
2.2	52	.63	1.91	1.2	1.93	86	.26	3	10.2	110	.08	.79	4-40
4.1	4.7	.818	2.19	1.36	1.96	100	.5	5	.73	7	1.5	.69	4-63

TABLE A-8 *(continuation 4)*

| x	$\dfrac{x}{c_f \tau}$	$p_0 \times 10^{-5}$	β_0	$R_0 \times 10^3$	$\dfrac{p_1}{p_0}$	U	d_B	$\dfrac{d_B}{U} \times 10^3$	W_6	$\nu_l \times 10^6$	$\tau \times 10^2$	F_{exp}	exp. number
m		N/m^2	$\%$	m		m/sec	m	sec		$\dfrac{m^2}{sec}$	sec		
4.1	4.4	.814	2.86	1.48	1.97	79	.4	5	.5	7	1.7	.43	4-64
2.2	3.3	.69	1.87	1.19	1.99	88	.26	2	.57	7	1.1	.68	5-42
2.2	3	.69	3.91	1.48	2	62	.25	4	.42	7	1.7	.6	5-41
2.6	3.6	.65	1.4	1.17	2.08	88	.35	4	.91	7	1.1	.73	4-62
2.5	2.9	.65	3.6	1.6	2.11	58	.23	4	.37	7	2	.6	4-64
2.2	3	.6	1.04	1.13	2.13	122	.31	5	.5	7	1	.8	4-17
2.5	3.1	.65	2.75	1.45	2.17	66	.26	4	.48	7	1.7	.63	4-63
2.2	3.8	.6	2.39	1.21	2.2	69	.14	4	.5	7	1.2	.76	4-16
2.2	3.8	.6	3.37	1.32	2.25	60	.18	4	.53	7	1.4	.73	4-18
1.2	30	.511	2.36	1.29	2.33	77	.31	4	16	110	.09	.84	4-40
1.2	2.2	.49	4.13	1.41	2.33	53	.11	2	.42	7	1.6	.83	4-18
1.2	2.2	.49	2.93	1.29	2.34	62	.12	2	.44	7	1.3	.79	4-16
1.2	2.6	.44	2.19	1.17	2.38	70	.14	2	.41	7	1.1	.64	5-42
1.2	1.8	.49	1.28	1.21	2.38	88	.18	2	.56	7	1.2	.8	4-17
1.2	2.3	.443	4.56	1.45	2.46	49	.2	4	.47	7	1.7	.57	5-41
2.2	3.8	.53	1.43	1.11	2.51	93	.19	5	.57	7	.98	.74	4-21
2.2	3	.53	2.39	1.29	2.54	79	.12	5	.44	7	1.3	.82	4-20
2.1	3.6	.53	3.49	1.39	2.56	58	.12	4	.36	7	1.5	.76	4-19
2.2	3.4	.55	3.76	1.47	2.63	57	.17	3	.44	7	1.7	.7	5-43
2.2	4.5	.46	2.77	1.24	3.04	70	.09	4	.33	7	1.2	.79	4-23
2.2	4	.39	2.77	1.36	3.47	67	.1	4	.42	7	1.5	.81	4-26
1.2	3.3	.31	2.26	1.14	3.67	75	.15	2	.52	7	1	.62	5-44
1.2	2.8	.31	4.63	1.43	3.71	53	.16	3	.46	7	1.6	.57	5-43
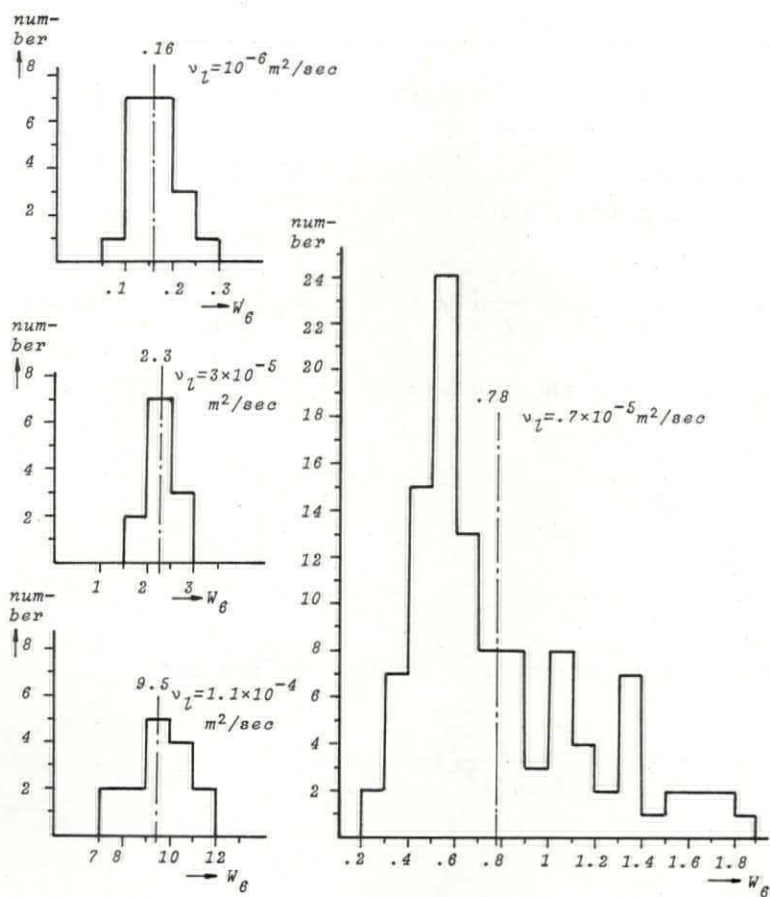
FIGURE A3-6. Distribution functions for W_6 from (8.25) for different viscosities of the liquid. The mean values are also indicated.

APPENDIX 4.

THE SHOCK STRUCTURE FOR A CONSTANT VALUE OF C_D.

The equations are:
equation of motion for a bubble

$$\frac{d}{d\eta}\left\{y\ \frac{v-u}{U}\right\}\ +\ \frac{3C_D}{4(3\alpha_o)^{\frac{1}{2}}}|y\ \frac{v-u}{U}|\left\{y\ \frac{v-u}{U}\right\}\ =\ 2\alpha_o y\ \frac{dy}{d\eta}\ ,\qquad (A3.1)$$

momentum equation for the mixture

$$y^{2/3}\left\{(1+4\alpha_o y)\frac{d^2 y}{d\eta^2}\ +\ \delta^\Delta\ \frac{dy}{d\eta}\right\}\ +\ (1-y)(y-M_o^{-2})\ +$$

$$\frac{v-u}{U}\ M_o^{-2}\ =\ 0\ .\qquad (A3.2)$$

The resulting equation for the smooth profile is

$$\frac{d}{d\eta}[(1-y)(y-M_o^{-2})]\ +\ \frac{3C_D}{4(3\alpha_o)^{\frac{1}{2}}}(1-y)^2(y-M_o^{-2})^2\ =$$

$$-2\alpha_o y\ \frac{dy}{d\eta}\ ,\qquad (A3.3)$$

where yM_o^{-2} is taken equal to unity. The derivatives in
(A3.2) are left out of account, since we consider changes
on the scale of the smooth profile.
We obtain from (A3.3)

$$\frac{M_o^{-2}-(1-2\alpha_o)}{(1-M_o^{-2})^2(1-y)}\ +\ \frac{M_o^{-2}-1-2\alpha_o M_o^{-2}}{(1-M_o^{-2})^2(y-M_o^{-2})}\ +$$

$$\frac{2\alpha_o(M_o^{-2}+1)}{(1-M_o^{-2})^3}\ln\left\{\frac{y-M_o^{-2}}{1-y}\right\}\ =\ -\ \frac{3C_D}{4(3\alpha_o)^{\frac{1}{2}}}\ \eta\ .(A3.4)$$

For $M_o^2<1+2\alpha_o$ this represents a wave profile in which y de-
creases smoothly from 1 to M_o^{-2}.

The shock thickness d_C becomes

$$d_C \sim \frac{16 R_o \alpha_o}{3 C_D (1-M_o^{-2})^3} 10 .$$
(A3.5)

With $C_D = 1.5$, $R_o = 10^{-3} m$, $\alpha_o = O(10^{-2})$ and $M_o^2 - 1 = O(10^{-1})$, d_C amounts to a couple of meters.

The length of the smooth region of a S_B shock cannot be approximated so easily. A rough estimate is found from replacing

$$\left| y \frac{v-u}{U} \right| y \frac{v-u}{U} \text{ by } \alpha_o (1-y^2) y \frac{v-u}{U} ,$$

where we used the unresisted bubble velocity as a first approximation. In that case d_B is

$$d_B \simeq \frac{4 R_o}{3 C_D \alpha_o (1-M_o^{-4})} \frac{\ln 20}{} .$$
(A3.6)

For our experiments d_B as given in (A3.6) is of the order of one meter.

LITERATURE.

Abramowitz, M., Stegun, I.A. 1965. *Handbook of Mathematical Functions*. Dover Publications New York.

Ackeret, J. 1930. *Techn. Mech. Therm.* 1, 53.

Batchelor, G.K. 1967. *An Introduction to Fluid Dynamics*. Cambridge at the University Press.

Batchelor, G.K. 1969. In *Fluid Dynamics Transactions*, ed. W. Fiszdon, P. Kucharczyk, W.J. Prosnak, vol. IV. Warszawa: Polish Scientific Publishers (PWN).

Benjamin, T.B., Bona, J.L., Mahony, J.J. 1972. *Phil. Trans. Roy. Soc. London* A 272, 47.

Broer, L.J.F. 1964. *Appl. Sci. Re.* B11, 273.

Campbell, G.A., Forster, R.M. 1948. *Fourier Integrals*. D. van Nostrand Company.

Campbell, I.J., Pitcher, A.S. 1958. *Proc. Roy. Soc. London* Ser. A243, 534.

Chapman, R.B., Plesset, M.S. 1971. *J.Basic Eng.* 93, 273.

Chisnell, R.F. 1955. *Proc. Roy. Soc. London* A232, 350.

Courant, R., Friedrichs, K.O. 1948. *Supersonic Flow and Shock Waves*. Interscience Publishers, Inc. New York.

Crespo, A. 1969. *Phys. Fluids* 12, 2274.

Darwin, C.G. 1953. *Proc. Camb. Phil. Soc.* 49, 342.

Devin, C., Jr. 1959. *J. Acoust. Soc. Am.* 31, 1654.

Eddington, R. 1970. *AIAA J.* 8, 1.

Erdelyi, A. 1954. *Tables of Integral Transforms*. Vol. I. Mc Graw-Hill Book Comp. Inc.

Foldy, L.F. 1945. *Phys. Rev.* 67, 107.

Grad, H., Hu, P.N. 1967. *Phys. Fluids* 10, 2596.

Haberman, W.L., Morton, R.K. 1954. *Trans. Am. Soc. Civ. Eng.* published as Proc. Sep. no. 387.

Hadamard, J.S., Rybczyncki, W. 1911. Reported in H. Lamb. 1932. *Hydrodynamics*. Cambridge at the University Press.

Hsieh, D.Y., Plesset, M.S. 1961. *Phys. Fluids* 4, 970.

Johnson, R.S. 1970. *J. Fluid Mech.* 42, 49.

Kosterin, S.I. 1949.*Bulletins of the Academy of Science of the USSR*. 12, 1824.

Lamb, H. 1932. *Hydrodynamics*. Cambridge at the University Press.

Levich, V.G. 1949. Reported in L.D. Landau, E.M. Lifshitz. 1959. *Fluid Mechanics*. Vol. VI. Pergamon Press.

Levich, V.G. 1962. *Physicochemical Hydrodynamics*. Prentice Hall.

Lick, W. 1970. *Ann. Rev. Fluid Mech.* 2, 113.

Lighthill, M.J. 1956. In *Surveys in Mechanics*, ed. G.K. Batchelor, R.M. Davies. Cambridge at the University Press.

Mallock, A. 1910. *Proc. Roy. Soc. London* Ser A84, 391.

Meyer, E., Skudrzyk, E. 1953. *Akust. Beih.* 3. 434.

Minnaert, M. 1933. *Phil. Mag.* 16, 235.

Moore, D.W. 1963. *J.fluid Mech.* 16, 161.

Morse, P.M., Feshbach, H. 1953. *Methods of Theoretical Physics*. Part I and II. Mc Graw-Hill Book Comp. Inc.

Noordzij, L. 1971. *Phys. Comm.* Twente Univ. Techn. 3, 1. To be published also in *Proc. IUTAM Symposium on Unsteady Flow of Water at High Speeds* Leningrad 1971.

Noordzij, L., Wijngaarden, L. van. 1973. *Mech. Comm.* Twente Univ. Techn. 2, 1.

Nunzatio, J.W., Walsh, E.K. 1972. *Phys. Fluids* 15, 1397.

Ockendon, H., Spence, D.A. 1969. *J. Fluid Mech.* 39, 329.

Parkin, R., Gilmore, F., Brode, H.L. 1961. Rand Corp. Mem. R.M.-2795-PR.

Peregrine, D.H. 1966. *J. Fluid Mech.* 25, 321.

Pfriem, H. 1940. *Akust. Z.* 5, 202.

Pfrisch, D., Sudan, R.N. 1971. *Phys. Fluids* 14, 1033.

Plesset, M.S. 1964. In *Cavitation in Real Liquids*, ed. R. Davies. Elsevier Amsterdam New York.

Riemann, B. 1859. *Götting. Abh.* 8, 43.

Strachan, J.D., Huni, J.P., Alborn, B. 1970. *J. Fluid Mech.* 43, 487.

Silberman, E. 1957. *J.Acoust. Soc. Am.* 29, 925.

Taylor, G.I. 1954. *Proc. Roy. Soc. London* Ser. A225, 273.

Whitham, G.B. 1958. *J. Fluid Mech.* 4, 337.

Whitham, G.B. 1959. *Comm. Pure and Appl. Math.* 12, 113.

Wijngaarden, L. van. 1964. *Proc. 11^e Int. Congr. Appl. Mech.* ed. H. Görtler. Springer Verlag Berlin 854.

Wijngaarden, L. van. 1968. *J. Fluid Mech.* 33, 465.

Wijngaarden, L. van. 1970. *Appl. Sci. Res.* 22, 366.

Wijngaarden, L. van. 1972a. *Ann. Rev. Fluid Mech.* 4, 369.

Wijngaarden, L. van. 1972b. *Progr. Heat Mass Transf.* 6, 637.

Woo, S.H., Paslay, P.R. 1967. *J.Acoust. Soc. Am.* 1, 114.

OVERZICHT.

Het doel van het onderzoek was de bestudering van de ver-
schillende schokgolfstructuren bij één dimensionale stro-
ming van een mengsel van vloeistof en gasbellen.
Beschouwd is een mengsel met een gasfractie van enkele pro-
centen. De gasbellen hebben plaatselijk allen dezelfde dia-
meter. Deze bedroeg ongeveer $10^{-3}m$. We zijn er vanuit ge-
gaan dat de bellen niet opbreken ten gevolge van een druk-
golf. Ook is er geen massatransport tussen bellen en vloei-
stof. Verder wordt voor de bellen aangenomen dat deze bol-
vormig blijven.
Voor de beschrijving van golfverschijnselen in dergelijke
mengsels kiezen we een model dat een beschrijving met be-
hulp van de continuums theorie mogelijk maakt. Hierbij
gaan we uit van een gemiddelde druk, snelheid en dichtheid.
De middeling wordt uitgevoerd over een volume element van
het mengsel. Dit volume element bevat veel bellen, maar
heeft afmetingen die klein zijn ten opzichte van een karak-
teristieke lengte voor de golfverschijnselen.
We gaan er bij de beschrijving vanuit dat in rust toestand
druk en dichtheid uniform zijn. Deze aanname is met betrek-
king tot de experimentele omstandigheden niet juist omdat
we een druk- en dichtheidsverdeling hebben ten gevolge van
de zwaartekracht.
Het mengsel is een compressibel medium met een compressibi-
liteit overeenkomstig aan die van de gasfase en een dicht-
heid overeenkomstig aan die van de vloeistof. De resulte-
rende geluidssnelheid in mengsels met een gasfractie van
enkele procenten is dan ook laag, lager dan die in lucht.
In genoemde mengsels beschouwen we verschillende typen
schokken. Voor deze schokken worden, net als in de gas-
dynamica, relaties geformuleerd tussen grootheden ver voor
en ver achter de schok, gebaseerd op behoud van massa,
impuls en energie. Met behulp van deze zogenaamde Hugoniot
relaties kunnen we de voortplantingssnelheid van de schok
in termen van bekende grootheden voorspellen. Ook wordt de
structuur, i.e. de druk als functie van bijvoorbeeld de

plaatscoördinaat, van deze schokken bepaald. Bij het ont-
staan van een stationaire schok speelt de relatieve bewe-
ging van de gasbellen een belangrijke rol. We kunnen twee
relatieve bewegingen onderscheiden en wel de radiale be-
weging van het gasbel oppervlak en de translatie van een
gasbel ten opzichte van de vloeistof. De eerste veroorzaakt
een zogenaamd dispersie effect op een golf en de tweede
veroorzaakt een relaxatie effect. Verschillende typen schok-
ken kunnen gevonden worden uit evenwicht van de verschillende
effecten. Er is een schok waarbij de structuur volgt uit de
vergelijking voor het evenwicht van niet lineaire compressie,
het belangrijkste niet lineaire effect, en de dissipatie
samenhangende met de volume oscillaties van een gasbel. Dit
resulteert in een schok waarvan de structuur gelijk is aan
de Taylor schok in de gasdynamica. Er is verder een schok
gebaseerd op evenwicht van niet lineaire compressie, dis-
persie en de bijbehorende dissipatie. Dit noemen we een S_A
schok. Het dispersie verschijnsel hangt samen met de traag-
heid van de radiaal bewegende vloeistof bij een pulserende
gasbel. Tenslotte kan een schokstructuur gevonden worden
uit een evenwicht van niet lineaire compressie en de dis-
sipatie samenhangend met de relatieve translatie van een
gasbel.

De eerste schok kon niet experimenteel aangetoond worden.
Voor niet te zwakke schokken geldt dat voor een S_A schok,
bij verwaarlozing van viskeuze effecten samenhangend met
de relatieve translatie, de structuur hoofdzakelijk bepaald
wordt door evenwicht van niet lineaire compressie en dis-
persie. Enige dissipatie is noodzakelijk voor het verkrijgen
van een stationaire schok. De verwaarlozing van viskeuze
effecten samenhangend met de relatieve translatie is gerecht-
vaardigd gedurende een zekere tijd nadat de schok opgewekt
is. Gedurende de experimenten bleek dan ook dat de struc-
tuur van de S_A schok veranderde bij voortplanting door een
schokbuis van enige lengte. Deze verandering hangt samen
met de genoemde viskeuze effecten welke na enige tijd ef-
fectief worden. Dit verschijnsel kan beschreven worden in

termen van relaxatie, overeenkomstig thermische relaxatie
bij schokgolven in gassen. De relaxatietijd behorende bij
de relatieve translatie is de tijd waarin een gasbel met
een beginsnelheid ten opzichte van de vloeistof door vis-
keuze krachten afgeremd wordt tot de vloeistof snelheid.
Een schok waarvan de S_A-structuur veranderd is door relaxatie
noemen we een S_B schok. Deze schokken treden op wanneer de
drukverhouding van de drukken achter en voor de schok boven
een zekere kritische waarde ligt. Beneden deze waarde ver-
andert de S_A schok op den duur in een S_C schok waarvan de
structuur bepaald wordt door niet lineaire compressie en
relaxatie.

Uit de theorie volgt dat de relaxatie de golfsnelheid en
de structuur van de golf beinvloedt. Experimenteel was de
invloed van de relaxatie op de golfsnelheid niet te bepalen,
omdat het effect klein is voor mengsels met enkele volume
procenten gas. De relaxatie effecten op de structuur waren
goed te meten.

Na een algemene inleiding wordt in Hoofdstuk 1 het gedrag
van een individuele gasbel in vloeistof besproken. In Hoofd-
stuk 2 wordt aandacht besteed aan de algemene eigenschappen
en de bewegingsvergelijkingen voor vloeistof-bellen meng-
sels. In de Hoofdstukken 3 tot en met 5 worden de verschil-
lende schokstructuren beschreven. Op de invloed van relaxatie
op de ontwikkeling van de schok wordt in Hoofdstuk 6 nader
ingegaan. In de experimenten speelt de zwaartekracht een rol
doordat gebruik gemaakt wordt van een verticaal opgestelde
schokbuis. In Hoofdstuk 7 wordt de invloed van de zwaarte-
kracht en de daarmee samenhangende druk- en dichtheidsver-
deling op de golfvoortplanting onderzocht. In Hoofdstuk 8
wordt de experimentele opstelling beschreven en de experi-
mentele resultaten vergeleken met de theoretisch afgeleide
grootheden.

De algemene conclusie luidt dat de experimenten goed met de
theorie overeenstemmen.

CURRICULUM VITAE.

De auteur van dit proefschrift werd op 1 december 1942 geboren te Rotterdam. Na de MULO in Enschede bezocht te hebben volgde hij aldaar een studie aan de Hogere Technische School, waar hij in 1962 het diploma in de werktuigbouwkunde behaalde. Na een onderbreking door militaire dienst studeerde hij werktuigbouwkunde aan de Technische Hogeschool Twente te Enschede. Zijn afstudeerwerk verrichtte hij in de groep Stromingsleer onder leiding van Prof. Dr. Ir. L. van Wijngaarden.
In 1969 behaalde hij het ingenieurs diploma met lof. Sindsdien is hij werkzaam als wetenschappelijk medewerker in de groep Stromingsleer van de afdeling Technische Natuurkunde aan de T.H.T.

STELLINGEN

I

De aanname van Levich dat een gasbel als een bol met een vrij oppervlak kan worden beschouwd, wordt, voor de door hem aangegeven begrenzing van het Reynoldsgetal, ondersteund door de experimentele resultaten voor translatie-relaxatie-schokken.

Levich, V.G. 1962. *Physicochemical Hydrodynamics*. Prentice Hall.
Dit Proefschrift.

II

De bewering van Ackeret, dat "solange unsere empirische Kenntnisse nicht grösser sind, hat es meiner Meinung nach nicht sehr viel Wert, die Rechnungen strenger durchzuführen" is met betrekking tot cavitatieschokken nog steeds juist.

Ackeret, J. 1930. *Tech. Mech. Therm.* 1, 63.

III

Het door Parkin e.a. beschreven schokprofiel kan alleen dan optreden, wanneer de drukverhouding tussen de drukken achter en voor de schok groter is dan γ en wanneer translatie-relax-atie geen rol van betekenis speelt. γ is de verhouding tussen de soortelijke warmte bij constante druk en de soortelijke warmte bij constante dichtheid van het gas.

Parkin, R., Gilmore, F., Brode, H.L. 1961. Rand Corp. Mem. R.M.-2795-PR.
Dit Proefschrift.

IV

De door Batchelor in 1969 gemaakte veronderstelling, dat de
translatie van de gasbellen ten opzichte van de vloeistof
een belangrijke rol kan spelen bij schokgolven in mengsels
van vloeistof en gasbellen is juist.

Batchelor, G.K. 1969. In *Fluid Dynamics Transactions*, e.d.
W. Fiszdon, P. Kucharczyk, W.J. Prosnak, vol. IV. Warszawa:
Polish Scientific Publishers (PWN).
Dit Proefschrift.

V

In sectie 85 van het boek *Fluid Mechanics* van Landau en
Lifshitz wordt wel het werk van Kontorovich genoemd, maar,
ten onrechte, niet het werk van Burgers.

Landau, L.D., Lifshitz, E.M. 1959. *Fluid Mechanics*. Vol. VI.
Pergamon Press.
Burgers, J.M. 1946. *Proc. Kon. Ned. Akad. v. Wetensch.*
Vol. XLIX, 273.

VI

De aanname van Crespo dat de warmteoverdracht tussen de
gasbel en de haar omringende vloeistof bepaald wordt door
de warmteweerstand aan vloeistofzijde van de gasbel is
onjuist.

Crespo, A. 1969. *Phys. Fluids* 12, 2274.

VII

De Nederlandse bevolking zal massaal tot actie tegen de
milieuverontreiniging overgaan, wanneer eigendommen, zoals
automobielen, door genoemde verontreiniging beschadigd worden.

VIII

De benaming smartlap voor het levenslied kan in vele gevallen
als geuzennaam opgevat worden.

IX

In een vloeistof-gasbellenschokbuis wordt de toelaatbare
lengte van de luchtkolom boven het mengsel bepaald door de
sterkte van de te produceren schok. Dit verklaart waarom
de luchtkolom voorkomende in de experimenten van Campbell
en Pitcher kort genoeg was.

Campbell, I.J., Pitcher, A.S. 1958. *Proc. Roy. Soc. London*
Ser. A243, 534.

X

Het is te verwachten dat bij toepassing van turbotreinen
voor railvervoer aanzienlijke kostenbesparingen kunnen wor-
den bereikt in vergelijking met de kosten die gemaakt worden
voor electrische treinen, waarbij energie voor de aandrijving
verkregen wordt uit bovenleidingen.

Guskovski, G.E. 1972. Zeleznodorozny Transport 1, 42.

XI

De auteur J.M.A. Biesheuvel meent dat K. van het Reve god is.
Dit is minder verontrustend dan wanneer laatstgenoemde zich
als zodanig zou gaan gedragen.

Biesheuvel, J.M.A. 1972. *In De Bovenkooi.*

XII

Als de bewering van de columnist N. Scheepmaker, dat een
grote kijkdichtheid een criterium voor een goed televisie-
programma is, vertaald wordt in termen van journalistiek
en politiek, leidt dit tot de bewering dat de Telegraaf een
goede krant is en Richard M. Nixon een goed president.